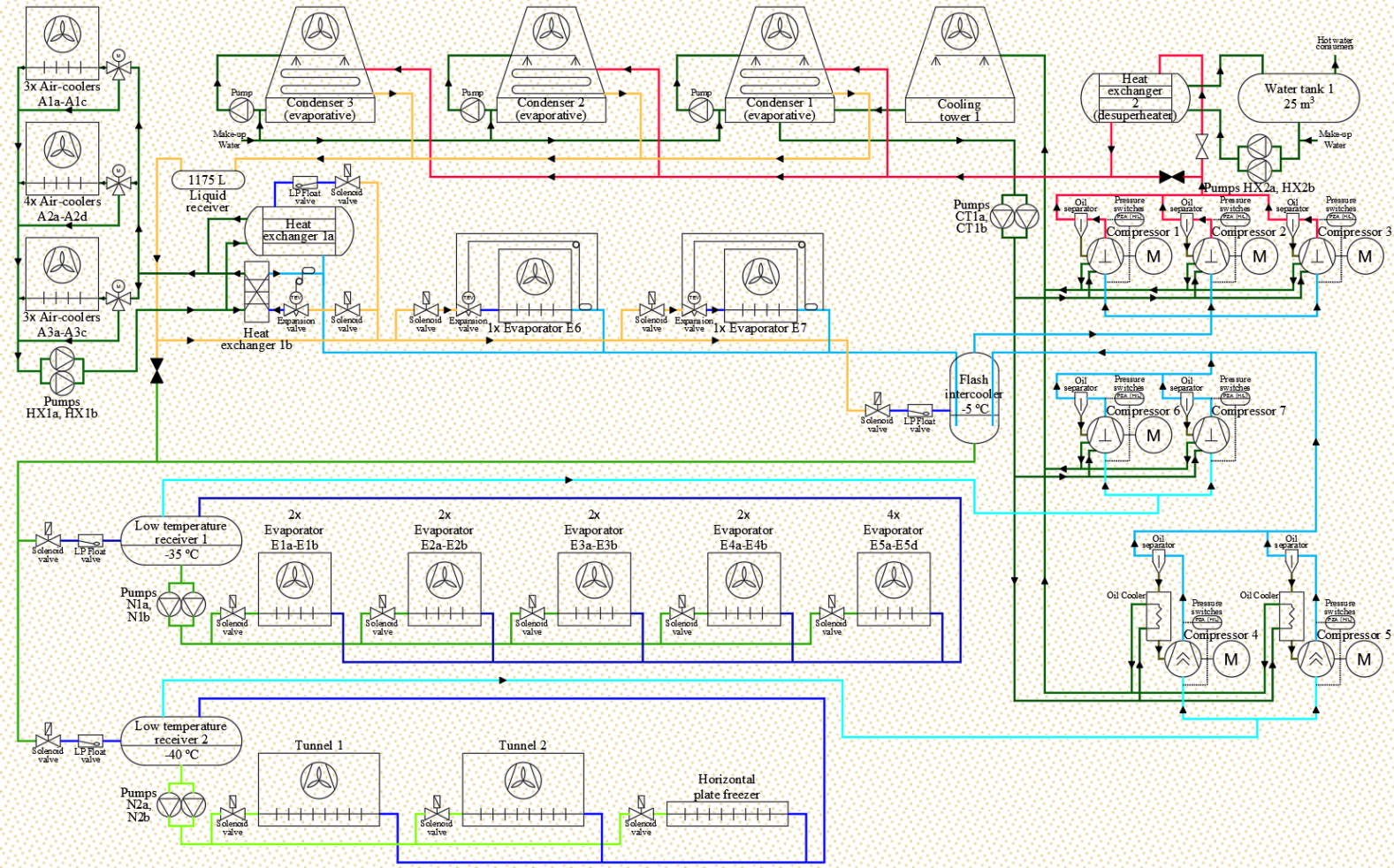

Francisco José Craveiro Bispo Pocinho Lamas

INDUSTRIAL REFRIGERATION
TECHNOLOGICAL OVERVIEW AND ENERGY-EFFICIENCY METHODOLOGIES

Master thesis on Energy for Sustainability supervised by Assistant Professor Adélio R Gaspar, and submitted to the Department of Mechanical Engineering, Faculty University of Sciences and Technology from the University of Coimbra

February, 2017

· U C ·

UNIVERSIDADE DE COIMBRA

UNIVERSIDADE DE COIMBRA

INDUSTRIAL REFRIGERATION
Technological overview and energy-efficiency methodologies

by

Francisco José Craveiro Bispo Pocinho Lamas

A thesis submitted in partial fulfillment of
the requirements for the degree of

Master of Science

Energy for Sustainability

DEPARTMENT OF MECHANICAL ENGINEERING

FACULTY OF SCIENCES AND TECHNOLOGY

UNIVERSITY OF COIMBRA

Thesis advisor

Adélio R. Gaspar, Assistant Professor

February, 2017

This work has been framed under the Energy for Sustainability Initiative of the University of Coimbra

ABSTRACT

Energy efficiency has become one of the most iconic issues/themes from the European Union's energy and environmental policies, being the key element to reach the goals of the "20-20-20 Programme" by 2020. Regarding the turnover, the activity related to the use of refrigeration equipment for food processing and cold storage corresponds to a high representative industry sector, either in Portugal, in the European Union, or even worldwide. In this context, both facilities and refrigeration systems have been identified as being areas having the greatest potential for the implementation of energy-efficiency and energy-saving measures.

Overcoming the lack of regulations applicable to the predominance of small and medium-sized enterprises, some energy-efficiency programmes have been implemented. However, they have proven to be insufficient on transferring results and recommendations to the agro-food industry. In this context, it is expected that the use of energy simulation tools applied to the refrigeration systems and facilities, and to other energy systems, would be able to provide reliable and useful information for this industrial sector. The dynamic simulation methodology demands an appropriate validation, comparing results with consumption breakdowns and energy analysis, obtained from detailed energy audits. On the other hand, the simulation model, and particularly the energy systems models must be correctly parameterized, in order to achieve an accurate convergence for the annual energy consumption. Nevertheless, the parameterization and technical characterization of the refrigeration systems, as well as simplification techniques commonly-used in dynamic simulation, require a thorough knowledge on the existing technological solutions, supported by theoretical fundamentals from the thermodynamic cycles taking place in it.

Thus, a technological overview is presented, based on the theoretical analysis of the vapor compression cycle (among others, briefly analyzed), along with its components and most-common configurations, regarding always the energy efficiency and the environmental issues. An analysis of the most widely used systems, configurations, equipment types and refrigerants is also carried out at a global level, and then in Portugal, in particular, being the latter supported by the information from a national research project on the energy-use and energy consumption of the refrigeration systems in the agro-industry sector.

Finally, a brief historical remark is presented aiming the evolution of the energy simulation programs, essential tools in the evaluation of energy-efficiency measures, culminating in the analysis of the technical feasibility on using the EnergyPlus software for modelling industrial refrigeration systems. Following this perspective, procedures and paths to be taken in future works, to perform detailed exercises on energy simulation of industrial refrigeration systems and facilities, are identified in order to demonstrate their added value for the study of energy-efficiency measures.

Keywords: industrial refrigeration; energy efficiency; agro-food industry; energy simulation; EnergyPlus.

RESUMO

A eficiência energética tornou-se um dos assuntos/temas mais emblemáticos das políticas energética e ambiental da União Europeia, sendo o elemento-chave para se atingirem os objetivos do "Programa 20-20-20", até 2020. A atividade relacionada com a aplicação da refrigeração para a transformação e conservação de alimentos corresponde a um sector industrial com elevada representatividade em termos de volume de negócios, seja em Portugal, na União Europeia ou mesmo a nível mundial. Neste contexto, as instalações e sistemas de refrigeração têm sido identificados como sendo as áreas com maior potencial para a implementação de medidas de eficiência energética e de poupança de energia.

Para ultrapassar a falta de regulamentação aplicável à predominância das pequenas e médias empresas, têm sido implementados alguns programas de eficiência energética. No entanto, têm-se mostrado insuficientes na transferência dos resultados e recomendações à indústria agroalimentar. Neste sentido, é expectável que o uso de ferramentas de simulação energética aplicadas às instalações, sistemas de refrigeração e outros sistemas de energia, possa fornecer informações fidedignas e úteis para este setor industrial. A metodologia de simulação dinâmica requer uma validação apropriada, comparando os resultados com a desagregação de consumos e análise energética, obtidos a partir de auditorias energéticas detalhadas. Por outro lado, o modelo de simulação e, em particular, os modelos dos sistemas energéticos têm de ser parametrizados corretamente, de forma a obter uma convergência precisa para o consumo anual de energia. Contudo, a parametrização e caracterização técnica dos sistemas de refrigeração, bem como as técnicas de simplificação utilizadas em programas de simulação dinâmica, exigem um conhecimento aprofundado das soluções tecnológicas existentes no mercado, consolidado na fundamentação teórica dos ciclos termodinâmicos que dentro deles ocorrem.

Desta forma, é apresentada uma revisão tecnológica, fundamentada na análise teórica do ciclo de compressão de vapor (entre outros, sumariamente analisados), juntamente com seus componentes e configurações mais comuns, tendo sempre em perspetiva a eficiência energética e as questões ambientais. É igualmente elaborada uma análise dos sistemas, configurações, tipos de equipamentos e fluidos refrigerantes mais utilizados a nível global, e em particular em Portugal, sendo esta última constituída de acordo com a informação de um projeto de investigação nacional sobre a utilização de energia e o consumo energético dos sistemas de refrigeração no sector agroindustrial.

Finalmente, é apresentado um breve registo histórico da evolução dos programas de simulação energética, ferramentas essenciais na avaliação de medidas de eficiência energética, culminando com a análise da viabilidade técnica do *software* EnergyPlus, para modelação de sistemas de refrigeração industrial. Nesta perspetiva, identificam-se os procedimentos e caminhos a seguir em trabalhos futuros para a realização de exercícios detalhados de simulação energética de instalações industriais de refrigeração, que permitam evidenciar a sua mais-valia no estudo de medidas de eficiência energética.

Palavras-chave: refrigeração industrial; eficiência energética; industria agroalimentar; simulação energética; EnergyPlus.

ACKNOWLEDGMENTS

To the few that lost their patience with me but never lost their hope, to those who lost their hope but never lost their patience, and to all, even (almost) losing both, never distanced themselves from me...

My deepest and sincere gratitude.

CONTENTS

LIST OF FIGURES

LIST OF TABLES

LIST OF ABBREVIATIONS AND ACRONYMS

ADAI	*Associação para o Desenvolvimento da Aerodinâmica Industrial* (In Portuguese)
AHRI	Air-Conditioning, Heating, and Refrigeration Institute
AMR	Active Magnetic Regenerator
ANSI	American National Standards Institute
ASHRAE	American Society of Heating, Refrigerating and Air-Conditioning Engineers
BAT	Best Available Techniques
BAU	Business-As-Usual
BPHX	Brazed Plate Heat eXchanger
CCHP	Combined Cooling, Heat and Power
CFC	Chlorofluorocarbon
CFD	Computational Fluid Dynamics
CHP	Combined Heat and Power
CHRP	Combined Heating, Refrigeration and Power
COP21	21st Conference of the Parties
COS	Condenser Outlet Split
DC	Direct Current
DOS	Diffuser Outer Split
DX	Direct-Expansion
EC	European Commission
EN	European Standard
EPCC	European Plan on Climate Change
ETS	Emissions Trading System
EU	European Union
FIPA	*Federação das Indústrias Portuguesas Agro-alimentares* (In Portuguese)
FPSC	Free-Piston Stirling Coolers
GAX	Generator-Absorber heat eXchanger
GHG	Greenhouse Gas
GVA	Gross Value Added
HC	Hydrocarbons
HCFC	Hydrochlorofluorocarbons

HFC	Hydrofluorocarbons
HFO	Hydrofluoroolefins
HVAC	Heating, Ventilation and Air-Conditioning
IEA	International Energy Agency
IEC	Intensive Energy Consumers
INDC	Intended Nationally Determined Contributions
IPB	*Instituto Politécnico de Bragança* (In Portuguese)
IPCB	*Instituto Politécnico de Castelo Branco* (In Portuguese)
IPCC	Intergovernmental Panel on Climate Change
IPP	*Instituto Politécnico de Portalegre* (In Portuguese)
IPVC	*Instituto Politécnico de Viana do Castelo* (In Portuguese)
ISQ	*Instituto de Soldadura e Qualidade* (In Portuguese)
LFL	Lower Flammability Limit
LSHX	Liquid-Suction Heat eXchanger
MCE	Magneto Calorific Effect
MEPS	Minimum Energy Performance Standards
NCCP	National Climate Change Programmes
NEEAP	National Energy Efficiency Action Plans
ODS	Ozone-Depleting Substances
OECD	Organization for Economic Co-operation and Development
OEL	Occupational Exposure Limit
POFC	*Programa Operacional Fatores de Competitividade* (In Portuguese)
QREN	*Quadro de Referência Estratégica Nacional* (In Portuguese)
RPM	Revolutions Per Minute
SGCIE	*Sistema de Gestão dos Consumos Intensivos de Energia* (In Portuguese)
SME	Small and Medium-sized Enterprises
TEAP	Technology and Economic Assessment Panel
TEV	Thermostatic Expansion Valve
TM	Thermal Machine
UBI	*Universidade da Beira Interior* (In Portuguese)
UC	*Universidade de Coimbra* (In Portuguese)
UNFCCC	United Nations Framework Convention on Climate Change
USA	United States of America

LIST OF SYMBOLS

C	Carbon
CO_2	Carbon Dioxide
F	Fluorine
H	Hydrogen
H_2O	Water
LiBr	Lithium Bromide
N_2	Nitrogen
NH_3	Ammonia
OH	Hydroxyl
%	Percentage
€	Euro
°C	Celsius degree
CO_2e / CO_2-eq	Carbone Dioxide equivalent
Gt	Gigaton
hr	Hour
K	Kelvin degree
L	Liter
Mtoe	Mega ton of oil equivalent
ppm	Parts per million
toe	Ton of oil equivalent
W	Watt
yr	Year

Greek symbols

∂	Partial derivative [relative to the unit of the respective variable]
Δ	Variation [relative to the unit of the respective variable]
ΔT_1	Temperature difference between $T_{fs,in}$ and T_{evap} [°C] or [K], for absolute temperature difference
ΔT_2	Temperature difference between $T_{fs,out}$ and T_{evap} [°C] or [K], for absolute temperature difference

ΔT_{fs}	Temperature difference between $T_{fs,out}$ and $T_{fs,in}$ [°C] or [K], for absolute temperature difference
ΔT_{lm}	Logarithmic mean temperature difference [°C] or [K], for absolute temperature difference
α_{ab}	Seebeck differential coefficient [dimensionless]
γ	Specific heat ratio [dimensionless]
ε_{LSHX}	Effectiveness of the liquid-suction heat exchanger [dimensionless]
η_{II}	Second Law efficiency based on the COP [dimensionless]
η_s, η_c	Isentropic efficiency or adiabatic compression efficiency [dimensionless]
η_{th}	Thermal efficiency [dimensionless]
η_v	Volumetric efficiency [dimensionless]
η_{vc}	Clearance volumetric efficiency [dimensionless]
θ	Total specific energy [J. kg^{-1}]
μ_{JT}	Joule-Thompson coefficient [°C.Pa^{-1}]
ρ	Density [kg. m^{-3}]

Symbols

A	Area [m^2]
$C_1, \dots C_{10}$	Regression coefficients [dimensionless]
c_p	Constant-pressure specific heat [J.kg^{-1}.K^{-1}]
$\bar{c_p}$	Mean constant-pressure specific heat [J.kg^{-1}.K^{-1}]
$\bar{c_p}_l$	Mean constant-pressure specific heat, for liquid phase [J.kg^{-1}.K^{-1}]
$\bar{c_p}_v$	Mean constant-pressure specific heat, for vapor phase [J.kg^{-1}.K^{-1}]
c_v	Constant-volume specific heat [J.kg^{-1}.K^{-1}]
COP	Coefficient of performance [dimensionless]
$COP_{R,Carnot}$	Coefficient of performance of a Carnot refrigerator [dimensionless]
COP_{rev}	Coefficient of performance of a reversible (ideal) refrigerator [dimensionless]
COP_{II}	Second Law efficiency based on the COP dimensionless]
COP_R	Coefficient of performance of a refrigerator [dimensionless]
COP_{th}	Thermal coefficient of performance [dimensionless]

D	Diameter [dimensionless]
$DT1$	Temperature difference between $T_{fs,in}$ and T_{evap} [°C] or [K], for absolute temperature difference
g	Gravitational acceleration [m.s^{-2}]
GWP	Global Warming Potential [dimensionless]
h	Specific enthalpy [J.kg^{-1}]
h_{fg}	Latent heat of vaporization or enthalpy of vaporization [J.kg^{-1}]
HRR	Condenser-to-evaporator heat rejection ratio [dimensionless]
IE	Isentropic efficiency [dimensionless]
L	Length [m]
$LMTD$	Logarithmic mean temperature difference [°C] or [K], for absolute temperature difference
$\dot{m}$	Mass flow rate [kg.s^{-1}]
N	Number of revolutions per minute [RPM]
n	Chemical amount [mol]
n_{cir}	Circulating number or rate [dimensionless]
n_{ovf}	Overfeed rate [dimensionless]
ODP	Ozone Depletion Potential [dimensionless]
P	Pressure [Pa]
P_{disc}	Pressure on the discharge side of the compressor [Pa]
P_{suct}	Pressure on the suction side of the compressor [Pa]
PR, r_P	Pressure ratio [dimensionless]
Q	Heat [J]
q	Specific heat [J.kg^{-1}]
$\dot{Q}_{evap}$	Refrigeration capacity [W]
Q_{des}	Isobaric desorption [J]
Q_{drive}	Driving heat [J]
q_{evap}	Refrigeration effect [J.kg^{-1}]
R	Ideal gas constant [J.mol^{-1}.K^{-1}]
S	Entropy [J.K^{-1}]
s	Specific entropy [J.kg^{-1}.K^{-1}]
s	Stroke length [m]

SEI, COP_{II}	System efficiency index [dimensionless]
T	Temperature [°C] or [K], for absolute temperature
T_G	Thermodynamic temperatures of the generator (high-temperature source) [K]
T_H	Thermodynamic temperatures of the condenser medium-temperature source) [K]
T_{hot}	Maximum temperature provided by the external heat source [°C] or [K], for absolute temperature difference
T_L	Thermodynamic temperatures of the evaporator (low-temperature source) [K]
T_m	Mean fluid stream temperature [°C]
$TEWI$	Total Equivalent Warming Impact
u	Specific internal energy [J. kg^{-1}]
U	Overall heat-transfer coefficient [W.m^{-2}.K^{-1}]
V	Volume [m^3]
v	Specific volume [m^3.kg^{-1}]
v	Velocity [m.s^{-1}]
$\dot{V}$	Volume flow-rate measured at the compressor [m^3.s^{-1}]
$\dot{V}_d$	Displacement rate [m^3.s^{-1}]
V_i	Volume index [dimensionless]
VE	Volumetric efficiency [dimensionless]
W	Work [J] or [N.m]
w	Specific work [J. kg^{-1}]
x	Quality of biphasic mixture [dimensionless]
x_{max}	Maximum amount of adsorbed refrigerant per unit of dry adsorbent or loading [dimensionless]
x_{min}	Minimum amount of adsorbed refrigerant per unit of dry adsorbent or loading [dimensionless]
z	Number of cylinders [dimensionless]
z	Height [m]
ZT	Figure of merit [dimensionless]

Subscripts

$1, 2, 3, 4, \ldots$ n	Evolution points for the cycle
a', b', c', d'	Evolution points for actual compression
$absor$	Absorption
$adsor$	Adsorption
$adsorbent$	Adsorbent
$bubble$	Bubble point
$comp$	Compressor or compression
$cond$	Condenser or condensation
db	Dry bulb
dew	Dew point
$disc$	Discharge (compressor outlet)
$evap$	Evaporator or evaporation
exp	Expansion or expander
$exp - gain$	Expansion gain
f	Saturated liquid
fs	Fluid stream
g	Saturated vapor
gen	Generator
$ideal$	Ideal compression
in	In or Inlet
int	Intermediate
liq	Liquid
out	Out or Outlet
$phial$	Phial
$pump$	Pump
r	Refrigerant
s	Isentropic value for point i $(s_{is} = s_{i-1})$
$suct$	Suction (compressor inlet)
$system$	System
tot	Total
$valve$	Valve
vap	Vapor

w	Water
wb	Wet bulb

1. INTRODUCTION

1.1. FRAMEWORK

The energy sector has been going through the major revolution ever, in the last decades. Since the post-war period (War World II), there have been several distinct events, but it was undoubtedly the first oil crisis, with the Arab oil embargo in 1973, that triggered a turning point on the awareness of how energy was being produced (transformed, would be more correct) and consumed worldwide.

Particularly in European Union (EU), where the energy structure has remained heavily dependent on fossil fuels [1], [2], and on its external energy supplies [3], [4], several initiatives have been promoted towards energy demand reduction, increased energy efficiency, energy source diversification, and decoupling energy demand from economic growth. It is then, not surprising that policy statements place energy policy and climate protection among the top priorities of the EU [1]. Attentive and aware of the consequences of a potentially dangerous polynomial: economic growth, energy consumption, greenhouse gas (GHG) emissions and energy dependency, the EU is at the forefront on energy and climate policy, shown by the numberless ongoing initiatives, programmes, directives and regulations. Among these energy policies [5], [6], spanned in the timescale from 1996 to 2020 and distributed in several phases (Figure 1.1), some still in progress, others recently completed:

- Renewable Energy Directives, an ambitious plan leading to an overall target of 20 % renewables across all energy sectors by 2020;
- EU Emissions Trading System (ETS), aiming 20 % GHG reduction until 2020;
- National Energy Efficiency Action Plans (NEEAPs), with 9 % energy saving target until 2016. According to the Energy Services Directive, these plans should be drawn by the Member States for each of the three year-period periods covered by the Directive. It also states that, in order to improve energy efficiency, it should be specified policy instruments to remove market barriers to efficiency, and created conditions to develop a market energy service and mechanisms for efficiency measures [7].

Between 2007 and 2008, the European Commission (EC) presented a package of proposals regarding GHG emissions and energy consumption reduction, extending ETS

and renewable energies' promotion, resulting on the European Council's approval of the so-called "20-20-20 programme" - the European Plan on Climate Change (EPCC).

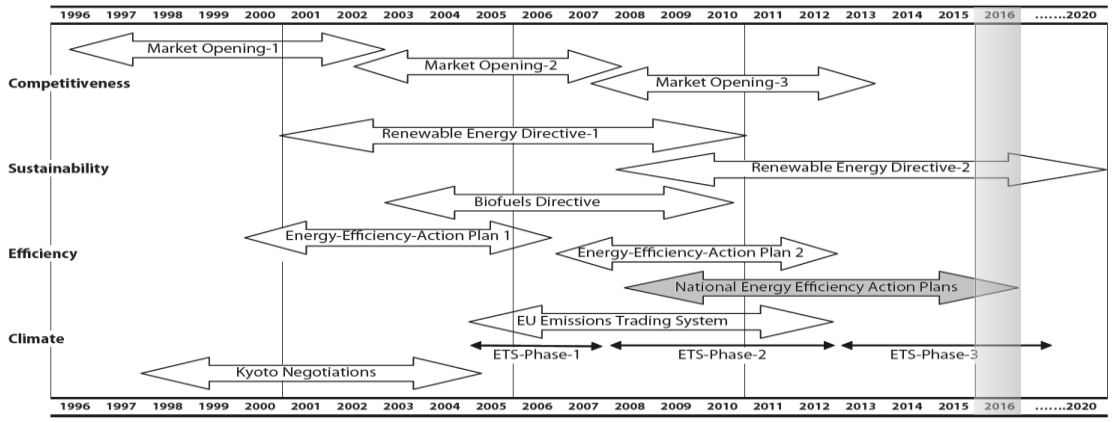

Figure 1.1: Development of EU energy policies over time (source: adapted from [7])

Recent economic and financial crisis reduced the capacity on investment of EU Member States, delaying, postponing or simply not starting up the implementation of all energy policies [7]. Even though, new targets and policies have already been defined for 2030, aligned with the 2050 roadmaps [6], namely [7]: reduction of 40 % on GHG emissions (compared to 1990 levels); minimum of 27 % share of renewable-energy consumption; at least 27 % of energy savings, through energy-efficiency measures, compared to a business-as-usual (BAU) scenario; reformation on EU ETS; *etc*. These ambitious commitments were based on the assumption of full implementation of the 20-20-20 targets [7].

1.2. MOTIVATION

Refrigeration plays a crucial role in industry and society. As freezing inhibits the microbiological growth, reducing chemical reactions and delaying physical transformations, it is possible to preserve food, maintaining its quality without spoiling, during long storage periods. This capacity is vital for the increasingly-demanding modern society. At the same time, it represents an extremely important economic activity, making food and beverage, one of the biggest, if not the biggest, industrial sector(s) worldwide. In addition, with a world population projected on almost 10 billion (9.6×10^9) by 2050, food storage for medium and long-term, at appropriate conditions for human consumption, will be a challenging task. Only actuating directly over the economic and environmental domains, improving energy-efficiency, reducing energy-consumption and -waste, reducing GHG emissions, *etc*., will balance this delicate social sphere, reaching

the desired sustainable development. Of course, it will not be shameful to admit that, besides the altruistic perspective, there is an economic interest, since the agro-food sector is the largest and the leading employer manufacturing sector, either in Portugal or in the European Union, registering the highest turnover of the entire industry sector. Regarding the technological aspects, and contrarily to the heating, ventilation and air-conditioning (HVAC) systems where thermal plants are usually factory-assembled packages, industrial refrigeration systems are commonly built-up, due to the enormous variety of installations and their operating conditions, providing diverse technical challenges to the mechanical engineer. It will also be an opportunity to deepen the knowledge on applied thermodynamics, for cycles, which will certainly lead to a proficient lecturing and/or vocational training performance.

1.3. RESEARCH OBJECTIVES

This thesis aims at baselining a future work, contributing for the global effort on achieving the EPCC's goals for 2020/2030, increasing energy-efficiency in the refrigeration systems of the agro-food industry. Several studies have been made, and this sector has undergone some energy-efficiency programmes throughout the last years. Nevertheless, the results of potential energy savings, from the application of a specific energy-saving measure, are presented at excessively large intervals (*e.g.* floating head pressure control: energy saving up to 30 % [8]). On the other hand, studying measures for a particular facility, demands previous detailed and costly energy audits.

The purpose of a future research is to use energy simulation software (and later an artificial neural network, eventually) coupled to optimization algorithms, to determine suitable energy-efficiency measures and elect the best options, providing reliable and useful information for this industrial sector. For the time being, it is necessary to pave the way for such a demanding and ambitious task.

To support the extensive data entry in detailed energy simulation models, a comprehensive characterization of different refrigeration systems (either with vapor or non-vapor compression cycles), components and configurations is demanded. In parallel, a characterization of the most common technologies, systems, components, and refrigerant types, globally and then particularly for Portugal, will direct the research towards the national industry reality. The technical adequacy of the energy simulation component’s models will be verified, and preliminary tests will be conducted.

1.4. THESIS OUTLINE

This dissertation, which reflects the work developed during an extensive research period, is structured in five chapters.

In the first and present chapter, the importance of energy is highlighted in different strands, namely in the efficiency, consumption, dependency and security on supply, and the related GHG emissions. Motivation and research objectives are also identified in this chapter.

The second chapter presents the context that supports all this work, reinforcing the role of the energy efficiency and energy consumption in the industry competitiveness, without disregarding environmental issues. In addition, a critical analysis of the energy legislation is made, particularly for Portugal, where some energy-efficiency programmes have been implemented in an attempt to reverse the lack of energy-efficiency measures oriented to SMEs, traditionally non-intensive energy consumers. A comprehensive technological overview is then presented. The analysis is also extended to the main components and most-common configurations of the refrigeration systems, always regarding the energy efficiency and environmental issues, such as the GHG emissions, owing the energy input during operation, and ozone depletion and global warming impacts, due to refrigerant leakages, during the operation, or in maintenance and dismantling procedures.

In the third chapter, an analysis of the most widely used systems, configurations, equipment types and refrigerants is carried out at a worldwide level, and then in Portugal, in particular. The characterization and examination of the Portuguese case, has been supported by the information from a national research project on the energy-use and energy consumption of the refrigeration systems in the agro-industry sector.

Described in the fourth chapter, energy simulation programs arise as being essential tools for the evaluation of energy-efficiency measures. Along with a brief historical remark on their evolution, a set of energy simulation software is referred. The technical feasibility on using EnergyPlus for modelling industrial refrigeration systems is discussed, as well as its adequacy for supporting an accurate methodology for evaluating energy-efficiency measures.

Finally in the fifth chapter, conclusions and future research work are presented.

2. CONTEXT AND STATE-OF-THE ART

2.1. ENERGY EFFICIENCY: THE MAIN KEY TO GHG ABATEMENT

Energy efficiency is a universal vector for all the goals of EU's energy and climate packages, covering GHG emission reduction and security of energy supply, providing affordable energy services for all consumers, and improving economic competitiveness, especially in the industry sector, while reducing its vulnerability either to sudden climate or energy price changes [2], [7]. This statement is not only applicable to the EU, but globally, as supported by the giant multinational corporation of oil and gas, ExxonMobil, in its document "The Outlook for Energy: A View to 2040" [9]. The International Energy Agency (IEA) also recognizes energy efficiency as a key option to explore intensively as a policy instrument, as "it plays a critical role in limiting world energy demand growth to one-third by 2040" [10].

Formerly, the IEA presented forecasts for the global energy consumption established in three different scenarios [11]:

- Current Policies Scenario, assuming no changes in policies from the mid-point of the year of publication (previously called Reference Scenario);
- New Policies Scenario, considering policy commitments, plans and measures announced by countries, including national commitments to reduce GHG emissions and plans to phase out fossil-energy subsidies;
- 450 Scenario, an alternative projection, defining an energy pathway in order to limit global temperature increase to 2 °C, stabilizing the concentration of GHG in the atmosphere at a concentration of 450 ppm of carbon dioxide (CO_2).

Recently, and recognizing that the door of "2 °C was closing" [12], the IEA raised an unprecedented challenge to the participant countries of the 21st Conference of the Parties (COP21) for the United Nations Framework Convention on Climate Change (UNFCCC) meeting in Paris, December 2015. In response to the forecast considering the pledges submitted by the COP21 participants, also known as Intended Nationally Determined Contributions (INDCs), and the planned energy policies in countries that still have not submitted their own, a bridging strategy has been proposed, imposing a near-term peak by 2020, demanding a strong political commitment to achieve the 2 °C climate goal [13].

Thus, IEA forecasts are presently established in two scenarios [13], in order to reach the 450 Scenario:

- INDC Scenario, which have a deceleration on GHG emissions, but have not a peak by 2030. This prognosis points out 2040 as the limit for CO_2 emissions consistent with a 50 % chance of surpassing the 450 Scenario (just eight months later than the forecast without INDCs);
- Bridge Scenario, including a set of essential measures in an energy sector transition compatible with the 2 °C goal, encouraging more research, development and deployment for key energy technologies. This scenario depends upon five measures: increasing energy efficiency within the industry, buildings and transport sectors; progressively reducing the use of the least-efficient coal-fired power plants and banning their construction; increasing investment in renewable-energy technologies in the power sector, gradually phasing out of fossil-fuel subsidies to end-users by 2030; and reducing methane emissions in oil and gas production.

A comparison between both scenarios can be seen in Figure 2.1, where energy efficiency is, once more, indicated as the measure with the highest CO_2 abatement potential. Nevertheless, the success of COP21 agreement will only be possible ensuring four pillar conditions: setting conditions for attainable global peak in energy-related emissions; providing periodical reviews (five-year review cycles) to set higher objectives over time; targeting worldwide 2 °C goal supported on national low-carbon economies; and building trust and confidence, consolidating a transparent tracking process to measure towards short- and long-term objectives [13].

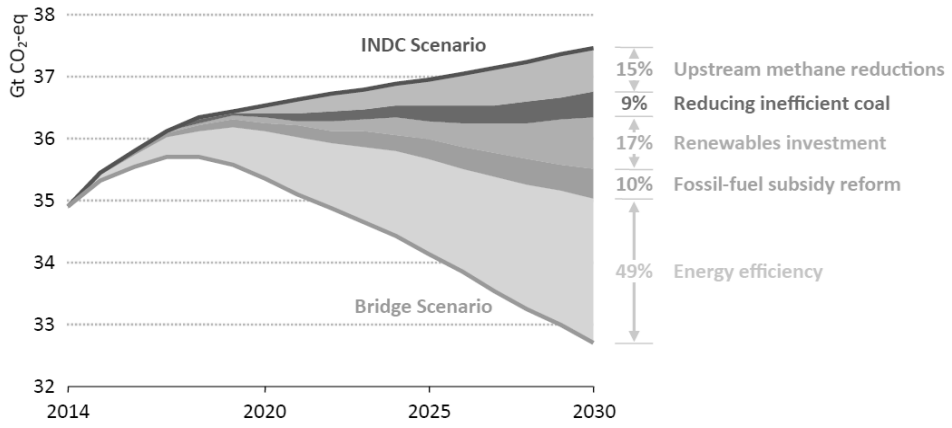

Figure 2.1: Global energy-related GHG emission by policy measure in the Bridge Scenario *Versus* INDC Scenario (source: [13])

2.1.1. THE ROLE OF INDUSTRIAL ENERGY EFFICIENCY

IEA's recommendations for reducing CO_2 emissions in industry are mainly related to energy efficiency: implementation of high-efficiency equipment and systems (*e.g.* mandatory adoption or variable-speed drives, when applicable); energy-efficiency services for Small and Medium-sized Enterprises (SMEs), as mandatory audit programmes; and complementary policies to support industrial energy efficiency, as minimum energy performance standards (MEPS) for electric motor systems, and incentives for heat pumps (low-temperature heat) [13], [14]. Another measure is related to the energy management [14], specifically with energy management protocols (*e.g.* ISO 50001). It is expected that industry will contribute almost 30 % of the total CO_2 savings potential from energy-efficiency recommendations, as depicted in Figure 2.2.

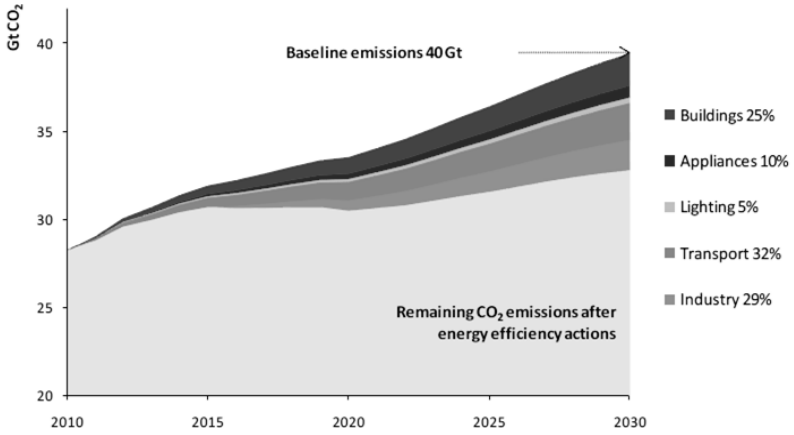

Figure 2.2: CO_2 saving potential (source: adapted from [15])

The assessment of the sectors where energy-efficiency measures might have a greater impact must be based on final energy consumption. In the EU, the final energy consumption is prevalent in three sectors (Figure 2.3): Transports (33 %), Industry (26 %) and Residential (25 %) [16]. In the Portuguese case, final energy consumption is dominated by Transports (41 %) and Industry (28 %) sectors [16].

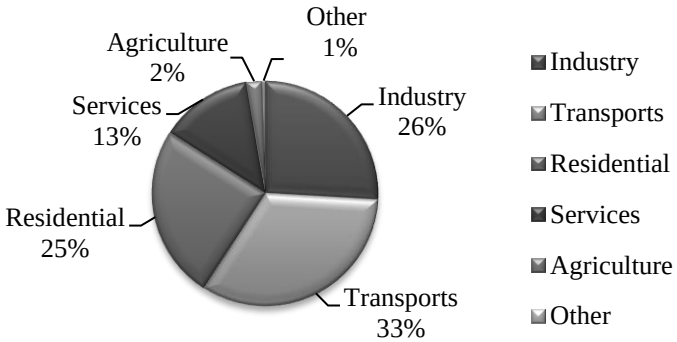

Figure 2.3: Gross final energy consumption, EU-28, 2014 (source: adapted from [16])

EU´s industry had a registered energy consumption of 297 Mtoe in 2005 and a forecast of 382 Mtoe, in a BAU scenario, by 2020, points it out as one of the sectors with largest potential savings: 95 Mtoe, representing 25% of the energy-use [17]. Recent studies [18] denote a lower final energy consumption in 2013, around 273 Mtoe, predicting a more conservative range, with reference to a BAU scenario, between 20 and 25 % of total energy-saving potential by 2030. Indeed, since 2005 EU industry's energy consumption has been registering an average annual growth rate of -2.1 % [16]. This trend is not only in accordance with the economy slowdown, but also with the adoption of energy-efficiency measures, as in the Portuguese case [19].

2.1.2. ENERGY POLICIES FOR THE EUROPEAN INDUSTRY

Currently, in the industrial sector, energy policies are used to enhance energy efficiency or to meet a specific energy-use. They have been used as a developing tool to a long-term strategic plan, covering from five to a ten-year period, for increasing energy efficiency and reducing GHG emissions [20]. As previously mentioned, EU's integrated energy and climate-change strategy and its energy-efficiency plans are the driving forces to reach the environmental goals by 2020 and 2030. Among other, these plans propose some actions to predict energy-efficiency requirements for industrial equipment, improved information provision for SMEs, and energy audits and energy management systems for bigger companies.

European Directives are transposed, into the national legislation of each EU State Member, through decrees or laws. These regulations are approved with the proper framework within the NEEAPs and National Climate Change Programmes (NCCPs) of each country (references [19] and [21], respectively, in their latest versions). Specifically for the Portuguese industry, it was created the regulation "*Sistema de Gestão dos Consumos Intensivos de Energia*" (SGCIE), a management system for Intensive Energy Consumers (IEC), established in order to promote energy efficiency and energy consumption monitoring of intensive energy consuming facilities [22]. The threshold for its application is established at 500 $toe.yr^{-1}$.

2.1.3. THE AGRO-FOOD INDUSTRY IN PORTUGAL AND IN THE EU

The Portuguese business sector is dominated by SMEs. By 2012, they were slightly more than one million, representing 99.9 % of the total of national non-financial enterprises. Approximately sixty-nine thousand belong to the manufacturing industry, corresponding to 6.5 % of the companies from non-financial sector [23]. According to the Portuguese agro-food sector association, "*Federação das Indústrias Portuguesas Agro-alimentares*" (FIPA) [24], its turnover and gross value added (GVA), 14.9×10^9 € and 2.6×10^9 €, respectively, make agro-food the largest Portuguese industry, representing almost 19 % of total manufacturing industry. This industry employs around one hundred thousand persons, distributed by few more than ten thousand enterprises [24]. In the EU, this phenomenon is also observed, with 15 % of the total manufacturing share, registering a turnover of $1\,244 \times 10^9$ € in 2013 (the largest sector in the EU), and a GVA of 206×10^9 € in 2012, being the leading employer manufacturing in EU, with more than four million person in almost three hundred thousand companies [25], [26].

2.1.4. PROJECT INOVENERGY: AN ATTEMPT TO MITIGATE THE GAP

From statistical studies [23], it is perceptible that the majority of Portuguese agro-food companies are SMEs. It has been estimated that their consumption is lower than 500 $toe.yr^{-1}$ [27], and therefore, not covered by the SGCIE (only approximately 10 % of the Portuguese agro-food industry is covered this legislation, leaving the remaining 90 % without any regulatory scope on energy consumption or energy efficiency [28]). This data corroborates Ferreira *et al.* statement [29], based on the Spanish experience, identifying this niche as having a interesting potential for energy savings.

In the recent past years, there were some programmes in Portugal. Among others, Efinerg and InovEnergy projects have been created to fill the gap left by the threshold of applicability of SGCIE and SMEs energy consumption, and/or to promote their competitiveness. The first one was more embracing, involving not only agro-food industries (reference [27]), but also ceramic and glass, wood and furniture, metalworking, and textile and apparel industries. By the other hand, InovEnergy project has been dedicated to the agro-food sector (six sub-sectors: meat, fish, dairy, wine, fruit & vegetables, and food conservation & distribution), and "...particularly focused on accounting energy use in the freezing and refrigerating chambers, since these facilities

represent the major energy consumption equipments of the mentioned industrial sector ... a value estimated to be about 30 % of a company's cost structure" [29].

The project "InovEnergy – *Eficiência Energética no Sector Agroindustrial*", resulted as a partnership between eight institutions, five public higher educational institutions: *Instituto Politécnico de Castelo Branco* (IPCB), as the project coordinator, *Universidade da Beira Interior* (UBI), *Instituto Politécnico de Bragança* (IPB), *Instituto Politécnico de Portalegre* (IPP), and *Instituto Politécnico de Viana do Castelo* (IPVC); one producers association: *Animaforum – Cluster Agroindustrial do Ribatejo*; one private laboratory: *Instituto de Soldadura e Qualidade* (ISQ); and one research unit: *Associação para o Desenvolvimento da Aerodinâmica Industrial* (ADAI), from the Department of Mechanical of the *Universidade de Coimbra* (UC) [30]. It was founded by the National Engineering Strategic Reference Framework, in Portuguese: *Quadro de Referência Estratégica Nacional* (QREN 2007-2013), Operational Programme for Competitiveness Factors, in Portuguese: *Programa Operacional Fatores de Competitividade* (POFC), 01/SIAC/2011, Ref.: 18642.

In summary, the purpose of this project was to overcome the lack of complete information on the energy-use of refrigeration and freezing processes. This data led to the identification of adequate energy-efficiency measures, enabling companies' competitiveness and contributing to the national (and European) effort regarding the energy independency and the reduction on GHG emissions. The assessment process, through energy audits, survey analysis, *etc.*, aimed not only an energy characterization of the agro-food sector, but also tools' development for energy-efficiency promotion [30].

Final results have been presented [30]: energy-saving potential range between 16.7 % and 24 %, depending on the sub-sector; a user-friendly predictive software COOL-OP (Cooling Optimization Program), developed for the assessment of energy performance in cold storage [31]; and the publication of a best-practice guidebook, where Best Available Techniques (BAT) were condensed in into a reference document [32]. Besides these technical outputs, some scientific production has been achieved under InovEnergy's scope, namely several MSc theses, peer-reviewed journal papers, conference papers, *etc.* [33].

2.2. INDUSTRIAL REFRIGERATION

2.2.1. INTRODUCTION

By definition, refrigeration is a process used for cooling or reducing the temperature of a space, product or process, moving the heat from one location to another using a refrigerant in a closed cycle (adapted from [34]), *i.e.* transferring heat from a low-temperature to a high-temperature source. It is a non-spontaneous process, contrarily to what might happen with cooling processes, and the final temperature of the heat source should always be lower than its surroundings.

2.2.1.1. Applications

Industrial refrigeration has a wide operating temperature range: evaporation may be as high as 15 °C, extending down to -60 °C or -70 °C. Cryogenics industry springs into action as the temperature requirements fall under -70 °C (for producing and using liquefied natural gas, liquid nitrogen, oxygen and other low-temperature substances) [35]. For agro-food industry, maintaining the temperature of perishable food keeping their nutrients intact, whatever the refrigeration method, is a key element to ensure food safety throughout the chain to the final consumer. In this sector, storage temperature is highly dependent on the type of product and on the product intended shelf life, but the majority of frozen food is stored between -18 °C and -35 °C [34]. Regarding the refrigerated facilities, two basic storage types are considered: cooler for commodities protection, usually at temperatures above 0 °C, and low temperature rooms, or freezers, operating at negative temperatures, preventing the product spoilage, maintaining or extending the product (or shelf) life [34].

For the classification of refrigerated storage for preservation of food quality, five categories can be found [34]:

- Controlled atmosphere (long-term fruit and vegetable storage);
- Coolers (positive temperatures above 0 °C);
- High-temperature freezers (temperatures between -2 °C and -3 °C);
- Low-temperature storages rooms (maintained at temperatures between -20 °C and -29 °C), for general frozen products;
- Low-temperature storages rooms (-20 °C to -29 °C), with a surplus of refrigeration capacity for freezing products received at above -18 °C.

2.2.1.2. Processes and methods

One of the most significant applications of refrigeration is food preservation. Freezing and cooling are common processes, as an effective reduction of microbial and enzymatic activity takes place [34]. Freezing inhibits normal microbiological development (due to water crystallization) and causes a delay in physical and chemical transformations, responsible for food deterioration [34]. Its temperature range is between -30 °C and -35 °C. In chilling processes, products are cooled and stored in a relatively high temperature range (-1 °C to -10 °C) [36]. Certain meat and poultry products can easily maintain their quality, remaining unfrozen, when stored superchilled at -1 °C. Some fruits can be stored at negative temperatures without freezing, due to sugars and other substances in the fruit water, lowering the freezing point below 0 °C [35].

Cooling, to be more precise, precooling processes are currently applied in fruits, vegetables and cut flowers' preservation. Prompt precooling, likewise a freezing process, inhibits the growth of microorganisms and enzymatic activity, besides reducing moisture loss and respiratory activity (an important heat gain in living commodities cooling or storing) [34]. In opposition to storage rooms, where products are hold at constant temperatures, precooling requires greater refrigeration capacity and cooling medium movement, once the heat is rapidly removed from the commodities [34]. For these processes, different cooling mediums, such as air, water or ice absorbing the heat from the commodities, result in distinct (pre)cooling methods, where residence time in the cooling medium is a crucial design criterion [34]:

- Hydrocooling. Method where chilled-water spray or agitated bath (immersion) removes heat from the commodities;
- Forced-air and forced-air evaporative cooling. In both methods, products are crossed by a cold air flow, providing much faster cooling than conventional room cooling methods. In the second method, mechanical refrigeration (used in the first case) is replaced by an evaporative cooler, passing air through a wet pad;
- Package icing. Spreading finely crushed or flaked ice, in shipping containers, directly over the food products (that are no harmed by the ice contact);
- Vacuum and water spray vacuum cooling. Cooling method through the rapid water evaporation off products surface, under low pressure flash chambers. In order to avoid mass loss, some vegetables are sprayed with water, before and during the cooling operation.

In freezing processes, the product temperature is reduced "while" most of its water is changed into ice. This process occurs in three separated phases (Figure 2.4). Firstly, from the initial temperature to the freezing point (sensible cooling above freezing), and after the water crystallization (fusion zone), temperature drops again reaching the storage temperature (sensible cooling below freezing) [34]. Thermal properties of foods, such as freezing point, latent fusion and sensible heats, will be addressed in Appendix A.

The three phases of freezing: (1) cooling, removing sensible heat and reducing the temperature to the freezing point, (2) latent heat of fusion removal, changing water to ice crystals, and (3) continuing cooling below the freezing point, removing more sensible heat and reducing the temperature to the desired or optimum frozen storage temperature. Latent heat of fusion removal (water turning to ice) is the longest part of the freezing process [34].

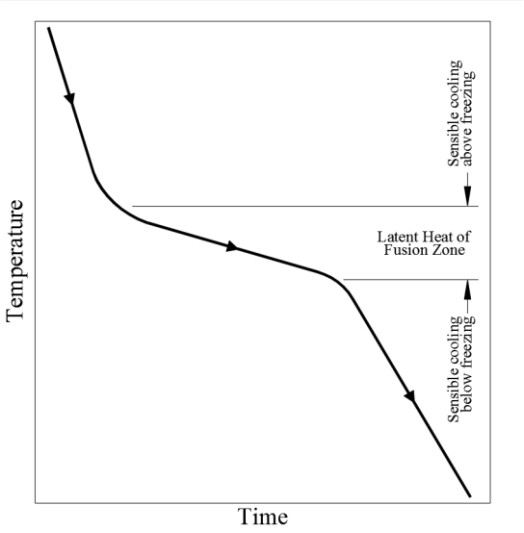

Figure 2.4: Typical freezing curve (source: [34])

Different methods, used in freezing processes, can be grouped by the heat-transfer mechanism [34]:

- Forced convection. Used in blast freezing, where cold air is circulated over the product at high velocity, removing the heat from the food product. The air is recirculated and the heat is removed in air-to-refrigerant heat exchanger;
- Natural convection. Used mainly in liquid immersions (*e.g.*, brines for packaged and fishery products);
- Conduction. Used in contact freezing method. The heat is extracted by conduction, from the food (packaged or unpackaged) to metal surfaces (cooled by a circulating refrigeration medium), where food is placed on or between.
- Convection and/or conduction. Used in cryogenic and cryomechanical freezing. In both cases, food is exposed to an environment below –60 °C (spraying liquid nitrogen or liquid carbon dioxide into the freezing chamber or container). In the second case, commodities are finish-frozen through mechanical refrigeration.

The working principles, equipment and refrigerants used by the systems behind the foregoing processes/methods, will be presented and analyzed in the following sections.

2.2.2. THE VAPOR-COMPRESSION CYCLE

Refrigeration cycles are a main topic in the majority of refrigeration and refrigeration-related literature [35], [37]–[42]. Alcaraz [37] presented an interesting thermodynamic approach to this subject: a thermal machine (TM) is considered, operating in a reversible closed cycle in steady-state regime, with heat transfer from two sources, HS_1 and HS_2 at different absolute temperatures, $T_2 > T_1$, and an external mechanical energy input, W (Figure 2.5a). After a loop or a time-interval, in which several loops have been completed, the TM has received an amount of external work, W, and transferred heat Q_1 and Q_2, from both sources. Entropy variation for the TM, Eq. (2.1), and heat sources, Eq. (2.2) and Eq. (2.3), are given by:

$$\Delta S = 0 \tag{2.1}$$

$$\Delta S = -\frac{Q_1}{T_1} \tag{2.2}$$

$$\Delta S = -\frac{Q_2}{T_2} \tag{2.3}$$

For the entire system, its entropy production is:

$$0 \leq \Delta S_{system} = -\frac{Q_1}{T_1} - \frac{Q_2}{T_2} \tag{2.4}$$

The energy conservation principle applied to this thermodynamic system results in the form of the First Law of Thermodynamics:

$$W = Q_1 + Q_2 = 0 \tag{2.5}$$

Rearranging Eq. (2.4) and Eq. (2.5), it is possible to obtain:

$$\begin{cases} W - Q_1 \times \dfrac{T_2 - T_1}{T_1} = T_2 \times \Delta S_{system} \geq 0 \\ W + Q_2 \times \dfrac{T_2 - T_1}{T_2} = T_1 \times \Delta S_{system} \geq 0 \end{cases} \tag{2.6}$$

In refrigeration equipment, the main purpose is the heat transfer from a cold source during its cycle operation. Thus, the amount of transferred heat from the cold source, during its operation, is positive, forcing to have a positive work, *i.e.* an input of mechanical energy, and having simultaneously a heat transfer into the hot source:

$$Q_1 > 0, W > 0 \text{ and } Q_2 < 0 \Longrightarrow |Q_2| > Q_1 \tag{2.7}$$

As shown, refrigerators transfer more heat to the hot source than the one taken from the cold source. For such reasons, refrigerators schemes can be adjusted and redrawn as follows in Figure 2.5b:

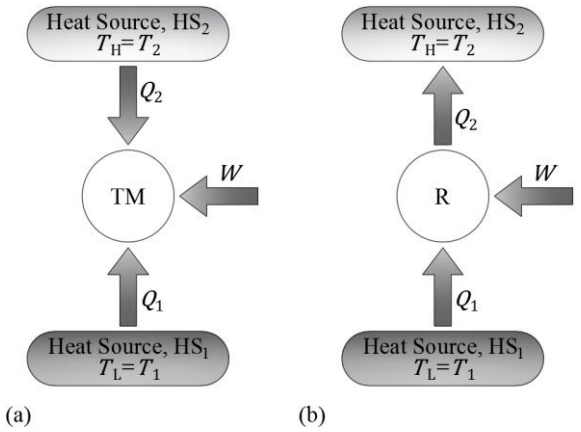

Figure 2.5: Schemes for (a) arbitrary thermal machine and (b) refrigerator (source: adapted from [37])

For refrigerators, the useful energy (energy extracted) is given by Q_1 while the energy consumption for the final purpose (work input) is given by W. The refrigeration "efficiency", can be measured by the ratio of these two quantities and is termed the Coefficient of Performance (COP) [38].

$$Q_1 = \frac{T_1}{T_2 - T_1} \times \left(W - T_2\, \Delta S_{system}\right) \tag{2.8}$$

$$COP_R = \frac{Q_1}{W} = \frac{T_1}{T_2 - T_1} \times \left(1 - \frac{T_2\, \Delta S_{system}}{W}\right) \tag{2.9}$$

From Eq. (2.9), it is noticeable that the maximum COP is given by $T_1/(T_2 - T_1)$. It is considered an ideal value, once real equipment has always a certain level of irreversibility. This "never-attainable-in-practice" COP, useful to compare the performance of real systems and evaluate their improvement potential, can be deduced from the reversed Carnot cycle (ideal refrigeration process), a four-process cycle after which it returns to original state [37], [38], as presented in Figure 2.6:

- Work input, resulting in an isentropic compression (adiabatic and reversible), vertical upwards evolution in the liquid-vapor area (1-2);
- Heat rejection to the high-temperature sink, with a complete condensation, at a constant temperature (isothermal) and pressure (isobaric), in a horizontal evolution (2-3);

  Isentropic expansion from the saturated liquid point to the corresponding pressure

of the cold source temperature, downwards to liquid-vapor mixture, in a vertical evolution (3-4);

- Heat addition, from the low-temperature source, with a partial vaporization at a constant temperature (isothermal) and pressure (isobaric), allowing to close the loop in a horizontal evolution (4-1).

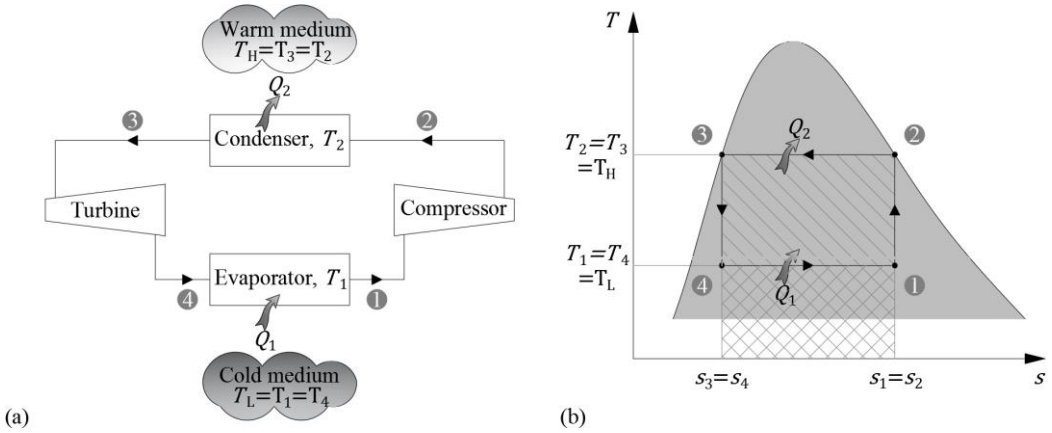

Figure 2.6: Ideal reversed Carnot cycle: (a) circuit and (b) T-s diagram (source: author)

From this cycle, the transferred heat from cold and hot sources is, respectively:

$$\begin{cases} Q_1 = T_1 \times (S_1 - S_4) = T_1 \times (S_2 - S_3) \\ Q_2 = T_2 \times (S_2 - S_3) \end{cases} \tag{2.10}$$

Applying the First Law of Thermodynamics:

$$W = Q_2 - Q_1 = (T_2 - T_1) \times (S_2 - S_3) \tag{2.11}$$

And therefore, the COP of Carnot refrigerators results as:

$$COP_{R,\,Carnot} = \frac{Q_1}{W} = \frac{T_1}{T_2 - T_1} = \frac{1}{T_2/T_1 - 1} \tag{2.12}$$

The improvement potential of an actual system can be then measured by COPs ratio of a real refrigeration system to a Carnot (reversible) cycle between heat-source and -sink temperatures. This ratio is known as System Efficiency Index (SEI) [38] or Second Law efficiency based on the COP [39], [43]:

$$SEI \text{ or } COP_{II} \text{ or } \eta_{II} = \frac{COP}{COP_{rev}} = \frac{COP_R}{COP_{R,\,Carnot}} \leq 1 \tag{2.13}$$

Defined as the ratio of the required minimum energy input for an ideal system to the actual energy input of a real system, its value gives an important indication of the effectiveness on the energy utilization [44].

2.2.2.1. Ideal *versus* actual vapor-compression cycle

Although the maximum efficiency provided by the reversed Carnot cycle, it is not a suitable model for refrigeration cycles, neither can be approximated in actual devices [39]. The unattainableness of such a working principle implies some modifications in the refrigeration cycle, leading to another conceptual definition: the ideal vapor-compression cycle. The differences between both cycles can be seen in Figure 2.7b, where the hatched areas represent the extra heat that could be avoided (region above condensing temperature, during compression and desuperheating processes) and the heat that could be potentially recovered (area below evaporating temperature, during the expansion) [38]. Therefore, the total vaporization of the fluid before compression and the replacement of the turbine by a throttling device (Figure 2.7a) eliminate the impracticalities associated with the reversed Carnot cycle, making the vapor-compression cycle the most widely used cycle in refrigeration, air-conditioning and heat pumps systems [39].

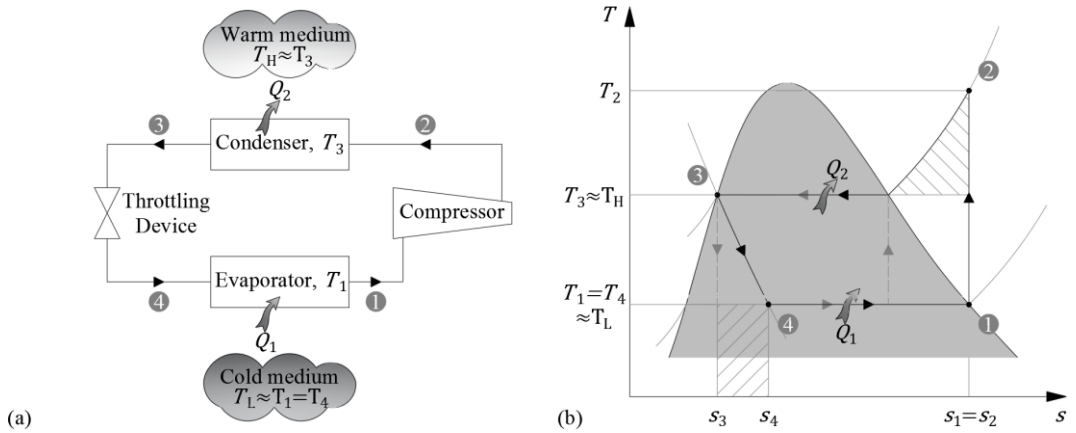

Figure 2.7: Ideal vapor-compression cycle: (a) circuit and (b) T-s diagram (source: adapted from [38])

The ideal vapor-compression cycle is also a four-process cycle. Its evolutions can be described as follows [35], [37]–[39], and as represented in Figure 2.8:

- Similarly to the reverse Carnot cycle, it presents an isentropic compression (adiabatic and reversible), although the process starts from a saturated vapor condition into the superheated vapor area (dry instead wet compression). This will increase the refrigeration effect and avoid liquid slugging in the compressor (1-2);
- Reversible heat rejection (2-3). Firstly, with a sensible cooling of the superheated vapor (desuperheating) and then by a complete condensation at constant temperature and pressure. In this evolution, the temperature of fluid must

be higher than its surroundings, but preserving the reversibility hypothesis, the temperature difference should be infinitesimal, and no pressure drops considered;

- Isenthalpic expansion, without heating absorption or rejection, and without mechanical work involved (3-4). Thus, in opposition to the reversed Carnot cycle expansion, this process is not reversible. The pressure reduction causes a corresponding temperature drop, due to the amount of energy removed from the partial (or flash) vaporization of the fluid. The amount of flash gas is responsible for increasing the volume of the working fluid, and therefore, the throttling valve is currently termed as expansion device. The application of isentropic expansion engines, such as turbines, are not a feasible option, being replaced by isenthalpic expansion devices (*e.g.* expansion valves, capillary tubes), whose simplicity and reliability are major advantages;
- Reversible heat addition (4-1) with a complete vaporization at constant temperature and pressure. As in the condensation process, the reversibility hypothesis imposes an infinitesimal temperature difference, infinite heat exchangers and the absence of pressure drops.

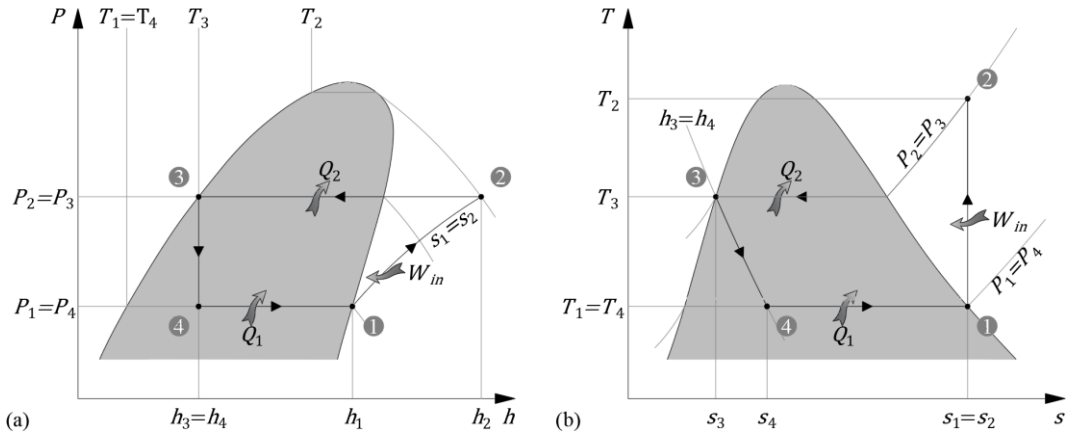

Figure 2.8: *P-h* (a) and *T-s* (b) diagrams for ideal vapor-compression cycle (source: author)

The major differences between the ideal and actual vapor-compression (Figure 2.9a) cycles are, according to [35], [37]–[39], in the:

- Heat exchangers, such as condensers and evaporators, having not infinite heat exchanging surfaces nor infinitesimal temperature differences with the heat sources (Figure 2.9b), and thus originating irreversible processes;
- Presence of liquid subcooling or vapor superheating, either individually and produced in the own heat exchanger, or simultaneously, in a Liquid-Suction Heat Exchanger (LSHX) – Figure 2.10. Although the increase of the refrigerating

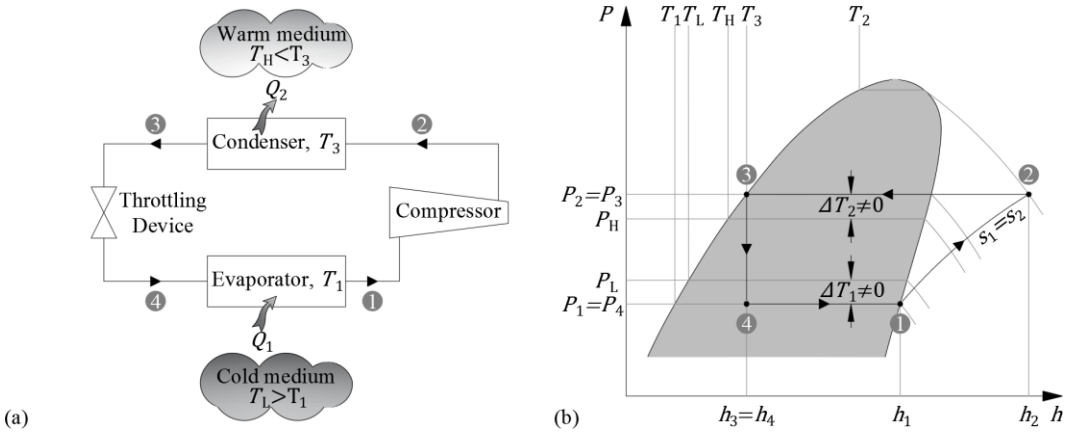

Figure 2.9: Actual vapor-compression machine: (a) circuit and (b) *P*-*h* diagram (source: author)

effect, subcooling is not normally desired once the totality of the heat-surface area of the condenser is not used for the condensation process. On the other hand, a slightly superheated vapor at the evaporator outlet is crucial for protection of the compressor; In the presence of an LSHX, and once the flow rate is the same, the ratio of enthalpy differences (or sensible evolutions, in liquid and vapor states) for subcooling to superheating processes is given by the LSHX effectiveness[1], ε_{LSHX}:

$$\varepsilon_{LSHX} = \frac{\Delta h_{1\to 7}}{\Delta h_{3\to 5}} = \frac{h_7 - h_1}{h_3 - h_5} = \frac{\bar{c}_{p_v}(T_7 - T_1)}{\bar{c}_{p_l}(T_3 - T_5)} = \frac{\bar{c}_{p_v}(T_7 - T_1)}{\bar{c}_{p_v}(T_3 - T_1)} = \frac{T_7 - T_1}{T_3 - T_1} \qquad (2.14)$$

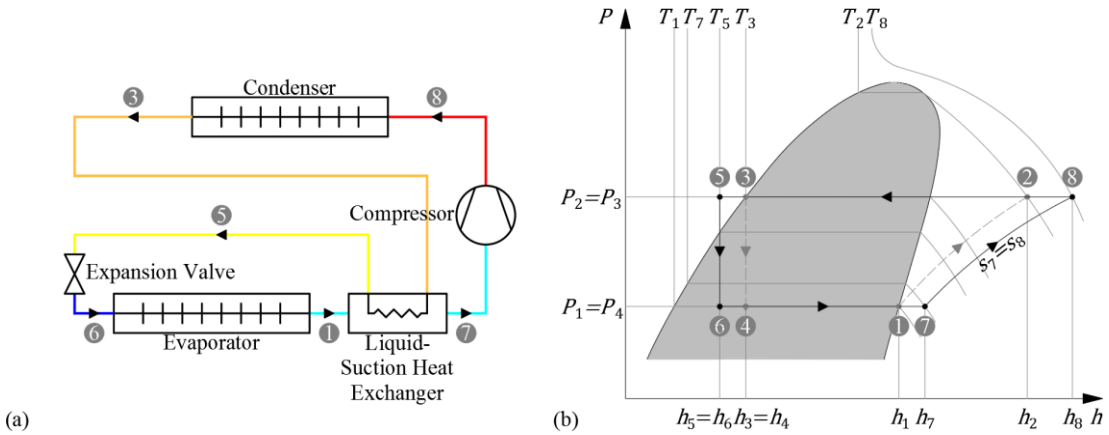

Figure 2.10: Liquid subcooling and vapor superheating with a LSHX: (a) circuit and (b) *P*-*h* diagram (source: author)

LSHXs are used to increase the cycle efficiency, to prevent flash gas formation at the expansion valve and completely evaporate any residual liquid that may remain at the suction line, before entering the compressor [34];

- Behavior of the real compressor, and subsequent reduction of the actual volumetric

[1] Terminology not consensual: some authors refer to this property as the *efficiency* of the heat transfer.

efficiency, VE [38] or η_v [35] (ratio of the volume rate entering the compressor to the compressor displacement rate, shown in Figure 2.11), due to: (1) the rise of the pressure ratio, PR [38] or r_P [35] (discharge pressure to suction pressure ratio), or the clearance volume (if adiabatic expansion: $PV^\gamma = \text{constant}$); (2) the existence of discharge and inlet valves, rising the pressure ratio; (3) heat addition from the compressor warm walls to the inlet vapor, increasing its specific volume and consequently decreasing the refrigerant mass flow rate; or the transferred heat through the compressor envelope, refuting the hypotheses of isentropic re-expansions and compressions and approaching the actual evolution to a polytropic evolution ($PV^n = \text{constant}$), involving some cooling; (4) the presence of lubricant and non-condensable residual matter (other fluids present in the refrigeration system), occupying volume destined to the refrigerant; and (5) leakages of refrigerant, reducing the volumetric efficiency proportionally to the lost mass flow rate. Another definition is used by [35] to characterize the volumetric efficiency, and call it the clearance volumetric efficiency, η_{vc} (ratio of effective swept, or intake, volume to the swept volume, as shown in Figure 2.11b).

$$VE \text{ or } \eta_v = \frac{\dot{V}}{\dot{V}_d} \tag{2.15}$$

$$\eta_{vc} = \frac{V_{a'} - V_{d'}}{V_{a'} - V_{c'}} \tag{2.16}$$

$$PR \text{ or } r_p = \frac{P_{disc}}{P_{suct}} \tag{2.17}$$

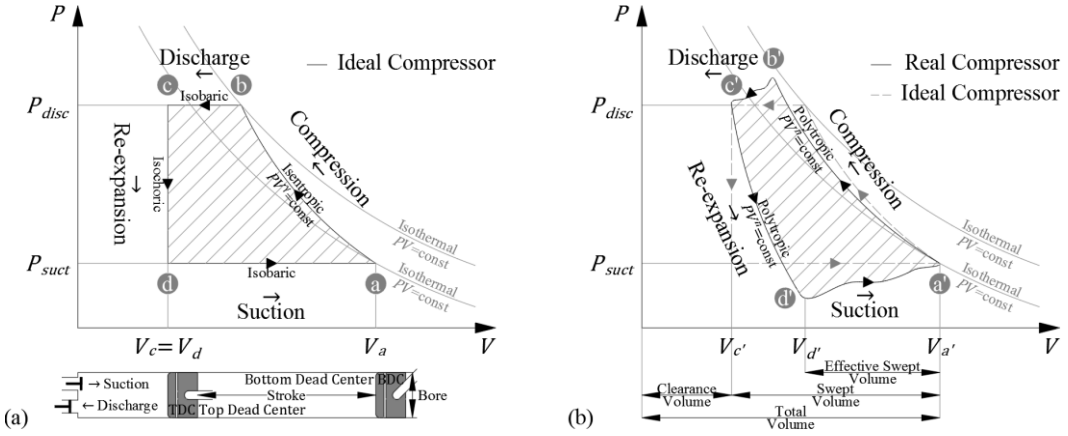

Figure 2.11: P-V or indicator diagrams for (a) ideal and (b) actual reciprocating compressors (source: adapted from [37])

Two compressors can be compared by the energy efficiency of compression. This term is defined by the ratio of the minimum work input required (isentropic work,

w_s or w_{ideal}) to compress a gas from P_1, T_1 to P_2, to the actual work input (w_{actual}, that includes several losses). It is known as the isentropic efficiency of a compressor, IE [38], η_s or η_c [39], or adiabatic compression efficiency, η_c [35]. Neglecting changes in kinetic and potential energy during the compression, the work input of an adiabatic compressor becomes equal to the change in enthalpy. The differences between ideal and actual evolutions can be seen in Figure 2.12 and Figure 2.14;

$$IE, \eta_s \text{ or } \eta_c = \frac{w_{ideal}}{w_{actual}} \cong \frac{\Delta h_{ideal}}{\Delta h_{actual}} = \frac{h_{8s} - h_7}{h_8 - h_7} \tag{2.18}$$

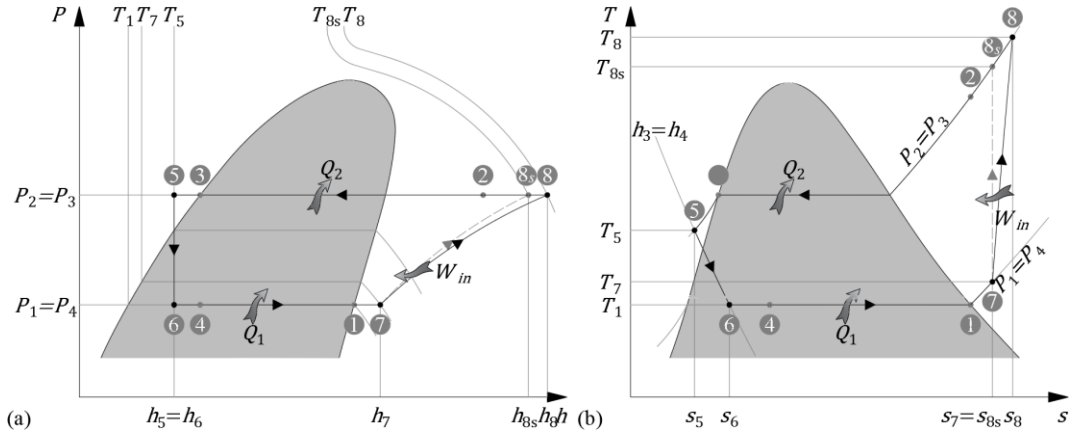

Figure 2.12: P-h (a) and T-s (b) diagrams representing ideal and actual compression (source: author)

- Existence of pressure drops also increases the pressure ratio, r_p, and is dependent on (1) the type and dimensions of the heat exchangers (*e.g.* condenser, evaporator); (2) the dimensions of the pipes and on the existence of valves and accessories; and (3) the physical properties of the refrigerant. These pressure drops can be divided in high (ΔP_2) and low pressure (ΔP_1) stages (Figure 2.14).

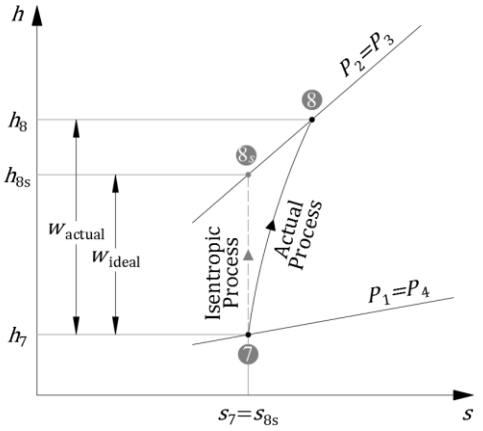

Figure 2.13: h-s diagram representing ideal and actual compression (source: adapted from [39])

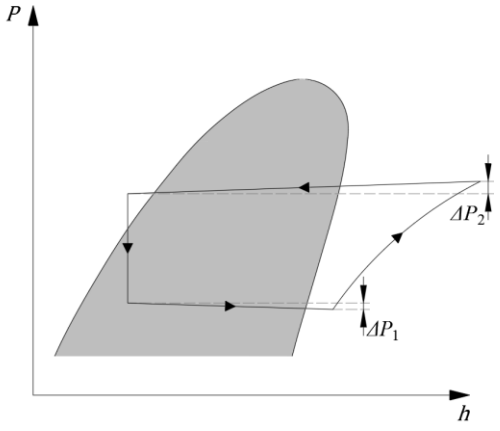

Figure 2.14: P-h diagram representing high- and low-pressure losses (source: adapted from [37])

Considering all the differences between ideal and actual vapor-compression cycles, abovementioned and represented in Figure 2.9 to Figure 2.14, the real cycle can be represented as follows (Figure 2.15):

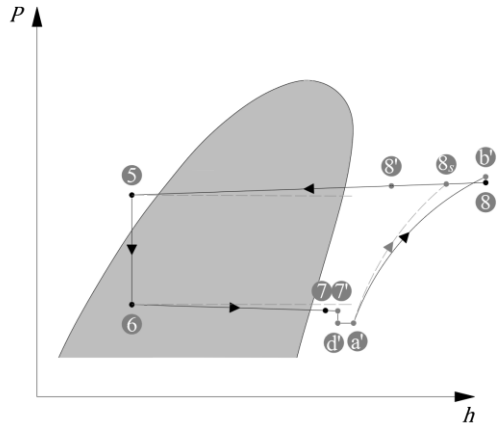

7–7': Reheating in compressor suction pipes;
7'–d': Vapor expansion in the suction valve;
d'–a': Vapor reheating entering the cylinder;
a'–b': Actual compression (non-isentropic);
b'–8: Gas expansion in the discharge valve;
8–8': Desuperheating in the connection pipes;
8'–5: Desuperheating, condensation and sub-cooling (subcooler may or may not exist);
5–6: Isenthalpic expansion in expansion valve;
6–7: Complete vaporization and superheating.

Figure 2.15: *P-h* diagram for actual vapor-compression cycle (source: adapted from [37])

2.2.2.2. Components used in vapor-compression systems

Evaporators, condensers, compressors and expansion devices are the crucial components of a vapor-compression refrigeration system. In the following subsection, their main characteristics, configurations and types are outlined, along with a brief thermodynamic and heat-transfer analysis of the evolutions occurring within each of them.

Applying the First Law of Thermodynamics, *i.e.* the conservation of energy principle to heat and thermodynamic processes, in an open system (Figure 2.16), such as those used in refrigeration systems (*e.g.*: heat exchangers – condensers and evaporators, compressors and expansion devices), the variation of the internal energy, on a unit mass basis, Δu, is given by the balance between the specific heat, q, added to (+, or removed from, −) the system and specific work, w, done on (+, or done by, −) the system, as expressed in Eq. (2.19).

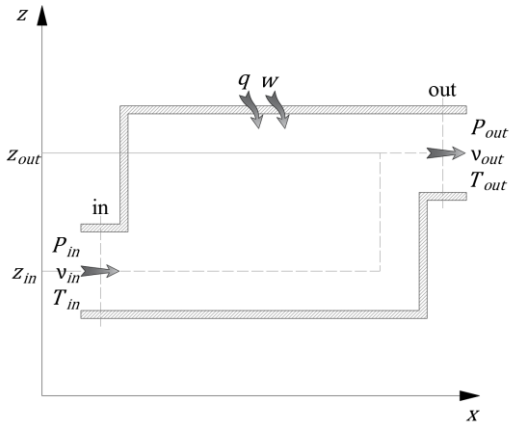

Figure 2.16: Open system balance (source: author)

$$\Delta u = u_{out} - u_{in} = q + w \tag{2.19}$$

For a working fluid, the variation of total energy, on a unit mass basis, $\Delta\theta$, is given by sum the variations of the specific flow energy, $\Delta(Pv)$, specific internal energy, Δu, kinetic

energy, $\Delta(v^2/2)$, and potential energy, $\Delta(gz)$ [39]. Considering both heat, q, and work, w, per mass unit, added to the system, the energy balance results as follows in Eq. (2.20):

$$\Delta\theta = P_{in}v_{in} + u_{in} + \frac{v_{in}^2}{2} + gz_{in} + q + w = P_{out}v_{out} + u_{out} + \frac{v_{out}^2}{2} + gz_{out} \quad (2.20)$$

One of the thermodynamic potentials, enthalpy, h, is by definition, a combination property used to characterize the state of a system (as it results from other state properties, as the internal energy, u, pressure, P, and specific volume, v):

$$h = u + P\,v \quad (2.21)$$

The energy balance expressed by Eq. (2.20) can be rewritten as:

$$h_{in} + \frac{v_{in}^2}{2} + gz_{in} + q + w = h_{out} + \frac{v_{out}^2}{2} + gz_{out} \quad (2.22)$$

Neglecting velocity (v) and heights (z) variations, respectively in kinetic and potential energy terms, the generic energy balance, results as:

$$h_{in} + q + w = h_{out} \quad (2.23)$$

Consider the refrigeration system in Figure 2.17a, whose components will be described, working in an ideal vapor-compression cycle (Figure 2.17b), to ease the explanation.

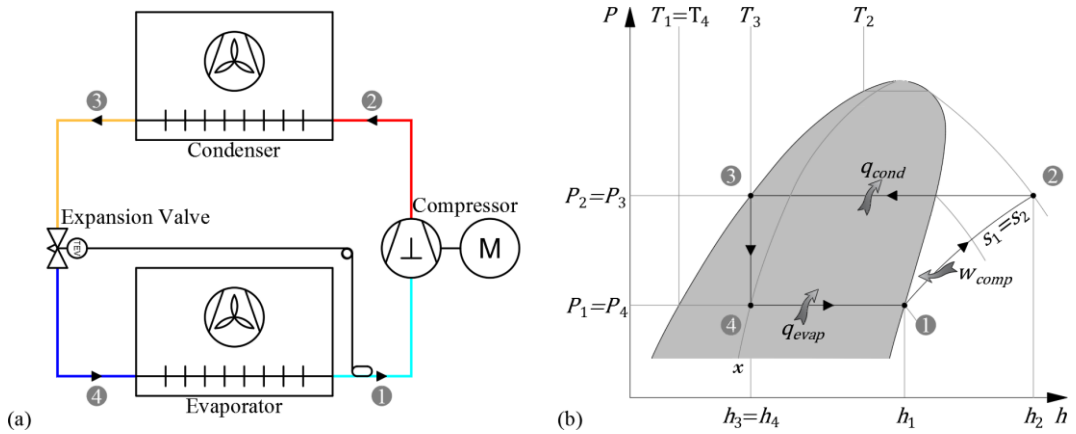

Figure 2.17: Single stage compression: (a) circuit and (b) ideal *P*-*h* diagram (source: author)

I. Evaporators

Evaporators are components of refrigeration systems "used to cool air, gases, liquids, and solids, condense volatile substances and freeze products" [34]. They are heat exchangers receiving low-pressure and -temperature fluid resulting from the expansion process, bringing it in close thermal contact with the load. From this load, and along the evaporator, the fluid absorbs its latent heat, ending this process as a dry gas [38].

In evaporators, as in heat exchangers in general, there is no mechanical energy involved. Thus, $w = 0$ and the energy balance is resumed to:

$$q = \Delta h = h_{out} - h_{in} \tag{2.24}$$

Using same the cycle numbering, shown in Figure 2.17, the quantity of heat absorbed in the evaporator, or the refrigeration effect, q_{evap}, [35], is as expressed in Eq. (2.25):

$$q_{evap} = \Delta h_{evap} = h_1 - h_4 \tag{2.25}$$

In ideal conditions, having saturated vapor at the evaporator outlet, it can be also obtained as a function of the quality of the biphasic mixture, x, (ratio of the mass of vapor to the total mass of a saturated mixture) and the latent heat of vaporization, c:

$$q_{evap} = (1 - x) \times h_{fg} \tag{2.26}$$

Finally, the refrigeration capacity, $\dot{Q}_{evap}$, can be defined as the heat transferred through the evaporator, from the load to the mass of refrigerant, per unit of time, (resulting as the refrigerant mass flow rate, $\dot{m}$, multiplied by the refrigeration effect):

$$\dot{Q}_{evap} = \dot{m} \times q_{evap} = \dot{m} \times (h_1 - h_4) \tag{2.27}$$

Notice that the correlation between Eq. (2.25) and Eq. (2.26) can be extremely useful to obtain the corresponding value of point ④ (Figure 2.18a), s_4, in the T-s diagram (Figure 2.18b), or any other property for that point. Quality results as the distance ratio $\overline{f4}/\overline{fg}$ on the P-h or T-s diagram, Figure 2.18 (with subscript f and g for saturated liquid and saturated vapor properties, respectively, and subscript fg for the total vaporization evolution): $x = 1 - (h_1 - h_4)/h_{fg} = \left(h_4 - h_f\right)/h_{fg} = \overline{f4}/\overline{fg}$. Therefore, the entropy value for point ④ can be obtained by $s_4 = s_f + x \times s_{fg}$.

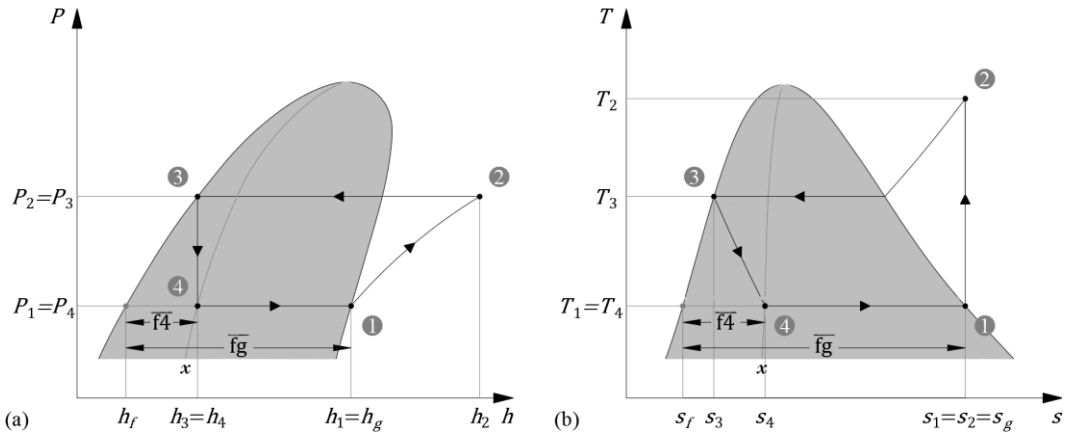

Figure 2.18: Quality relation to horizontal distances on (a) P-h and (b) T-s diagrams (source: author)

Consider now the cooling process of a fluid stream, with a mass flow rate $\dot{m}_{fs}$, represented in Figure 2.19a, and the corresponding temperature variation in Figure 2.19b. The fluid, whose constant-pressure specific heat is $\bar{c_p}$, enters at the evaporator with the initial temperature $T_{fs,in}$, and leaves it with the final temperature $T_{fs,out}$, while the refrigerant (subscript r) takes up its latent heat, keeping its temperature constant, T_{evap}.

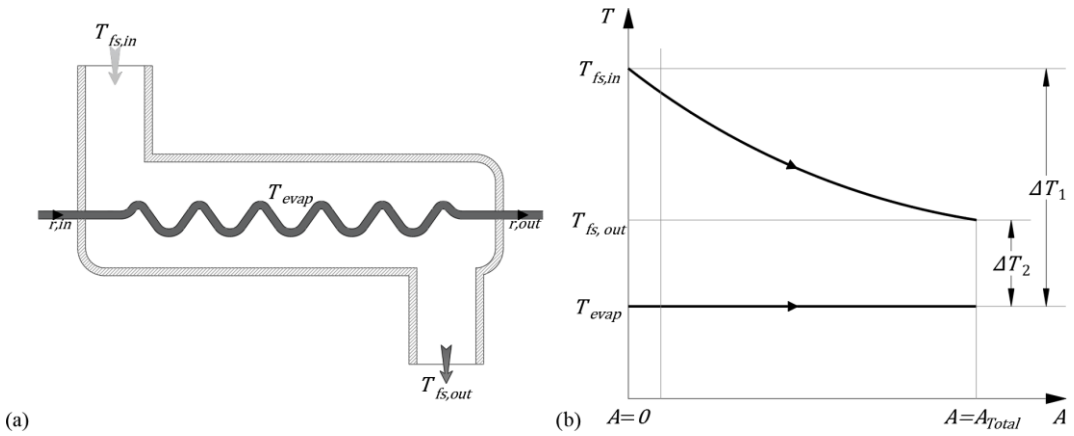

Figure 2.19: Evaporation process and temperature variation (source: adapted from (a) [45], (b) [37])

The heat-transfer rate between both (fluid stream and refrigerant) can be expressed as a function of the overall heat-transfer coefficient, U (considering the contribution of all individual heat-transfer coefficients), total heat-transfer area, A (contact area for each fluid side, include fins) and the logarithmic mean temperature difference, ΔT_{lm} or $LMTD$:

$$\dot{Q} = \dot{m}_{fs} \times \bar{c_p} \times \left(T_{fs,in} - T_{fs,out}\right) = U \times A \times \Delta T_{lm} \tag{2.28}$$

The logarithmic mean temperature difference, Eq. (2.33), is a function of the difference, ΔT, between the mean fluid stream temperature, T_m, and the refrigerant temperature, and of the differences between initial and final temperatures of the fluid stream, ΔT_1 and ΔT_2, and the refrigerant temperature, T_{evap}, as expressed from Eq. (2.29) to Eq. (2.32):

$$T_m = \frac{T_{fs,in} + T_{fs,out}}{2} \tag{2.29}$$

$$\Delta T = T_m - T_{evap} \tag{2.30}$$

$$DT1 \text{ or } \Delta T_1 = T_{fs,in} - T_{evap} \tag{2.31}$$

$$\Delta T_2 = T_{fs,out} - T_{evap} \tag{2.32}$$

$$LMTD \text{ or } \Delta T_{lm} = \frac{\Delta T_1 - \Delta T_2}{\ln \frac{\Delta T_1}{\Delta T_2}} = \frac{T_{fs,in} - T_{fs,out}}{\ln \frac{T_{fs,in} - T_{evap}}{T_{fs,out} - T_{evap}}} \tag{2.33}$$

The values of T_{evap} and ΔT are defined as characteristics of the evaporator [37]. However, for equipment selection, $DT1$ (ΔT_1) or $LMTD$ (ΔT_{lm}) are the major selecting parameters. Air temperature and humidity must be considered related to the final product, whenever air is the cooling medium. For these cases, it always exists a commitment between the dehydration sensitivity of the products, ΔT_1 (high values reduce size and coil costs) and T_{evap} (the lower it is, the lower it will be the compressor capacity and COP) [35], [38]. Due to the proximity of the air dew point and the fin surface of the evaporator, the inside air humidity is a function of $DT1$ (Figure 2.20), as the fin surface temperature falls down, more moisture will condensate, and so the lower will be the humidity [38]. Some guidance values for $DT1$ can be found in Table 2.1, according the humidity sensitivity [38].

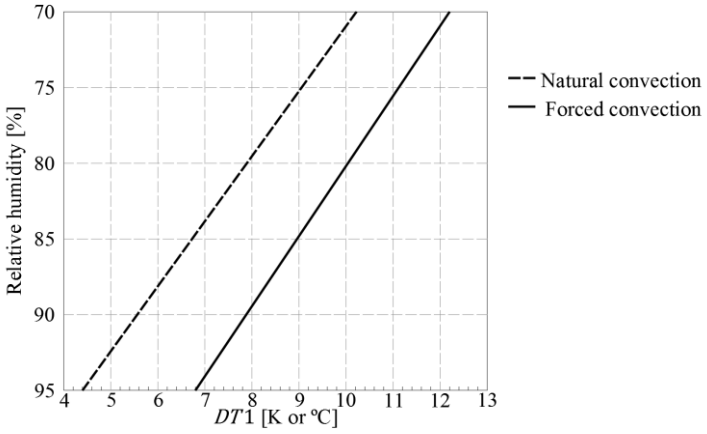

Figure 2.20: Relation between the relative humidity and $DT1$ (source: adapted from [37])

Table 2.1: Typical $DT1$ according to the humidity sensitivity (source: [38])

Humidity sensitivity	***DT*1 [K or °C]**
Products that dehydrate quickly, such as most fruits and vegetables	4
Products requiring about 85% saturated air	6
Products requiring 80% saturation or drier	8
Products not sensitive to dehydration	≥ 10

Other authors present same parameter as a function of the evaporator type ([37], [41]), Table 2.2, or according the application and humidity ([34], [35]), Table 2.3 and Table 2.4:

Table 2.2: Typical $DT1$ according to the evaporator type (sources: [37], [41])

Type of evaporator		***DT*1 [K or °C]**
Direct-expansion		8 to 12
Forced convection air		8
Immersion:	Water medium, without ice formation	5.5 to 8
	Water medium, with slight ice layer formation	8 to 12
	Refrigerant medium (except water or brine)	4.5 to 5.5

Table 2.3: Typical $DT1$ according to the type of application and humidity level I (source: [34])

Type of application		***DT*1 [K or °C]**
Medium-temperature applications above -4 °C:	Medium relative humidity (approximately 70 %)	9 to 7
	High relative humidity (approximately 80 %)	6 to 7
	Very high relative humidity (about 90 %)	4 to 5
Packaged products and workrooms		14 to 16
Paper storage or similar products (low humidity level)		11 to 16
Low-temperature applications below -4 °C		< 8

Table 2.4: Typical $DT1$ according to the type of application and humidity level II (source: [35])

Type of application		***DT*1 [K or °C]**
Below freezing:	Storage and blast freezing	5.5 to 6.5
Above freezing:	Low humidity	11 to 17
	High humidity	2.2 to 4.4

Evaporators can be classified according to their function (regarding the cooling medium), construction type and by the techniques for feeding refrigerant. Starting with functionality, they are divided in (1) air-coils and (2) liquid-cooling chillers.

In air-coils, the air stream is cooled by the refrigerant that flows inside finned tubes (Figure 2.21a), and the refrigerant supply method is inevitably by direct-expansion [38].

Direct-expansion evaporators (Figure 2.21) have a continuous flow through the heat exchanger, and the expansion valve regulation is done so that all the liquid is fully vaporized and slightly superheated (also termed "dry-expansion"), from 4 to 7 °C [35]. It is commonly used with halocarbon refrigerants, for moderate refrigerating temperatures, but for ammonia systems and low-temperature applications (suction temperatures below –18 °C [34]), its use is limited [35].

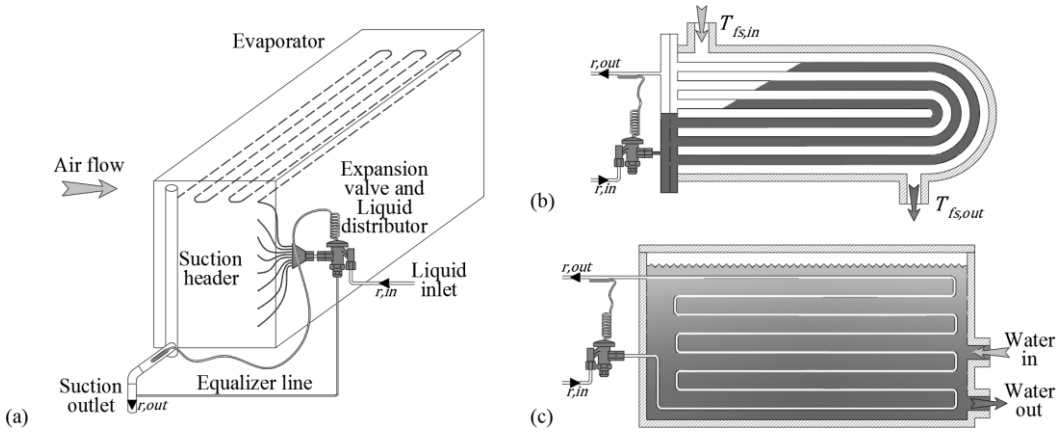

Figure 2.21: Direct-expansion evaporators: (a) air coil, (b) liquid cooler and (c) immersion tank (source: adapted from (a) [34], (b) [45], (c) [38])

Liquid-cooling chillers may have many configurations such as [38]: (1) immersion tank evaporators (with conventional or herringbone coils, totally immerged in the liquid); (2) shell-and-tube evaporators (liquid in pipes, shell ¾ full of liquid-boiling refrigerant); (3) shell-and-coil evaporators (water in the baffled shell and refrigerant inside the coil); (4) spray chillers (spray nozzles assure an evaporating liquid film over water or brine pipes, using much less refrigerating charge than conventional flooded evaporator); (5) brazed plate heat exchangers, BPHX, (widely used in current refrigeration systems, but only for small applications, once it has approximately two liters of refrigerant for each square meter of cooling area, (2 $L.m^{-2}$), which is ten times lower than multi-tube design); (6) plate-and-shell heat exchangers (for larger installations, similar principle to BPHX); (7) plate freezers (horizontal or vertical types, used to direct contact product freezing); and (8) Baudelot coolers (used when the water is close to its freezing point). Refrigerant supply method can be either by direct-expansion or flooded [38].

The flooded feed method is desirable for small temperature differences between the fluid and the refrigerant, $DT1$, and for low-temperature applications [34]. It is based on the liquid refrigerant circulation, through the evaporator (by gravity and a thermosiphon effect - Figure 2.22, or by forced convection, using a pump - also called "liquid recirculation" or "liquid-overfeed" method - Figure 2.23a), in a higher quantity than that it can evaporate [35]. The refrigerant is retained in a low-pressure receiver (surge drum or separating vessel), where it evaporates or is taken to individual coolers, returning as a liquid-vapor mixture [38]. The level of refrigerant is usually controlled by a high- or low-pressure valve, admitting the liquid refrigerant to replace the amount vaporized [35].

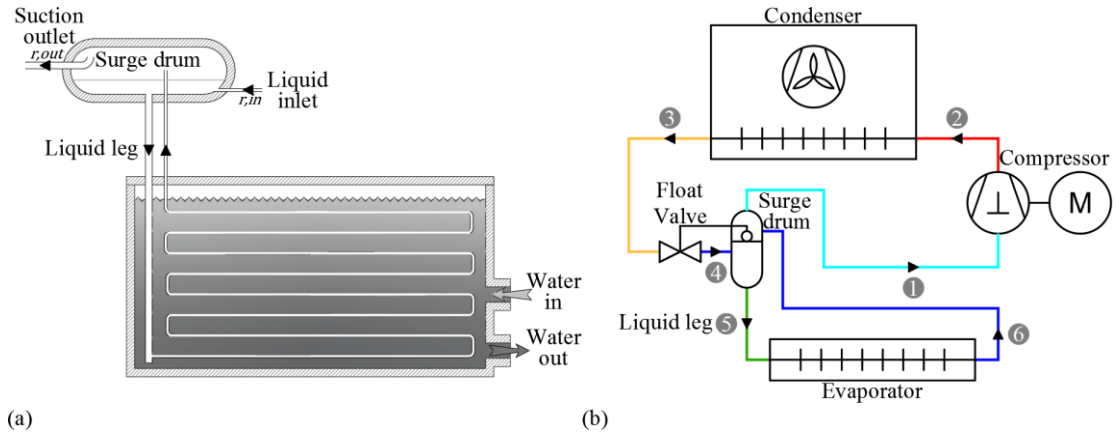

Figure 2.22: Flooded evaporators: (a) scheme and (b) circuit (source:(a) adapted from [38], (b) author)

In forced convection (liquid-overfeed) method, commonly used in ammonia systems due to its high efficiency, the high-pressure refrigerant flashes into a low pressure receiver, from which is pumped to the evaporators at an overfeed rate of 2.5 to 1 to 4 to 1 [34]. The circulating number or rate, n_{cir}, is defined as the mass ratio of (total) liquid circulated to the liquid vaporized ($n_{cir} = \dot{m}_{tot}/\dot{m}_{vap}$), and the overfeed rate, n_{ovf}, as the ratio of liquid to vapor returning to the low-pressure receiver ($n_{ovf} = \dot{m}_{liq}/\dot{m}_{vap}$) [34]. Each evaporator has an optimum circulating rate for every loading condition, giving the minimum difference and best evaporator efficiency, and this rate can also vary with the pipe diameter, circuit length and the number of parallel circuits [34]. As predicting ideal circulating rates or designing plants for automatic rate adjustment are practically impossible tasks, recommended circulation rates are frequently specified by evaporator manufactures, for their equipment [34]. The values shown in Table 2.5 are complying those recommendations. Figure 2.23b illustrates the influence of quality, x, in the position of point 6, at the *P-h* diagram (dark hatched area means possible recommended locations of h_6, at the interval Δh_6), as below demonstrated, is a consequence of n_{cir} value.

Table 2.5: Recommended minimum circulating rate (source: [34])

Refrigerant		**Circulating rate, n_{cir}**
R-717 (ammonia):	Downfeed (large-diameter tubes)	6 to 7
	Upfeed (small-diameter tubes)	2 to 4
R-22:	Upfeed	3
R-134a		2

As the amount of liquid vaporized is based on the latent heat of the refrigerant at the evaporator temperature, circulation and overfeed rates can be related to the quality. Thus, being quality the ratio of the mass of vapor to the total mass of a saturated mixture, considering the same time interval, Δt, and $\dot{m}_{tot} = \dot{m}_{liq} + \dot{m}_{vap}$:

$$x = \frac{m_{vap}}{m_{tot}} = \frac{\dot{m}_{vap}}{\dot{m}_{tot}} \Leftrightarrow x = \frac{1}{n_{cir}} \tag{2.34}$$

$$n_{ovf} = \frac{\dot{m}_{liq}}{\dot{m}_{vap}} = \frac{\dot{m}_{tot}}{\dot{m}_{vap}} - 1 = \frac{1}{x} - 1 \Leftrightarrow x = \frac{1}{n_{ovf} + 1} \tag{2.35}$$

Finally, using the correlations previously mentioned, the enthalpy of point 6 is given as:

$$h_6 = h_f + x \times h_{fg} = h_f + \frac{1}{n_{cir}} \times h_{fg} \Leftrightarrow h_6 = h_5 + \frac{h_1 - h_5}{n_{cir}} \tag{2.36}$$

For liquid-overfeed evaporators, the refrigeration effect, q_{evap}, and the refrigeration capacity, $\dot{Q}_{evap}$, are respectively expressed by Eq. (2.37) and Eq. (2.38):

$$q_{evap} = h_6 - h_5 = \frac{h_1 - h_5}{n_{cir}} \tag{2.37}$$

$$\dot{Q}_{evap} = \dot{m}_{tot} \times q_{evap} = \dot{m}_5 \times \frac{h_1 - h_5}{n_{cir}} \tag{2.38}$$

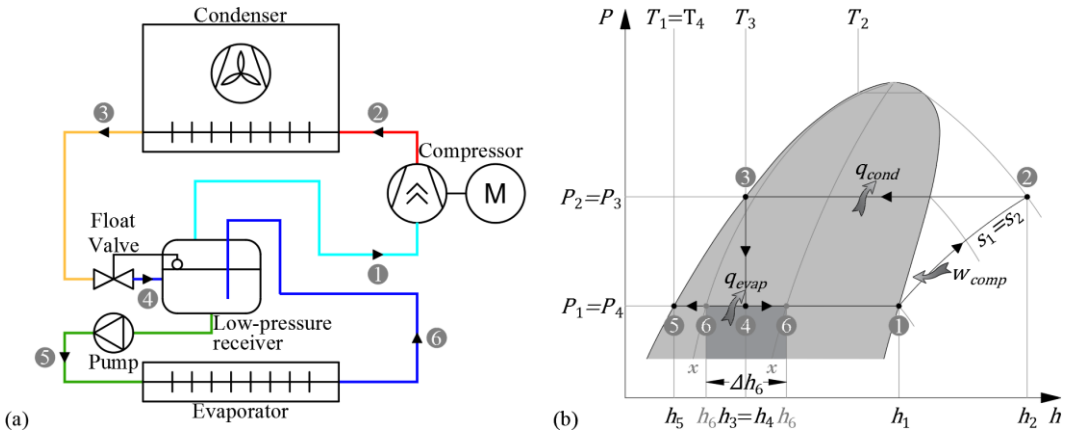

Figure 2.23: Flooded evaporators: (a) liquid-overfeed circuit and (b) P-h diagram (source: author)

The presence of the low-pressure receiver requires mass and energy balances, Eq. (2.39), (control volume along its surroundings, considering it having adiabatic boundaries) to determine the suction line mass flow rate, $\dot{m}_1$, which is not necessarily equal to $\dot{m}_{tot}$:

$$\begin{cases} \dot{m}_1 = \dot{m}_2 = \dot{m}_3 = \dot{m}_4 \\ \dot{m}_5 = \dot{m}_6 \\ \dot{m}_4 \times h_4 + \dot{m}_6 \times h_6 = \dot{m}_1 \times h_1 + \dot{m}_5 \times h_5 \end{cases} \tag{2.39}$$

Resulting as follows, Eq. (2.40):

$$\dot{m}_1 = \dot{m}_5 \times \frac{h_6 - h_5}{h_1 - h_4} = \dot{m}_5 \times \frac{q_{evap}}{h_1 - h_4} \tag{2.40}$$

When compared to the direct-expansion, flooded evaporators: (1) use more effectively the heat exchanging surface, because the internal tube surface is completely wetted; (2) have fewer severe problems in distributing refrigerant in parallel-circuit evaporators; and (3) induce lower discharge temperature in the compressor, as the entering suction gas temperature is also decreased, due to the entrance of saturated vapor instead of superheated vapor in the compressor. By opposition, direct-expansion evaporators:

(1) are less expensive and more feasible for small applications; (2) have less refrigerant charge; and (3) are not so complex nor require so much maintenance (flooded evaporators tend to accumulate oil in the surge, demanding a periodic or continuously oil removal [34], [35]. The initial costs for liquid-overfeed systems, compared to a gravity recirculated or flooded system, are more favorable the more evaporators used [34]. Liquid-overfeed major advantages are high system efficiency and low operating expenses, lower energy costs and fewer operating hours due to the [34]: (1) evaporating effectiveness (as aforesaid, heat exchanging surface is completely wet); (2) compressor protection (low-pressure receiver avoids liquid slugging in compressor); (3) lubrication and fouling prevention (lower discharge and condensing temperatures); (4) ease defrost of the evaporator (hot-gas defrosted with little disturbance to the system); (5) independency from environmental conditions (undisturbed by condensation conditions); (6) pressure drop decrease: flash vapor, resulting from refrigerant throttling losses, would not contribute to the pressure drop increase in the evaporator or overfeed lines, since it is directly deviated to the compressor, in the separating vessel; and (7) compressors longevity (less maintenance, fewer breakdowns) due to the ideal suction gas conditions; On the other hand, (1) uses large refrigerant charges than others; (2) need larger diameters in liquid feed and wet return pipes (higher refrigerant flow rate); (3) need more insulation to prevent condensation, frosting or heat gains (more expensive); (4) is not feasible for small installations (those with few than three evaporators); and (5) pumps require maintenance and the low available net positive suction pressure might cause cavitation problems.

Evaporators can also be classified into natural or forced convection, by draw- or blow-through arrangement of the fan and coil. All fan-coils normally operate below room dew-point conditions (below 3.3 °C [34]), enhancing frost formation around the coil, decreasing its heat-transfer efficiency (increase the heat exchange area and add another thermal resistance) or completely disabling its operation. For these cases, defrosting is necessary, and the method used is dependent on the air temperature, T_{air} (Table 2.6):

Table 2.6: Typical defrost methods according to the air temperature (source: [34], [38])

Defrost method	T_{air} **[°C]**
Stop refrigeration for a short period (if possible), allowing frost to melt out	≥ 4
Air, water, hot-gas or electric (electric resistances) defrost	≥ 2.2
Hot-gas or electric defrost	< 2.2

II. Condensers

Condensers are components used to reject the heat from the refrigeration system. They are exchangers receiving the hot, high-pressure gas resulting from the compression process, cooling it to remove, in first place, the superheat and then the latent heat, promoting the refrigerant condensation back to the liquid state, with a slight subcooling, in the majority of the cases [38]. As in evaporators (and heat exchangers in general), there is no mechanical energy involved, $w = 0$, however, contrarily to happen to those, heat is not added, but removed from the system, and the energy balance of Eq. (2.23) results as:

$$q = \Delta h = h_{in} - h_{out} \tag{2.41}$$

Using same the cycle numbering, shown in Figure 2.17 (p. 23), the amount of heat rejection at the condenser, q_{cond}, is as expressed in Eq. (2.42):

$$q_{cond} = \Delta h_{cond} = h_2 - h_3 \tag{2.42}$$

The heat-transfer rate rejection at condenser, (condenser capacity [35] or condenser load [38]), $\dot{Q}_{cond}$, can be defined as the heat transferred at the condenser, from the mass of refrigerant to the condensing medium, per unit of time:

$$\dot{Q}_{cond} = \dot{m} \times q_{cond} = \dot{m} \times (h_2 - h_3) \tag{2.43}$$

Plant size is normally characterized by the refrigeration capacity and it is translated to a condenser capacity through the condenser-to-evaporator heat rejection ratio, HRR [35]. This ratio (frequently used by manufacturers [38]), defines the heat rejected rate at the condenser as function of the refrigeration capacity, $\dot{Q}_{evap}$, and the compressor thermal equivalent power input, $\dot{W}_{in}$ [35] (Figure 2.24), neglecting other small gains/losses:

$$\dot{Q}_{cond} = \dot{Q}_{evap} + \dot{W}_{in} \tag{2.44}$$

$$HRR = \frac{\dot{Q}_{cond}}{\dot{Q}_{evap}} = \frac{\dot{Q}_{evap} + \dot{W}_{in}}{\dot{Q}_{evap}} \tag{2.45}$$

The HRR can also be defined as a function of evaporating and condensing temperatures (absolute temperatures, in [K], T_{evap} and T_{cond}), but is also influenced by the compressor type and additional or different cooling configurations [35]. The following expression, Eq. (2.46), empirically adjusted and derived from Carnot's correlations, and graphically represented in Figure 2.25, gives a reasonable approach for standard

configurations when the compressor data is not totally available [35]. It is valid for systems using ammonia or halocarbon refrigerants and open-type compressors [35].

$$HRR = \left(T_{cond}/T_{evap}\right)^{1.7} \tag{2.46}$$

The cooling method used on the compressor has a strong influence over the HRR, causing a variation over its values according to the type (*e.g.* small hermetic, oil-injected screw compressors, or reciprocating compressors using water-cooled head, *etc.*) [35], [38].

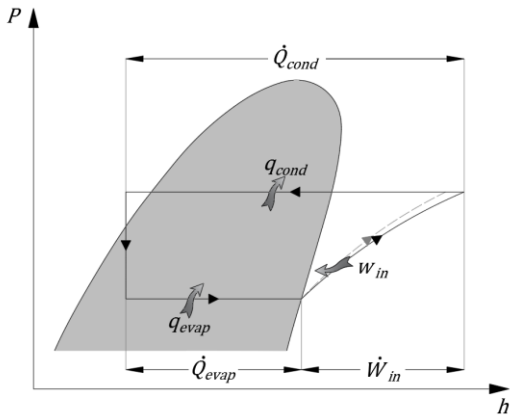

Figure 2.24: Relation between $\dot{Q}_{cond}$, $\dot{Q}_{evap}$ and $\dot{W}_{in}$ (source: author)

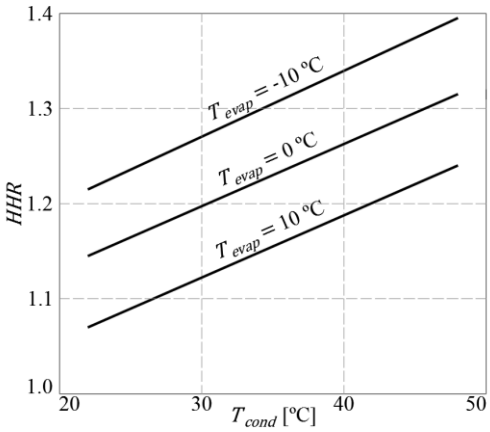

Figure 2.25: Typical values of HHR (source: adapted from [35])

Condensation process presents three distinguished phases, from the admission of the hot, high-pressure gas discharged by the compressor, until the ending subcooling stage. These phases are graphically represented in Figure 2.26, and described as follows [37]: (1) Desuperheating phase ❶: the hot-gas, proximally to the discharge conditions, is subjected to a sensible cooling, until it reaches the high pressure saturation temperature; (2) Condensation phase ❷: phase change at constant pressure, representing almost 90 % of the total heat exchange. The pressure drop in this stage should be 1.5 to 2 °C lower than the saturation pressure; and (3) Subcooling phase ❸: final sensible stage, and liquid-state refrigerant cooling due to the differences between saturation temperature, T_{cond}, and the incoming condensing agent flow stream temperature.

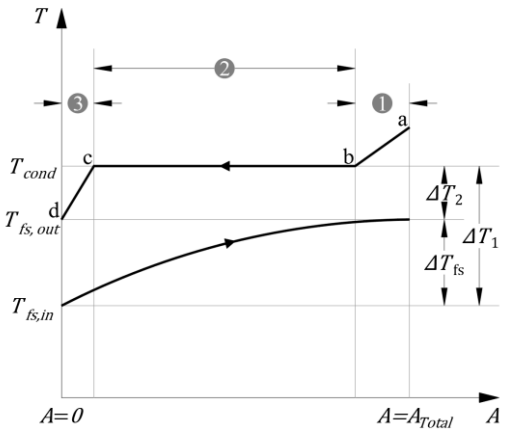

Figure 2.26: Phases of the condensation process (source: adapted from [37])

The cooling agent, usually water or air flow streams, undergoes a sensible heating, from its initial temperature, $T_{fs,in}$, until the final temperature at the condenser outlet, $T_{fs,out}$. Neglecting desuperheating and subcooling phases, due to the greater preponderance of pure condensation process over the total heat (latent heat is much higher than the sum of sensible heats from desuperheating and subcooling), as well as friction losses (promoting changes in the condensing temperature), the condenser heat-transfer rate is given by:

$$\dot{Q} = \dot{m}_{fs} \times \overline{c_p} \times \left(T_{fs,out} - T_{fs,in}\right) = U \times A \times \Delta T_{lm} \tag{2.47}$$

Where, analogously to was referred to the evaporators, ΔT_{lm} is the logarithmic mean temperature difference, and ΔT_1 and ΔT_2 are then related to the differences of the refrigerant temperature at the high pressure saturation conditions, T_{cond}, and respectively, the cooling agent fluid stream temperatures at condenser inlet, $T_{fs,in}$, and outlet, $T_{fs,out}$:

$$\Delta T_1 = T_{cond-}T_{fs,in} \tag{2.48}$$

$$\Delta T_2 = T_{cond} - T_{fs,out} \tag{2.49}$$

$$\Delta T_{fs} = T_{fs,out} - T_{fs,in} = \Delta T_1 - \Delta T_2 \tag{2.50}$$

$$LMTD \text{ or } \Delta T_{lm} = \frac{\Delta T_1 - \Delta T_2}{\ln\frac{\Delta T_1}{\Delta T_2}} = \frac{\Delta T_{fs}}{\ln\frac{\Delta T_1}{\Delta T_2}} = \frac{T_{fs,out} - T_{fs,in}}{\ln\frac{T_{cond} - T_{fs,in}}{T_{cond} - T_{fs,out}}} \tag{2.51}$$

Some values for the characteristic temperature differences of the condensers, ΔT_1, ΔT_2 and the temperature rise of the cooling agent, ΔT_{fs}, can be found in Table 2.7 ([38]), Table 2.8 ([46]) and Table 2.9 ([37]), according to the condenser type:

Table 2.7: Typical temperature differences according to condenser type I (source: [38])

Type of condenser		**ΔT_1 [K or °C]**	**ΔT_2 [K or °C]**	**ΔT_{fs} [K or °C]**
Air-cooled		15	-	9 to 12
Water-cooled:	Unlimited water flow: sea, river, *etc.*	-	-	5
	Limited flow, once through only	-	-	10 to 12
Evaporative		12 *[1]	-	-

*[1] Considering $T_{fs,in} = T_{wb,in}$ (wet bulb temperature of the incoming air)

Table 2.8: Typical temperature differences according to condenser type II (source: [46])

Type of condenser	**ΔT_1 [K or °C]**	**ΔT_2 [K or °C]**	**ΔT_{fs} [K or °C]**
Air-cooled	-	7 to 8	5 to 6
Water-cooled	-	5	5 to 12
Evaporative or atmospheric	-	10 to 12 *[2]	-

*[2] Considering $T_{fs,out} = T_{wb,out}$ (wet bulb temperature of the outgoing air)

Table 2.9: Typical temperature differences according to condenser type III (source: [37])

Type of condenser		**ΔT_1 [K or °C]**	**ΔT_2 [K or °C]**	**ΔT_{fs} [K or °C]**
Air-cooled:	Natural convection	15	8 to 10	10 to 15
	Force convection	15		
Water-cooled:	Tube-in-tube (or double pipe)	-	3 to 5	5 to 7, or to 10
	Shell-and-tube	10		5, or 5 to 10
Evaporative:	(optimal air velocity: 3 to 5 m.s^{-1})	8 to 10 *3	-	-

*3 Considering $T_{fs,in} = T_{wb,in}$ (wet bulb temperature of the incoming air)

Regarding general and industrial refrigeration systems, condensers have three main types: (1) Air-cooled (Figure 2.27); (2) Water-cooled (Figure 2.28); and (3) Evaporative [35] or regarding the cooling agent, Air-Water (Figure 2.29 and Figure 2.30) [37], [46]. Another type, the dry cooler, has similar construction to air-cooled condensers, with a sealed water system, dismissing water treatment and eliminating related hazards, but with some limitations or drawbacks [38]. Fluctuations in condensing temperature and pressure, as well as in the outside air temperature, might reduce the system performance or cause malfunctions [46], such as: (1) unsatisfactory defrost due to extremely low defrost-gas pressure; (2) inadequate pressure to guarantee a suitable flow rate of liquid into the compressor, when using oil-cooled screw compressors with direct injection of refrigerant; (3) inadequate feed of level control or expansion valves [35]. These phenomena occur especially during the "winter operation", in which both condensing and cooling medium temperatures fall, requiring means (control capacity) to ensure a functional, but lower-as-possible (reducing the consumption) condensing pressure level [38]. Further lowering of the condensing temperature, to reduce the compressor consumption, might be less than the possible saves in pumps and fan motors of the condensers. [35]. Reducing or cycling air or spray-water flows are two main methods of reducing the condenser capacity [35].

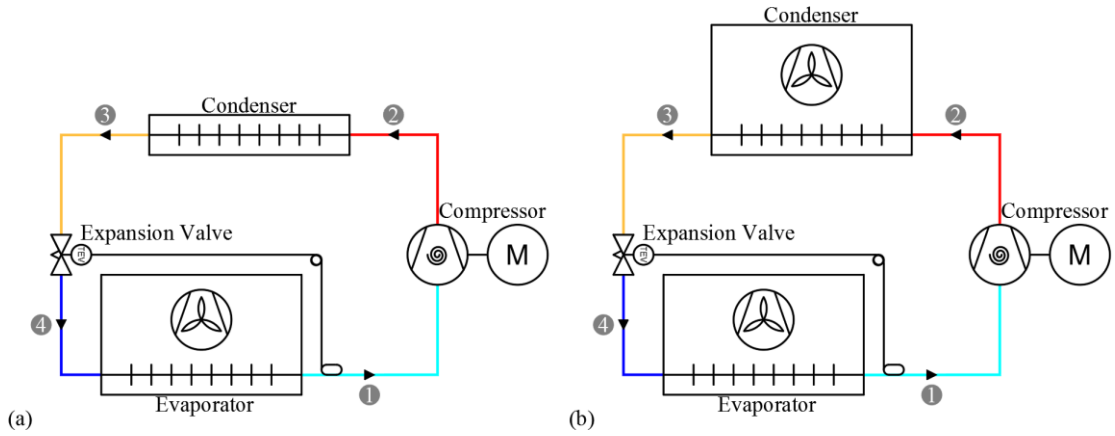

Figure 2.27: Air-cooled condensers: (a) natural- and (b) forced-convection (source: author)

When air is the cooling agent, the air flow over the condenser can be classified as (1) natural convection, for small retail units or domestic refrigerators and freezers; and (2) forced convection, using propellers or axial fans (normally single-stage fan) to remove the heat rejected by the condenser, blowing over the plate finned tubes, which outside to inside surface ratio is between 5 to 1 and 10 to 1 [38]. Air-cooled is the costless condenser type: the lowest acquisition and maintenance costs (no water circulates or evaporates) [35]. The preference given to its use, relatively to water-cooled condensers, is due to the deficit of water resources and environmental protection, but require a higher condensation pressure and have higher noise levels [37]. Regarding the capacity control, it can be achieved by taking off line parallel-mounted condensers, switching off fans or by varying the fan motor speed (two-speed or other variable speed control: e.g. variable-frequency drive) according to the condensing temperature [38], [46]. Other possibilities are: (1) control the refrigerant flow using a thermostatic expansion valve [46]; or (2) flood the condenser, reducing the available condensation heat-transfer area, using a by-pass valve fitted across the condenser, and discharging the hot-gas directly to the receiver [38]. From Eq. (2.47), the ratio of air mass flow to the condensing capacity, is:

$$\frac{\dot{m}_{fs}}{\dot{Q}} = \frac{\dot{m}_{fs}}{U \times A \times \Delta T_{lm}} = \frac{1}{\overline{c_p} \times \left(T_{fs,out} - T_{fs,in}\right)} = \frac{1}{\overline{c_p} \times \Delta T_{fs}} \tag{2.52}$$

This ratio is extremely useful for the comparison of the characteristics for the different condensers types (flow rates of different cooling agents, heat exchange areas, *etc.*). Considering the outdoor air temperature, $T_{fs,in}$, between 25 and 45 °C (and a moister content of 10×10^{-3} kg.kg^{-1}), an air temperature rise, $\Delta T_{fs} = 9.5$ K (mean value, coherent with those presented in Table 2.8 to Table 2.9) and a mean specific heat capacity $\overline{c_p} = 1.02$ kJ.kg^{-1}.K^{-1}, the ratio results as 0.103 kg.s^{-1}.kW^{-1} (0.091 m^3.s^{-1}.kW^{-1}).

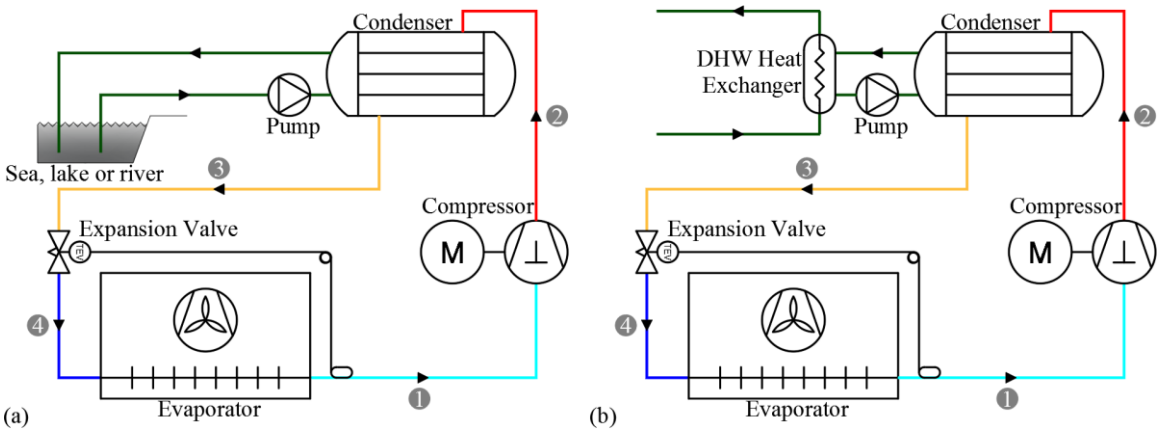

Figure 2.28: Water-cooled condensers: (a) unlimited flow and (b) limited flow (source: author)

The water thermal properties (high heat capacity and density) make it an ideal medium for condensation [38]. Shell-and-tube type is one of the most used in refrigeration systems [35], [46], particularly for medium and high capacity facilities [37], but other types, such as tube-in-tube or plate-type condensers (namely BPHX), particularly in low capacity systems [38], plate-and-frame, shell-and-coil, water cascading or sprayed over plate or coil serpentine models [35]. The condenser capacity can be controlled by throttling, or three-way valves; diverting valves can be used to take off line a complete condenser [38]. Considering the inlet water temperature, $T_{fs,in} = 20$ °C, a temperature rise, $\Delta T_{fs} = 11$ K (mean value), and a mean specific heat capacity $\overline{c_p} = 4.13$ kJ.kg^{-1}.K^{-1}, the ratio of water flow rate to condensing capacity is 0.022 kg.s^{-1}.kW^{-1} (0.022 × 10^{-3}m^3.s^{-1}.kW^{-1}).

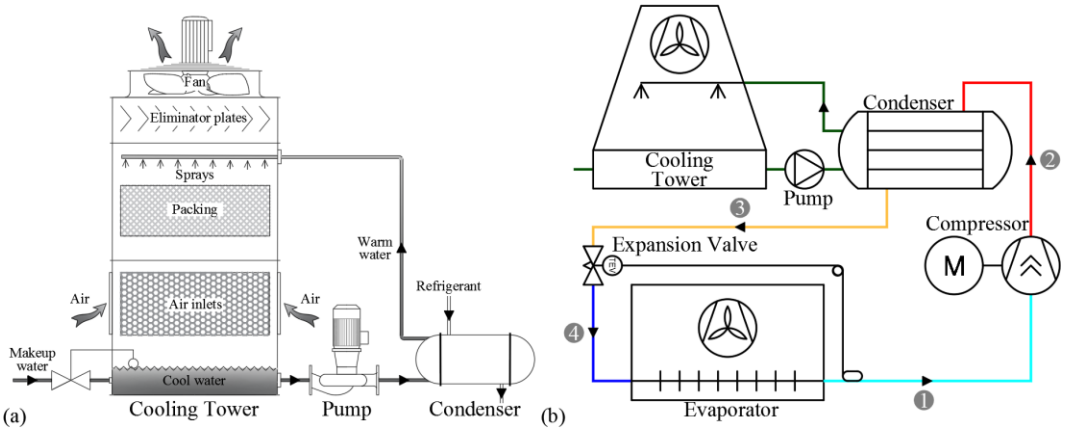

Figure 2.29: Cooling tower: (a) scheme and (b) circuit (source: author)

Air-Water cooled type is divided in (1) indirect or cooling towers; and (2) direct or evaporative condensers [37]. The major difference relies on the heat-transfer process: (1) in the indirect type (Figure 2.29), circulating cooling water removes heat from the condenser (water-cooled condenser), and once warmed, it is sprayed on the top the cooling tower, falling in the upgoing air stream, and evaporating while passing over the packing [38], which increases not only the heat exchange surface, but also increases the contact period between both streams, in a heat and mass transfer process [37]; (2) in the direct type (Figure 2.30), the heat transfer has two stages: a sensible heat transfer from the interior of the condensing coil to the involving water layer around the tubes (water acting as heat-transfer medium [38]), and a heat and mass transfer process (water acting as a coolant [38]), such as that occurring for the indirect type [37]. This happens due to the direct application of the water over the condenser coil, in such a flow ensuring the complete wetting of the tube surface, enhancing the efficiency of heat rejection [38].

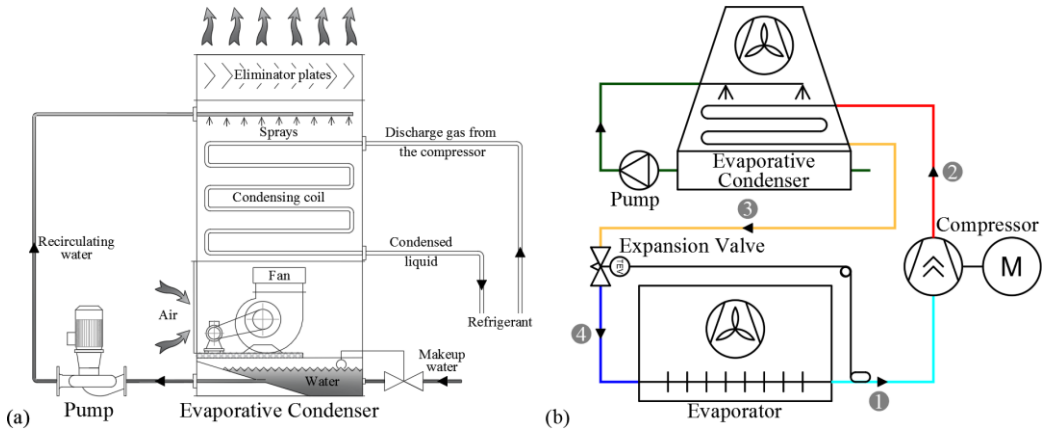

Figure 2.30: Evaporative condenser: (a) scheme and (b) circuit (source: author)

In the indirect type, the total tower duty is provided by latent heat taken up by the water evaporation, h_{fg} [38]. Thus, the ratio of evaporated water to the condensing capacity, is:

$$\frac{\dot{m}_{\mathrm{v}}}{\dot{Q}} = \frac{1}{h_{fg}} \tag{2.53}$$

Assuming the same outdoor air temperature considered previously, $T_{db,in} = 35$ °C (dry bulb), the same moister content of 10×10^{-3} kg.kg^{-1}, resulting in a wet bulb temperature, $T_{wb,in} = 20.9$ °C, and considering the cooled water leaving the tower 3 to 8 K warmer than the incoming air wet bulb ($T_{wb,in}$) [38], $T_{w,out} = 25.9$ °C and the water latent heat of vaporization at 25.9 °C, $h_{fg} = 2439.6$ kJ.kg^{-1}, the ratio of evaporated water flow rate to condensing capacity is 0.410×10^{-3} kg.s^{-1}.kW^{-1} (0.411×10^{-6} m^3.s^{-1}.kW^{-1}). Although the range of temperature differences between $T_{w,out}$ and $T_{wb,in}$ proposed by Hundy *et al.* [38], it is quite common, in catalog data of counter flow cooling towers, to approach the leaving water temperature to the wet-bulb temperature of entering air [35].

The complexity of the overall heat-transfer process occurring in evaporative condensers, entails the use of ratings determined from tests performed on complete condensers [38]. The ratio of the evaporation rate to condensing capacity is the same as described for cooling towers: 0.410×10^{-3} kg.s^{-1}.kW^{-1} (0.411×10^{-6} m^3.s^{-1}.kW^{-1}), the recommended water circulation rate varies between 80 to 160 times the quantity evaporated (respectively for $\Delta T = T_{w,out} - T_{wb,in} = 7.1$ and 3.6 K) resulting an interval from 0.033 to 0.066 kg.s^{-1}.kW^{-1} (0.029 to 0.058 m^3.s^{-1}.kW^{-1}), and an average value of 0.06 kg.s^{-1}.kW^{-1} (0.053 m^3.s^{-1}.kW^{-1}) is indicated for the ratio of mass air flow to the condensing capacity [38]. From this indicators is noticeable the proximity of the water and air mass flow rates operating in evaporative condenser. Another ratings are presented

more detailed, and most of them also related to the heat rejection capacity [35]: (1) heat-transfer area of 0.25 $m^2.kW^{-1}$; (2) air volume flow rate of 0.03 $m^3.s^{-1}.kW^{-1}$; (3) air pressure drop through the condenser (coils, plates, etc.) between 250 and 375 Pa; (4) rate of evaporated water of about 1.5 $L.hr^{-1}.kW^{-1}$ (0.418×10^{-6} $m^3.s^{-1}.kW^{-1}$); and (5) spray water circulating rate of 0.018 $L.s^{-1}.kW^{-1}$ (0.018×10^{-3} $m^3.s^{-1}.kW^{-1}$ or around 43 times the quantity evaporated) or up to 4.1 $L.s^{-1}.m^{-2}$ (4.1×10^{-3} $m^3.s^{-1}.kW^{-1}$).

Cooling towers: (1) operate with a lower condensing temperature, once the heat-transfer process occurs at wet-bulb rather than dry-bulb temperature, comparing to air-cooled evaporators, resulting in lower condensation temperatures, therefore, less consumption; (2) demands less refrigerant charge and have fewer friction losses in the refrigerant side, when the heat rejection point is far away from the compressors, sending water instead of refrigerant to the cooling tower (contrarily to evaporative or air-cooled condensers) [35]; (3) waste less water than water-cooled (once-through-only) and evaporative condensers. On its side, evaporative condensers are more compact and provide lower condensing temperatures than air-cooled condensers and also lower than cooling towers. Because of it, is widely used in industrial refrigeration, since low condensing temperatures moderate the compression discharge temperature (particularly important for ammonia applications), and consequently, reduce the energy consumption in the compression [35].

Some common disadvantages shared with evaporative condensers and cooling towers are: (1) the inevitably link with legionella, needing constant vigilance and water analysis [38]; (2) the costly water treatment, due to salts deposition and concentration increase [38]; (3) the risk of the spray water freezing, for outdoor temperatures fall to near or below freezing. This problem can be avoided locating the sump in a warm area, using sump water heaters, or shifting the condenser to a dry operation, stop water recirculation and drain the sump [35].

The last is also used as a capacity control measure, owing to the significantly reduction of the heat-transfer capacity under dry operation [35]. Besides the dry operation, other capacity control methods (to control the condensing pressure) can be used evaporative condensers [34]: (1) cycle the spray pump motor; (2) cycle both fan and spray pump motors; (3) throttle the spray water; (4) bypass air around duct and dampers; (5) throttle air via dampers, on either inlet or discharge; and (6) a combinations of five these methods.

Cooling towers and evaporative condensers can either be (1) forced draught or (2) induced

draught. While cooling towers are mainly induced (Figure 2.29a), using axial flow fans, evaporative coolers are predominantly forced draught type, using centrifugal fans (Figure 2.30a) or axial flow fans [35], [38]. Natural air draught evaporative condensers can also be found, being simplified versions of the evaporative type [38]; constructively, the atmospheric condenser, can have a parallel flow or counter flow (partially, for the Lebrun type, or totally, for the Block type [46]) configuration. This type of condenser should be mounted in airy areas (to ensure a functional air flow). It has a low overall heat transfer coefficient, its heat-transfer efficiency decays with the growth of the humidity outdoor conditions [46], and it is extremely bulky, (about 0.2 $m^2.kW^{-1}$ [38]).

III. Compressors

Compressors are the components of the vapor-compression cycle, responsible for the working-fluid motion generation, carrying it over all the refrigeration system. It is considered, therefore, the "heart" of the vapor-compression refrigeration system [37]. The compressor has two basic functions: (1) suction of \the low-pressure dry gas coming from the evaporator, removing it and avoiding its accumulating, which would increase the evaporating pressure and consequently, the corresponding temperature; and (2) the compression function, raising the low-pressure dry gas pressure to a level in which it can condensate, in an economical way, through an external cooling agent [37], [38].

Considering an adiabatic compressor, where there is no heat transfer during the compression, $q = 0$, and the energy balance from Eq. (2.23) is resumed to:

$$w = h_{out} - h_{in} \tag{2.54}$$

Once more, using same the numbering, shown in Figure 2.17 (p. 23), the amount of work done on the system, or the ideal work of compression [35], w_{comp}, is given by Eq. (2.55):

$$w_{ideal} = \Delta h_{ideal} = h_2 - h_1 \tag{2.55}$$

Finally, the power required, if the compression is adiabatic and frictionless, $\dot{W}_{ideal}$, is the result of the refrigerant mass flow rate, $\dot{m}$, multiplied by the ideal work of compression:

$$\dot{W}_{ideal} = \dot{m} \times w_{ideal} = \dot{m} \times (h_2 - h_1) \tag{2.56}$$

Regarding the method to obtain the compression effect, compressors can be divided in two groups: (1) volumetric or positive displacement, where the confined discrete volume of low pressure gas is mechanically reduced, causing a pressure increase; and

(2) dynamic, in which, the pressure rise is obtained by increasing the velocity of the low-pressure gas and afterwards, reducing it in a diffuser, transforming kinetical energy into a pressure rise [37], [38]. The different compressor types are may be found in Figure 2.31:

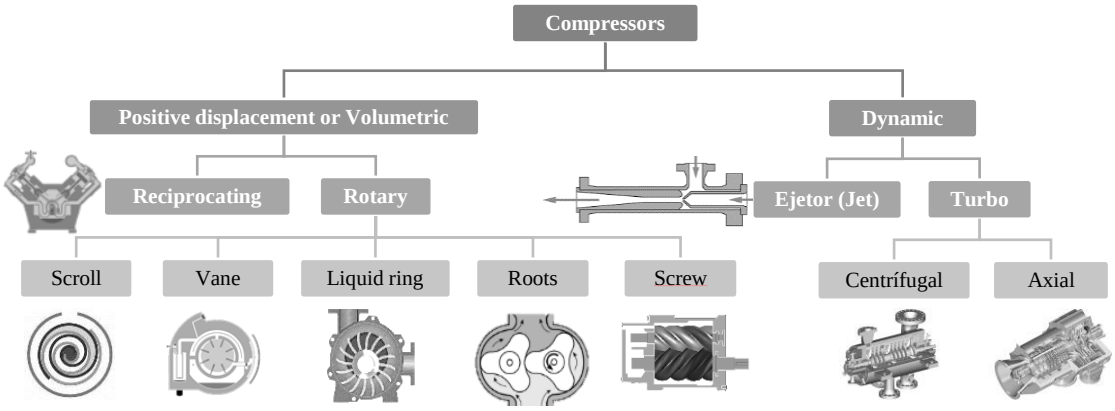

Figure 2.31: Compressor types (source: author)

In industrial refrigeration systems, the most-used types are screw and reciprocating (Figure 2.32), but also centrifugal (restricted to large-capacity chemical and process industry plants, or used in water chillers for HVAC applications) [35], [41]. Although the high-volume capacity of the rotary-vane compressor, suited for low-stage compression, it has been replaced by, the also-rotary, screw compressor [34], [35]. In recent years, scroll compressors (whose representing circuit symbols can be found in Figure 2.27) have been occupying a prominent place in HVAC equipment, due to their singular advantages [38], but are still not available in the normal sizes used in the industrial refrigeration [35].

Reciprocating compressors (Figure 2.32a) are the most common compressors applied in small (up to 75 kW) single-stage or multistage systems [34], although having an applicability range from 0.25 kW to 1000 kW [38]. They are adaptable in size, speed, drive method and number of cylinders, having two to four cylinders for small and simpler systems, whereas four- to eight-cylinder machines are usual in medium size systems [38]. A wide rage capacity can be found, from two to sixteen cylinders, mounted in “V”, “W” or “VV” configurations [37]. Their characteristic longitudinal movements, pressurize the enclosed gas by the reduction of its volume, and working in a two-stroke cycle, as shown in Figure 2.11, p. 20: (1) the pressure-actuated suction valve opens during the suction stroke, admitting gas coming from the evaporator and closing at the bottom of the stroke; (2) once reached the bottom dead center, it begins the compression stroke, and the discharge valve will open as soon as the cylinder pressure becomes higher than the discharge pressure, allowing the passage of the compressed gas to the condenser;

(3) owed to gas left in the clearance on the top of the stoke, the suction valve will only open again after the re-expansion of trapped gas, when the cylinder pressure is lower than the suction pressure [38]. Obviously, the largest the clearance volume is, the further the piston has to travel without admitting gas, and therefore, the higher the losses are [38].

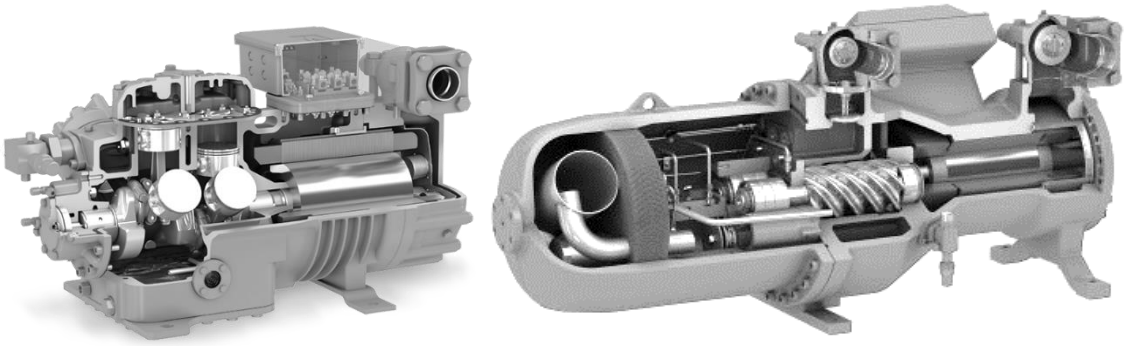

(a) (b)

Figure 2.32: Compressors: (a) reciprocating and (b) screw (source: Bitzer)

Constructively, the reciprocating compressors can be classified in: (1) open type, having a shaft extended out of the compressor and externally connected to driving motor, avoiding to superheat the gas before entering the cylinder, but increasing the risk of refrigerant leakage through the shaft coupling the motor and compressor [37]. The open-type is used in ammonia systems, since this refrigerant reacts, attacking the cooper windings of the motor (such does not happens with halocarbon refrigerants) [35], [38]; (2) enclosed type, which, by its turn, can be divided in: (2a) hermetically sealed, or simply fully hermetic, used for small appliances, such as domestic refrigerators and freezers, small air-conditioning equipment, and it has a completely welded shell, incapacitating its repair or maintenance, but assuring several years running with no leaks of refrigerant [38]. They have no lubrication pump system, since the lubrication is done by oil splashing over the moving parts [37]. In this type of compressors, the low-pressure and temperature gas, arising from the evaporator cools down the windings of the motor, spanning the motor service life, due to a non-useful heat gain (Figure 2.33). It cannot be used with ammonia or any other cooper-reacting refrigerant [37], [38]. As it

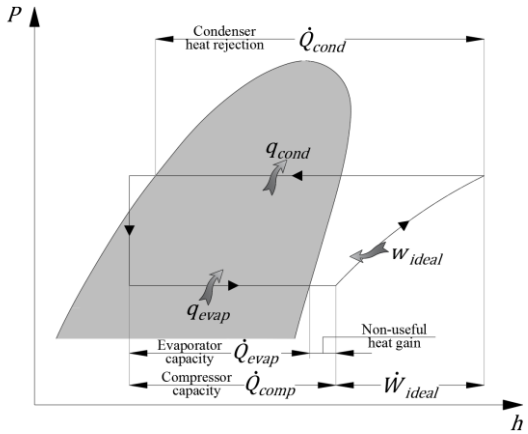

Figure 2.33: Compressor and evaporator capacities (source: adapted from [38])

is generally registered, almost 20 % of the compression capacity is lost, due to the raise of the gas temperature in the suction line, which can be reduced by the improvement of the insulation, mounting the compressor near to the evaporator, or using an LSHX [38]; (2a) semi-hermetic or accessible hermetic (Figure 2.32a) is similar to the fully hermetic compressor type, with exception to for the shell involving both the motor and compressor, which is accessible from the outside for maintenance and repair [37]. It is normally limited to a maximum refrigeration capacity of about 150 kW [35]. The motor windings are cooled by suction gases, by forced convection air flow or water jackets [38].

Cooling equipment is essential for the compressor protection, not only for the cylinder heads (refrigerants having high discharge temperatures demands water-cooled, such as ammonia), but also for oil coolers (which may also be water, air or refrigerant cooled), avoiding the risk of the oil or refrigerant decomposition [38]. Regarding suction and discharge pipe sizing, suction lines should have a total friction pressure drop in the range of 0.5 to 1.5 K equivalent (0.01 K.m^{-1}), and discharge lines between 7 and 15 kPa [34]. The range of pressure ratio, $r_P = \frac{P_{disc}}{P_{suct}}$, Eq. (2.17), is typically between 2.5 and 8 or 9 [35], and the volumetric efficiency, η_v, Eq. (2.15), can be estimated as a function that ratio, according to the empirical formula, valid for new compressors, $\eta_v = 1 - 0.05 \times r_P$ [42].

Besides the power requirement, the refrigerating capacity of the compressor is a key element for its characterization [35]. The compressor refrigerating capacity, $\dot{Q}_{comp}$, is proportional to the refrigeration effect, q_{evap}, and the refrigerant mass flow rate, $\dot{m}$, [37], being equal to the refrigeration capacity, $\dot{Q}_{evap}$, or not, if the non-useful heat gain is not negligible (Figure 2.33), and then $\dot{Q}_{comp} = \dot{Q}_{evap}$ + non-useful heat gain. It can also be defined as the capacity to compress the refrigerant flow rate from its suction pressure to its discharge pressure, providing a specified heat-transfer rate at the evaporator [35], and is given by Eq. (2.57), *where* $\dot{V}$ is the volume rate entering the compressor, $h_1 - h_4$ stands for the refrigeration effect (q_{evap}), $\dot{V}_d$ is the displacement rate, η_v is the volumetric efficiency, and v_1 is the specific volume of gas at the suction of the compressor:

$$\dot{Q}_{comp} = \dot{m} \times q_{evap} = \frac{\dot{V}}{v_1} \times (h_1 - h_4) = \frac{\dot{V}_d \times \eta_v}{v_1} \times (h_1 - h_4) \qquad (2.57)$$

This expression shows the influence of the evaporating temperature on refrigerating capacity, *i.e.*, when evaporating temperature drops, the specific volume increases,

decreasing both volume flow rate entering the compressor and the volumetric efficiency, causing a decline in the mass flow rate [35]. The decrease rate of the refrigerating capacity is around 4 and 9 % per °C, for high and low evaporating temperatures, respectively [35].

The capacity control of a multi-cylinder reciprocating compressor can be analyzed through the following expression, Eq. (2.58) [37], where D is the cylinder diameter, s is the stroke length (between top and bottom dead centers), z is th*e* number of cylinders, and N is the number of revolutions per minute (RPM) performed by the motor crankshaft:

$$\dot{Q}_{comp} = \dot{m} \times q_{evap} = \frac{\left(\pi \times \frac{\mathrm{D}^2}{4} \times \mathrm{s} \times \mathrm{z} \times \mathrm{N}\right) \times \eta_v}{v_1} \times (h_1 - h_4) \tag{2.58}$$

Therefore, the control capacity can be achieved by [37], [38], [47]: (1) block suction method (actuating over the "z" variable), it consists of taking cylinders out of service with blocked suction or the valve lifting mechanisms; it is an good energy-efficient control; (2) expansion of suction gas (actuating over "v_1" and "η_v"), reducing the suction pressure at the inlet of the compressor, and raising the specific volume and the volumetric efficiency; therefore, it is not a suitable control method, regarding the energy-efficiency; (3) control over the rotation speed (actuating over the "N" variable), using variable-frequency drives or electronic motors, varying the speed of synchronous motors by generating electrical waveforms of controllable frequency, commonly called inverters; (4) control the clearance volume (actuating over the "η_v"), connecting the cylinder to a variable-volume complementary cavity, varying the clearance volume and consequently having a stronger re-expansion, reducing the entrance of the low-pressure and temperature gas from the evaporator as well as the refrigeration capacity. It could be also: (5) on/off method, normally for low refrigeration capacity systems, through the actuation of the thermostat or, directly, by the low-pressure switch of the compressor; (6) discontinuous regulation, using the on-off strategy in a multi compressor system; and (7) external bypass method, using a valve between suction and discharge lines or across the inlet and outlet ports in the cylinder head; this method is extremely energy-inefficient.

Screw compressors (Figure 2.32b) are the most used above 75 kW, in both single- and multistage systems [34], and have an applicability range from that value to 6000 kW [38]. Belonging to the positive displacement type, similarly to the reciprocating compressors, compression process is obtained by reducing the volume occupied by the suction gas [37]. There are two major categories of this type of compressors: (1) twin screw and (2) single

screw, although the most usual configuration is the twin screw, having twin-meshing rotors on parallel shafts [38], with a male meshing lobe rotor (4 or 5 lobes) driving the female rotor (6 or 7 concave alveoli) [37]. Compression is processed by the engagement of both screws, in the flow direction, axial and circumferentially, completing the following steps [35], [37]: (1) suction and transport, while the rotors turn and the discharge port is kept closed, gas enters and occupies the space between two grooves, creating a pocket of gas; the dimension of the space grows longitudinally, on further rotation, until gas fills the complete extension of the rotor; at this moment the suction port is closed; (2) compression, the volume of the retained gas is progressively reduced by the screws engagement, as the chamber shrinks towards the discharge side, increasing the gas pressure; (3) discharge, the discharge port becomes uncovered allowing the complete expel of the compressed gas to the discharge line. These steps can be seen in Figure 2.34.

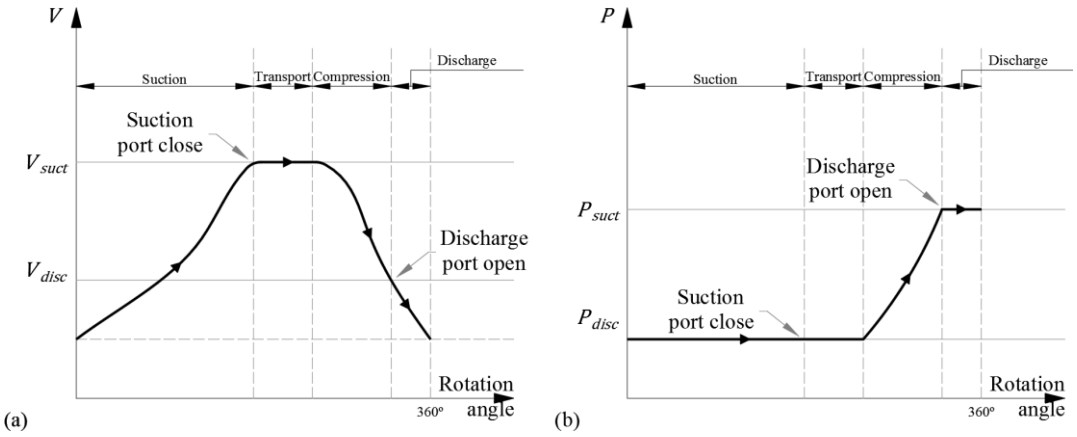

Figure 2.34: Screw Compressors: (a) volume and (b) pressure variation (source: adapted from [37])

The single screw has a single helical grooved rotor, with two flat star wheels, confining the pockets of gas in a similar process to that in twin-screw compression [35], [38]. The screw type compressor has been largely replacing the rotary vane in low-stage ammonia compression systems [34]. The recommendations for piping used for reciprocating compressors are also valid for screw compressors [34]. The maintenance of the lubrication process is essential, and its can be done, along with cooling process and sealing between moving parts, through oil injection along the length of the barrels [38], and lubrication systems require at least a 500 kPa pressure differential for proper operation [34]. At the discharge, the oil is separated, cooled and filtered, and then reintroduced in lubrication circuit [38]. The lubricant cooling can done by [34]: (1) liquid refrigerant injection, this method decreases compressor efficiency and capacity, but lowers the equipment cost; although, for low stage compression, it has a negligible

penalty, or no penalty at all; (2) indirect cooling with glycol or water in a heat exchanger, increase the compressor efficiency using an indirectly cooled lubricant cooler, which is cooled by an evaporative condenser or cooling tower, without being transmitted to the high-stage compressor; (3) indirect cooling with boiling high-pressure refrigerant used as the coolant in a thermosiphon process, this method is the industry standard where the high-pressure liquid, from the condenser, cools the lubricant in a tubular heat exchanger.

One fundamental characteristic of the screw compressor, and as it has a constant volume or displacement design [34], is its built-in volume ratio. Its defined as the proportion of the inlet volume reduced by the time the discharge port is uncovered [38], or more specifically the ratio of the volume in cavity when suction port closes to the volume in cavity when the discharge port uncovers, v_i [35], or simply, the internal volume ratio of the compressor, volume index ,V_i [34]. Typical values for this volume ratio, used by manufactures, are 2.6, 3.6, 4.2, and 5.0 [35], although these values can be presented according to the screw compressor type [34]: (1) fixed V_i with slide valve, ${V_i}^{\gamma} = r_p$, where the ratio of the specific heats $\gamma = \mathrm{c}_p/\mathrm{c}_v$ is 1.4 for ammonia [34] (approximately 1.29 [35]) and the pressure ratio, r_P (Eq. (2.17)), should selected for average conditions; (2) fixed V_i with bypass port, instead of slide valve, these compressor are often applied as booster compressors, and normally have an built-in volume ratio less than 2.9; (3) variable V_i with slide valve and slide top, the compressor volume ratio can vary from 2.0 to 5.0, resulting in a simpler compressor selection process, and matching the compressor internal pressure ratio with the external pressure ratio. Contrarily to the piston (reciprocating) machines, which are limited to pressure ratio of 8 or 9, screw compressors can work, without restrictions or any drawback, up to pressure ratios of 20 or more [35].

The capacity of the screw compressor is controlled by a sliding block or valve (or two, in the case of the single-screw), covering part of the barrel and allowing gas to pass back to the suction, varying the working stroke [38], and thus, the compressor capacity, from 100 to 10 % with a signal from an electric, electronic or microprocessor controller [34]. The slide valve is controlled by four-way control valves, positioning both slide valve, according to the load, and the slide stop, to adjust the compressor internal pressure ratio, in accordance to the external suction and discharge pressure [34]. Although having an excellent and smooth capacity control, this method results in a decline of the compression efficiency, particularly at part-load, variable-speed drives became alternatives (even though having also some drawbacks [47]), provided either by a two-speed motor or by a

frequency inverter [35]. Figure 2.35 shows the efficiency reduction, comparing to the ideal curve, relating the percentage of full power to the same percentage of full capacity. At part load, the percentage of full power always exceeds the percentage of full capacity, this effect has more impact in constant condensing and evaporating temperatures (black solid curves), rather than for adjustable condensing (drop) and evaporating (increase) temperatures, at part load (grey continuous curves) [35]. The reasons for the efficiency drop may be pointed out as owing to the: (1) friction of the gas, passing back to the suction; and (2) changing of built-in volume ratio of the compressor, which is assumed to be properly matched to the external conditions at full load [35].

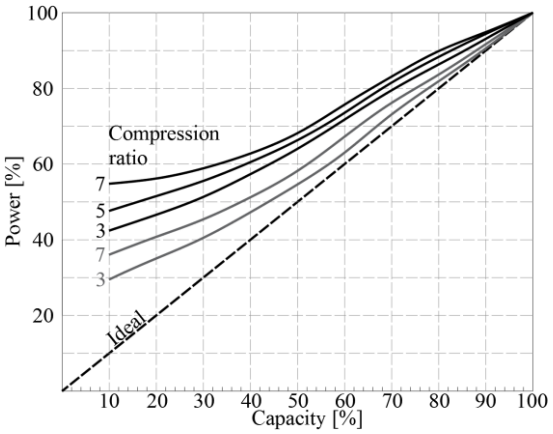

Figure 2.35: Part-load power requirements of a screw compressor (source: adapted from [35])

Rotary-screw compressors are subjected to constant circumferential movements, the suction and discharge gas flow-rate is continuous, and therefore, they are exposed to fewer mechanical vibrations and fewer pulsed discharges, when compared to reciprocating compressors [37]. Nevertheless, they also have compression and volumetric losses, resulting from the leakage of the refrigerant bypass to the suction, via built-in clearances [38], heating losses, *etc.* [37]. Screw compressors have higher volumetric efficiencies, under the same operation conditions, as they have not clearance volume, and consequently, no losses during its re-expansion [38]. Typical volumetric and isentropic efficiency values, η_v and η_s, are presented in Figure 2.36 and Figure 2.37, respectively.

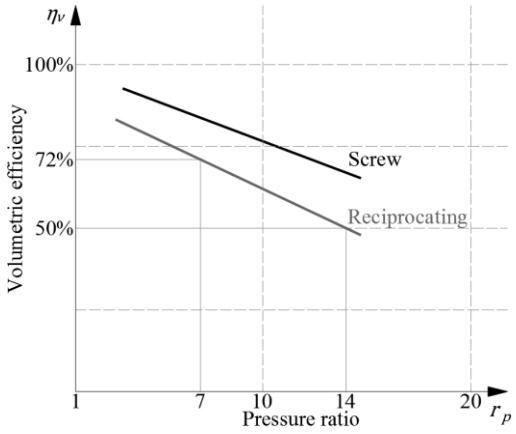

Figure 2.36: Typical η_v for different compressors (source: adapted from [38])

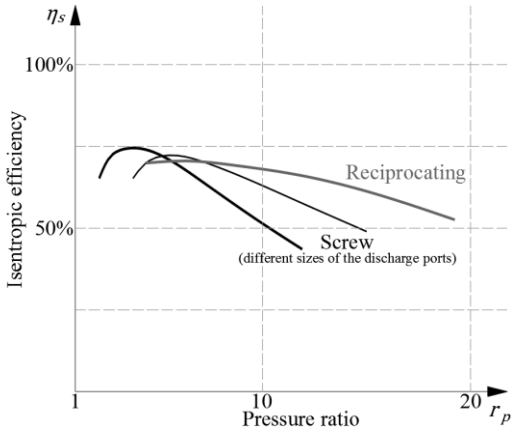

Figure 2.37: Typical η_s for different compressors (source: adapted from [38])

As previously referred, the isentropic power (in an ideal evolution) is always lower than actual power, due to the motor losses (around 10 %, for an efficiency of 90 %), friction losses (around 10 %), and over compression, pressure drops; leakages, oil pump, *etc.*, grouped in flow and heat transfer losses (around 10 %) [38]. These inevitable efficiency-reductions, lead to a threshold of isentropic efficiencies at 70 %. Thus, machines having an isentropic efficiency above 70 % are considered reasonably efficient compressors [38].

For equipment selection, rating information should comply with international standards, normally referenced to standard vapor-compression cycles, with complementary information for subcooling and superheating, namely the European Standard EN 12900 [38], or the ANSI/AHRI Standards 500 series, based in the ANSI/ASHRAE Standard 23. Detailed information is also essential to define the compressor power curve and perform energy simulations. For that effect, it is used the following bi-cubic equation, as specified in ANSI/AHRI Standard 540 (reference [48]), as a function of the saturation temperatures corresponding to the suction and discharge pressures, respectively, T_{suct} and T_{disc} (which can be, considering the equivalent pressure drops [34], related to the evaporating and condensing temperatures, $T_{evap} - 1$ and $T_{cond} + 0.5$ °C) and the regression coefficients, provided by the manufacturer, C_1 to C_{10}. In the expression Eq. (2.59), X can assume the input power [W], the refrigerant mass flow rate [kg.s^{-1}] or the refrigeration capacity [W]:

$$\begin{aligned} X = {} & C_1 + C_2 \times T_{suct} + C_3 \times T_{disc} + C_4 \times {T_{suct}}^2 + C_5 \times T_{suct} \times T_{disc} + \\ & + C_6 \times {T_{disc}}^2 + C_7 \times {T_{suct}}^3 + C_8 \times \left(T_{disc} \times {T_{suct}}^2\right) + \\ & + C_9 \times \left(T_{suct} \times {T_{disc}}^2\right) + C_{10} \times {T_{disc}}^3 \end{aligned} \tag{2.59}$$

Although reciprocating and screw compressors (as the other types in general) are well-defined products, further improvements, in efficiency and reduction in size and cost can be possible [49], [50]. Moreover, the economic and technological competition is so fierce that no detail is left to chance. Meticulous attention must be paid to in housing ports, bearings, seals, and the lubrication system, but also to rotor profiles [51]. Powerful three-dimensional computational fluid dynamics (CFD) programs have been widely used, to simulate, detect and evaluate conceptual or manufacturing defects (such as leakages registered in reciprocating compressors, through the piston-cylinder clearance [50]), providing useful information that would not be considered in simpler numerical models.

IV. Expansion devices

Expansion devices have a dual function in the vapor-compression refrigeration cycle: (1) control the refrigerant flow, necessary to the evaporating equipment for removing the heat load; and (2) the reduction of the system pressure, from the high-pressure of the condensing side into the low-pressure side, essential in the evaporation process [37], [38]. Besides these two essential functions, they may also be used to control the liquid level in vessels, injection of low-pressure and temperature refrigerant in suction lines, *etc*. [37].

Consider the presence of an obstruction in the fluid flow, in a vapor-compression cycle, such as throttling valve, an ordinary adjustable valve, capillary tube, or a porous plug. The refrigerant will experience a pressure drop, and once the heat transfer (as well as kinetical and potential energies) is negligible, $q = 0$, and no work is done on or by the system, $w = 0$, the energy balance from Eq. (2.23) is resumed to:

$$h_{in} = h_{out} \tag{2.60}$$

The expansion of a high-pressure fluid is an isenthalpic phenomenon followed by a temperature reduction (or sometimes, a temperature rise [39]). This occurrence is known as the Joule-Thompson effect [39], [40]. Using, once more, the same numbering used in Figure 2.17 (p. 23), the expansion process of a simple vapor-compression cycle is:

$$h_3 = h_4 \tag{2.61}$$

During an isenthalpic expansion, the temperature behavior can be described by the Joule-Thompson coefficient, μ_{JT}, which is described as follows in Eq. (2.62), where T is the temperature, P is the pressure, h is the enthalpy, c_p is the specific heat (constant pressure) and v is the specific volume. It can be also seen as a measure of the temperature change with pressure during a constant-enthalpy process [39]. If $\mu_{JT} < 0$ the temperature increases, if $\mu_{JT} = 0$ the temperature remains constant, and if $\mu_{JT} > 0$, the temperature decreases, during a throttling process. The Joule-Thompson coefficient represents the slope of the isenthalpic lines on a T- P diagram, as can be observed in Figure 2.38.

$$\mu_{JT} = \left(\frac{\partial T}{\partial P}\right)_h \quad \text{or} \quad \mu_{JT} = \frac{1}{c_p}\left(T \times \left(\frac{\partial v}{\partial T}\right)_P - v\right) \tag{2.62}$$

The isenthalpic line present an inversion point (point of zero slope or zero Joule-Thompson coefficient). The curve that passes through all these points is called the inversion line, and the temperature at these is termed inversion temperature.

The intersection point where the inversion curve crosses the $P = 0$ line is called the maximum inversion temperature. The conjugation of temperature and pressure values inside (right bounded) the area delimitated by the inversion curve, represents a temperature decrease during a throttling process ($\mu_{JT} > 0$). By opposition, if it is out of the boundary, the temperature increases during the throttling process ($\mu_{JT} < 0$). In a cooling process of a gas, using the isenthalpic expansion method, it has to occur, inevitably, inside the inversion curve area, where $\mu_{JT} > 0$, below its maximum inversion temperature. A common example is the hydrogen (H_2), whose maximum inversion temperature is −68 °C. Therefore, it must be cooled below this temperature if any further cooling is intendent to be achieved by this method [39], [40].

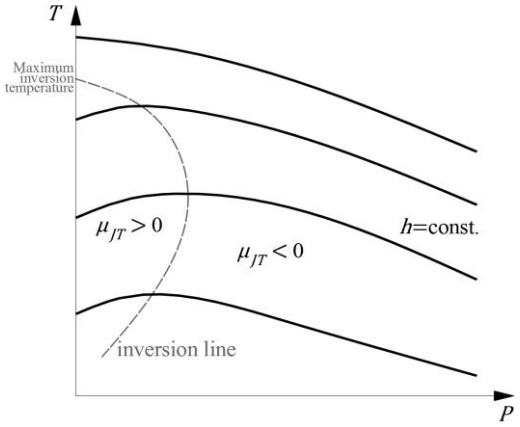

Figure 2.38: Constant-enthalpy lines on a T-P diagram (source: adapted from [39])

Expansion devices can be classified according to the driving and controlling method [37], [38]. Firstly, they can be tagged as: (1) manual, *e.g.* an ordinary adjustable valve, manually opened or closed, in which the refrigerant flow is a function of the opening degree and the pressure difference between in- and outlet of the valve; its use is restricted, normally only for redundant control of level controlled or flooded systems [37]; (2) constant cross section area expansion devices, such as capillary tubes (tube bores with 0.5, 0.6 or 0.8 to 2.5, 2.3 or 2 mm, and lengths from 0.5 or 1 to 5 or 4 m, respectively, or L/D between 1000 to 5000, depending on the authors, [37], [38], [40]), and restrictors (precision-drilled orifices, with a free-moving bullet in horizontal direction, fixed in the condenser outlet), are predominantly used in small household and air-conditioning systems; low price, reliability, limitation of the refrigerant mass-flow and the absence of high and low-pressure separation are their advantages, but an incorrect selection and the almost-inexistent adaption to floating heat loads might be main drawbacks [37]; these equipment are factory selected and cannot be adjusted [37], [38]; and (3) automated expansion devices, which can be subdivided in four types: (3a) thermostatic expansion valve (TEV), mainly used in direct-expansion (DX) circuits (Figure 2.39a), it is the most-used expansion device in industry; although the designation "thermostatic" may suggest an evaporating temperature control, it is the evaporator outlet

superheating-level that is controlled (Figure 2.39b), usually in the order of 5 K [38]; a common practice, owing to the lack of standards for valve rating conditions, is to consider a nominal capacity for the condensation at 38 °C, 4 °C for the evaporation, 1 K for subcooling and 3 to 4 K for superheat [38]; the superheating degree is the temperature difference, ΔT, between the low-pressure gas temperature, at the evaporator outlet, and the evaporating temperature; the TEV has a phial, mounted in full contact with the suction pipe, charged with the same refrigerant used in the circuit, acting like a detector and power element, and connected to the set diaphragm – spring – valve, by a capillary tube; it has also a superheat setting spindle (or spring), allowing the adjustment of the balance between the refrigerant pressure inside the phial, P_{phial}, at the temperature T_{phial} (commonly predetermined for vaporizing at 0 °C [38]), and the evaporating pressure of the circuit, P_{evap}, at the corresponding temperature T_{evap}, through the gas law $P_{phial}/P_{evap} = T_{phial}/T_{evap}$ [38]; its basic principle is ruled by the response of the pressure variation of the refrigerant inside the phial, to the superheat degree of the circuit refrigerant, at the evaporator outlet: the valve element is moved along the stem (opening or closing the passage orifice) due to the pressure done over the diaphragm by the phial refrigerant, which is counteracted by the pressure exerted by the spring; thus, once the thermal load increases, a fast vaporization occurs, causing a high superheat degree at the evaporator outlet, and consequently, the valve will open; by opposition, if the thermal load decreases, the vaporization will proceed slowly, achieving the outlet of the evaporator, originating a low superheat degree, and resulting in the closing of the valve;

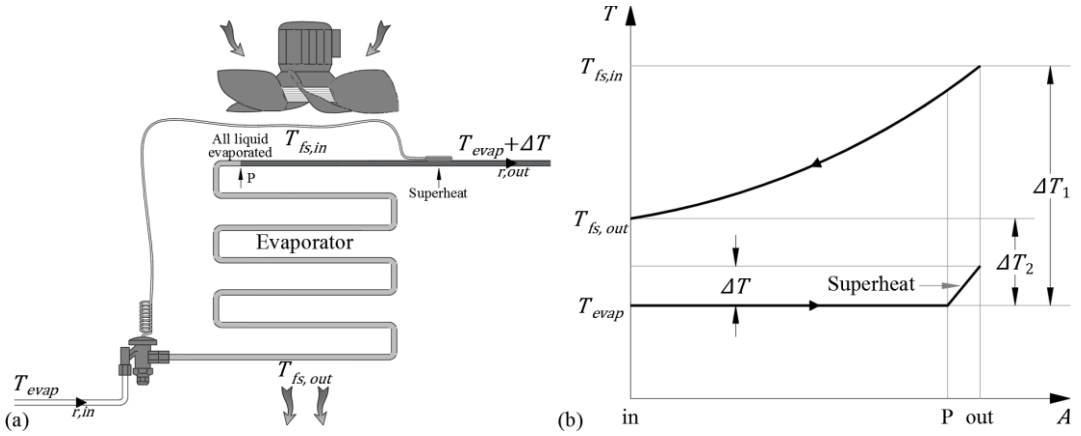

Figure 2.39: Evaporation with superheat (source: adapted from (a) [38], (b) [37])

whenever the system is turned-off, a thermal equilibrium is rapidly obtained, no superheat will be registered, hence, the valve will close; between two consecutive start-over, the slow superheat decrease will hold the valve open for a while, exposing the

compressor to a liquid slugging, and for this reason a solenoid valve should be mounted; the superheat degree can be fixed by the adjustment of the superheat setting spindle, [37]: a high degree is acceptable for high $DT1$ values (*e.g.* in HVAC), and low for low-temperature applications; commonly, the superheat degree is defined from 5 to 7 °C; the phial may be charged with a mixture of two or more volatile fluids, adapting its characteristic curve and enlarging the application range, of a specific valve, or using silica gel or charcoal, through the principle of gas adsorption by a porous materials [37]; external equalizers (Figure 2.47) are used ever since there is a high pressure drop, due to the evaporator dimension and configuration, or a distribution device (are used to equalize the pressure drop in parallel passes of an evaporator coil, Figure 2.21a, commonly around 1 to 2 bar), avoiding undesirable superheat and consequent reduction of the useful heat-transfer area; this equipment has a middle chamber and an equalizing connection, at the evaporator outlet in suction line near to the phial position, reducing the pressure difference between both sides of the diaphragm, helping on the valve control and reducing the occurrence of undesirable excessive superheating [38];

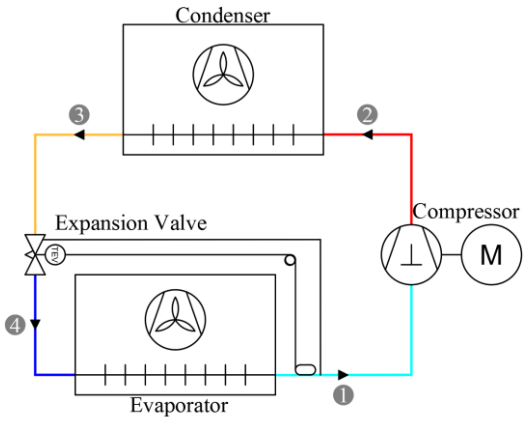

Figure 2.40: TEV with external equalizer (source: author)

TEV can also have some variations, for instance, the capillary tube and phial are replaced by a passage back through the valve; as major advantages, TEV induce high performance in the evaporating process (due to the control of the superheat), are extremely reliable, provide a long time service, and it can be used for all refrigerants [37]. As disadvantages, the evaporating temperature is not kept constant, *i.e.* a predefined superheat degree, as the thermal load changes, the mass-flow rate also changes, varying both pressure and temperature, the temperature variation could trigger a decrease on the relative humidity, with all the subsequent consequences to the products, and liquid slugging might also be a problem, however, a solenoid valve can be used to avoid the occurrence of that [37]; (3b) electronic expansion valve, which is very similar to the mechanical TEV, although having a higher precision (in the order of less than 1 °C [37]); offers a rapid response to load changes, better control at low superheats, flexibility in the system layout (due to electrical instead piping connections) and does not need a solenoid valve, for the system shut-down [38]; these valves are being widely used for many applications,

not only by the advantages presented above, but also to its adaptability on different control tasks, such as: expansion valve (for superheat control), suction pressure control (for capacity control), liquid injection for desuperheating of compressor, condensing pressure control and hot gas bypass control, compensating the excessive compressor capacity and avoiding the evaporating pressure falls below a set point [38]; (3c) high-pressure float valves (Figure 2.41a): used in flooded systems, maintaining the liquid level in a float chamber, at the condenser outlet, by the actuation of a float, *i.e.*, the valve opens if the liquid level at the vessel, which it is at the condenser pressure, increases; this device has not a direct control over the evaporation flow rate, once a constant refrigerant flow is provided to the evaporator (demanding a low-pressure receiver to avoid liquid entering at the compressor, but dismissing a high-pressure receiver); they are appropriate to constant thermal loads, such as liquid chilling processes [37]; (3d) low-pressure float valves (Figure 2.41b): similarly to the high-pressure ones, they are used to maintain the liquid level in a float chamber, by the actuation of a float, although, in this case, the valve opens if the liquid level, which it is at the evaporator pressure, decreases; furthermore, the low-pressure valves control the refrigerant flow rate entering the evaporator, as a function of the thermal load, passing liquid in the same amount of the one that is vaporized at the evaporator; they could be divided in continuous and non-continuous response action, which differ in the immediate response for any change on the liquid level (continuous), or a discrete response within a range, with a minimum and a maximum value (non-continuous) [37]; Their major drawback relies on the recovery of the lubrication oil, once it hinders the oil return into the sump, in highly-mixable refrigerant/oil, especially some halogenated derivatives [37]; This type of valves is much more common in industrial refrigeration than the high-pressure float valve [35].

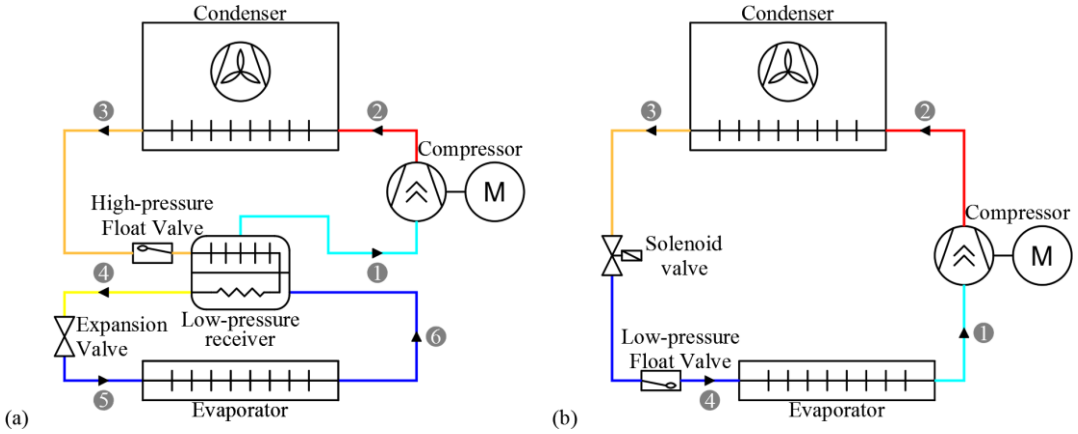

Figure 2.41: Float valves: (a) high pressure and (b) low pressure

(source: (a) adapted from [38], (b) author)

As it was aforementioned, throttling devices are much more simple and reliable, and more feasible than expansion engines (section 2.2.2.1). Nevertheless, there is always a power loss, wasted during the expansion, which if recovered and used, could relieve the compressor, during the compression cycle. The research and implementation of such equipment are not new: Stoecker [35] reported the existence of, at least, one water chiller, working with R-134a (in late 90s of the last century), using a turbine as an expansion engine, delivering power to the compressor through a direct shaft connection, as shown in Figure 2.42; and ejectors (Figure 2.87) have been under the scope of researchers for many decades [52]. Nevertheless, it was with the restrictions of the latest environmental regulations over energy efficiency and refrigerants (section 2.2.3), that these components gained a new impetus. Recent theoretical studies, highlighted expanders as being financially feasible when applied in systems using CO_2 and R-1234yf, particularly attractive to low temperature refrigeration systems (-30 °C), and in commercial refrigeration, in both conventional and transcritical CO_2 systems [53]. The enhancement of the COP is given by the enthalpy gain due to the near-isentropic expansion, $\Delta s_{exp} \approx 0$, ($\Delta h_{exp} = h_3 - h_{4e} \neq 0$, and comparing to the isenthalpic expansion of the conventional throttling devices, $\Delta h_{valve} = h_3 - h_{4v} = 0$, as depicted in Figure 2.42b), increasing the refrigeration capacity of the system, $\dot{Q}_{evap}$, and allowing the reduction of the compressor size; the work produced by the expander, $\dot{W}_{exp}$, also helps to reduce the electrical power supplied to the compressor, $\dot{W}_{in}$, [53], as expressed in the following equation, Eq. (2.63).

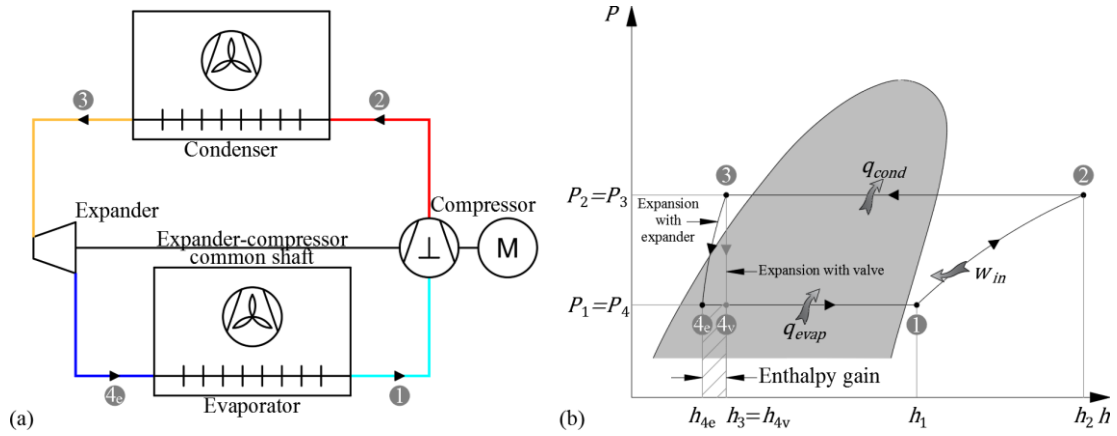

Figure 2.42: Expansion cycle with expander (a) circuit and (b) *P-h* diagram (source: adapted from [53])

$$COP_{exp} = \frac{\dot{Q}_{evap} + \dot{Q}_{exp-gain}}{\dot{W}_{in} - \dot{W}_{exp}} = \frac{\dot{Q}_{evap} + \dot{m} \times \Delta h_{exp-gain}}{\dot{W}_{in} - \dot{m} \times \Delta h_{exp} \times \eta_{exp}} \tag{2.63}$$

where $\Delta h_{exp-gain}$ is the enthalpy gain ($h_{4v} - h_{4e}$), and η_{exp} is the expander efficiency.

Ironically, the ejector has the precise opposite working principle of an expansion device, being indeed a dynamic compressor (Figure 2.31). However, it has been experimented and recently implemented in the expansion process. The first use of a two-phase ejector (Figure 2.43) was proposed in 1931 [54], [55], However, it was only in 1990 that a thermodynamic model (Figure 2.43), for the expansion process in the ejector, was developed, achieving an increased COP, decreased compressor displacement and decreased compression ratio, when compared to a conventional vapor-compression cycle, under the same conditions, using R-12 [52]. In this standard configuration, the liquid-vapor separator could impair the performance of the ejector cycle, if liquid and vapor are not properly separate from each other [54]. Other configurations have been tested for low-pressure refrigerants (R-134a and R-1234yf), such as the diffuser outer split (DOS) [55], and the condenser outlet split (COS) ejector cycle [54], showed in Figure 2.44. Numerical studies proved the same COP for both standard and COS ejector cycles, although the last offers more practical advantages, as the application for multiple evaporation temperatures [54]. COS ejector cycles can have a COP 10 % higher than the conventional cycles [55].

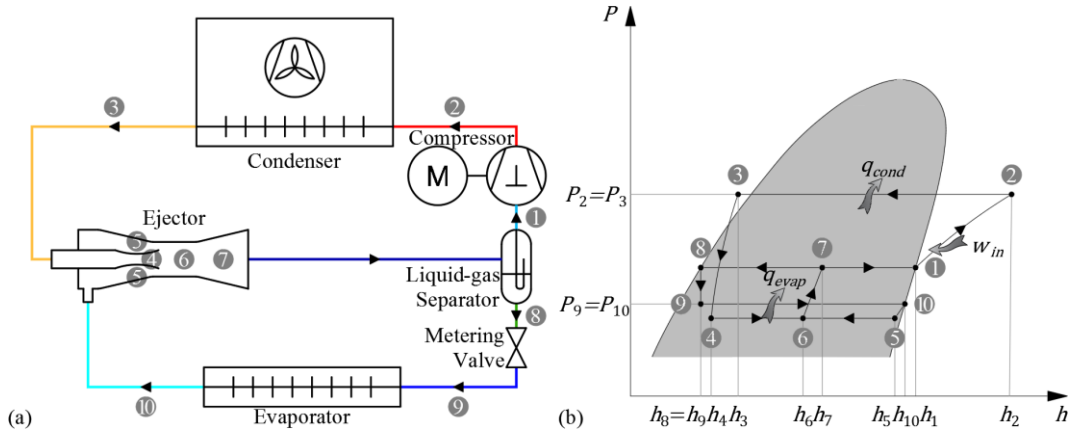

Figure 2.43: Standard two-phase ejector cycle: (a) circuit and (b) *P-h* diagram (source: adapted from [54])

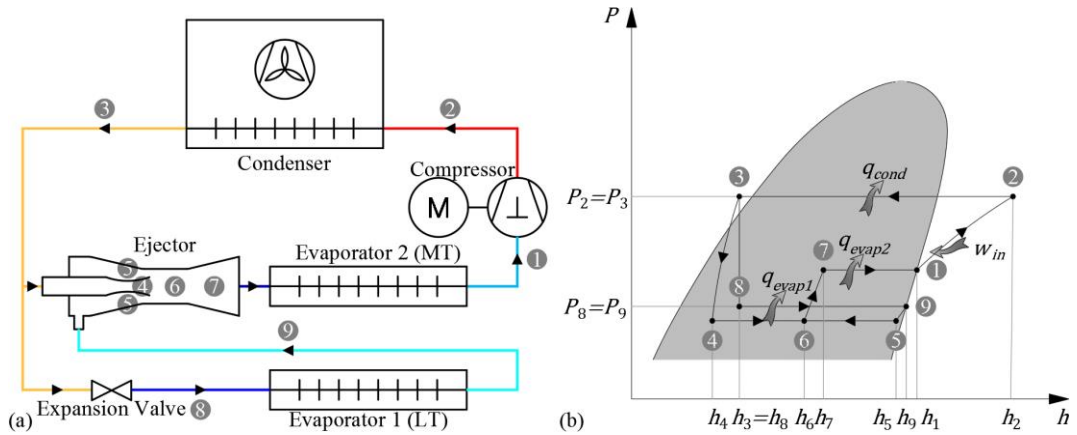

Figure 2.44: COS ejector cycle: (a) circuit and (b) *P-h* diagram (source: adapted from [54])

Many other studies have been performed, denoting higher COP values for the new generation refrigerants, such as the R-1234yf and the R-1234ze(E), than for other low-GWP refrigerants, in multistage cycles with two-phase refrigerant injection [56], [57]. However, it has been for transcritical CO_2 cycles that these components have been mostly studied (Figure 2.45), for its larger throttling loss and a lower cycle efficiency [57]–[59].

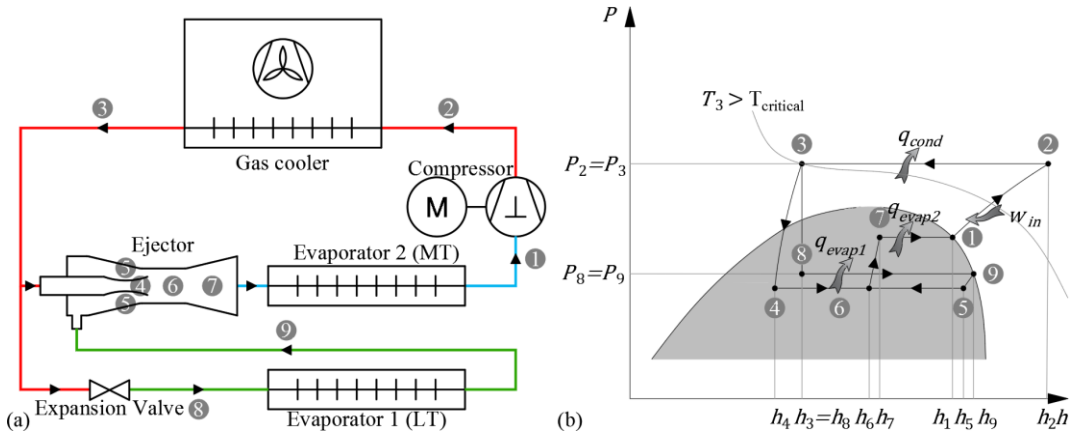

Figure 2.45: Transcritical CO_2 ejector cycle: (a) circuit and (b) P-h diagram (source: author)

Recently, these theoretical concepts have been implemented in refrigeration facilities, namely in new transcritical CO_2 systems for commercial refrigeration in supermarkets, bringing an enormous expectation regarding the energy savings. The system presented in Figure 2.46 is announced by a consulting engineering company (Frigo-Consulting Ltd., Switzerland), as having 15 % of energy savings when compared to regular CO_2 systems.

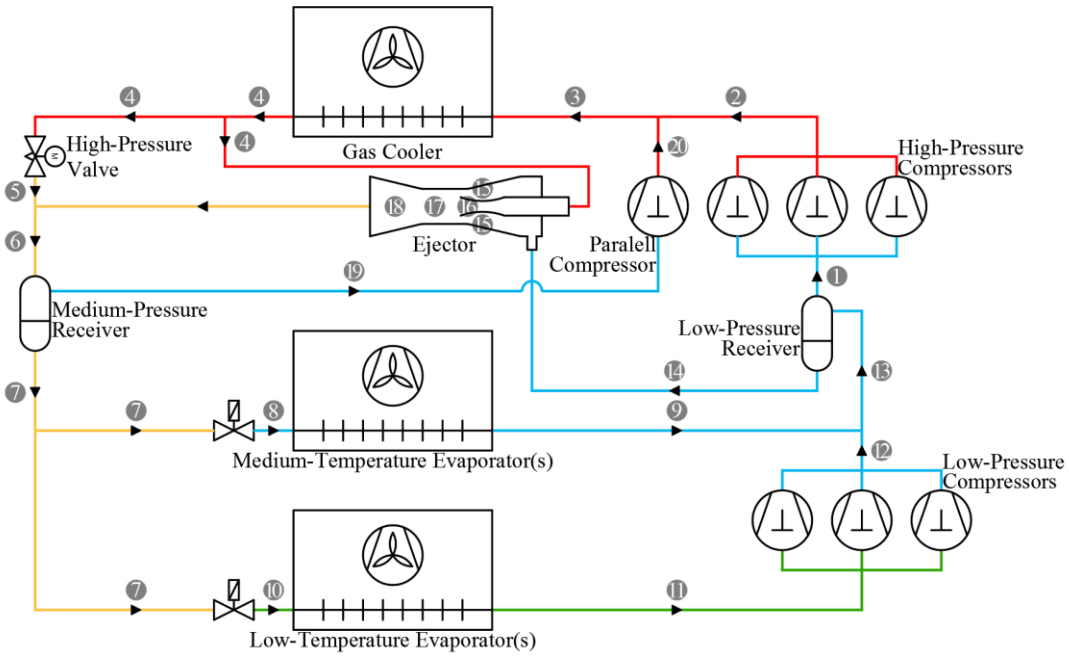

Figure 2.46: Schematic of a transcritical CO_2-refrigeration system with an integrated ejector (source: adapted from Frigo-Consulting Ltd.)

V. Other components

Besides the abovementioned equipment, many other components are used in refrigeration systems. These components are required for safety, control and maintenance, and fitted according to the system size and complexity. Some of them, described as follows and based on references [37], [38], can be found in Figure 2.47:

- Oil separator ❶: lubrication is essential for a proper operation of the compressor, but some oil leaves the compressor with the discharge gas. Particularly in complex systems with remote or flooded evaporators, and to reduce the oil carry-over to the system, it is desirable to fit an oil separator in the discharge line, as the presence of oil in the refrigeration circuit reduces the system global performance;
- Liquid receiver ❷: vessel used to store: (1) the refrigeration charge within the system, temporarily, or (2) the excess of refrigerant arising from the changing operation conditions. It can also act as a pump-down reservoir. For expansion and safety reasons, the refrigerant volume should never surpass 85 % of liquid receiver total capacity. It can nullify the subcooling obtained in the condenser;
- Filter-driers ❸ (liquid and suction line): particularly with halocarbon refrigerants, the reduction of water content is mandatory. The dryer is composed by a capsule charged with a drying agent: a solid desiccant material, such as activated alumina, calcium oxide or sulfate, silica gel or zeolite. Filter-driers are fitted in the liquid line, upstream to the expansion valve, or in the suction line for cleaning up after repairs, until the pressure drop exceeds 1 K (when compared to new one);
- Sight glass moister indicator ❹: mounted in the liquid line, from the receiver to the expansion valve (closest to the last). It is used to verify the presence of gas (bubbles formation due to a refrigerant shortage, *e.g.* denoting the need for filter charging or recharging) where only liquid should pass. A moisture-sensitive chemical is inserted to indicate the excess of water, by a change of color;
- Solenoid valves ❺ (liquid line, bypass, *etc.*): electrically operated shut-off valves. The most-common working configuration is opening through the solenoid energization and closing by de-energization. Used to: block the entrance of refrigerant in the evaporator when the compressor is off, control the refrigerant flow entering in the expansion valve, divert hot gas for defrosting the evaporator;
- Evaporator pressure regulation valve ❻: used in the suction line, to prevent the evaporator pressure falling below a predetermined or controlled value, even if the compressor suction pressure is lower. Its applied to (1) allow different load

temperatures in two or more evaporators working with the same compressor; (2) modulate the evaporator pressure, controlled by the load temperature, according to a varying load; (3) prevent damages owing to freeze or frost forming, either in a liquid chilling evaporator or an air cooling evaporator respectively, or to a temporary malfunction disabling the interruption operation; (4) act as a solenoid valve for on/off operations;

- Suction accumulator ⑦ (also known as knockout drum or suction trap): vessel normally used in halocarbon refrigerant systems to separate the return liquid and prevent its passage to the compressor (liquid slugging), allowing, however, the oil present in the liquid to be sucked back to the compressor. It can have an additional hot-gas heating coil to promote the evaporation of the trapped liquid;

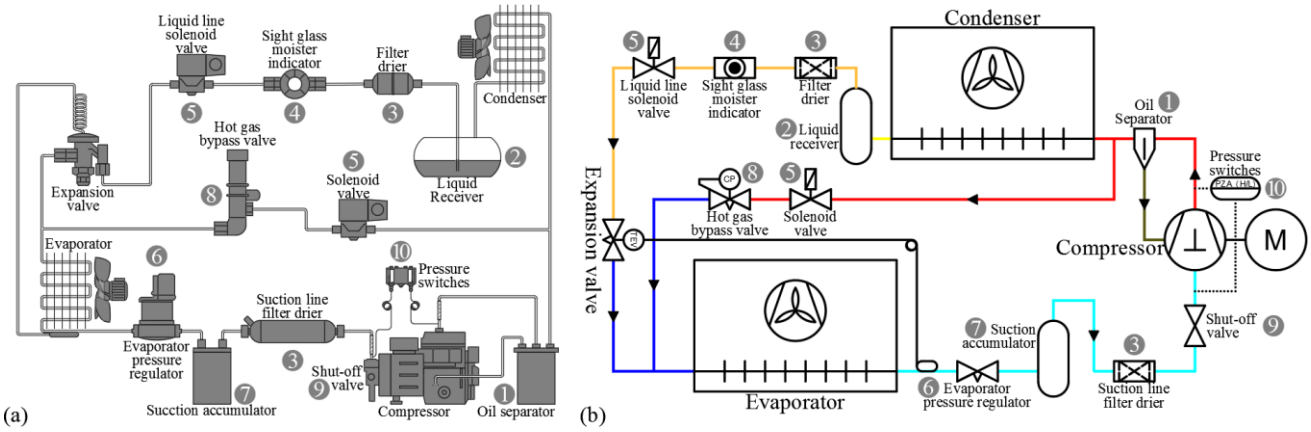

Figure 2.47: Components for direct-expansion circuits (source: (a) adapted from [38], (b) author)

- Hot gas bypass valves ⑧: used to when the compressor has no capacity reduction device, and the on-off switching does not provide an adequate control to the refrigeration process. Therefore, the cooling capacity is regulated by discharging back the hot gas at the entrance of the evaporator, keeping it at a constant pressure, regardless of the load. This control method is extremely energy wasteful;
- Shut-off valves ⑨: used to manually isolate branches or equipment, during partial operation, service or maintenance;

  Pressure and oil switches ⑩: used to stop the compressor, if necessary. The high-pressure cut-out point should be regulated 2 bar than the expected peak operation pressure, and if reached, indicates a system malfunction, such as a condenser fault or incorrect valve closures. In opposition, the low-pressure cut-out should be 0.6 to 1.0 bar below the design evaporation pressure (but is strongly dependent on the system type), and anomalous low suction pressures will lead to high discharge

temperatures, caused by the high compression ratio, excessive frost in air cooling coils, and the malfunction of other components. Oil switches are used in mechanical lubrication systems, to prevent the compressor damage owing an oil shortage or a pump fault in the oil supply;

- Pressure gauges: mounted near or on the compressor (suction, discharge and oil delivery) to give a direct indication of the operating conditions. Condensation and evaporation pressures (and the corresponding condensing and evaporating temperatures) can be measured on these pressures gauges with a reasonable accuracy level, since the pressure losses in discharge and suction lines are comparatively small the rest of the system;
- Thermostats and humidistats: used to maintain a predetermined level of temperature of humidity, respectively, stopping the equipment or reducing its capacity when the required conditions are reached. Typically, thermostats can be mechanically triggered by: (1) movement of a bimetallic element; (2) expansion of a fluid; (3) vapor pressure of a volatile fluid; or alternatively by an electrical sign, which must be measured and amplified, to operate the controlled device: (4) electric resistance or (5) electronical. Normally, a 2 K temperature differential is recommended to prevent excessive cycling. Humidistats are either (1) mechanical (using materials whose dimension is moister sensitive) or (2) electronical (using a hygroscopic salt);
- Suction to liquid heat exchanger: as previously mentioned, LSHXs are used to increase the refrigeration effect, along with the compressor protection. However, the efficiency enhancement should be evaluated against the effect of pressure drop through the suction side of the exchanger (forcing the compressor to operate at a lower suction pressure) [34], [37]. This pressure loss triggers a sequence of losses: the reduction of the density of the refrigerant, ρ, resulting in reduced refrigerant mass flow rate, $\dot{m}$ ($\dot{m} = \rho\dot{V}$ and from Eq. (2.15), $\dot{m} = \rho\left(\eta_v \dot{V}_d\right) = \eta_v \dot{V}_d / v$) that in turn, reduces the refrigeration capacity; additionally, more work per unit mass, w, is required to increase the pressure to the level in the condenser, and the volumetric efficiency, η_v, is reduced [60]. In conclusion, LSHX is detrimental to system performance in systems using R-22, R-32 and R-717. Nevertheless, it is useful for systems that have heat exchangers with minimal pressure losses in the

low-pressure side, and using R-12, R-134a, R-290, R-404A, R-407C, R-410A, R-507A or R-600 [60];

- Condenser pressure regulators: in the off-peak-season, operation may lead to malfunctions, as the low condensing temperature and pressure induce a low-pressure difference across the thermostatic expansion valve. It is necessary to prevent the condenser pressure from falling too low, and the condenser pressure regulator can be a pressure-operated bleed valve in a bypass across the condenser, diverting hot gas to the receiver. In air-cooled condensers and water cooling towers, pressure is controlled indirectly, by controlling the condensing temperature through the air-flow by automatic dampers, fan speed control or switching off fans. For water-cooled condensers, a water-regulating valve operated by the condenser pressure or a three-way blending valve in the water circuit, are suitable solutions;
- Relieve valves: mandatory equipment to relief the pressure under several possible conditions of malfunction. It is normally fitted between the inlet and discharge connections, to prevent overpressure within the compressor;
- Strainers: fitted in the compressor suction to trap small particles of dirt and swarf;
- Non-condensable traps: purging devices to remove incondensable gases (*e.g.* air);
- Charging connection: used to admit the initial refrigerant charge into the circuit recharge it, when needed. Normally located ahead of the expansion valve, controlling the flow and preventing liquid reaching the compressor;
- Check valves: check valves or non-return valves, used (1) on reversible heat pumps, preventing flow through expansion valves that are not in service for the active cycle; (2) on hot gas circuits, preventing the das entering another evaporator; (3) to prevent liquid condensing back to out of duty compressors, in a configuration where several compressors discharge into a common condenser; (4) when different evaporators work at different pressures, avoiding suction gas flowing back to the colder ones;
- Vibration eliminators: mounted in compressors and pumps. For the firsts, they are inserted in suction and discharge lines, placed as close to the compressor as possible. Flexible connectors are used to isolate water and brine pumps;
- Liquid refrigerant pumps: used in forced circulation evaporators, to circulate the refrigerant from the suction separator (or surge drum) through the evaporators and back. Mainly used in ammonia and CO_2 (subcritical) systems.

2.2.3. PARAMETERS INFLUENCE OVER THE SYSTEM PERFORMANCE

The system performance, or COP, is a result of the ratio of the extracted energy (from the refrigeration load, Q_{evap}) to the consumed energy for that purpose (W_{in}), as expressed in Eq. (2.9). This expression could be also written as a relation between the specific properties (*i.e.* per mass unit, m) refrigeration effect (q_{evap}) and work input to the compressor (w_{in}), or even, considering the mass flow rate ($\dot{m}$), as the ratio of refrigeration capacity ($\dot{Q}_{evap}$) to the power supplied to the compressor ($\dot{W}_{in}$), as presented in Eq. (2.64).

$$COP = \frac{Q}{W} = \frac{m \times q_{evap}}{m \times w_{in}} = \frac{\dot{m} \times q_{evap}}{\dot{m} \times w_{in}} = \frac{\dot{Q}_{evap}}{\dot{W}_{in}} \tag{2.64}$$

As it was formerly described (sections 2.2.2.1 and 2.2.2.2), parameters such as the working pressures or temperatures (condensing and evaporating pressure or temperature), subcooling and superheating degree (presence of subcooled liquid and/or superheated vapor) and the existence of pressure drops, will influence the system performance, either over the refrigeration effect/capacity, the compressor work/power input, or both. In order to evaluate the variation of the COP, owing to the variation of these parameters, Alcaraz [37] deduced the following expressions, where Δ stands for the variation of the associated variable ($\dot{Q}_{evap}$, q_{evap}, η_v, η_s, v_1, $\dot{W}_{in}$ or w_{ideal}), η_v is the volumetric efficiency, η_s is the isentropic efficiency, v_1 is the specific volume at the suction conditions (compressor inlet), and w_{ideal} is the ideal (isentropic) work input.

$$\frac{\Delta \dot{Q}_{evap}}{\dot{Q}_{evap}} = \frac{\Delta q_{evap}}{q_{evap}} + \frac{\Delta \eta_v}{\eta_v} - \frac{\Delta v_1}{v_1} \tag{2.65}$$

$$\frac{\Delta \dot{W}_{in}}{\dot{W}_{in}} = \frac{\Delta w_{ideal}}{w_{ideal}} + \frac{\Delta \eta_v}{\eta_v} - \frac{\Delta v_1}{v_1} - \frac{\Delta \eta_s}{\eta_s} \tag{2.66}$$

$$\frac{\Delta COP}{COP} = \frac{\Delta q_{evap}}{q_{evap}} + \frac{\Delta \eta_s}{\eta_s} - \frac{\Delta w_{ideal}}{w_{ideal}} \tag{2.67}$$

The COP calculations were performed with CoolPack™, version 1.50 [61]. For the baseline cycle, it was considered some of the rating conditions for the low temperature range of the European Standard EN 12900: T_{evap} = -35 °C, T_{cond} = 40 °C and subcooling 0 K. An initial superheating of 0 K was considered, and the calculations were executed for R-22, R-404A, R-407C, R-410A and R-717, in a one-stage cycle with DX evaporator, having no LSHX and no pressure nor thermal losses, and an isentropic (ideal) compressor.

2.2.3.1. Influence of condensing and evaporating pressure/temperature

Assuming an ideal refrigerating machine (Carnot refrigerator), whose maximum efficiency is a function of the working temperatures, given by Eq. (2.12), a temperature variation, ΔT, in the evaporating temperature, T_{evap}, has a higher impact than the same variation in the condensation temperature, T_{cond} [37]. This statement can be proven by:

$$\frac{\partial COP_{R,\,Carnot}}{\partial T_{cond}} = T_{evap} \times \frac{\partial}{\partial T_{cond}}\left(\frac{1}{T_{cond}-T_{evap}}\right) = -\frac{T_{evap}}{\left(T_{cond}-T_{evap}\right)^2} \tag{2.68}$$

$$\frac{\partial COP_{R,\,Carnot}}{\partial T_{evap}} = \frac{\frac{\partial (T_{evap})}{\partial T_{evap}} \times \left(T_{cond}-T_{evap}\right) - \frac{\partial (T_{cond}-T_{evap})}{\partial T_{evap}} \times T_{evap}}{\frac{\partial}{\partial T_{cond}}\left(\frac{1}{T_{cond}-T_{evap}}\right)} = \frac{T_{cond}}{\left(T_{cond}-T_{evap}\right)^2} \tag{2.69}$$

Once $T_{cond} > T_{evap}$, it results as $\partial COP_{R,\,Carnot}/\partial T_{evap} > \partial COP_{R,\,Carnot}/\partial T_{cond}$ [37].

Analyzing the condensation evolutions represented in Figure 2.48a, and considering the reduction of the condensing temperature or pressure, it is noticeable that the suction conditions are kept constant (specific volume, $\Delta v_1 = 0$), while there is an increment in the refrigeration effect ($q'_{evap}/q_{evap} > 1$, being greater, the greater is the specific heat for the liquid phase, $\overline{c_{p_l}}$), the isentropic work decreases ($w'_s/w_s < 1$, once the enthalpy variation along an isentropic evolution decreases with the decrease on the condensation temperature), both volumetric and isentropic efficiencies increase in the same magnitude order ($\eta'_v/\eta_v > 1$ and $\eta'_s/\eta_s > 1$, due to $P'_{cond} < P_{cond}$, *i.e.*, as the pressure ratio r_P decreases, both η_v and η_s increase, as shown in Figure 2.36 and Figure 2.37, p. 47, having more impact for reciprocating compressors, while for screw compressors, particularly the twin screw type, the isentropic efficiency may decrease, for low pressure ratios in off-design conditions) [37]. Thus, it results $\Delta\dot{Q}_{evap}/\dot{Q}_{evap} = \Delta q_{evap}/q_{evap} + \Delta\eta_v/\eta_v > 0$, $\Delta\dot{W}_{in}/\dot{W}_{in} = \Delta w_{ideal}/w_{ideal} + \Delta\eta_v/\eta_v - \Delta\eta_s/\eta_s < 0$, and finally $\Delta COP/COP > 0 \Leftrightarrow \Delta COP > 0 \Leftrightarrow COP' > COP$ [37]. As a final remark, the reduction of the condensing temperature, or pressure, leads to an increase of the system efficiency (Figure 2.49). This impact can be observed in the Carnot efficiency, Eq. (2.12): the temperature difference between the heat sources is decreased, and the low-source temperature is kept constant).

The variation of the evaporating temperature or pressure is represented in Figure 2.48b. Considering the increase of this variable, it is observed that the isentropic work decreases ($w'_s < w_s$), as above-mentioned, the decrease of the pressure ratio, r_P, increases both η_v and η_s ($\eta'_v > \eta_v$ and $\eta'_s > \eta_s$, owing to $P'_{evap} > P_{evap}$), the specific volume decreases

($v_s' < v_s$), and the variation of the refrigeration effect ($q'_{evap} - q_{evap} = h'_5 - h_5$) is dependent on the variation of specific enthalpy of the saturated vapor ($h_v = h_l + h_{fg}$) with the pressure ($\partial h_v/\partial P = (\partial h_v/\partial T)/(\partial P/\partial T)$) [37]. Admitting that the latent heat of vaporization (h_{fg}) has a decreasing linear relation with the temperature, with slope α ($\partial h_{fg}/\partial T = -\alpha$), considering the Clausius-Clapeyron equation for vapor regions far from the critical point $\left(\partial P/\partial T = h_{fg}/(T \times v_v)\right)$ and the variation of specific enthalpy of the liquid, being (almost) exclusively dependent on the temperature ($\partial h_l/\partial T = \bar{c_{p_l}}$), the variation of specific enthalpy of the saturated vapor with the pressure results as $\partial h_v/\partial P = (\bar{c_{p_l}} - \alpha) \times (T \times v_v)/h_{fg}$ [37]. Since $(\bar{c_{p_l}} - \alpha) > 0$ for all commonly-used refrigerants, in normal working conditions, it results always an increase of the vapor enthalpy with the increase of the evaporating temperature, along with the increase on the refrigeration effect [37]. Thus, $\Delta\dot{Q}_{evap}/\dot{Q}_{evap} = \Delta q_{evap}/q_{evap} + \Delta\eta_v/\eta_v - \Delta v_1/v_1 > 0$, and $\Delta\dot{W}_{in}/\dot{W}_{in} = \Delta w_{ideal}/w_{ideal} + \Delta\eta_v/\eta_v - \Delta\eta_s/\eta_s - \Delta v_1/v_1 \cong 0$, finally resulting $\Delta COP/COP = \Delta q_{evap}/q_{evap} + \Delta\eta_v/\eta_v - \Delta w_{ideal}/w_{ideal} > 0$ [37]. The increase of the evaporating temperature, or pressure, results in an increased system efficiency (Figure 2.50), although the increment is limited by the conditions of the refrigerated medium, and by $DT1$ [37].

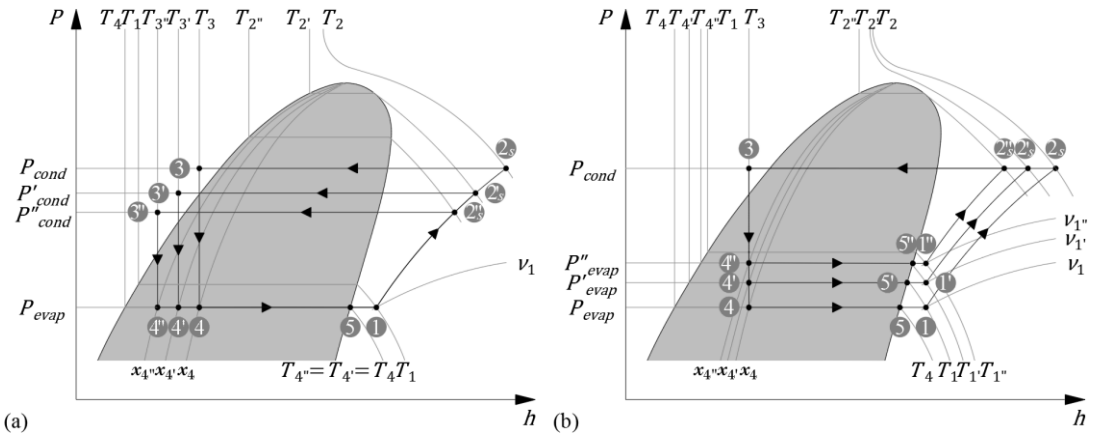

Figure 2.48: Influence of the (a) condensing and (b) evaporating pressure/temperature (source: author)

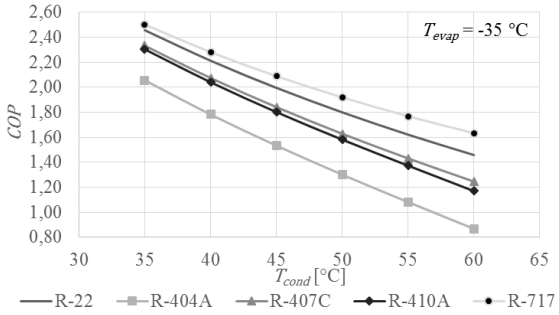

Figure 2.49: COP *vs* T_{cond} (source: author)

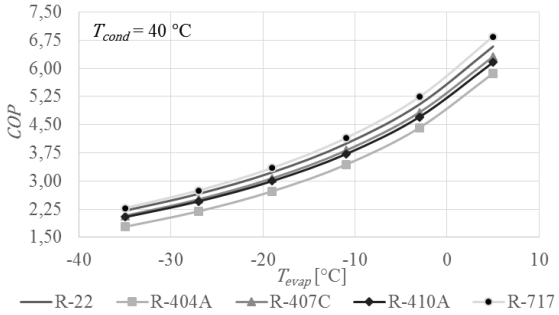

Figure 2.50: COP *vs* T_{evap} (source: author)

2.2.3.2. Influence of subcooling and superheating degree

Considering the subcooling evolutions represented in Figure 2.51a, obtained through the heat transfer from the liquid to an external agent, it is noticeable that all the suction conditions are kept constant (particularly the specific volume, $\Delta v_1 = 0$), as well as the ideal (isentropic) work input ($\Delta w_{ideal} = 0$), and the pressure ratio, $\Delta r_P = 0$. For such conditions, either the volumetric or the isentropic efficiency are practically invariable ($\Delta\eta_v \cong 0$, $\Delta\eta_s \cong 0$) [37]. Resulting $\Delta\dot{Q}_{evap}/\dot{Q}_{evap} > 0$ and $\Delta\dot{W}_{in}/\dot{W}_{in} > 0$, and finally $\Delta COP/COP > 0 \Leftrightarrow \Delta COP > 0 \Leftrightarrow COP' > COP$. Resuming, an increase in the subcooling degree leads to an increase of the system efficiency (Figure 2.52), being more important as higher is the subcooling degree, and the lower is the refrigeration effect [37].

In the analysis of the superheating degree, represented in Figure 2.51b, there are two distinguished effects: (1) the "useful heat", related to the heat transfer from the cooling medium and whose superheating degree is limited to the temperature of the medium, and (2) the "non-useful heat" which is related to gains from motor windings, *etc.*, as explained in section 2.2.2.2. For the same pressure ratio, r_P, it can be considered almost negligible the variation of both volumetric and isentropic efficiencies ($\Delta\eta_v \cong 0$, $\Delta\eta_s \cong 0$)[2], although having variations in the specific volume and in the isentropic compression ($\Delta v_1 > 0$ and $\Delta w_{ideal} > 0$), resulting then $\Delta\dot{Q}_{evap}/\dot{Q}_{evap} = \Delta q_{evap}/q_{evap} - \Delta v_1/v_1$ and $\Delta\dot{W}_{in}/\dot{W}_{in} = \Delta w_{ideal}/w_{ideal} - \Delta v_1/v_1$. For the "non-useful heat", there is no variation in the refrigeration effect (the heat gain is not in the evaporator, $\Delta q_{evap} = 0$), while the specific volume increases after leaving the evaporator. Therefore, $\Delta\dot{Q}_{evap}/\dot{Q}_{evap} = -\Delta v_1/v_1 < 0$, $\Delta\dot{W}_{in}/\dot{W}_{in} \cong 0$ and $\Delta COP/COP \cong \Delta\dot{Q}_{evap}/\dot{Q}_{evap} < 0 \Leftrightarrow \Delta COP < 0 \Leftrightarrow COP' < COP$, and meaning that the "non-useful gain" from the superheating degree leads to a decrease of the system efficiency [37]. By the other hand, for the "useful heat", the signal of the ratio $\Delta\dot{Q}_{evap}/\dot{Q}_{evap}$ is highly dependent on the fluid specific volume, which can have a stronger or weaker variation than variation of the refrigeration effect in the cycle, leading respectively to $COP' < COP$ or $COP' > COP$, once $\Delta\dot{W}_{in}/\dot{W}_{in} = 0$. The superheating degree has a negative impact on the system

[2] It is considered that both volumetric and internal efficiencies are solely dependent on the pressure ratio; However, some studies demonstrated that the volumetric efficiency tends to increase with the superheating degree [37].

efficiency for some refrigerants, *e.g.* ammonia (Figure 2.53), and an enhancing effect over the efficiency for some others [37], corroborating the conclusions of Klein *et al.* [60].

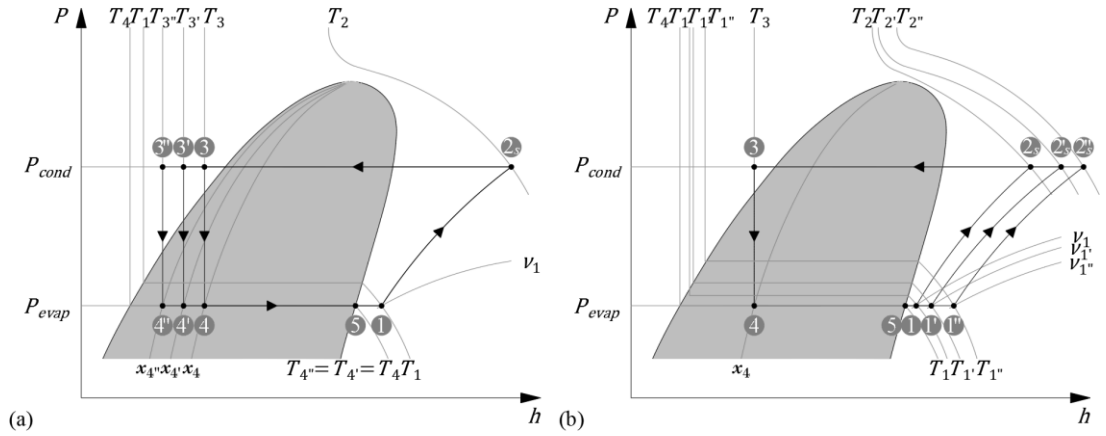

Figure 2.51: Influence of the (a) subcooling and (b) superheating degree (source: author)

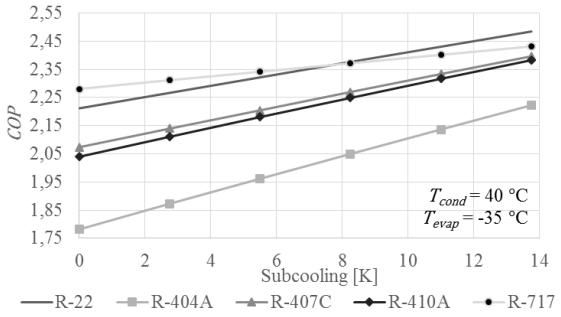

Figure 2.52: COP *vs* subcooling (source: author)

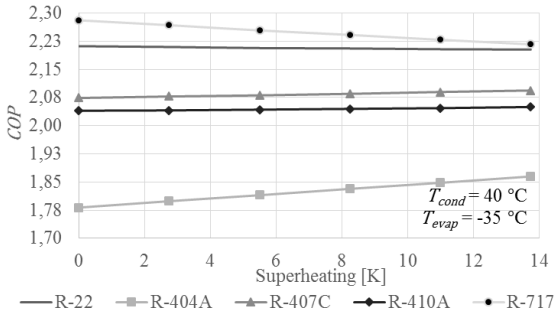

Figure 2.53: COP *vs* superheating (source: author)

2.2.3.3. Influence of the combined effect of subcooling and superheating

The combined effect of subcooling and superheating degree using a LSHX, represented in Figure 2.10, p.19, is similar to the superheating degree, insofar as it depends on the strength of the variation of the specific volume *versus* the increment on the refrigeration effect. In general, the global effect is in the unit order for all refrigerants (higher for halogenated derivatives) and lower than the unit for ammonia [37].

2.2.3.4. Influence of the pressure drops

As it was aforementioned, the existence of pressure drops, either in low- or high-pressure side (which can be seen in Figure 2.14 and Figure 2.15) increases the pressure ratio, r_p, increasing the necessary specific work. Another impact of the pressure drops (in the low-pressure side) is the increase of the specific volume, v_1, which associated to the decrease on the volumetric efficiency, η_v, leads to a reduction in the mass flow rate, $\dot{m}$ [37].

2.2.4. MULTISTAGE COMPRESSION

Single stage systems (presented in the previous section) are pretermitted by multistage arrangements whenever the compression process is not economically feasible. As referred previously, the rise of the pressure ratio, r_P, *i.e.* the rise of the evaporating and condensing temperature difference (temperature lift), brings the following consequences [34], [35], [37], [38]: (1) unacceptably high discharge temperature, causing lubricant deterioration; (2) serious drop in the volumetric efficiency, η_v, where high pressure leaking back to the low pressure side, through the compressor clearances, originates a decrease on the refrigeration capacity, as a direct consequence of the decrease on the refrigerant flow; (3) excessive stress on the compressor moving parts; and (4) an increase on the work input, increasing the energy consumption for compression, during the working period. These effects are particularly harmful for reciprocating compressors, and for this reason, multicylinder reciprocating machines are limited for maximum pressure ratios from 7 to 9 (suction gage pressure is limited to between 35 and 70 kPa) [34], causing the use of a two-stage compressor, to limit the ratio to a typical value of 8, exceeded at evaporating temperatures below -6 °C [35]. However, this limitation is not applicable for screw compressors, which incorporate cooling, being able to operate with pressure ratios up to 20 and achieving low-suction temperatures of about -40 °C, although having a severe efficiency deterioration at high pressure ratios [34], [35]. Whenever these pressure ratio limits are excessed, multistage compression is used, in which the gas coming from the evaporator to the condenser is compressed in several stages, reducing the pressure ratio across each compressor [34], and operating more efficiently [35].

The initial cost of a multistage system is substantially higher than those for single stage, and therefore, the energy savings and the other advantages of the multistage design must compensate [35]. As these savings increase as evaporating temperature drops, the decision of implementing, or at least considering, a two-stage system is taken when the evaporator temperature is below -10 °C [35], and they are commonly used to produce temperatures within the range of -25 °C to -60 °C [34], or when the temperature lift is higher than 50 °C to 60°C, for ammonia, 65 °C for R-22, or 70 °C for R-502 [37]. Below the lower limit of -60 °C, three-stage arrangements should be considered [34] (*e.g.* cryomechanical and cryogenic freezing). In addition to the increase on the overall system operating efficiency, multistage compression also offers the accommodation of multiple loads, at different temperatures and pressures, in the same refrigeration system [34].

Besides of avoiding the deterioration of the lubricant and mechanical stability of the compressor, the main goal of multistage refrigeration is the minimization of the compression work. The minimization of the compression work can either be achieved by: (1) approximating to an internally reversible process as much as possible, through the minimization of the irreversibilities (friction, turbulence, and non-quasi-equilibrium compression), which is taken so far as the technological and economic feasibility allows; or, (2) in a more practical way, keeping the specific gas volume as small as possible during the compression process, maintaining the gas temperature as low as possible during the process [39]. This procedure is achieved cooling the gas while it is compressed, and it can be better understood through the analysis of the integration of Eq. (2.70), for three reversible processes: an isentropic process ($PV^{\gamma} = \text{constant}$, where $n = \gamma$, involving no cooling, Eq. (2.71)), a polytropic process ($PV^{n} = \text{constant}$, where $1 < n < \gamma$, involving some cooling, Eq. (2.71)) and an isothermal process ($PV = \text{constant}$, where $n = 1$, involving maximum cooling, Eq. (2.72)), executed within the same pressure range (P_1 and P_2), and behaving as an ideal gas ($Pv = RT$) [39].

$$w_{ideal} = \int_1^2 v \, \mathrm{d}P = \int_1^2 \frac{RT}{P} \, \mathrm{d}P \tag{2.70}$$

$$w_{ideal} = \frac{n \times R(T_2 - T_1)}{n-1} = \frac{n \times RT_1}{n-1}\left[\left(\frac{P_2}{P_1}\right)^{(n-1)/n} - 1\right] \quad \begin{matrix} n = n \text{ (polytropic)} \\ n = \gamma \text{ (isentropic)} \end{matrix} \tag{2.71}$$

$$w_{ideal} = RT \ln \frac{P_2}{P_1} \tag{2.72}$$

As it can be observed in Figure 2.54, the minimum work required (left-side area below the curves) is the one for the isothermal compression ($n = 1$), while the maximum is for the isentropic compression (adiabatic and reversible, $n = \gamma$). For the polytropic case ($1 < n < \gamma$), the work input requirement will be the lowest as it leans towards the isothermal compression, obtained when enough heat is removed during compression, and the polytropic exponent, n, is decreased approaching unity [39]. Cooling the gas during compression could be achieved using cooling jackets around

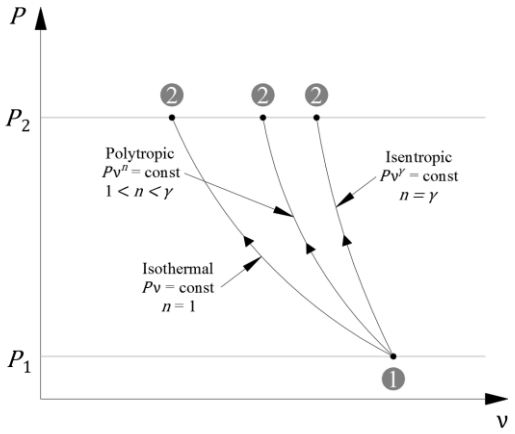

Figure 2.54: P-v diagram of isothermal, isentropic and polytropic compression (source: adapted from [39])

the casing of the compressors. However, this technique is not suitable for all the cases, particularly in medium and large-size equipment, where an inter-stage desuperheating of the discharge vapor from the low-stage compressor (booster), or intercooling, is needed [35], [39]. In an ideal intercooling process, cooling occurs at a constant pressure, and the gas is cooled to the initial temperature T_1 at each desuperheating stage, being firstly compressed from P_1 to an intermediate pressure P_{int}, and then compressed to the final stage pressure P_2 (in a two-stage arrangement), as shown in Figure 2.55a and Figure 2.55b.

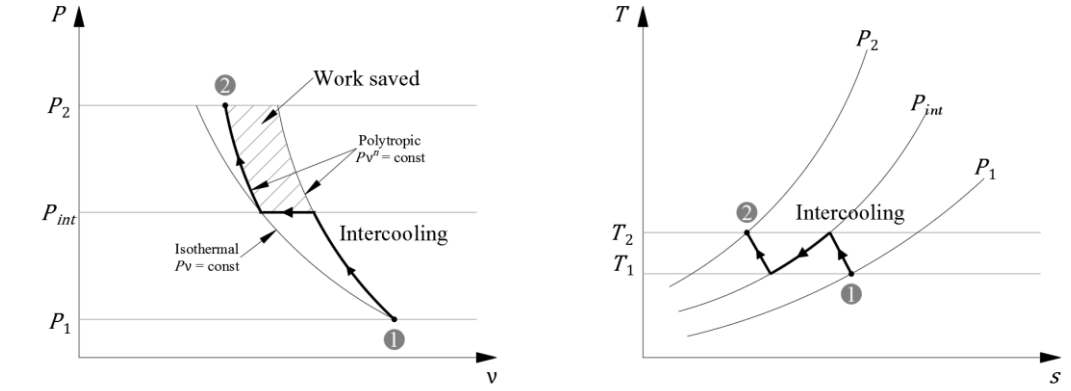

Figure 2.55: P-v and T-s diagram for a two-stage steady-flow compression (source: adapted from [39])

The total work input for a multistage compression is the sum of the work input of each stage of compression, which for a two-stage (I + II) compression results, from Eq. (2.71):

$$w_{ideal\,\text{total}} = w_{ideal\,\text{I}} + w_{ideal\,\text{II}} = \frac{n \times RT_1}{n-1}\left[\left(\frac{P_{int}}{P_1}\right)^{(n-1)/n} - \left(\frac{P_2}{P_{int}}\right)^{(n-1)/n}\right] \quad (2.73)$$

and it can be minimized by differentiating this expression with respect to P_{int}, yielding:

$$\frac{P_{int}}{P_1} = \frac{P_2}{P_{int}} \Leftrightarrow r_{p\,\text{I}} = r_{p\,\text{II}} \quad \text{or} \quad P_{int} = \sqrt{P_1 \times P_2} \quad (2.74)$$

Thus, in a two-stage compression, the minimum work is obtained when the pressure ratio, across each stage of compression, is the same ($r_{p\,\text{I}} = r_{p\,\text{II}}$) [39], which is (approximately) equal to the square root of the overall pressure ratio ($r_{p\,\text{I}} = r_{p\,\text{II}} = \sqrt{P_2/P_1} = \sqrt{r_p}$) [34]. For a three-stage system, each compressor is exposed to a pressure ratio (approximately) equal to the cubic root of the overall pressure ratio [34]. This calculation does not guarantee the system optimization when screw compressors are used [34], and alternative correlations were experimentally obtained: (1) Sandholt: $P_{int} = \sqrt{P_1 \times P_2} + 0.35$ kg.cm^{-2}; or (2) for determining the optimal temperature: (2a) Behringer: $T_{opt} = T_{int} + \Delta T$, where

ΔT =5 °C, T_{int} is the corresponding temperature for the intermediate pressure of Eq. (2.74)(2.88), for an evaporating temperature range from -35 to -10 °C and condensing temperatures within 20 to 35 °C, for ammonia; or (2b) Czaplinsky $T_{opt} = \sqrt{T_1 \times T_2}$ [37].

A single equipment can operate in a two-stage cycle, which is the case of the (1) internally compounded reciprocating compressors, particularly used in small systems requiring low temperature [34]. In these multicylinder compressors, cylinders are grouped in low- and high-compression stages, isolated from each other, and the hot discharge gas from first compression stage is cooled, before the high-stage compression: (1a) in an intercooler, [34], [38]; (1b) in a water-cooler heat exchanger (*i.e.*, an external cooling agent, although with limited efficiency, owed to the impossibility of reducing temperature below the condensing value and to the low heat-transfer coefficient in the vapor side) [37], [38]; or (1c) mixing with intermediate pressure (and temperature) gas, as depicted in Figure 2.56.

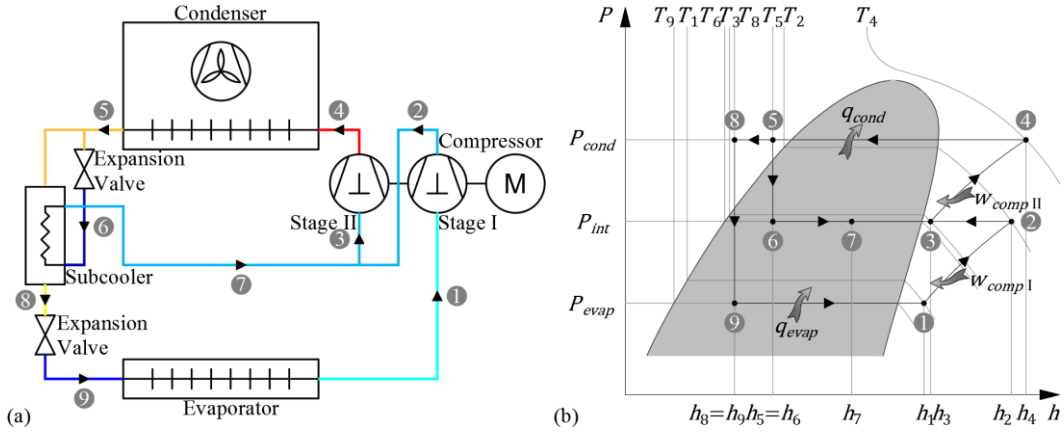

Figure 2.56: Two-stage cycle compounded compressor: (a) circuit and (b) *P*-*h* diagram (source: author)

Other arrangements, can be found, such as (2) the simple injection of a controlled amount of liquid refrigerant, from the condenser, mixing with the intermediate pressure gas [38]; (3) multipurpose systems with a single compressor, commonly used in ordinary refrigerator–freezer units [39], having different temperatures for freezer and refrigerator compartments, whose schematic circuit and *P*-*h* diagram are represented in Figure 2.57; (4) flash-gas removal, drawing off the vapor from the separating vessel, or flash tank, (mass and energy balances in Eq. (2.75)) then compressing and joining it to the vapor from the main compressor (mass and energy balances in Eq. (2.76)), at the condensing pressure [35], as observed in Figure 2.58, bringing two benefits: the useless vapor from the partial expansion is recompressed, in a lower pressure ratio, r_p, and the main engine compresses less mass flow, reducing the power supplied to the compressor, $\dot{W}_{in}$;

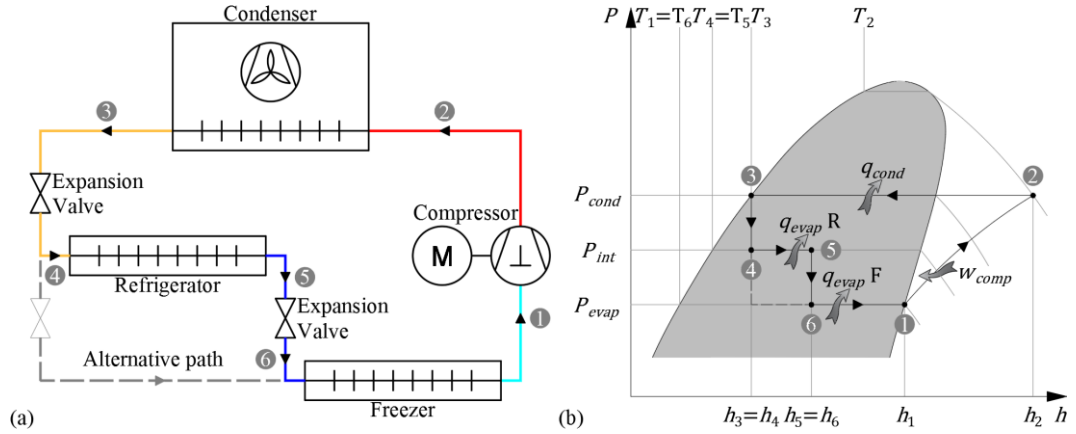

Figure 2.57: Multipurpose systems with a single compressor: (a) circuit and (b) P-h diagram (source: (a) adapted from [39], (b) author)

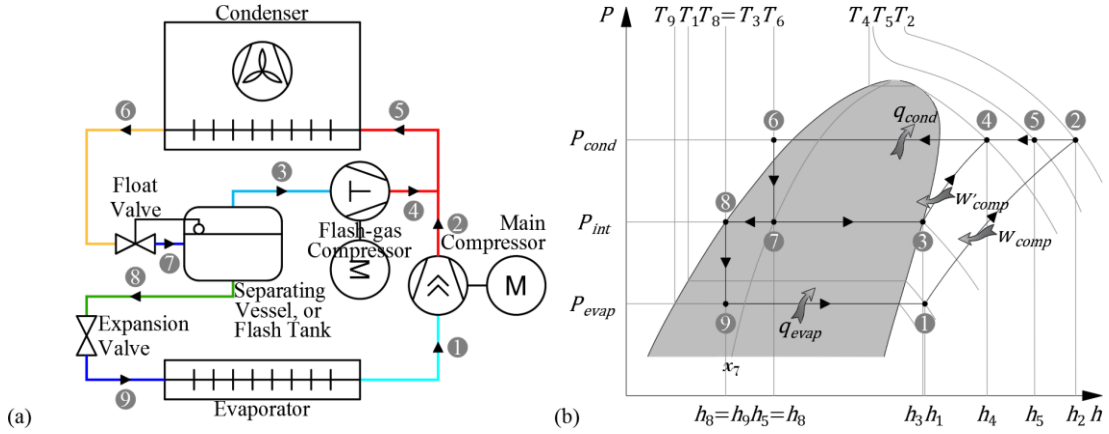

Figure 2.58: Two-stage cycle with flash-gas removal: (a) circuit and (b) P-h diagram (source: author)

$$\begin{cases} \dot{m}_7 = \dot{m}_3 + \dot{m}_8 \\ \dot{m}_7 \times h_7 = \dot{m}_3 \times h_3 + \dot{m}_8 \times h_8 \end{cases} \tag{2.75}$$

$$\begin{cases} \dot{m}_5 = \dot{m}_4 + \dot{m}_2 \Leftrightarrow \dot{m}_7 = \dot{m}_3 + \dot{m}_8 \\ \dot{m}_7 \times h_5 = \dot{m}_3 \times h_4 + \dot{m}_8 \times h_2 \end{cases} \tag{2.76}$$

(5) economized systems (Figure 2.59), frequently used with screw compressors and most beneficial at high pressure ratios, subcooling the refrigerant, in the shell-and-coil economizer (mass and energy balances in Eq. (2.77)), before entering the evaporator, increasing the refrigeration effect, and injecting the vapor generated (during subcooling) in the compressor (mass and energy balances in Eq. (2.78)), decreasing the compressor work (as explained previously); the simultaneous effects increase the system efficiency, reaching similar levels of those achieved by two-stage systems, although being less complex and having simpler maintenance; however, economized systems should be

carefully selected for variable loads (particularly below 75 % capacity), owing the aperture of the economizer port in the compressor suction area, derived from the slide valve position, reverting the efficiency to single-stage compression levels; alternatively, flash economizers are used (as shown in Figure 2.78), due to their higher efficiency [34].

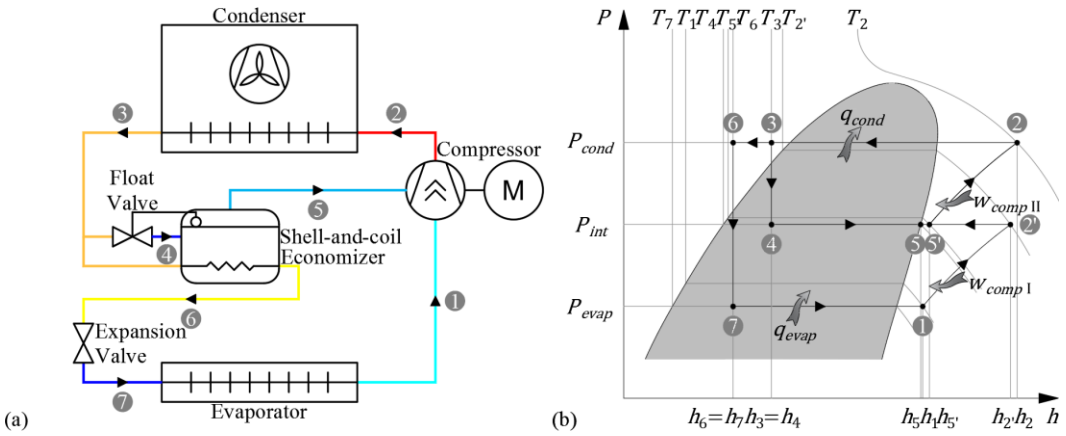

Figure 2.59: Two-stage cycle with shell-and-coil economizer: (a) circuit and (b) *P*-*h* diagram (source: author)

$$\begin{cases} \dot{m}_3 = \dot{m}_5 + \dot{m}_6 \Leftrightarrow \dot{m}_2 = \dot{m}_5 + \dot{m}_1 \\ \dot{m}_2 \times h_3 = \dot{m}_5 \times h_5 + \dot{m}_1 \times h_6 \end{cases} \tag{2.77}$$

$$\begin{cases} \dot{m}_2 = \dot{m}_5 + \dot{m}_1 \\ \dot{m}_2 \times h_2 = \dot{m}_5 \times h_5 + \dot{m}_1 \times h_1 \end{cases} \tag{2.78}$$

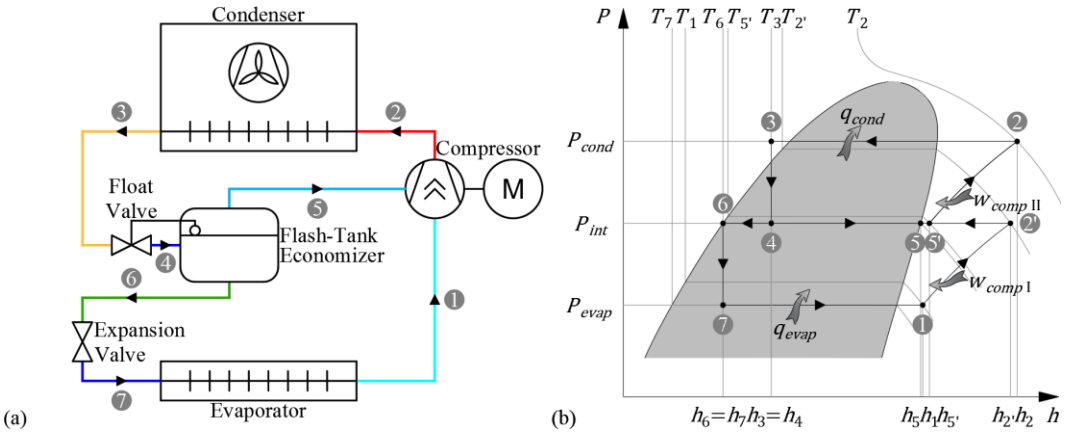

Figure 2.60: Two-stage cycle with flash economizer: (a) circuit and (b) *P*-*h* diagram (source: author)

Multistage compression can be classified in: (1) direct multistage, using the same refrigerant throughout a common circuit; or (2) indirect multistage compression, or simply cascade refrigeration system, operating with one or more refrigerants and having two separate refrigeration systems, one acting as a condenser of the other [37], [38].

2.2.4.1. Direct multistage compression

Regarding the cooling agents used in desuperheating processes, they could either be categorized as external or internal. External cooling agent systems, normally using water or air, are often deprecated due to their restrictions (the aforementioned temperature and heat-transfer coefficient limitations, besides being restricted to systems having dedicated cooling water pump systems, such as trucks), whereby most of the direct multistage compression systems use an internal cooling agent [37]. The most-used interstage desuperheating strategies are[35], [37]: (1) liquid injection (directly or passing through a heat-exchanger), (2) liquid subcooling (using a flash or a shell-and-coil economizer), and (3) intercooling (simple, total injection with flash-gas removal or partial injection).

I. Liquid injection

The injection of liquid refrigerant (shown in Figure 2.61 and mass and energy balances in Eq. (2.79)), at the outlet of the low-pressure compressor, is the simplest, most compact and least-expensive desuperheating strategy, demising suction filter in the high-pressure side, discharge oil separator in the low-pressure side, and demanding a simple operating control [37]. This strategy is advantageous for cycles using ammonia, disadvantageous for R-502, it has practically no benefits for R-22 (depends on the specific volume, v), and it is used in low and medium-capacity systems, using ammonia and R-22 [37].

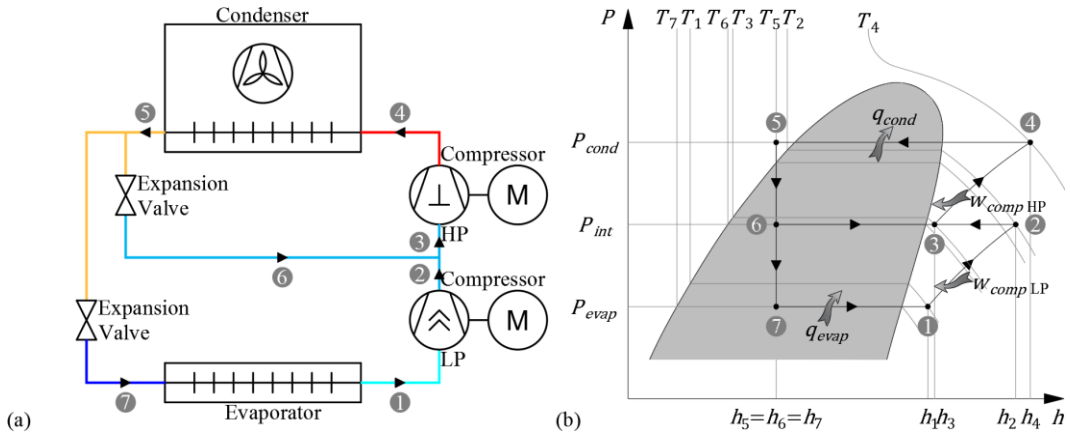

Figure 2.61: Two-stage cycle with liquid injection: (a) circuit and (b) P-h diagram (source: adapted from [37])

$$\begin{cases} \dot{m}_5 = \dot{m}_6 + \dot{m}_7 \Leftrightarrow \dot{m}_3 = \dot{m}_6 + \dot{m}_2 \\ \dot{m}_5 \times h_5 = \dot{m}_6 \times h_6 + \dot{m}_7 \times h_7 \Leftrightarrow \dot{m}_3 \times h_5 = \dot{m}_6 \times h_6 + \dot{m}_2 \times h_7 \\ \dot{m}_3 \times h_3 = \dot{m}_2 \times h_2 + \dot{m}_6 \times h_6 \end{cases} \quad (2.79)$$

II. Liquid subcooling

The liquid subcooling method allows to reduce the irreversibility issue of the isenthalpic expansion, through a multistage expansion (technically limited to the number of levels minus one) [37]. It avoids the useless and energy-consuming full compression of flash-gas, formed during the first-stage expansion, at the intermediate pressure, increasing the heat transfer rate in the evaporator, inasmuch the presence of vapor decreases the thermal efficiency of the evaporator; finally, the flash-gas mixing with the low-pressure discharge gas produces a desired subcooling degree before the high-pressure compression [37]. A two-stage cycle with subcooling and flash-tank can be seen in Figure 2.62 (mass and energy balances in Eq. (2.80)), and another usual configuration, with a shell-and-coil economizer can be seen in Figure 2.63 (mass and energy balances in Eq. (2.81)).

In these systems, the refrigeration effect increases, being higher than that provided by standard systems, without subcooling, although the mass flow decreases, which can be an undesirable effect depending on the operating conditions and on the used refrigerant [37]. It is advantageous for systems using R-502, but should not be used with R-22 or ammonia (owed to the high vapor temperatures achieved during the compression) [37]. To solve this constrain, allowing the use of this method for all refrigerants and enabling a security bypass of the economizer (in fault case), an additional direct liquid injection is used [37].

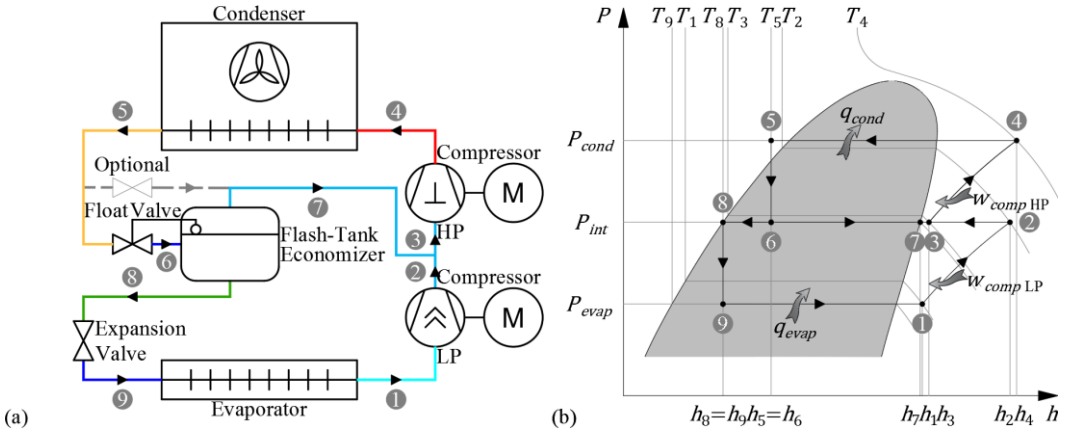

Figure 2.62: Two-stage cycle with subcooling and flash tank: (a) circuit and (b) *P*-*h* diagram (source: adapted from [37])

$$\begin{cases} \dot{m}_6 = \dot{m}_7 + \dot{m}_8 \Leftrightarrow \dot{m}_3 = \dot{m}_7 + \dot{m}_2 \\ \dot{m}_6 \times h_6 = \dot{m}_7 \times h_7 + \dot{m}_8 \times h_8 \Leftrightarrow \dot{m}_3 \times h_6 = \dot{m}_7 \times h_7 + \dot{m}_2 \times h_8 \\ \dot{m}_3 \times h_3 = \dot{m}_2 \times h_2 + \dot{m}_7 \times h_7 \end{cases} \quad (2.80)$$

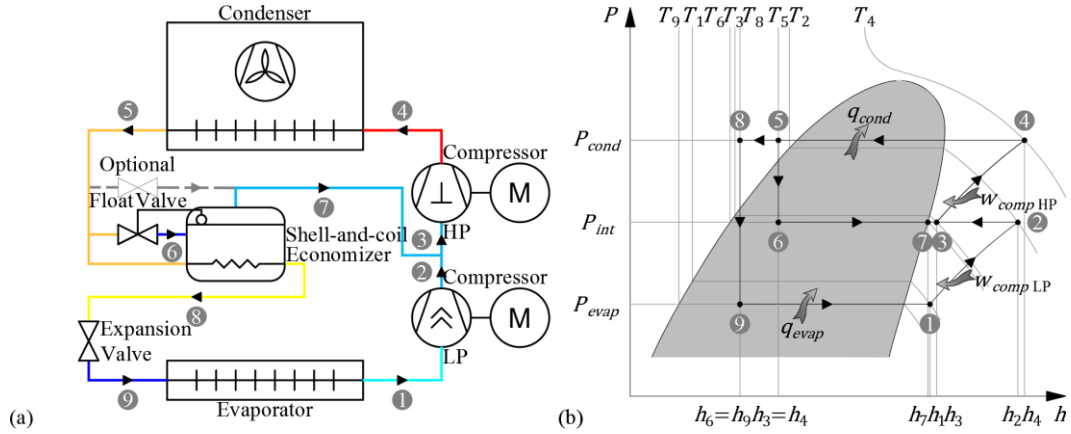

Figure 2.63: Two-stage cycle with subcooling and shell-and-coil tank: (a) circuit and (b) *P-h* diagram (source: adapted from [37])

$$\begin{cases} \dot{m}_5 = \dot{m}_7 + \dot{m}_8 \Leftrightarrow \dot{m}_3 = \dot{m}_7 + \dot{m}_2 \\ \dot{m}_6 \times h_6 + \dot{m}_8 \times h_5 = \dot{m}_7 \times h_7 + \dot{m}_8 \times h_8 \Leftrightarrow \dot{m}_3 \times h_5 = \dot{m}_7 \times h_7 + \dot{m}_2 \times h_8 \\ \dot{m}_3 \times h_3 = \dot{m}_7 \times h_7 + \dot{m}_2 \times h_2 \end{cases} \quad (2.81)$$

III. Liquid injection with subcooling

An alternative to the former liquid subcooling methods, avoiding the problems that a partial evaporation of the saturated liquid might bring before the second-stage expansion, in the cycle represented in Figure 2.62a, or the constrains imposed for R-22 or ammonia, is the liquid injection with subcooling, presented in Figure 2.64 (mass and energy balances similar to Eq. (2.81), differing the location of 7, compared to Figure 2.63b) [37]. The major part of the flow passes through the low-pressure branch, implying a second-stage valve working for the total rate (being advantageous), this system is more expensive (owed the heat exchanger), having similar application to the liquid injection systems [37].

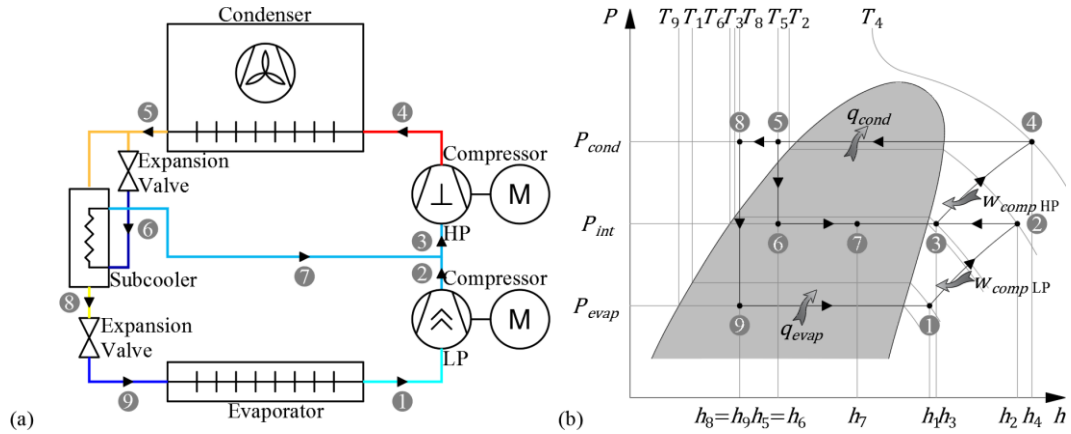

Figure 2.64: Two-stage cycle with liquid injection and subcooler: (a) circuit and (b) *P-h* diagram (source: adapted from [37])

IV. Intercooling

Intercooling is an efficient interstage desuperheating method, particularly for high-capacity and low-temperatures applications using ammonia (as shown in Figure 2.65a) [35], [37], where the combined effect of liquid subcooling, in multistage expansion, and desuperheating is crucial for an adequate and efficient system operation. For other refrigerants, such as R-134a and R-507 (replacement options for R-22) in other applications, the flash-gas removal, alone or combined with desuperheating, is the method that provides a higher percentage of energy savings, when comparing to a single-stage compression (Figure 2.65b, considering 100 % efficiency compressors) [35].

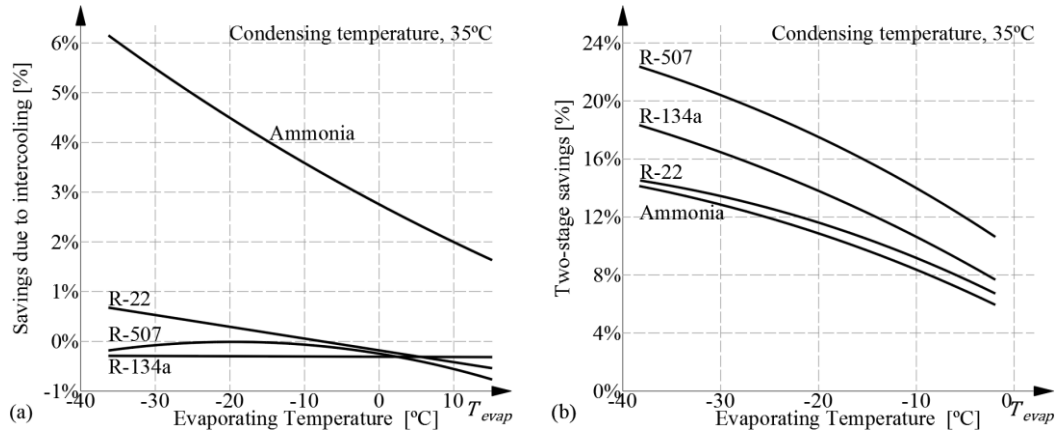

Figure 2.65: Energy savings with: (a) simple intercooling and (b) two-stage compression with flash-gas removal and desuperheating (source: adapted from [35])

Figure 2.65a represents the energy savings of a simple intercooling cycle, as the one represented in Figure 2.66a, whose mass and energy balances in expressed by Eq (2.82).

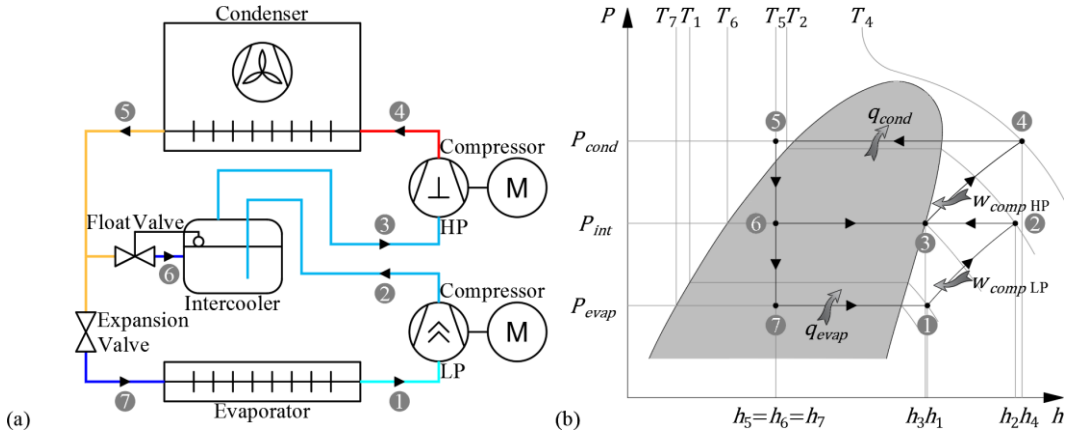

Figure 2.66: Two-stage cycle with simple intercooling: (a) circuit and (b) *P*-*h* diagram (source: adapted from [35])

$$\begin{cases} \dot{m}_3 = \dot{m}_6 + \dot{m}_2 \Leftrightarrow \dot{m}_5 = \dot{m}_6 + \dot{m}_7 \\ \dot{m}_3 \times h_3 = \dot{m}_6 \times h_6 + \dot{m}_2 \times h_2 \Leftrightarrow \dot{m}_5 \times h_3 = \dot{m}_6 \times h_6 + \dot{m}_7 \times h_2 \end{cases} \quad (2.82)$$

Additionally to the simple intercooling process, a liquid subcooling can be incorporated, providing interstage expansion and thus, increasing the overall efficiency. Such systems can be classified as (1) total injection, using a flash (or open) intercooler (Figure 2.67, mass and energy balances in Eq. (2.83)); or (2) partial injection, using a shell-and-coil (or closed) intercooler (Figure 2.68, mass and energy balances in Eq. (2.84)) [37].

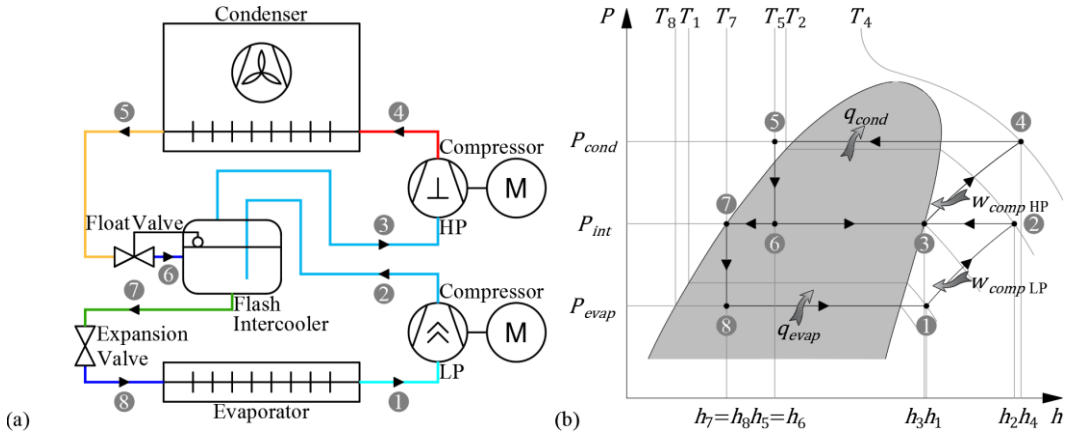

Figure 2.67: Two-stage cycle with flash intercooler (total injection): (a) circuit and (b) P-h diagram (source: adapted from [37])

$$\begin{cases} \dot{m}_2 + \dot{m}_6 = \dot{m}_3 + \dot{m}_7 \\ \dot{m}_2 \times h_2 + \dot{m}_6 \times h_6 = \dot{m}_3 \times h_3 + \dot{m}_7 \times h_7 \end{cases} \tag{2.83}$$

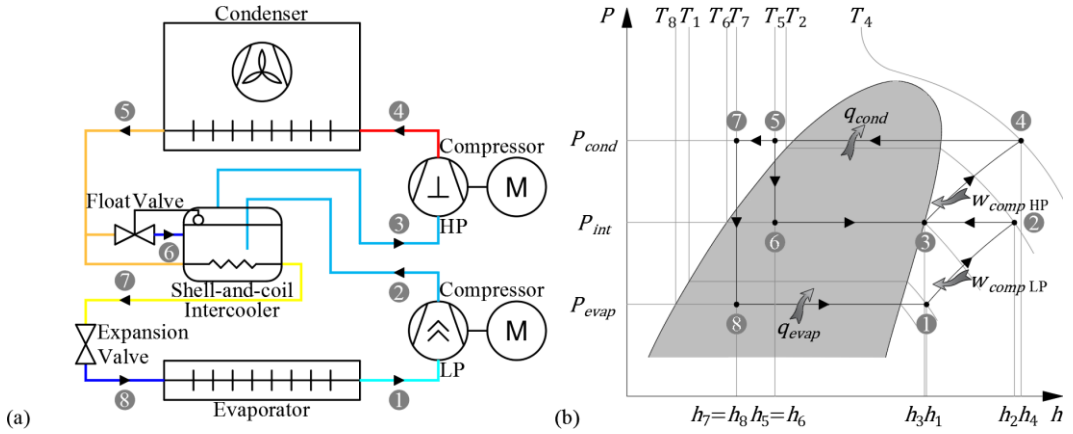

Figure 2.68: Two-stage cycle with shell-and-coil intercooler (partial injection): (a) circuit and (b) P- h diagram (source: adapted from [37])

$$\begin{cases} \dot{m}_2 + \dot{m}_5 = \dot{m}_3 + \dot{m}_7 \\ \dot{m}_2 \times h_2 + \dot{m}_5 \times h_5 = \dot{m}_3 \times h_3 + \dot{m}_7 \times h_7 \end{cases} \tag{2.84}$$

The shell-and-coil methods, although being less efficient by several percent (owing to the finite heat-transfer surface limitation, implying always $T_7 < T_6$, Figure 2.68b) than the total injection type ($T_7 = T_6$, Figure 2.67b), allows the operation of the expansion

valve between both condensing and evaporating pressures, providing more working stability and for this reason, it is normally preferred in these applications [34], [37]. The overall efficiency of intercooling systems can be increased, to the highest available values, if indirect lubricant cooling is used, particularly in screw compressors working with ammonia [34]. The following scheme, Figure 2.69, exhibits a typical two-stage screw compressor system, for high- and low-temperature applications, provided with a flash-intercooler doubling as a medium-temperature receiver, and thermosiphon lubricant cooling. An energy efficiency enhancement is obtained using the indirect lubricant cooling [34]: (1) the heat removal from the low-stage (booster) motor relieves approximately half of this load from the high-stage compressor, dismissing the liquid injection cooling (10 % less efficient); (2) the heat removal from the high-stage motor increases on about 15 % of the overall efficiency, when compared to systems without intercooling, or injection cooling; (3) electric energy savings around 20 to 30 %, during low-temperature months, due to the reduction of the condensing (gage) pressure to 600 to 700 kPa, contrasting to the threshold of 850 to 900 kPa when using injection cooling. The intermediate pressure is controlled by the relative pumping rates of both compressors, and the pressure of the low-pressure evaporator is regulated by the pumping capacity of the booster, while the intermediate is regulated by the pumping capacity of the other compressor; however, both stages should work in unison, as the high-stage compressor must pump the same mass flow rate as the low-stage, plus that resulting from flash and desuperheating gas, as well as the one from the intermediate-temperature evaporator [34].

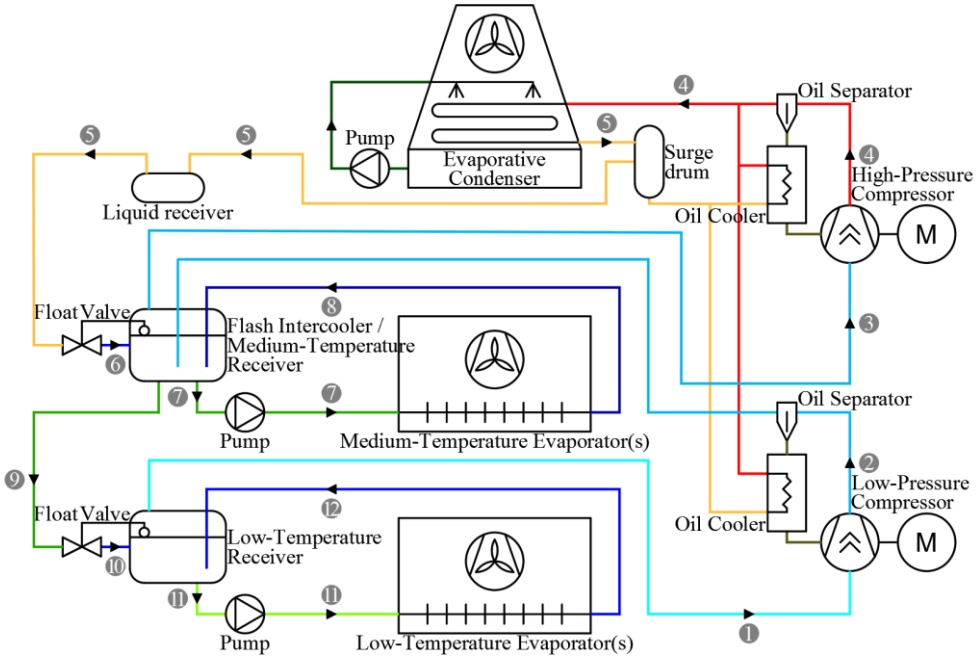

Figure 2.69: Two-stage system with thermosiphon cooled screw compressors (source: adapted from [34])

2.2.4.2. Indirect multistage compression or cascade refrigeration

In some refrigeration applications, the low-temperature requirements may raise some difficulties to conventional refrigerants, owing [37]: (1) the low evaporating pressure, lower than atmospheric pressure, exposing the system, in case of rupture, to the entrance of moist air; (2) the temperature decrease, and both increase on the specific volume, v, (at the compressor inlet) and displacement rate, $\dot{V}_d$, to assure the desired mass flow rate, $\dot{m}$; and (3) the reduction of the refrigeration effect, q_{evap}, due to the increase on the vapor quality, x, as the evaporating temperature falls down. Even specific refrigerants, specially developed for low-temperature applications, failed in operability, demanding extreme robustness either in equipment or operation [37], or leading to poor performances of the compressors [39]. These constraints can be surpassed performing the refrigeration process in stages, having two or more refrigeration cycles operating in series, in an indirect multistage compression process, also known as cascade compression [37], [39].

Figure 2.70 shows a two-stage cascade refrigeration system, where both cycles (upper and lower cycle) are connected through a heat exchanger in the middle, serving as an evaporator for upper cycle and as a condenser for the lower cycle. Assuming an ideal heat exchanger, the heat transfer rate from the lower to upper cycle stands as expressed in Eq. (2.85) and the COP equation as expressed in Eq. (2.86).

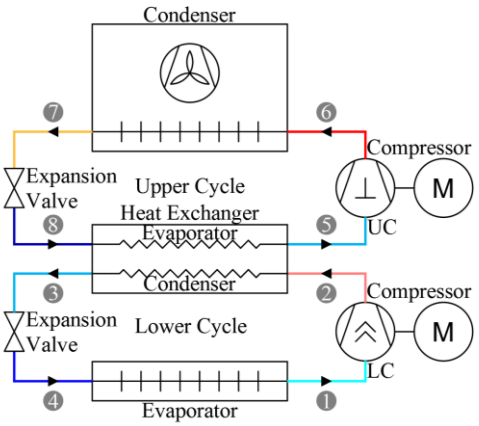

Figure 2.70: Two-stage cascade refrigeration system (source: author)

$$\dot{m}_{\mathrm{UC}} \times q_{evap\,\mathrm{UC}} = \dot{m}_{\mathrm{LC}} \times q_{cond\,\mathrm{LC}} \Leftrightarrow \dot{m}_5 \times (h_5 - h_8) = \dot{m}_3 \times (h_2 - h_3) \tag{2.85}$$

$$\begin{aligned} COP_{cascade} &= \frac{\dot{Q}_{evap}}{\dot{W}_{in}} = \frac{\dot{m}_{\mathrm{LC}} \times q_{evap\,\mathrm{LC}}}{\dot{m}_{\mathrm{LC}} \times w_{in\,\mathrm{LC}} + \dot{m}_{\mathrm{UC}} \times w_{in\,\mathrm{UC}}} \\ &= \frac{\dot{m}_3 \times (h_1 - h_4)}{\dot{m}_3 \times (h_2 - h_1) + \dot{m}_5 \times (h_6 - h_5)} \end{aligned} \tag{2.86}$$

Cascade systems normally have different refrigerants in each system, using those with the most desirable characteristics for each cycle [39], although the analysis on the impact in the system performance is easier to expose considering the same fluid in both cycles, as represented in the following P-h and T-s diagrams, Figure 2.71. As it can be seen, the

compressor work decreases and refrigeration capacity increases, comparing to a single-stage cycle, therefore, cascading improves the COP of a refrigeration system [39]. Theoretically, cascade systems can have an infinite number of stages, inasmuch as the COP increases with the number of stages. However, this grow has an important initial increment on efficiency, from single- to two- or three-stage cycles, and eventually until the fourth stage (depending on the properties of the refrigerants), and the increment will be smoother as the number of stages increases [37]. Two-stage cycle is the most used configuration, although some systems use three or four stages of cascading [39].

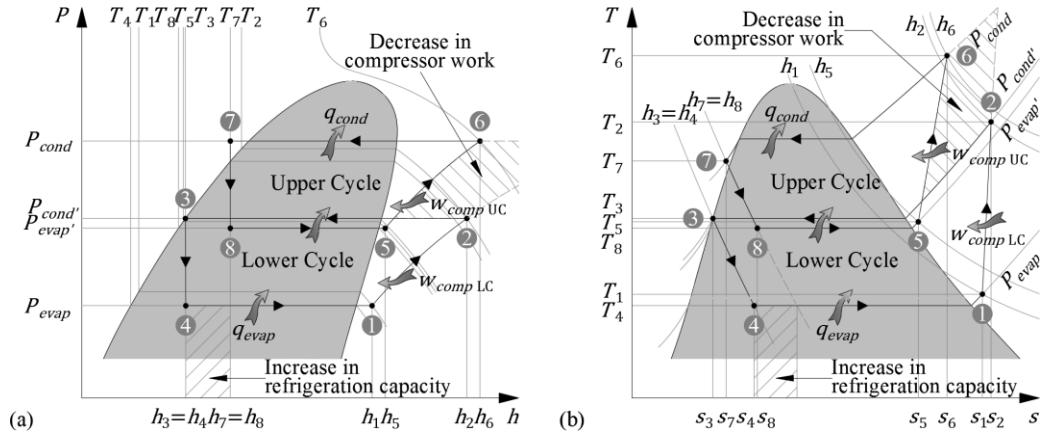

Figure 2.71: P-h (a) and T-s (b) diagrams for a two-stage cascade (source: author)

Regarding the technological aspects, cascade condensers can be manufactured in many forms, depending on the system size and end-use: (1) for industry, shell-and-tube, submerged, direct-expansion double coils, embossed and welded-plate heat exchangers; or (2) for commercial use, brazed-plate, coaxial and tube-in-tube heat exchangers [34]. Due to the high pressures and temperature fluctuations of both refrigerants, the cascade heat exchanger vessels must be constructed under strict requirements, also preventing internal leakages, consequent cross-contamination and combined reaction of both fluids, which might damage the entire refrigeration system (particularly in NH_3/CO_2) [34].

Another important aspect on using cascade cycles is the reduction of the refrigerating charge, owing the low quantity demand in the high-temperature cycle. In commercial applications, such as supermarkets, the reduction of the primary refrigerant charge can be as much as 75 %, while in industry, and particularly in systems using ammonia, its charge can be reduced by approximately 90 %, compared to a conventional ammonia system of the same capacity [34]. This advantage is very important either in industrial applications, minimizing the amount of ammonia on site (normally limited to the compressor room and the condenser flat), or in commercial systems, reducing hydrofluorocarbons (HFCs)

refrigerant losses (and consequent emissions), simplifying regulatory requirements, or reducing operator staff [34]. Besides ammonia, in the upper cycle, R-22, azeotropes, and refrigerant blends or zoetropes are used, while in the lower cycle, R-23 (a HFC) and, presently and mostly R-744 (carbon dioxide, CO_2, a natural refrigerant) is used [34]. Furthermore, and additionally to their great impact on the reduction of HFCs, CO_2 cascades enable the use of existing equipment (compressor and condenser), except for the low-side evaporator and piping and the additional CO_2 pump, which allied to simpler and easier maintenance, and fewer tuning control, make these systems a versatile and feasible option when refurbishing a facility [34]. Although the introduction of a CO_2 circulator pump, the energy consumption is not significantly changed, owing to the reduction on suction losses and the increment on the evaporator heat transfer process, which may raise the evaporating temperature in about 5 to 6 K [34].

NH_3/CO_2 cascades refrigeration systems (normally used in industry [34], and with a potential use in the conversion of large food storage facilities operating with ammonia [62]) are more efficient than two-stage ammonia systems, especially for temperatures below -40 °C, and in case of having plate freezers, the high heat transfer and low pressure drop combination gives CO_2 an incomparable advantage [63]. NH_3/CO_2 cascades are used in industrial low-temperature applications such as ice machinery, spiral and belt freezers, blast freezers, freeze drying, and in many other food and industrial product freezing systems [34]. HFCs/CO_2 cascades are normally used in commercial applications (HFCs as primary refrigerants), being commonly design to operate multi-temperature evaporators (*e.g.* display cases) and providing heat recovery to generate service hot water or space heating [34], as depicted in Figure 2.72.

All cascade refrigeration systems face an inherent problem, related to the high-temperature difference between the evaporator outlet and the environment air, which although all the insulation care, produces a superheating degree, particularly undesired for refrigerants commonly used in the low-temperature cycles (such as ammonia, and as explained previously) [37]. Owing this inevitability, these systems are provided with heat exchangers (Figure 2.73), offering a useful heat transfer, by: (1) the vapor superheating of the suction gas from the low-pressure compressor in two steps, firstly, subcooling the liquid from the lower cycle and then same with the liquid from the upper cycle (increasing the refrigeration effect, and also avoiding the compressor operation in extreme temperature conditions); and by (2) the additional gas cooling (with an gas cooler or

another heat exchanger), reducing the thermal load transferred to the upper cycle, through the cascade condenser, and limiting the superheating of the upper cycle suction gas [37]. The effect of these subcooling and desuperheating processes, not only reduces the energy requirements, as it helps on the reduction of oil carryover (due to desuperheating) [34].

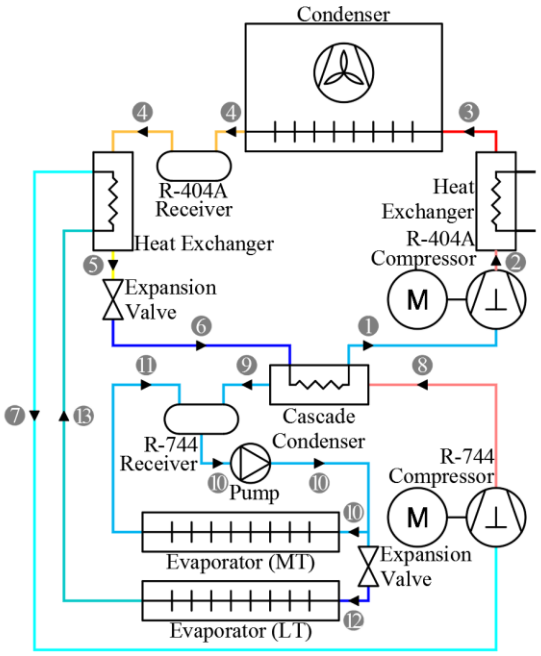

Figure 2.72: Dual temperature system cascade R-404A/CO_2 (source: adapted from [34])

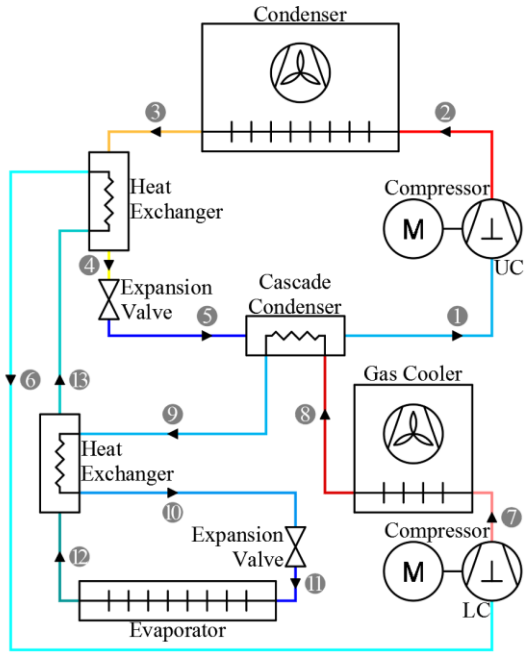

Figure 2.73: Complete cascade system (source: adapted from [37])

Environmental restrictions on the use of fluorinated gases, and the urgency to provide energy-efficient and environmental-friendly solutions, has been triggering a huge effort in research and engineering fields [64]. In the last few years, many experimental research using CO_2 cascades have been performed, either for ammonia (NH_3 or R-717 [65]) or HFCs (*e.g.* R-134a [66], R-404A [67]), preceding the European (and worldwide, particularly in the United States of America (USA) [68]) trend on using CO_2 cascades in commercial refrigeration [69]. According to a survey (data reported to the year 2013), there was a minimum of 1638 stores in Europe using HFCs/CO_2 cascade systems, with the majority of the cases registered in central Europe (Germany, Switzerland and Netherlands) and also in Italy [70]. The same study also indicates 19 stores using NH_3/CO_2 and 5 using hydrocarbons (HC)/CO_2 cascade systems [70]. None of them (HFCs, ammonia or HC/CO_2 cascade systems) was registered in Portugal.

2.2.5. OTHER VAPOR-COMPRESSION CYCLES

As aforementioned, and corroborated by several authors ([38], [40], [59], [62], [64]–[72]), CO_2 has been recovering its place in vapor-compression systems. Being a natural refrigerant, it accomplishes with the increasingly restrictive environmental legislation. However, its low COP comparing to other refrigerants (as shown in Table 2.10, within a temperature range from -15 to 30 °C), inhibits its use in conventional vapor-compression systems [40], [71]. This limitation is related to its critical point: low critical temperature and high critical pressure (31.06 °C, at 7.38 MPa [61]), as the cycle efficiency drastically decreases with the approximation of the condensing temperature to the critical value [38]. As advantages, CO_2 presents high latent heat and a heat transfer coefficient, which combining with the high pressure and density operating conditions, results in a high volumetric refrigeration capacity (3 - 10 times larger than synthetic and hydrocarbon refrigerants), using very small compressors and small diameter pipelines, besides being environmental harmless, (virtually) nontoxic, nonflammable and inexpensive [38], [68]. For these reasons, CO_2 is commonly used: (1) as a secondary refrigerant, (1a) in the low-stage of cascade systems, using vapor-compression cycles (as presented previously); or (1b) in secondary loop system (having no compressors, only with liquid circulation); or (2) as a primary refrigerant in transcritical cycles, which is slightly different from standard vapor-compression cycles [34], [38]. Both systems, secondary loop and transcritical cycle will be presented ahead, with an especial focus on the CO_2.

Table 2.10: Thermodynamic efficiency (COP) of different refrigerant (source: author)

Refrigerant / System	$\boldsymbol{COP}$
Carnot refrigerator $COP_{R,\,Carnot} = T_{evap}/(T_{cond} - T_{evap})$	5.74
R-717 (NH_3, ammonia)	4.75
R-22 (Chlorodifluoromethane)	4.66
R-407C (R-32/125/134a (23/25/52))	4.53
R-410A (R-32/125 (50/50))	4.46
R-404A (R-125/143a/134a (44/52/4))	4.19
R-744 (CO_2, carbon dioxide)	2.72

The COP calculations, in the foregoing table, were performed using CoolPack™, version 1.50 [61], considering a subcooling and superheating level of 0 K, in a one-stage cycle with DX evaporator, having no LSHX and no pressure nor thermal losses, and an isentropic (ideal) compressor.

2.2.5.1. Secondary loop systems

Secondary loop systems, also known as liquid-chilling systems, are comprised of two circuits, in the same way as cascade systems, although, only the primary circuit is vapor-compressed, while the secondary loop is pumped, being both circuits coupled by a secondary fluid heat exchanger [68], [73], [74]. Alternatively, a thermosiphon can replace the forced circulation in the secondary loop, especially for CO_2, eliminating the pumping consumption [74]. Secondary loop systems use two kinds of secondary refrigerants: (1) single phase fluids, such as water, brine or other aqueous (using glycol, ethyl alcohol, chloride salts, potassium acetate and formate) or non-aqueous antifreeze solution (diethylbenzene or hydrocarbon mixtures, hydrofluoroether, and polydimethylsiloxane); or (2) two-phase secondary refrigerants, taking advantage from the high latent heat during the phase change process, such as ice slurries (having 4 to 6 times more cooling capacity than chilled water, depending on ice fraction), and mostly, in the last few years, CO_2 [74]. The high-temperature circuit is based in a DX configuration, and the primary refrigerant depends on the final use of the refrigeration system, mainly R-404A for commercial refrigeration [68], ammonia for industrial low-temperature refrigeration and in the food industry (normally using chilled water or propylene glycol in the secondary loop) [34], [73], and R-134a, R-407C, R-410A (among others) for water chilling in HVAC systems, which is the most common application for secondary loops [73]. Likewise cascade systems, the major advantage is the reduction of the refrigerating charge, owing the low quantity demand in the primary cycle, comparing to standard vapor-compression systems.

A CO_2 secondary loop, with R-404A as primary coolant, is shown in Figure 2.74, although other configurations are possible, *e.g.* a combined CO_2 secondary cascade (Figure 2.72).

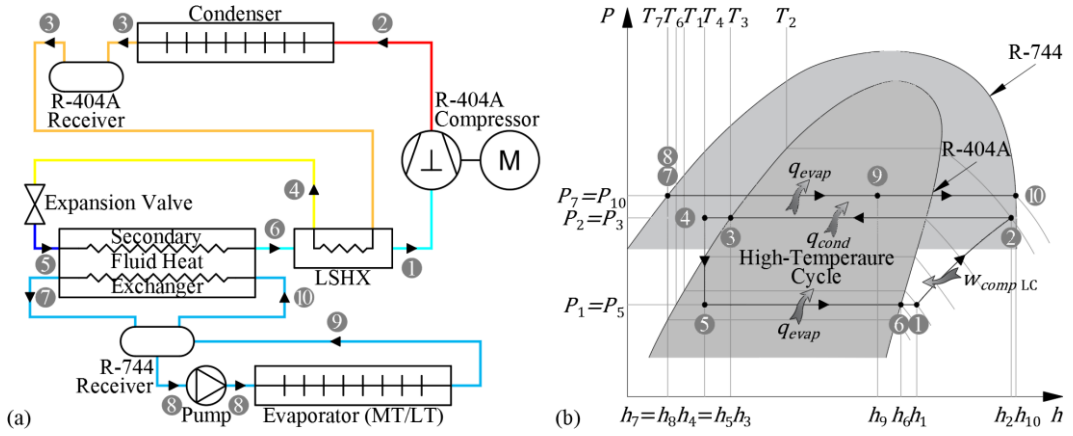

Figure 2.74: CO_2 secondary loop system: (a) circuit and (b) *P-h* diagram (source: adapted from [68])

2.2.5.2. Transcritical carbon dioxide cycle

Although being mostly categorized as “vapor-compression”, the transcritical CO_2 cycle is sometimes regarded as “non vapor-compression” [38]. The explanation for such disagreement is probably relying on the fact of (1) the heat rejection for a transcritical process does not result in a phase change of the working fluid (*i.e.* no condensation), as it happens in conventional vapor-compression cycles, owing the occurrence of heat rejection above the critical temperature of the refrigerant; and (2) to the liquid formation only taking place during the expansion evolution, where a partial condensation occurs, once the cooled gas turns into a mixture of liquid and gas, after passing through the throttling device [34], [38], [71]. Nonetheless, most of the evolutions of the transcritical cycle are identical to those from the conventional (subcritical) vapor-compression cycle: heat addition, compression and expansion, if neglecting that it starts in supercritical gas conditions, instead of saturated or subcooled liquid [71], as represented in Figure 2.75. As a matter of fact, one of the major disadvantages from the transcritical cycle is the large throttling irreversibility, owing high-pressure difference during the expansion, whose losses can be partially recovered using ejectors [57]–[59], or expanders (reducing the enthalpy during the expansion process, recovering some work and reducing the electric input of the compressor) [34], [53]. Other disadvantages such as the larger irreversibilities in the heat exchanging and higher working pressures, are supplanted by better transport properties (particularly in the region of the critical point), and better compressor efficiencies, owing to their lower pressure ratios [71]. Current technology used in component design, as the development of hermetic and semi-hermetic multistage CO_2 compressors, have made it possible to operate in previously unattainable pressure ranges, and in an efficient, reliable and cost-effective way [34], [42].

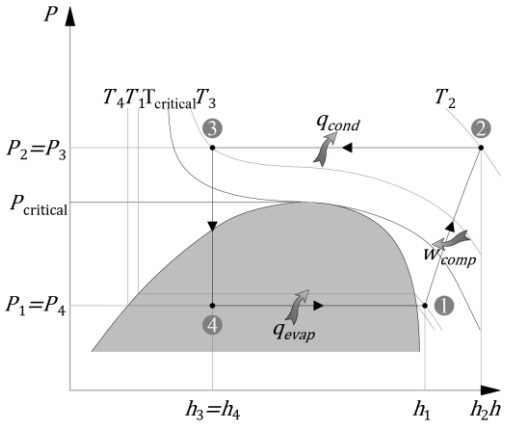

Figure 2.75: P-h diagram for a transcritical cycle (source: author)

The transcritical CO_2 cycle was presented in the 1990s as a measure to reduce the global warming impact from the HFC-based air conditioning and refrigeration systems [40], [71]. However, it has been a non-consensual issue, inasmuch as the climate impact depends not only on the refrigerant global warming potential (GWP) and its leak rate, but

also on the system efficiency, particularly for individual applications [71]. The main reason is related to the outdoor operational conditions, *e.g.* in colder climates (such as northern regions of Europe and USA), the energy consumption of transcritical CO_2 systems can be 5 % lower than typical direct HFC systems, while for warmer climates (such as southern regions of Europe and USA), the energy consumption may increase by 5 % [34], [68]. Indeed, the use of transcritical CO_2 systems has been limited to temperate climates, since its efficiency and refrigeration capacity undergo a rapid deterioration in hot climates [75]. However, there has been a research and technological effort to increase the efficiency of the transcritical CO_2 systems and to make it applicable to warmer climates [64], [68], enabling the so-called "CO_2 efficiency equator" moving further south.

The energy efficiency of transcritical CO_2 systems can be maximized by: (1) minimizing the irreversibilities (*e.g.* using ejector technology, Figure 2.46, presented previously); (2) determining the optimum operating pressure, which can be obtained between the balance of the highest-achievable cooling effect and the smallest amount of energy input (as the discharge pressure is raised, the resulting enthalpy of the cold gas is reduced); and (3) enabling the operation of the gas cooler as a condenser, in colder weathers, and its control, switching from gas cooler operation (with a restricted outflow passing through the air-cooled heat exchanger) to condenser operation (having no restrictions, as conventional subcritical systems) [34], [38]. In the first case, additional technological solutions have been recently implemented to increase the overall efficiency, and achieve an efficient operability under warmer conditions, such as parallel (or bypass) compression, as shown in Figure 2.46 and Figure 2.76b, high-pressure subcoolers, water spray systems, or adiabatic cooling curtains (www.r744.com). In the second case, several optimizing algorithms have been developed, measuring saturated suction pressure and gas cooler outlet temperature and regulating the refrigerant flow, maintaining the desired optimum discharge pressure [34]. Finally, in the third case, the success of transcritical CO_2 systems, particularly in Northern Europe, relies on its operation in subcritical mode, in the majority of time (owing the low external conditions [38]), achieving higher-efficiency levels [68]. This dual control is not necessary in heat-pumps, or in refrigeration systems with heat recovery, due to their permanent transcritical operating conditions [34].

The decision of opting for a transcritical cycle is supported by the usage-capacity for the high enthalpy from the discharge-superheated gas [40]. Besides heat-pump water heating and automotive air conditioning [34], [40], [71], [76], transcritical CO_2 systems have been

increasingly used in commercial refrigeration (supermarkets) [34], [56], [64], [68]–[70], [75], [77], [78], where the heat rejection is often recovered to indoor air or service water heating, endowing these systems with a highly economic competitiveness [75]. This statement is confirmed by the growing number of systems installed in European supermarkets, during the last few years. From 2011 to 2013, the number of transcritical CO_2 stores grew more than the double (1330 to 2885), mostly of them implemented in Central and Northern Europe, and in the United Kingdom, as well [70]. In contrast, only four transcritical CO_2 systems were installed in Portugal, all during 2016, (www.r744.com). In Figure 2.76, two currently-used transcritical CO_2 booster systems are exhibited, one in the standard configuration (Figure 2.76a), and the other, with parallel (bypass) compression (Figure 2.76b), a mandatory configuration for southern countries.

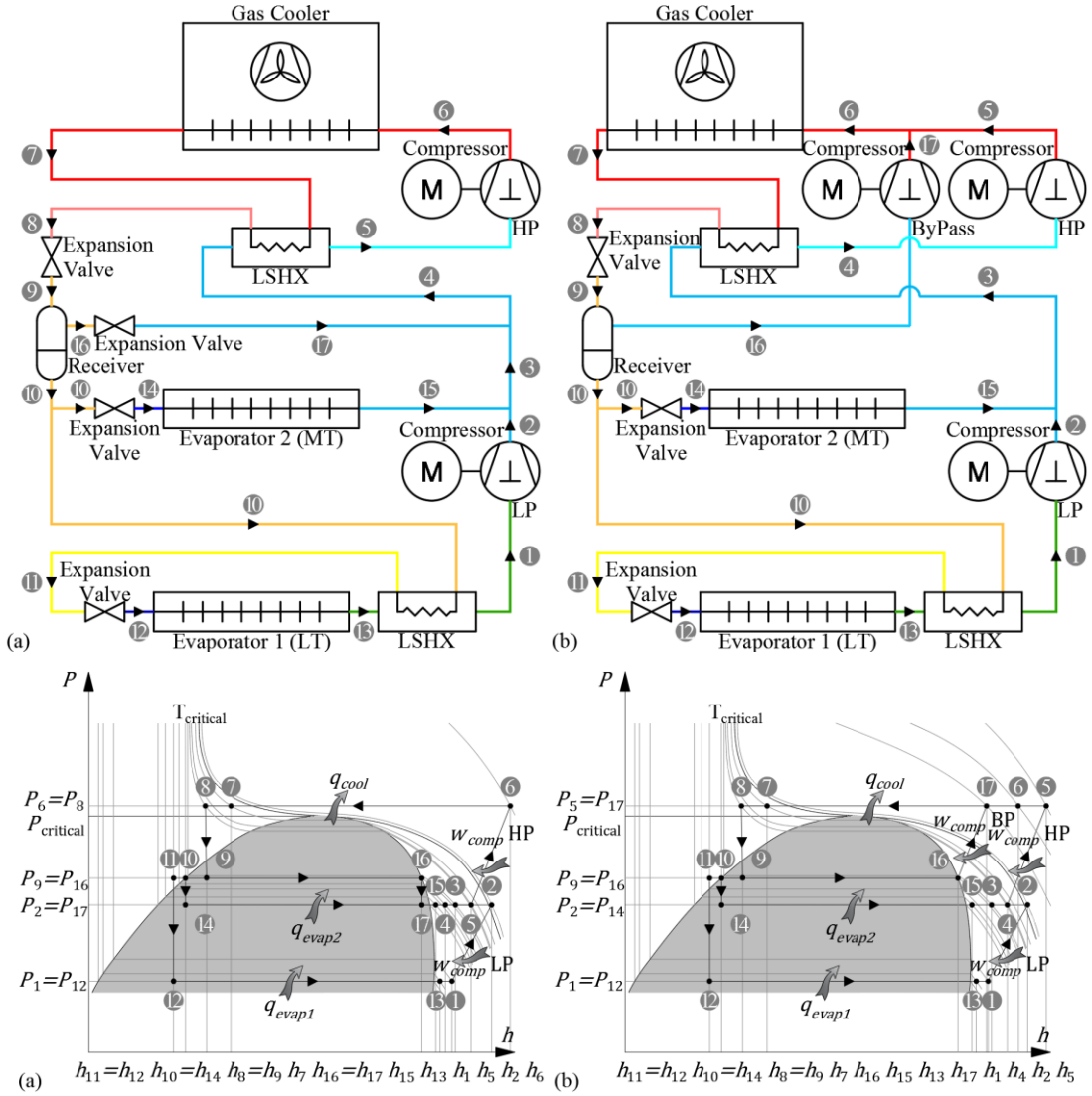

Figure 2.76: CO_2 transcritical booster system circuits and *P*-*h* diagrams for: (a) standard configuration and (b) with bypass compressor (source: adapted from [68])

2.2.6. NON VAPOR-COMPRESSION CYCLES

2.2.6.1. Absorption cycle

Regarding the refrigeration effect, *i.e.*, the heat absorption at a low temperature, both absorption and vapor-compression systems are similar: it occurs through the vaporization of a liquid, in a low-pressure evolution [37]. The main difference relies on the procedure taken after the vaporization of the refrigerant, which is, in an absorption system, dissolved in a liquid, before it is compressed [39]. This difference implies that, as depicted in Figure 2.77, in lieu of a compressor (mechanical work), a generator/absorber pair and a mechanical pump drive the working fluid (thermal drive), being complemented with a valve and a rectifier (used in ammonia-water adsorption systems) [39], [71]. The suction of the refrigerant vapor, leaving the evaporator, is a consequence from the ability of a substance (a solution of liquid absorbent) to absorb another (refrigerant vapor) [37].

The absorption refrigeration systems are divided in two main categories: (1) those that use water as refrigerant (H_2O) and lithium bromide (LiBr) as the absorbent, in a salt-liquid mixture (LiBr - H_2O); or (2) those that use ammonia (NH_3) as refrigerant and water as the absorbent, in a liquid-liquid mixture (H_2O - NH_3) [34]. Absorption equipment using salt-liquid mixtures (LiBr - H_2O) can also be classified according to (1) the heat input: (1a) indirect-fired, using steam, hot liquids, or various waste fluids as the heat source; or (1b) direct-fired, when using direct combustion or fossil fuels as heat gases; or (2) whether the absorption cycle is: (2a) single-effect (Figure 2.78), using low pressure steam or hot water (between 80 to 120 °C); or (2b) multiple-effect (double and triple, working with temperatures around 120 °C or higher than 200 °C, respectively), using high pressure steam or being gas-fired ("whenever the unit cost of thermal energy is low and is projected to remain low relative to electricity" [39]), and having more equipment than the single-effect chillers, such as middle and/or high-temperature generator(s), middle and/or high-temperature condenser(s) (allowing them to boil-off more refrigerant from the absorbent solution, providing higher efficiencies than the single-effect chillers), additional heat exchangers, or optional condensate subcooling heat exchangers [34], [79].

The saturated vapor leaves the evaporator and enters the absorber (sharing the same pressure, in a near-vacuum environment), mixing, dissolving and reacting with the absorbent solution, in an exothermic reaction, where the heat is released to an external agent [34], [39]. Along with this condensation and dilution heat, a volume contraction

also occurs due to the low-pressure level [34]. As the temperature is inversely proportional to the amount of the refrigerant dissolved in the absorbent, it is essential to cool the absorber, maintaining its temperature as low as possible, and maximizing the concentration of the refrigerant in the solution [39]. This solution, with a high concentration of refrigerant - "rich" or "strong liquor", is accumulated in the absorber sump, and then pumped (through the solution pump) to the generator, at the condenser pressure. Owing to the liquid state of the fluid, the compression developed by the pump demands much less work input, than that it would be required by a vapor-compressor machine, being often neglected in the cycle analysis (on the order of 1 % of the heat supplied to the generator) [37], [39]. Before it enters in the condenser, the refrigerant is desorbed from "strong liquor" (and weak in absorbent), during a heat-transfer from the primary heat source (high-level temperature), at the generator. The separation produces: (1) a flow stream of refrigerant vapor, pure or with an extremely weak absorbent concentration (purged at the rectifier, in ammonia-water cycles, refluxing the water), and (2) a highly concentrated absorbent solution, (weak refrigerant concentration, or "weak liquor"), which is throttled to the pressure of the absorber, where it is sent back, restarting the absorption of the refrigerant vapor coming from the evaporator [37]. At the condenser, the refrigerant vapor is condensed on the outside of water tubes, cooled in a heat sink (*e.g.* cooling tower), passing then through an expansion device, and entering the evaporator, at a low-pressure level, receiving the heat from the cooling medium [34]. The system overall efficiency can be improved through a heat exchanger, as shown in Figure 2.78, transferring the heat from the "weak liquor", *i.e.* the absorbent solution coming from the generator to the "strong liquor", which is pumped to the generator [34].

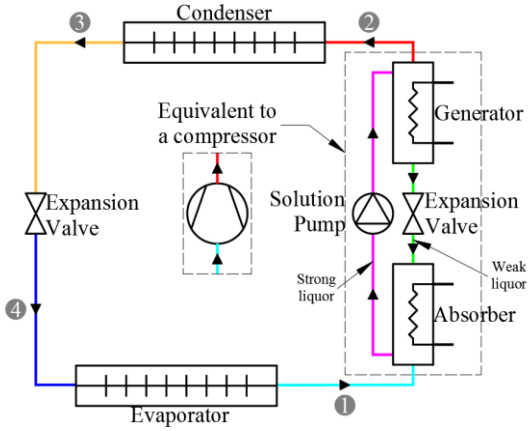

Figure 2.77: Absorption cycle: basic circuit (source: author)

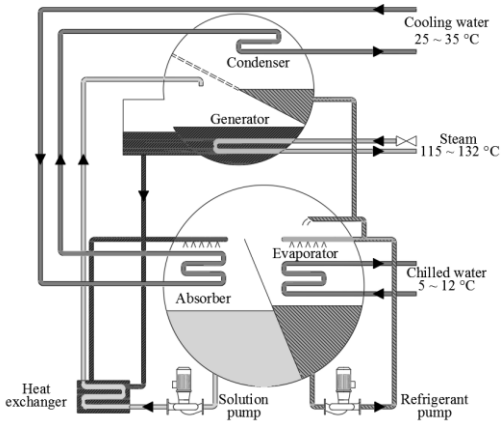

Figure 2.78: Two-shell lithium bromide cycle water chiller (source: adapted from [34])

Equipment working with salt-liquid mixtures, such as water-lithium bromide and water-lithium chloride, are limited to HVAC appliances, where the minimum working temperature is above the freezing point of the water, which is the refrigerant [39]. For refrigerating appliances where negative temperatures are required, such as food processing and cold storage, ammonia-water absorption systems are used. They are able to achieve temperatures as low as -57 °C, although being commonly rated within the range from -29 °C to -46 °C [34]. Due to the variability in the cooling capacity, chilling temperature, driving heat, heat rejection mode and other key parameters, these systems are essentially custom units [34]. Having water as absorbent, which is extremely volatile (and so the regeneration of weak absorbent to strong absorbent is a fractional distillation process), it is always necessary to purify the vapor formed in the generator (rectification process), and ensure that the evolution in the condenser-expansion mechanism-evaporator circuit is made with (almost) pure ammonia [34]. Actually, rectification is never a complete process, and therefore, the cycle efficiency decreases. The working principle of ammonia-water chillers is identical to those working with salt-liquid mixtures [80] (*e.g.* water-lithium bromide). The difference relies on the existence of a purification column, or an analyzer and a rectification section, which purifies the vapor leaving the generator (also called "desorber"), as shown in Figure 2.79.

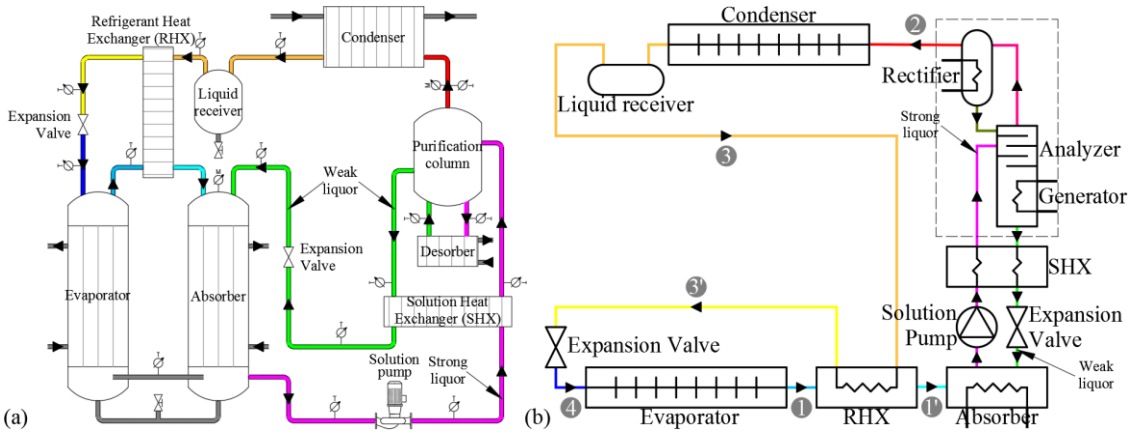

Figure 2.79: Ammonia-water absorption chiller: (a) scheme and (b) circuit (source: (a) adapted from [80], (b) author)

The thermal COP (ratio of the desired cooling output to the required thermal input) of an absorption system, $COP_{th,\ absor}$ can be defined by Eq. (2.87), where Q_{evap} is the desired refrigeration effect (for the total refrigerant mass), Q_{gen} is the driving heat, transferred through the generator, from the high-level temperature heat source, and W_{pump} is the work input of the pump, which is negligible comparatively to the others [37], [39].

$$COP_{th,\,absor} = \frac{Q_{evap}}{Q_{gen} + W_{pump}} \approx \frac{Q_{evap}}{Q_{gen}} \tag{2.87}$$

And the maximum COP of an absorption refrigeration system, assuming the total reversibility of the cycle, is given by Eq. (2.88), where T_L, T_H, and T_G are the thermodynamic temperatures of the evaporator (low-temperature source), of the condenser (medium-temperature source), and of the generator (high-thermal level source), respectively. The expression considers that the heat from the high-thermal level energy source, Q_{gen}, is transformed, in a Carnot heat engine, into a work output, $W = \eta_{th,\,rev} \times Q_{gen}$, which is supplied to a Carnot refrigerator, in order to remove the heat from the refrigerated space through the evaporator, Q_{evap}. [39]. Considering a new arrangement of Eq. (2.12), where $Q_1 = Q_{evap}$, $T_1 = T_L$ and $T_2 = T_H$, it results as $Q_{evap} = W \times COP_{R,\,Carnot}$ and therefore, $Q_{evap} = \eta_{th,\,rev} \times Q_{gen} \times COP_{R,\,Carnot}$.

$$COP_{rev,\,absor} = \frac{Q_{evap}}{Q_{gen}} = \eta_{th,rev} \times COP_{R,\,Carnot} = \left(1 - \frac{T_L}{T_G}\right) \times \left(\frac{T_L}{T_H - T_L}\right) \tag{2.88}$$

Single-effect absorption chillers have COPs from 0.6 to 0.8 out of an ideal 1.0, while double-effect equipment reaches approximately 1.0 (1.1 to 1.2 [34], *e.g.* water-lithium bromide chillers can reach 1.2 [81]) out of an ideal 2.0, and triple-effect chillers are expected to have COPs between 1.4 to 1.6 [79] (theoretically, 1.7 is the maximum [34]), which could represent 40 - 70 % higher than those of the double-effect, and as much as 300 % than the single-effect efficiency [71]. The introduction of the generator-absorber heat exchanger (GAX) technology (using the absorber heat in the lower-temperature section of the generator, as well as in the strong liquor, rich in ammonia) has increased the COP of these systems [34], [71]. Besides being more expensive, absorption refrigeration systems are also more complex, bulkier, more difficult to service and less efficient than the vapor-compression systems [39]. Although, they could be an interesting option whenever waste heat or fluids are available [34], [39], [62], or in solar applications. In an energy conservation perspective, the absorption refrigeration technology can be extremely interesting, when integrated in a co-generation plant, *i.e.* a Combined Heat and Power (CHP) system coupled to a thermally driven refrigeration equipment, providing not only electrical power and heating, as well as cooling. These systems are known as Combined Cooling, Heat and Power (CCHP) or Combined Heating, Refrigeration and Power (CHRP), and can achieve overall efficiencies of 90 %, which is incomparably high relatively to the 33 - 35 % for the electricity generation in central power plants [62].

2.2.6.2. Adsorption cycle

Similarly to the absorption refrigeration technology, adsorption equipment is thermally driven (Figure 2.80), and can be powered by waste heat or solar energy [82]. The main difference between both sorption technologies is based on the sorbent state, being a solid (adsorbent) in the adsorption systems - "solid sorption", instead of being a liquid (absorbent) as it happens for the absorption equipment. The conventional adsorbent cycle includes two phases [62], [82]: (1) adsorbent heating with desorption process, or generation (heating-desorption-condensation phase: evolutions ❶-❷-❸, as depicted in Figure 2.81), *i.e.*, when the adsorbent is heated, it desorbs the refrigerant at the condenser pressure (the heat generation process can be provided by a low-grade heat source, such as solar or waste heat, and as the temperature adsorbent increases, also the pressure increases); at the condenser, the refrigerant vapor is liquefied, releasing the heat into the environment, and then forwarded to the evaporator, at a lower pressure, due to the passage through an expansion device (such as a capillary tube or expansion valve); (2) adsorbent cooling with adsorption process (cooling-adsorption-evaporation phase: evolutions ❸-❹-❶, as shown in Figure 2.81), *i.e.*, when the adsorbent is cooled, it re-adsorbs the refrigerant, maintaining the evaporator at a low pressure; the cooling or refrigeration effect is obtained through both sensible and latent heat, transferred from the cooling medium (usually air from a refrigerated space or water) to the liquid refrigerant, promoting its heating and vaporization, respectively. The adsorptive cycle is an intermittent process, because the adsorbent must be regenerated when is saturated, and therefore, the adsorber is alternatively connected to a condenser and to an evaporator. To overcome the intermittency issue, and providing a continuous operation, multiple adsorbent beds are used (multi-bed systems) [81].

Adsorption processes can be classified as [81], [83]:(1) physical adsorption (also called "physisorption"), which is caused by the van der Waals force between the molecules of the adsorbent (activated carbon fiber, silica gel, zeolite or alumina) and the adsorbate (refrigerants as ammonia, water, methanol, ethanol or calcium chloride, are the most common); these adsorbents have highly-porous structures with surface volume ratios in the order of several hundred, having the ability to selectively catch and hold the refrigerant molecules; once saturated, the adsorbent can be regenerated by being heated; and (2) chemical adsorption (also called "chemisorption"), caused by the reaction, a strong chemical bond, between the contact of the adsorbate molecules and

the adsorbent surface molecules; this process is difficult to reverse, requiring more energy to remove the adsorbed molecules than that used in the physical adsorption.

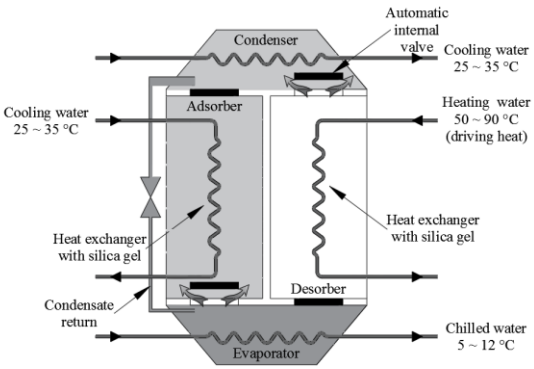

Figure 2.80: Schematic diagram of adsorption refrigeration system (source: adapted from [62])

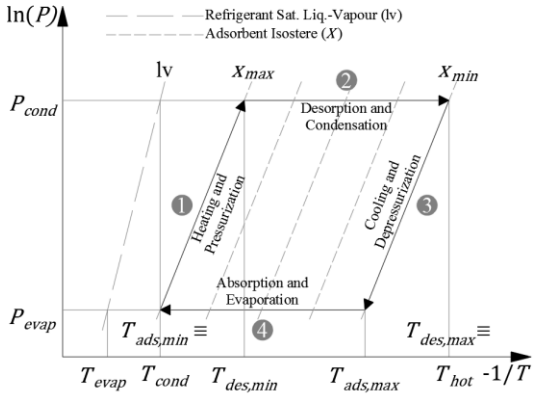

Figure 2.81: Clapeyron diagram for an ideal adsorption cycle (source: adapted from [84])

The adsorbent-adsorbate working pairs have been tested and documented through several studies. The main characteristic of working pair (adsorbent-adsorbate) is the amount of adsorbed refrigerant per unit of dry adsorbent. The loading $x = m_{refrigerant}/m_{adsorbent}$ is a function of refrigerant pressure and temperature, $x = x(T, P)$, and can be represented in isosteric (an adsorption equilibrium relationship[3]) diagrams [84]. Besides the two-phase cycles referred previously, an adsorption refrigeration cycle can be detailed described by the four following steps [84], shown in Figure 2.81: (1) isosteric heating, ❶: the loaded adsorbent is heated at constant maximum loading x_{max}; The equilibrium pressure in the system increases until the condensation pressure (P_{cond}) of the refrigerant (at condensation temperature, T_{cond}) is reached; (2) isobaric desorption, ❷: the adsorbent is still being heated, and consequently desorbed at constant pressure; this process ends as soon as it is reached the maximum temperature provided by the external heat source (T_{hot}). It is an endothermic process, taking up the desorption heat and the released refrigerant is then condensed in the condenser; (3) isosteric cooling, ❸: the desorbent is cooled down until the equilibrium pressure in the system reaches the evaporation pressure of the refrigerant in the evaporator (P_{evap}); (4) Isobaric adsorption, ❹: the adsorbent is still being cooled, resulting in the adsorption process; the refrigerant is evaporated in the evaporator, thus producing the desired cooling

[3] "The isostere is a plot of the $\ln(P)$ *versus* $1/T$ at a constant amount of vapour adsorbed. Adsorption isotere lines are usually straight for most adsorbate-adsorbent systems. The isostere is important in that the slope of the isostere (approximately) corresponds to the heat (enthalpy) of adsorption" [139].

effect and taken up by the adsorbent; this process ends as soon as the adsorbent temperature reaches the heat rejection temperature. The thermal COP of an adsorption system, $COP_{th,\,adsor}$, can be estimated using the following expression, Eq. (2.89), where, Q_{evap} is the cooling or refrigeration energy, Q_{drive} is the driving heat ($Q_{drive} = Q_1 + Q_{des}$), Q_1 is the isosteric heat, Q_{des} is the isobaric desorption, h_{evap} is the evaporation enthalpy, and $(x_{max} - x_{min})$ is the loading difference [84]:

$$COP_{th,\,adsor} = \frac{Q_{evap}}{Q_{drive}} = \frac{h_{evap} \times (x_{max} - x_{min})}{Q_1 + Q_{des}} \tag{2.89}$$

Comparatively to the adsorption refrigeration systems, the majors advantages of those of adsorption are [83], [84]: (1) operability by sources with a wide temperature range, it can use heat sources with temperatures as low as 50 °C (absorption systems require, at least 70 °C) up to 500 °C, without causing any corrosion problems (in absorption systems, sever corrosion start occurring for temperatures above 200 °C); (2) suitability for vibration conditions: adsorption systems can be used in fishing boats and locomotives, once vibrations produce great instability in absorption systems; (3) simplicity and robustness, less complex than absorption systems, for instance it is not required to deprive the absorbent, by evaporation or distillation, as it happens to water in an ammonia-water absorption system; and there is no risk of crystallization; (4) the common-used materials are environmentally friendly (zeolite, silica gel); (5) possess low number of moving parts, lowering maintenance efforts and costs; (6) high potential of cost reduction in series production (small number of individual parts). Adsorption systems can be applied in food applications, whenever waste heat is available to drive the adsorption system, and it can be used in food factories and transport refrigeration, as well as, in tri-generation systems, working conjunctively with combined heat and power systems to provide cooling [62].

Their major drawbacks are low COP and low specific cooling power, which can be improved by (1) increasing adsorption properties of the working pairs, and (2) by the optimization of the heat management during the adsorption cycle, resulting in the enhancement of the heat and mass transfer properties at the absorber [82], or (3) using generation heat provided by a large solar system, where its low power density is not a problem [81]. Some commercial equipment, driven by low grade heat (50 – 90 °C) and within a model range from 70 up to 1300 kW, present COPs values around 0.7 [62].

2.2.6.3. Ejector refrigeration cycle

The ejector or jet pump refrigeration is a thermally driven technology [62], whose principle is based on the change of state, likewise the vapor-compression or absorption systems, occurring in a liquid refrigerant when subjected to a heat supply, at a certain pressure [37]. The system is composed by two loops, refrigeration and power loop (in which is used a boiler or a generator), as represented in Figure 2.82. The ejector is used in the suction of the low-pressure vapor (secondary fluid or refrigerant), due to the Venturi effect caused by the high-speed and -pressure primary fluid passing through the nozzle at a supersonic velocity, and posteriorly decreased to a subsonic regime, after the mixing of both fluids, generating a shock wave which causes an irreversible compression [37], [62]. It is a longstanding technology, which has been used for many years, but it was replaced by vapor-compression systems when the CFCs emerged [62]. Presently, it is restricted to chemical and process industries [37], [62], or used in food processing factories, where waste heat is available to drive the ejector [62]. One of the most promising and interesting applications of these kind of cycles, is at tri-generation systems, working conjunctively with combined heat and power systems to provide cooling [62].

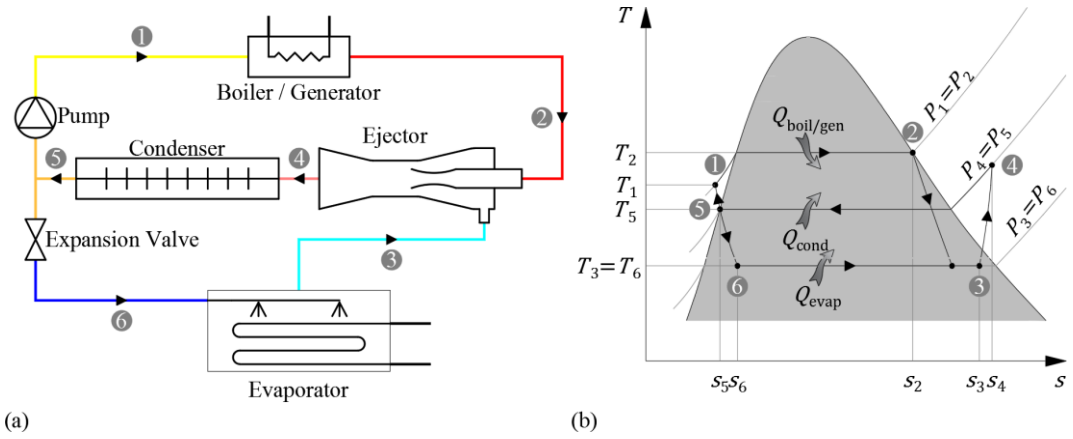

Figure 2.82: Ejector cycle: (a) circuit and (b) T-s diagram (source: adapted from (a) [37], (b) [62])

The COP of an ejector refrigeration system (ratio of the refrigeration effect to the heat input of the boiler, if the pump work is neglected), is incomparably lower than the vapor-compression system, less than 0.2 or 0.3 [62]. Water is used as the working fluid, which, although being innocuous, low-cost and widely available refrigerant, inhibits the use for temperatures below its freezing point, restricting its use to cooling, more than refrigeration processes. Its major advantage relies on the possibility to use waste heat or

solar , as heat sources at 80 °C for obtaining the refrigeration process, besides having no moving parts, and being a less complex mechanism [62].

2.2.6.4. Gas refrigeration cycle

The refrigeration effect can be achieved subjecting a gaseous refrigerant to a cycle involving compression, followed by the heat removal and expansion, in a turbine, in which the gas temperature drops below that it had before it was compressed, and finally the heat absorption, by the gas from the refrigerated space [38], [39], [62]. Such cycle is called the reverse Brayton or Joule cycle, and air is the must-used gas. The air cycle refrigeration can generate temperatures down to -100 °C or below (with a niche position in the -50 to -100 °C range, perfectly suitable for cryogenic applications), or temperatures over 200 °C, offering the possibility to use both potential to cooking and refrigeration processes [62]. Is mainly applied in air-conditioning and pressurization of aircraft, where mass (and consequently, weight) is a critical parameter, owing its low specific capacity (per mass unit) [37], and also due to its simpler and lighter components [39]. Modifications in the standard reverse Brayton cycle, as the inclusion of regenerators (or regenerative heat exchangers) and multistage compression with intercooling (as shown in Figure 2.83), makes them suitable for liquefaction of gases and cryogenic applications [39]. This technology has been also evaluated for application in “rapid chilling and/or freezing (including air blast, tunnel, spiral, fluidized bed and rotary tumble equipment); cold storage, refrigerated storage cabinets, refrigerated transport (trucks, containers, rail freight); and for integrated rapid heating and cooling (cook–chill–freeze or hot water/steam raising and refrigeration)” [62]. It can be classified as (1) closed (sealed

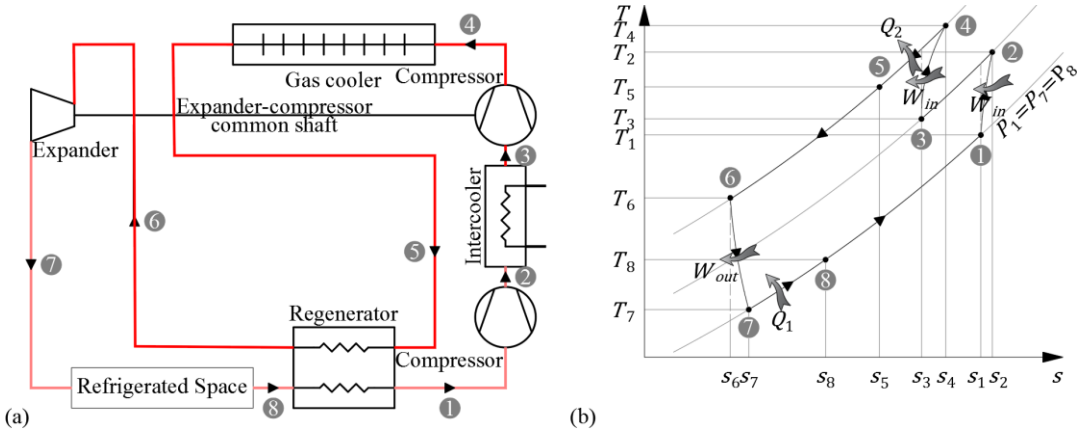

Figure 2.83: Gas cycle (two-stage, intercooling and regenerator): (a) circuit and (b) *T*-*s* diagram (source: adapted from [62])

system, without direct contact with the working fluid and the refrigerated product), (2) open or (3) semi-open/closed (both open to the refrigerated space, respectively, with no air recovery at all, either in low- and high-pressure side, or drawn back to the compressor) [62]. The COP is lower than other systems, and severely limited by the efficiencies of the compression and expansion components, as well as the heat exchangers. Current COP values can be found within the range of 0.4 to 0.7 [62].

2.2.6.5. Stirling refrigeration cycle

The Stirling cycle is made up of four totally reversible processes, shown in Figure 2.84, [39]: (1) a constant temperature expansion, with a heat transfer from the external source; (2) constant volume regeneration (internal heat transfer from the fluid to the regenerator); (3) constant temperature compression, with a heat transfer to the external sink; and (4) constant volume regeneration (internal heat transfer from the regenerator back to the working fluid). The piston alternatively compresses and expands the gas, while the displacer shuttles gas back and forwards, between the cold end (where heat is absorbed), and the warm end (where the heat is rejected) [62], as shown in Figure 2.85.

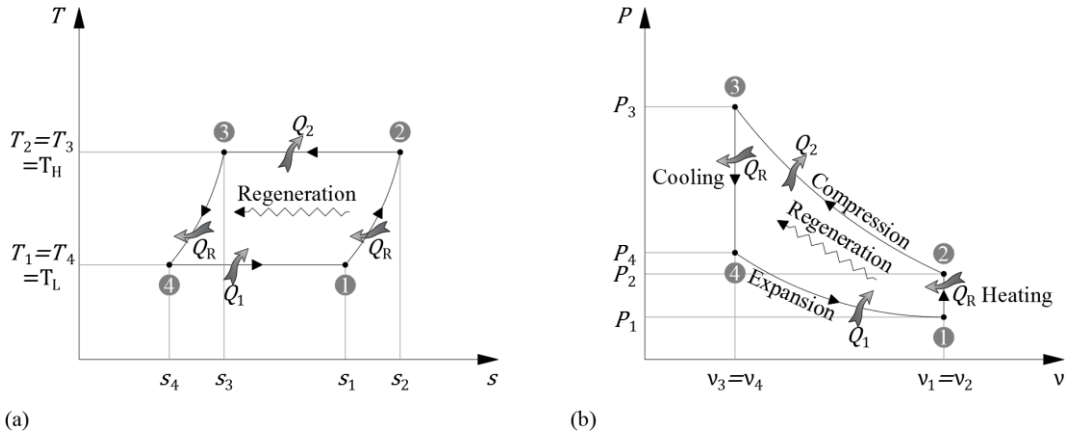

Figure 2.84: Stirling cycle: (a) T-s diagram and (b) P-v diagram (source: adapted from [39])

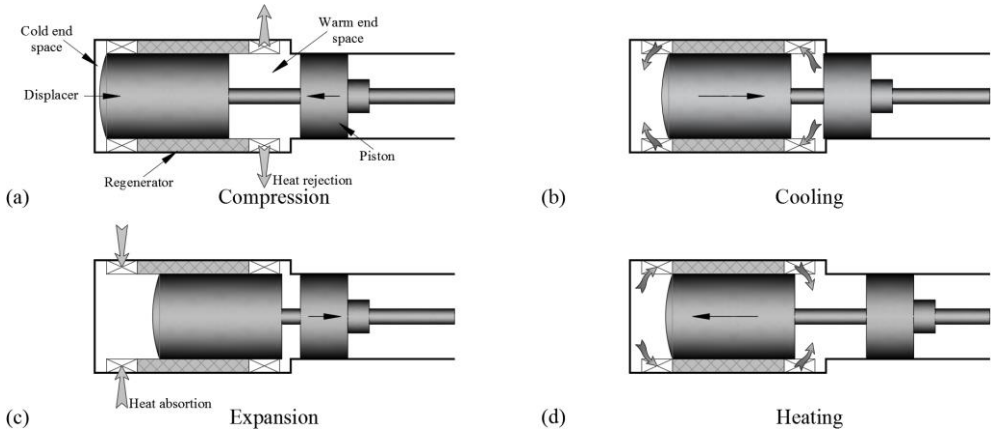

Figure 2.85: Piston and displacer movements during the Stirling cycle (source: adapted from [62])

During the compression, the piston moves compressing the gas, while the heat rejection occurs at the warm end (Figure 2.85a). Afterwards, the displacer moves the compressed gas to the cold end space, though the regenerator (Figure 2.85b), in the so-called "regenerating cooling" process. Then, the piston moves back, expanding the gas, and at the same time there is a heat absorption at the cold end (Figure 2.85c). And finally, the displacer moves back the gas to the warm end space, through the regenerator, in the so-called "regenerating cooling process" (Figure 2.85d). This cycle is used in free-piston Stirling coolers (FPSCs) and cryocoolers [62] (commonly used in several medical, instrumentation, security, astronomy, telecommunications, and pharmaceuticals applications). Thus, operating in the cryogenic temperature range, can be used in many food refrigeration applications, although having low cooling capacities, and lower COP and higher costs than vapor-compression systems [62]. It is suitable for household and portable refrigerators and freezers, as well as in food processing, such as butter churning [62]. FPSCs present measured values of COP, operating with warm head temperatures around 30 °C and cold head temperatures of 0 °C, typically between 2 and 3, falling to around 1, when the cold head decrease to -40 °C [62].

2.2.6.6. Total loss refrigerants

Cryogenic freezing systems, use often volatile fluids, such as liquid nitrogen, N_2, and liquid (or solid) carbon dioxide, CO_2, directly over the perishable products [38], [85]. These refrigerants are both stored as liquids, under a combination of pressure and low temperatures, and then released to produce the required cooling, or refrigeration, effect, resulting in their total loss into the atmosphere [38]. Due to this loss, only environmental innocuous and readily available fluids should be use, which is the case of the both mentioned and water (in the solid state, used as ice) [38], [85]. The refrigerating process results not only on the latent heat absorption by liquid, while boiling, but also on the sensible heat gain, due to the low temperature of the resulting gas [85]. The CO_2 is sublimated (from the solid state, "dry ice") at -78.4 °C while the N_2, is evaporated at -198.8 °C [38], for standard temperature and pressure. Cryogenic systems have often considerably higher cooling rates than other refrigeration systems, owing to the extremely-low working temperature and high surface heat transfer coefficients between product and medium [85]. These systems are mainly used in small products, spraying liquid N_2 or CO_2 into the freezing chamber, container or food-conveyed tunnel [34], [85].

2.2.6.7. Thermoelectric refrigeration

The physical principle of the thermoelectric cooling is based on the Peltier effect, developing a temperature difference between the junctions of two dissimilar metal conductors, when subjected to an electric current and at the same initial temperature [37], [62]. Current commercial thermoelectric cooling devices use N-type and P-type doped semiconductor materials [62], [71]. The pair of these thermal elements is jointed at one of the ends by a conducting metal strip, forming a junction (cold side), while the other end is wire-connected, as depicted in Figure 2.86. This "thermoelectric couple", is then connected electrically in series, but thermally connected in parallel, and whereas the N-type semiconductor has a negative Seebeck coefficient (with the majority of negative charge carriers, or electrons), the P-type semiconductor has a positive Seebeck coefficient (majority of positive charge carriers, or holes) [37], [62]. When a direct current (DC) is applied, the temperature of the junction decreases, while the thermal energy is absorbed from the cold side, as electrons move to a higher energy level from the P-type to the N-type material [62]. The heat is transferred by the majority charge carriers, to the hot side, where the heat is rejected, as the electrons return to the lower energy level [62]. Thermoelectric materials are characterized by a function of the their properties (the Seebeck differential coefficient, α_{ab}, the conductance, C, and the electric resistance, R), denominated as the figure of merit, $Z = {\alpha_{ab}}^2/(C \times R)$, and the absolute temperature, T [37], [62], [71], resulting in the dimensionless figure of merit, ZT. Higher ZT values result in higher COP [71], and the evolution on the production of semiconductors, has been enhancing improvements in this cooling method [38]. The maximum theoretical efficiency, assuming total reversibility, comparing to a Carnot refrigerator, working within the range of T_H and T_L, and considering the irreversibility degree of the involved processes [37], is given by the following expression, Eq. (2.90):

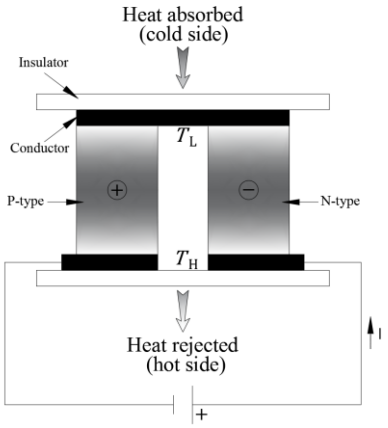

Figure 2.86: Thermoelectric cooling (or Peltier) couple (source: adapted from [62])

$$COP_{rev,\,thermoelec} = \left(\frac{\sqrt{1+ZT} - T_H/T_L}{\sqrt{1+ZT}+1}\right) \times \left(\frac{T_L}{T_H - T_L}\right) \tag{2.90}$$

State-of-the-art N-type and P-type thermoelements are bismuth telluride (Bi_2Te_3) based materials, having a $ZT \cong 1$, result in a maximum efficiency around 10% of the corresponding reversed Carnot cycle efficiency, and a maximum temperature difference of around 70 K; research, and not-yet commercialized materials, clamming $ZT = 2.4$ at 300 K, would result in a maximum of 0.37¸while, in order to achieve a theoretical COP_{max} of 0.50, which is comparable to current vapor-compression technology, it would be required a material with $ZT \cong 4$ [62], [71]. Although its non-competitiveness, comparing to the vapor-compression technology, thermoelectric cooling is used in some small military, aerospace, laboratorial and medical, or electronic cooling applications [38], [71]. This niche results of its high reliability and virtual maintenance free (owing the lack of moving parts), the absence of noise and vibration, the compactness and low-weight construction, and its precision in temperature control [62]. Regarding food applications, thermoelectric cooling technology is used in "compact refrigerators (15–70 L) for hotel rooms (mini bar), mobile homes, trucks, recreational vehicles and cars; wine coolers, portable picnic coolers, beverage can coolers and drinking water coolers" [62]. Measured COP values of 1.2 have been achieved in household refrigerators prototypes, and an also-prototype of a refrigerator-freezer achieved an overall COP of 0.44 [62].

2.2.6.8. Magnetic refrigeration

The magnetic refrigeration is based on the magnetocalorific effect (MCE) [38], [62], [71]. The MCE, caused by the exposition to a magnetic field, originates a temperature change in most of the magnetocalorific materials, which is either a heating or cooling process, if the material is magnetized or demagnetized, respectively [71]. The magnetic refrigeration systems are developed for near room temperature applications, operating in the active magnetic regenerator (AMR) cycle, where the magnetocalorific material assumes simultaneously the function of refrigerant and regenerator bed [62]. Two working principles are used in most of the prototypes: (1) a water-based solution is forced to change direction through a static porous AMR bed, owing to the periodical application and removal of the magnetic field, promoting a heat pumping effect [62], [71], or (2) applying a static magnetic field with moving magnetocalorific materials, using also an external heat transfer fluid [71]. For cooling and refrigeration processes, the most suitable materials are those with Curie Points (temperature at which a ferromagnetic material losses its permanent magnetism and becomes paramagnetic) near the room temperature,

such as the gadolinium, a rare earth metal [71]. This cooling method has a potential application within the near room temperature to cryogenic temperature range [62], [71], and expecting commercial applications for "low capacity stationary and mobile refrigeration and freezing systems [62]. The magnetic processes are virtually loss free, and the solid state refrigerant eliminates the ODP and GWP issues [62]. Experimental equipment presented COP values below 2 (more precisely 1.8 and 1.6), for low cooling capacities and reduced temperature lifts (0.2 °C and 2 °C, respectively) [62], [71].

2.2.6.9. Thermoacoustic refrigeration

The thermoacoustic refrigeration is based on the conversion of acoustic energy into thermal energy, using standing or traveling sound waves, which expand or contract a non-flammable mixture of inert gas (helium, argon or air), or a mixture of gases, in a resonator [62], [71]. During the gas expansion, its pressure and temperature are reduced, while in the compression, they are both increased, and these pressure differences induce the movement of the working gas, enabling the heat transfer to an external fluid through heat exchangers [71]. Constructively, the thermoacoustic devices are composed by (1) a closed cylinder, (2) two heat exchangers, (3) an acoustic driver (a loudspeaker, radiating the acoustic energy in a resonator) and (4) a porous component called "stack" or "regenerator" (where the gas flows oscillating back and forth, while transferring the thermal energy between the heat exchangers, removing heat from the cold side, and rejecting it to the hot side) [62], [71]. The temperature difference results mainly from the compression and expansion of the gas by the sound pressure, while the rest is owed to the heat transfer between the gas and the regenerator [62]. Technically, they are classified, in accordance to the acoustic wave type, as (1) standing-wave stack-based devices, or (2) traveling-wave (acoustic-Stirling or pulse tube regenerator-base devices), which is more complex than the first, and theoretically able to achieve the Carnot efficiency, as it based on the Stirling cycle [71]. Similarly to the magnetic refrigeration, this method has the potential to cover a wide temperature range, from refrigeration to cryogenics applications [62]. It has been used in cycle-based military and aerospace prototypes [71], while, particularly for food preservation, it is expected its implementation in "low capacity equipment, such as domestic and commercial refrigerators, freezers and cabinets" [62]. A predicted COP, from a refrigerator prototype, led to an acceptable value of 1.7, although having a COP_{II} within the 0.03 to 0.21 range (vapor-compression range: 0.3 to 0.5) [71].

2.2.7. REFRIGERANTS

Refrigerants are the working fluids in refrigeration, as well as in air-conditioning and heat-pumping systems [86]. In refrigeration systems, they are used for heat transfer, absorbing the heat at a low temperature and pressure, transferring it to a higher temperature and pressure, usually with a change of state, and its refrigeration effect is produced by expansion or vaporization [34]. Historically, refrigerants have been used since the end of the 19th century, as working fluids of the first mechanical refrigeration and vapor-compression-cycle apparatus. Air was used in the earliest mechanical refrigeration systems, and with the arise of the vapor-compression systems, although with some inadequacies, methyl chloride (toxic and unpleasant, used in small systems), carbon dioxide (requiring high pressures) and ammonia (toxic and unsuitable for the meat preservation method, used at that time) started to be use [38]. A revolution was trigged in the early 1930s, with the invention of the chlorofluorocarbon (CFC) R-12, eliminating both toxicity and inflammability problems, and guaranteeing good thermodynamic properties and oil miscibility characteristics [38], and paving the future for the hydrochlorofluorocarbons (HCFC) [37], [38], such as the well-succeed R-22 (HCFC-22).

Although complying with almost of the technical properties required for refrigerants, CFCs, HCFCs affect both stratospheric ozone and climate change [86], and for these reasons they have been progressively phased out, since the Montreal (1987) and Kyoto (1997) protocols, along with many others multilateral environmental agreements (*e.g.* Vienna Convention, in 1985, UNFCCC, in 1992, the several Conferences of Parties, *etc.*) [37]. In the USA, the production and importation CFCs was completely banned in 1996 (aligned with the industrialized countries), while HCFCs are being phased down towards the complete phase-out in 2030 [86]. Regarding the HCFCs, the EU imposed more stringent restrictions [34], as expressed in the Regulation (EC) No 2037/2000 [87], banning all the new equipment in 2004, banning the sale of virgin refrigerant from maintenance and service in January 2010, and the total phase out, including recycled refrigerants, in 2015 [38]. These two groups of refrigerants, CFCs and HCFCs, are commonly refereed as being powerful ozone-depleting substances (ODS), possessing not only a significant ozone depletion potential (ODP), owed to their chlorine content (higher for CFCs), having, as well, a high global warming potential (GWP) [34]. Both referred environmental-impact properties, ODP and GWP, will be described ahead.

To solve the chlorine containing problems of CFCs and HCFCs, the chemical companies developed a range of substitutes, the hydrofluorocarbons (HFCs) [38].The HFC methanes (fluoromethanes), ethanes (fluoroethanes), and propanes (fluoropropanes) have been extensity used in refrigeration, such as mixtures including R-32, or the R-23 for very-low-temperature applications, the R-134a extensively used in the direct replacement of R-12 or R-22, in high-temperature systems, the R-125 and R-143a, R-245ca, *etc.* [34]. Although being harmless to the ozone layer (zero ODP), generally non-toxic and non-flammable, HFCs are thermodynamically less efficient than the HCFC R-22 and may not match exactly to the chemical properties of the refrigerant they intended to replace [38]. Moreover, these fluorinated gases have high GWP values, contributing thereby to global warming, when released into the atmosphere. The first European regulation on fluorinated greenhouse gases, the also-called "F-gas Regulation", Regulation (EC) No 842/2006 [88] and its actualization, Regulation (EU) No 517/2014 [89], introduced and strengthened the existing measures, respectively, for controlling the emission from the fluorinated greenhouse gases (F-gases). While the fist was solely centered on the containment, use, recovery and destruction of the F-gases [88], current regulation is also addressed to trade phase-down, use banning and prevention of gas-emissions from existing equipment [89].

2.2.7.1. Ozone depletion potential

The effect that a certain refrigerant has over the atmospheric ozone, is represented by its ozone depletion potential, or simply ODP, whose reference point is usually adopted for the CFC R-11, with a unitary ozone depletion potential, $ODP = 1$ [38]. ODP values were established through the Montreal Protocol and are unlikely to change [34]. As mentioned before, the absence of chlorine atoms in the HFCs chemical structure, result in $ODP = 0$.

2.2.7.2. Global warming potential and total equivalent warming impact

The global warming potential, or simply GWP, can be defined as an index comparing the climate impact of a greenhouse-gas emission (*i.e.* released into the atmosphere) to that of released out by the same amount of CO_2 (whose GWP is 1), and its effect is integrated for a time horizon of hundred years, allowing the time decay of the substance [38], and for this reason may be designated as GWP_{100} [34]. GWP values were established as a reference point using the 1995's Intergovernmental Panel on Climate Change (IPCC) assessment values, and have been reviewed since then [34]. Another important indicator is the total equivalent warming impact ($TEWI$). It is used to characterize the overall

environmental impact, for which a particular refrigerant has over the lifetime warming impact of a system [38].The $TEWI$ of a refrigeration system is the sum of direct refrigerant emissions (direct global GWP, accounting leakages and recovery losses), expressed in terms of CO_2 equivalents, and indirect emissions of CO_2 (indirect global GWP) from the energy use over the system service life [86], as expressed in Eq. (2.91), where GWP is the global warming impact [CO_2-related], L is the leakage rate per year [kg], n is the system operation time [years], m is the refrigerant charge [kg], $\alpha_{recover}$ is the recycling factor, E_{annual} is the energy consumption per year [kWh], and β is the CO_2-emission per kWh, which is dependent on the energy-mix of each country:

$$TEWI = (GWP \times L \times n) + \left(GWP \times m \times (1 - \alpha_{recover})\right) + (n \times E_{annual} \times \beta) \quad (2.91)$$

◄—— Leakages ——► ◄———— Recovery losses ————► ◄— Energy consumption —►
◄———————— Direct GWP ————————► ◄—— Indirect GWP ——►

Refrigerants such as ammonia, HCFCs, most HFCs, hydrocarbons (HC) such as R-290, R-600 and R-600a, and the newest generation refrigerants, the hydrofluoroolefins (HFOs) such as the R-1234yf and R-1234ze, have shorter atmospheric lifetimes than CFCs, due to their massive destruction in the lower atmosphere by reactions with hydroxyl (OH) radicals, generally resulting in lower ODP and GWP values [86].

2.2.7.3. Classification

Refrigerants can be classified either according to: (1) their typical application temperature range [38], which can be (1a) high temperature (from +10 to −5 °C); (1b) medium temperature (from −5 to −25 °C); and (1c) low temperature (from −25 to −40 °C); or (2) the corresponding working pressure range [37], where it can be (2a) low pressure, with high evaporation temperatures at the atmospheric pressure, covering high-temperature working range; (2b) medium pressure, working at very low pressure in the low-pressure side, and low pressure values at the high-pressure side; (2c) high pressure, having low temperatures at the atmospheric pressure, working at low pressure in the low-pressure side, and high pressure values at the high-pressure side; and (2d) very high pressure, covering very low temperature range, working at very high pressures and having low evaporating temperatures, at the atmospheric pressure.

Relatively to the nomenclature, (1) halogen refrigerants are defined by the ASHRAE classification system, consisting in the "R" followed by the number, m, of the carbon (C) atoms -1 (omitted digit if zero), the number, n, of hydrogen (H) atoms +1, and the number,

p, of fluorine (F) atoms [37], [38], through the following chemical arrangement $\mathrm{C}m\mathrm{H}n\mathrm{F}p\mathrm{Cl}q$, where it always complies with $n + p + q = 2m + 2$ [37]. This means that knowing the number of the atoms of carbon, hydrogen and fluorine, the numbering system waives the quantity of chlorine atoms [37]. For example, the HFC R-134a has the following formulation CH_2FCF_3, and the lowercase letter indicates a specific isomer [38]. (2) Mixtures are identified by serial numbers designating, for instance, (2a) zeotropic mixtures, in the 400 series (*e.g.* the R-407C, where the "07" is a chronological number designating the components of the mixture, but not the percentage of the constituents, and the uppercase letter denotes a specific composition, *i.e.* the percentage of the components: R-407C is a mixture of R-32/R-125/R-134a in the following proportions 23/25/52); (2b) azeotropic mixtures, in the 500 series (*e.g.* R-507 is a mixture of R-125/R-143a in a 50/50 proportion); (2c) miscellaneous organic compounds, in the 600 series (*e.g.* butane, R-600 and isobutane, R-600a); and (2d) the 700 series identifies inorganic compounds (such as ammonia NH_3, R-717, where the "17" stands for ammonia molecular mass) [38].

Refrigerants can either be (1) pure substances or (2) mixtures or blends of two or more individual chemicals, as the case of many HFCs. By its turn, mixtures can be [38]: (2a) azeotropes (from the 500 series; blends dates back to the CFCs: the first azeotropic was the R-502), behaving as single substances, presenting a single boiling point, at one particular pressure, resulting in unique evaporating and condensing temperatures; (2b) near azeotropes, exhibiting a glide less than 2 K, which can be treated as single substances for practical purposes, as the case of both largely-used R-404A and R-410A; or (2c) zoetropes (from the 400 series, whose representative R-407C is from far, the most used), denoting the behavior shown in Figure 2.87: constant line pressures are represented horizontally, but the isothermal lines (constant temperature lines) are sloping. Thus, during the evaporation process, the refrigerant enters at the evaporator at the temperature T_4 ($T_{evap\ (inlet)}$), leaving it at the saturation temperature T_1 ($T_{evap\ (dew)}$), creating a temperature glide, in which $T_{evap\ (inlet)} < T_{evap\ (dew)}$, showing the earlier evaporation of lighter components of the mixture, relatively to the heavier. By

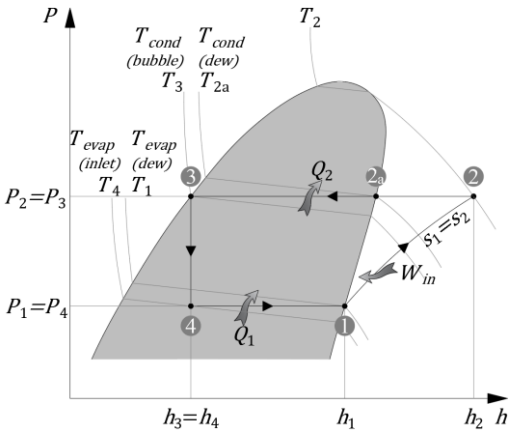

Figure 2.87: Vapor-compression cycle with a zeotropic refrigerant (source: author)

opposition, the condensation process starts taking place at the saturation temperature T_{2a} ($T_{cond\,(dew)}$), and progressively falls down until the bubble point temperature, T_3 ($T_{cond\,(bubble)}$), is reached, originating a temperature glide: $T_{cond\,(bubble)} < T_{cond\,(dew)}$. Zeotropic mixtures should not be used in flooded evaporators whenever the temperature glide is greater than 5 K [38]. One of the major disadvantages from the mixtures is the refrigerant leakage, which can change the proportion of the components, although having a negligible effect over the system performance [38]. Refrigerant charging should always be done in the liquid phase, for a correct setting of the component concentrations, and always avoiding the ingress of air [38].

2.2.7.4. Safety, toxicity and flammability

Relatively to this issue, refrigerants are classified by the European Standard EN 378 [90] and ANSI/ASHRAE Standard 34 [91], according to their toxicity level, by the occupational exposure limit (OEL) and the flammability potential, as shown in Table 2.11:

Table 2.11: Safety groups according EN 378/ANSI/ASHRAE Standard 34 (source: [90], [91])

Flammability hazard	**Toxicity hazard**	
	A - Lower toxicity (OEL ≤ 400 ppm)	**B – Higher Toxicity (OEL > 400 ppm)**
1 - No flame propagation	A1	B1
2 - Lower flammability*[4,5]	A2 (+ A2L*[7])	B2 (+ B2L*[7])
3 – Higher flammability*[4,6]	A3	B3

*[4] Flammable in vapor form at any concentration in the air [90]; Exhibits flame propagation in air at 60 °C and 101.3 kPa [91];

*[5] Lower flammability limit (LFL) ≥ 3.5 % V/V when they form a mixture with air [90]. LFL > 0.10 kg.m^{-3} at 23.0 °C, 101.3 kPa, and heat of combustion < 19.000 kJ.kg^{-1} [91];

*[6] LFL < 3.5 % V/V when they form a mixture with air [90]; LFL ≤ 0.10 kg.m^{-3} at 23.0 °C, 101.3 kPa, or heat of combustion ≥ 19.000 kJ.kg^{-1} [91];

*[7] Optional class, for lower flammability refrigerants with a maximum burning velocity of no more than 10 mm.s^{-1}, at 23.0 °C and 101.3 kPa [91].

The European Standard EN 378 has a simplified classification: L1 for high-security level (low-toxicity and non-flammable, exclusively for the group A1, including among others the R-12, R-22, R-125, R-134a, R-404A, R-407C, R-502 and the R-744 [37]); L2 for medium-security level (low flammability and non-flammable but toxic groups A2, B1 and B2, including the R-30, R-40, R-160, R-611, R-717, R-764 and the R-1130 [37]);

and L3 for low-security level (high flammability hazard groups A3 and B3, including the refrigerants R-170, R-290, R-600, R-600a and the R-1150 [37]).

2.2.7.5. Properties required for refrigerant candidates

The ideal properties for a refrigerant, can be listed as follows [37], [38]:

- Thermodynamic characteristics, such as (1) high latent heat of vaporization, for maximization of the refrigeration effect, with the lowest mass flow; (2) low liquid specific heat, to ease the subcooling process; (3) high vapor specific heat, avoiding undesired vapor superheating; (4) critical temperature and triple point well outside the working range, providing efficient and adequate condensation and evaporation processes; (5) positive but not excessive pressures at evaporating and condensing conditions, avoiding moist air infiltrations, and minimizing initial and operation costs; (6) low pressure ratio, so the discharge temperature is the lowest as possible; (7) high suction gas density, *i.e.*, low specific volume, which increases the volume flow rate entering the compressor and its volumetric efficiency;
- Chemical and physical characteristics, such as (1) chemical stability, compatible with construction materials, such as metals and alloys, plastics or elastomers; (2) adequate miscibility with lubricants, *i.e.* no miscible at all in the case of ammonia, miscible under certain conditions or fully miscible, affecting the refrigerant properties; (3) high dielectric strength, especially when used in hermetic compressors; (4) behavior in the presence of water; (5) efficient heat transfer, having high heat-transfer coefficients, both in liquid and vapor states;
- Safety and environmental characteristics: the refrigerants should be (1) non-corrosive, non-toxic and non-flammable; and (2) environmentally friendly, having low GWP value and zero ODP;
- Abundancy and low production costs are also important requirements.

2.2.7.6. Current applications and new trends

The HFCs mono-compound R-134a (demanding higher system costs, due to requirements on the compressor displacement and larger piping and accessories, relatively to R-22, although with a wide appliance) and mixtures such as R404A (which is widely applied in commercial refrigeration, and exhibits higher performances than other HFCs, in low temperature applications), R-407C (whose properties are very similar to the R-22) and R-410A (although having apparent low performance, when applied in optimized systems,

present higher COPs than R-22 and R-407C equivalent systems) have been replacing R-22 in many applications [38], [76]. Despite of the performances, their contribution to the global warming imposes restrictions on their continuity, and natural refrigerants, such as the "olds" ammonia and carbon dioxide have been through a renewed interest [69], [76]. Ammonia, NH_3 or R-717, is widely used in industrial refrigeration [34], [38], [63], especially for food and beverage processing and storage [69]. It has a well-established technology to deal with its high toxicity and low flammability [38]. The characteristics of the carbon dioxide, CO_2 or R-744, such as non-flammability, non-toxicity, the absence of carcinogenic, mutagenic, or other toxic effects, and dangerous products of combustion, allied to the fact that refrigeration systems containing it could be considered as a form of carbon capture, have launched, once again, a great interest over this refrigerant [34]. It has been increasingly applied, especially in the UE, in commercial (supermarkets) refrigeration, both as a refrigerant and in indirect or "secondary loop" [69], [76]. Due to its low critical temperature (31.06 °C, at 7.38 MPa [61]), it is used in transcritical cycles predominantly in small-scale or retail applications, mobile air conditioning, heat pumps, domestic appliances, and supermarket display freezers [34]. In these cases, CO_2 is the sole refrigerant, working with operation pressures much higher than those of HFCs and ammonia systems, imposing higher costs in the system construction and operation [34]. The use of CO_2 as secondary refrigerant is presently restricted to commercial and industrial refrigeration, in two-phase cascade systems, typically with ammonia (the most analyzed cascade refrigeration system [66]) or R-507A, in large industrial systems, or HFCs, in medium-sized commercial systems, in the high-temperature-stage [34]. Many equipment producers promote R-134a/CO_2 cascades as high-security low-GWP solutions for centralized commercial refrigeration systems (once NH_3/CO_2 systems are not recommended for safety reasons), overcoming this away F-gas regulation [66]. It was in quick response to that directive that manufactures launched the last generation of refrigerants [69], wherein the synthetic fluids HFOs fit. The R-1234yf, an HFO, has been tested a and is regarded as most promising candidate to replace R-134a [57]. The same goes to the R-1234ze(E), which has been under the scope of recent research, denoting its suitability, demanding although some modifications within the system, in order to maintain the energy performance [56]. Many others refrigerants have been recently developed, but are still being studied prior to being commercialized [56], and other already available, as the case of HFO blends Solstice™ L40 and N40 (from Honeywell), and DR-7 and DR-33 (from DuPont), are adequate low GWP substitutes for R-404A, [92].

3. GLOBAL FRAMEWORK AND CURRENT STATUS

According to the Intergovernmental Panel on Climate Change's (IPCC) special report, Chapter 4 - Refrigeration [36] - made in collaboration with Montreal Protocol's Technology and Economic Assessment Panel (TEAP) - the most important refrigeration application is in food processing and in cold storage, being extremely important economically, both in developed and developing countries. Simply notice that, during the first half of the last decade from the last millennium, global consumption of frozen food was about 30 $Mt.yr^{-1}$ (representing a consumption of 63 kg per capita in the USA, 56 kg in the EU and 16 kg in Japan) [36]. It was registered a growth in beginning of the present millennium, over 50 %, which kept growing, besides the enormous amount of stored refrigerated food, which was, in 1995, around 350 $Mt.yr^{-1}$ [36].

From the same report and regarding the used technologies, most of the refrigeration systems used in food processing and cold storage are based on vapor-compression systems of the direct-expansion type [36]. Indirect systems, based on liquid chillers or ice banks are also commonly used, especially for fruit and vegetable packing, meat processing, *etc.* [36]. The system size is variable: from low cooling capacities (few kilowatts, for cold storage), to large processing plants (several megawatts); and the most-used compressor types are reciprocating and screw: for lower capacity range, the reciprocating compressor is the most frequently used, whilst for larger systems, the screw compressor type is the commonest [35], [36]. Ammonia (alias NH_3 or R-717, the leading refrigerant for food processing and cold storage applications), the HCFC R-22, the CFC R-12 and the CFC azeotropic-blend R-502, have been the historically used refrigerants, although have been gradually replaced by HFC refrigerants (*e.g.* R-134a and HFC blends such as R-404A, R-407C, R-410A and R-507A) [34], [36]–[38], [63], [69]. The main refrigerant technological options, along with the annual emissions for food processing, cold storage and industrial refrigeration applications can be found in following Table 3.1.

Table 3.1: Food processing, cold storage and industrial refrigeration (2002) (source: [36])

	CFCs (R-12, R-502)	**HCFC (R-22)**	**Ammonia (NH_3, R-717)**	**HFCs (R-134a, R-404A, R-410A, R-507A)**
Cooling capacity range [kW]	25 - 1 × 10^3	25 - 30 × 10^3	25 - 30 × 10^3	25 - 1 × 10^3
Emissions, [$t.yr^{-1}$]	9 500	23 500	17 700	1 900
Refrigerant in bank, [t]	48 500	127 500	105 300	16 200
Emissions, [$\%.yr^{-1}$]	20 %	16 %	17 %	12 %

Carbon dioxide has been gaining (again) a prominent place in the vapor-compression technology ([36], [38], [40], [59], [62], [64]–[72]), due to its environmentally friendly behavior (almost negligible GWP value and zero ODP), and it is commonly used as a secondary refrigerant, predominantly in NH_3/CO_2 cascade systems [36], [38], [66].

Vapor absorption technology may be a feasible alternative. However, it is often limited to sites where waste heat can be used, such as in CHP or CHRP systems [34], [36], [39], [62]. These systems require excessively high investment costs, since vapor absorption still is an emerging and in-development technology [36], [39], [62], [71]. Other emerging technologies have been recently implemented in cooling and refrigeration systems, beyond the research field. Some of them are used: (1) in niche applications, such as: (1a) thermoelectric coolers, especially designed for temperature cycling applications, night vision glasses and imaging systems, commonly used in aerospace and defense technologies, or in the temperature stabilization of bolometers and ferroelectric detectors, laser diode arrays in fiber optics systems and in ink jet printers (www.marlow.com), or even for small air-conditioners, cold plates or liquid chillers (www.thermoelectric.com); (1b) free-piston Stirling equipment, used in ultra-low temperature storage freezers for biorepositories, pharmaceutical companies and hospitals (www.stirlingultracold.com), in cryogenic solutions for liquid nitrogen production (also for oxygen, methane, argon, helium and carbon dioxide), or even in cryocooling applications for high temperature superconductors, space simulation chambers, MRI (Magnetic Resonance Imaging) magnet cooling, and research applications, such as nuclear physics, cooling of laser amplifiers, liquid argon neutrino detectors, measurement of radioactivity, shielding of low temperature devices, and heat shielding and vacuum cryopumping for space propulsion motors test chambers (www.stirlingcryogenics.com, www.sunpowerinc.com); or (2) in HVAC applications, from small unitary systems to large centralized systems: (2a) thermoacoustic technology used in small air-conditioners (www.coolsound.us); (2b) adsorption chillers with zeolite and using water as refrigerant, for HVAC applications, providing chilled water (5 °C to 15 °C) from hot waste water (60 °C to 80 °C), or from renewable or unused energy (www.mayekawausa.com); and some others (3) in refrigeration systems, either in commercial or in food preservation industry, namely (3a) magnetic refrigeration systems, with high efficiency and no CO_2 emissions, being safe and reliable, and having reduced maintenance costs, applied in display cases, yet, in a near future, in medium-size refrigeration systems (www.cooltech-applications.com); and

(3b) gas refrigeration cycle, using an air cycle for ultra-low temperature storage (within a temperature range from -100 °C to -50 °C), without environmental impacts - zero ODP and GWP - and with an integral turbine expander-compressor (www.mayekawausa.com).

The vapor compression cycle is a mature technology and it is strongly implemented in the food industry [62], [71]. It is quite probable that this panorama will remain as it is, in the next decades, taking into to account the consolidation of the vapor-compression technology in the market, the latest advances in the development of low-environmental-impact refrigerants, improvements in the insulation systems, high-efficiency motors' technology, etc. Regarding energy efficiency, the gap between vapor-compression and other technologies is still an advantage for the first, as it can be concluded by the comparison of the energy performance coefficients, as those considered for a freezer, operating at -18 °C and an outdoor environment of 32 °C: (1) thermoelectric technology, approximately 0.1 W/W; (2) absorption technology, approximately 0.2 W/W; and (3) vapor compression technology, within a range from 1.3 W/W to 1.7 W/W, [34], [39].

In the Portuguese agro-food industry, besides the lower capacity of the refrigeration systems (from few kilowatts, to no more than a couple of megawatts), current status is perfectly suitable in the report presented by the IPCC [34], more than a decade ago. According to the data gathered during the course of the InovEnergy project, particularly surveys and information acquired during the energy audits, under the responsibility of ADAI, performed in 32 companies from the agro-food sector (9 from the fish sub-sector, 8 from the meat, 4 from the food conservation & distribution, 4 from the fruit & vegetables, 1 from the dairy and 6 from the wine), it was registered as follows:

- Absolute domain of the vapor-compression technology, as shown in Figure 3.1;
- Reciprocating compressors leading the table of the most-used compressor types (77 + 19 = 96 %), followed by screw compressors (4 + 19 = 23 %). In fact, 19 % of the companies use both types (particularly for multistage compression, in larger systems), as shown in Figure 3.1. These values do not include the compressors from the companies of the wine sub-sector, owing to lack of reliable information for all the companies. From the available documentation (photos, surveys, audits, *etc.*) it was only possible to assure the existence of two cases using screw compressors, in air-cooled water chillers;
- Extensive use of direct-expansion evaporators (77 %), except for ammonia-based flooded evaporators (23 %), liquid-overfeed method, as depicted in Figure 3.2;

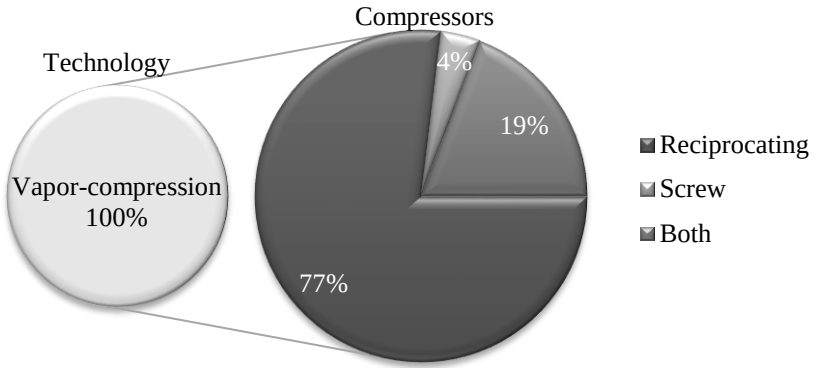

Figure 3.1: Most-used technology and compressor types: InovEnergy project - ADAI (source: author)

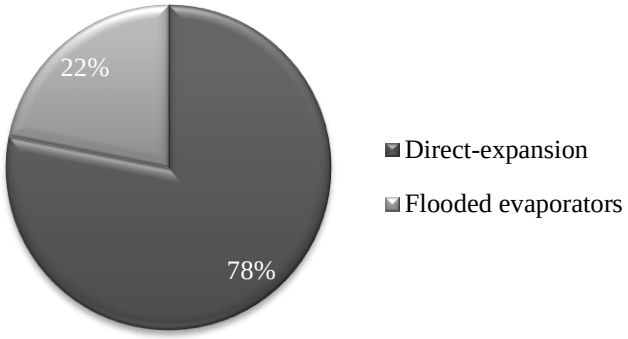

Figure 3.2: Most-used refrigerant supply method: InovEnergy project - ADAI (source: author)

- Owed to the systems size and age, and the existence of multiple unitary systems, the leading refrigerant is the R-404A (56 %). It is followed by the R-717 (ammonia, with a share of 22 %, and in this case, exclusively applied in larger central systems) and by the R-22 (with 9 %). In *ex aequo*, in the fourth place and registered in one company each (3 %), the R-13, R-417A, R-410A and R-407C (the last two are used in air-cooled water chillers, with scroll compressors, in the wine sub-sector), as illustrated in Figure 3.3. From a more extensive survey, performed on 148 companies (31 under the responsibility of IPCB, 30 of UBI, 29 of IPVC, 15 of IPP , 11 of IPB and 32 of ADAI), the results were slightly different, nevertheless, having the same causes. Likewise, it was registered a categorical first place for the R-404A (40 %), followed by a significant portion of R-22 systems (26 %) and then, with similar shares, the R-407C, R-717 and R-410A (respectively, 8 % and 7 % for the last two). It was also registered the use of refrigerants such as the R-422A (3 %), R-507C and R-417A (2 % for both), and a residual use of other refrigerants (5 %), such as the R-13, R-40, R-134A, R-417B, R-422D and the R-432A (with approximately 1 % each), as shown in Figure 3.4.

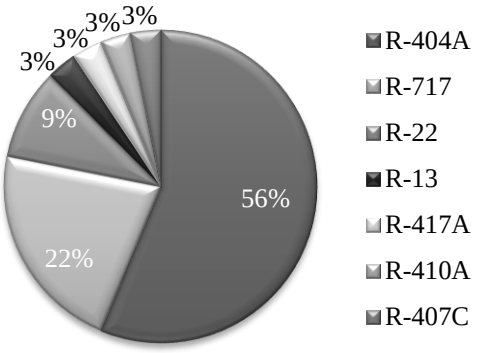

Figure 3.3: Most-used refrigerants: InovEnergy project - ADAI (source: author)

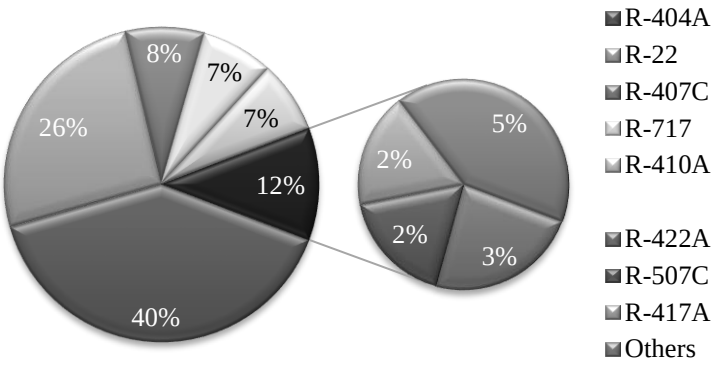

Figure 3.4: Most-used refrigerants: InovEnergy project (source: adapted from [93])

Partially supporting these observations, Nunes c presents in his research, particularly focused in the meat, dairy, and fruit & vegetables sub-sectors, some similar conclusions:

- From the 87 companies audited (33 from the meat sub-sector, 31 from dairy and 23 from the fruit & vegetables), vapor-compression is the unique technology observed in 537 different refrigeration systems, having a total of 621 compressors;
- The reciprocating compressor is the dominant type (99 %, 553 out of 557), followed by an insignificant share of the scroll type (1 %, 4 out of 557), and no screw compressors are pointed out. These values are only referenced to the meat and dairy sub-sectors, once it is not specified any compressor type for the 64 units registered in the fruit & vegetables sub-sector. However, those proportions are unlikely to be significantly changed, since most of these compressors are probably from the reciprocating type (scroll compressors are more common in condensing and in compact units, representing, respectively, 18 % and 3 % of the 40 systems of this sub-sector [8]). The majority of the compressors are semi-hermetic (76 %), followed by the hermetic (16 %) and the open e (8 %, in older equipment);
- Direct-expansion is the most-used evaporator feed system (approximately 100 %).

Surprisingly, the R-22 appears as the leading refrigerant (66 %), followed by the R-404A

(24 %), the R-134a (9 %) and, applied in only one system, the R-717 (0.2 %) [8]. Such distribution denounces the advanced age (67 % have more than 10 years), fragmentation and diversity of those systems: unitary systems, condensing units, compressor racks (direct and secondary loop), compact units and air handling units (drying processes) [8]. The following figures illustrate the most-used technology and compressors (Figure 3.5), and refrigerants (Figure 3.6), from the data collected in the aforementioned study, [8].

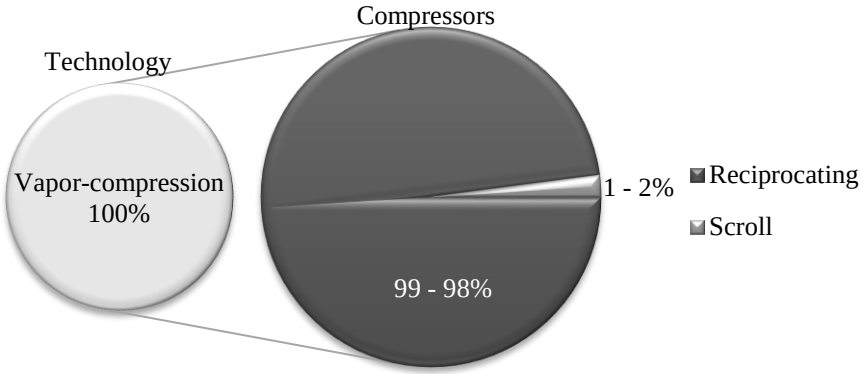

Figure 3.5: Most-used technology and compressor types in meat, dairy and fruit & vegetables sub-sectors in the province of Beira Interior, Portugal (source: adapted from [8])

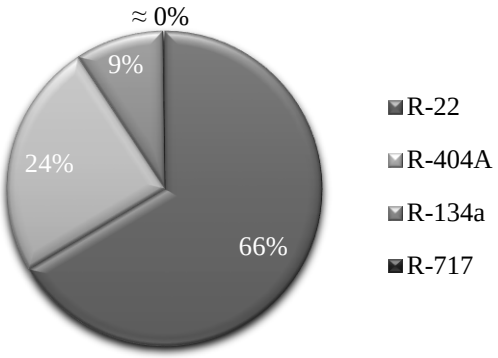

Figure 3.6: Most-used refrigerants in meat, dairy and fruit & vegetables sub-sectors in the province of Beira Interior, Portugal (source: adapted from [8])

No CHP nor CHRP systems have been detected in any of both studies. It will be quite unlikely to find such equipment in the Portuguese agro-food industry, except for the small percentage of intensive energy consumers, normally food transformation companies (meat, fish, dairy, *etc.*), where heating is also an essential process. In Portugal, the CHP market has been through deep changes in the present decade. Although the recognized importance of these systems for achieving the European targets for 2020, the introduction of the CHP legal and remuneration regime, in 2010 (Decree-Law No. 23/2010 [94]), has proven to be particularly harmful and unattractive to new investments, and neither its recent amendment (Decree-Law No 68-A/2015 [95]) seems able to revert this trend [96].

4. ENERGY SIMULATION OF REFRIGERATION SYSTEMS

Energy simulation programs are extremely useful tools to develop and evaluate alternative scenarios for energy analysis. Traditionally associated to buildings (mainly commercial and services, but also residential), energy simulation programs have been gaining a growing popularity in the refrigeration industry, predicting the impact of energy-efficiency measures and optimizing the design of refrigeration systems [97], [98]. Contrarily to the design based on steady-state models (current practice), "dynamic models allow prediction of the time-variability of heat loads and the response of refrigeration systems to such loads, and hence selection of system designs, control strategies and controller designs to both minimize energy use and improve temperature control" [99]. Regardless the final application, these tools provide rapidness and accuracy, avoiding the use of prototype modelling, along with all their technical and economic charges [98].

Both building and refrigeration energy simulation programs share the same chronological origin, in the 1960s. However, it was the arising development on digital computer technology that brought their full development in late 1970s, early 1980s [100]–[102]. By the time building energy simulation programs, such as BLAST and DOE-2 (whose fusion would result in the origin of EnergyPlus [103]), TRNSYS [104] and others, were already being used in the USA, in New Zealand, Cleland was developing and performing experimental validation on a numerical method, culminating in a commercial computer package for Refrigeration Analysis, Design and Simulation: RADS [105]–[107]. Years later, in 1992, Lovatt [102], in a PhD thesis supervised by Cleland, proposes a new methodology, embodied in a computer program: RefSim, obtaining better results and proving to be more flexible than RADS, respectively, version V2.2 and V3.1 [102], [108].

Equations-solving programs also have been used in energy simulation of refrigeration systems. Programs such as the EES (Engineering Equation Solver) [109], or the MATLAB (MATrix LABoratory) platform [110], have been widely used to create and solve computational models, analyze and design engineering systems, or to develop simulation models used in other programs (*e.g.* the EESCoolTools from CoolPack [61]). Regarding the EES, its high-accuracy thermodynamic and transport property database features, along with its internal procedures, makes it perfectly suitable for computer modelling of refrigeration systems and refrigerated product, namely for designing and

identifying the most suitable operating techniques in order to maximize the system performance [111], simulating the effects resulting from different operations strategies under real-time pricing [112], or performing comparative analyses of low temperature industrial refrigeration systems (comparison of NH_3/CO_2 cascades *versus* two-stage NH_3 systems) [113], [114], among others. The EES has also the ability for a close integration with TRNSYS [112], and it has macros that can control EES programs and allow it to interface to other programs, such as the LabVIEW, Excel or MATLAB. Owing the multi-functionality of MATLAB, which can be used either for programming, simulation and calculation, it is widely used in academia and industry [115]. This versatility allows, for example, the description of all major features of cold-stores operations, through simple equations, with a limited number of model parameters, and the acquisition of the remaining parameters through physical reasoning, in a top-down modelling approach (contrarily to the majority of the models for the overall dynamic behavior of cold store plants) [116]. Furthermore, besides optimizing the energy use, MATLAB based models can easily integrate, among others, sensitive analysis through random parameter variation (*e.g.* Monte Carlo) or optimization tools (*e.g.* multi-objective optimization), such as those provided by the FRISBEE tool, developed within the FRISBEE (Food Refrigeration Innovations for Safety, consumers' Benefit, Environmental impact and Energy optimisation along the cold chain in Europe) project [117]. Using another feature from MATLAB, the graphical user interface GUIDE, Nunes *et al.* developed a predictive tool, the COOL-OP (Cooling Optimization Program) for the assessment of the energy performance in the Portuguese agro-food industry, allowing to identify weaknesses or strengths, and providing energy-efficiency measures, through statistical correlations on energy-related characteristics, gathered in a large sample of Portuguese companies [31].

In another category, the Coolpack and the Pack Calculation Pro (both developed by IPU, Denmark), are respectively a collection offering different models for refrigeration systems, allowing cycle analysis, dimensioning of main components, energy analysis and –optimization, and an application for calculating and comparing the yearly energy consumption of refrigeration systems and heat pump. Although being very interesting tools (from the educational point of view), some drawbacks have been reported: the inability of CoolPack to simulate the performance of a refrigeration system whose load varies according to ambient conditions (that vary with the weather), and the incapacity of Pack Calculation II (a former version of Pack Calculation Pro) to model a temperature-

dependent refrigeration load, ignoring the effects of weather data on refrigeration load (conduction and infiltration) [118]. The last remains unchanged in Pack Calculation Pro.

Numerical studies have also been found during this literature review, among others, the design and performance evaluation of reciprocating refrigeration systems, based in a property dependent finite-time thermodynamic model [119], the development of methodologies for simulation and optimization of energy consumption in cold stores, improving constructive and operating parameters [98], or mathematical models embodied in user-friendly excel spreadsheets, as the case of the ICE-E model (under the scope of the Improving Cold storage Equipment in Europe project), allowing easily to predict cold store energy consumption, when refrigeration loads vary according to ambient weather conditions, supported by large databases of products and theirs thermal properties [118].

In addition to the abovementioned examples, and apart from a handful of commercial software, it seems that the development of energy simulation tools, and research as well, of industrial refrigeration systems is losing ground to a wave of recent research interest: the commercial refrigeration in supermarkets. In this field, there are various software codes available, some of them with the ability of simulating entire supermarkets, *i.e.* able to simulate both the refrigeration and HVAC systems in supermarkets [77], [115], [120].

In 2005, resulting from his PhD thesis, Arias presents the release version of CyberMart [121], [122], a dedicated stand-alone program for estimating the annual energy consumption of an entire supermarket, with a user-friendly interface and allowing, not only the comparison of energy consumption, but also the environmental impact ($TEWI$) and the Life Cycle Cost (LCC) of different refrigeration systems. This tool offers a large set of system configurations (DX, completely and partly indirect systems, cascades, parallel systems with subcooling and district cooling), and it has been widely referenced in the literature [77], [115], [117], [118], [120]. However, some drawbacks are reported by Ge and Tassou [77], namely the zoning limitation (it considers the building as a singular zone), and the simple data requirement at two conditions (winter and summer conditions). According to the same authors [77], these limitations and other constrains (*e.g.* calculation of heating and cooling loads in steady-state operation with monthly mean climatic data, prediction of internal space parameters in a daily base, *etc.*), are shared by the RETScreen software, a clean energy project analysis software, used “to evaluate the

energy production and savings, costs, emission reductions, financial viability and risk for various types of Renewable-energy and Energy-efficient Technologies (RETs)" [123].

Some researchers have been using Modelica [124], an object-oriented modelling and simulation language, implemented by several software tools, and used to model large, complex and heterogeneous physical systems [115], [125], [126]. All Modelica models are mathematically described by differential, algebraic and discrete equations. Such fact provides this object-oriented modelling language, the adequate suitability for the physical modelling and transient simulation of CO_2-refrigeration cycles [125], or to develop and verify the performance and robustness of systems controls (in the absence of physical prototypes) of a CO_2 booster configuration in supermarket refrigeration systems [126].

Other simulation programs are referenced in the literature [77], [115], [117], [118], [121], [127]–[131], some of them already mentioned in the section of the industrial refrigeration's energy simulation software (Coolpack, Pack Calculation Pro, EES and MATLAB), others with multiple applications in the refrigeration sector, including supermarket equipment, such as the IMST-ART (*Investigación y Modelado de Sistemas Térmicos* – Advanced Refrigeration Technologies [132]), or even specifically used for supermarket refrigeration systems, such as the Econu Koeling (TNO, in The Netherlands) and the ORNL Supermarket Spreadsheets (Oak Ridge National Laboratory, in the USA).

4.1. THE ENERGYPLUS SOFTWARE

Besides CyberMart and RETScreen, two more energy simulation software with built-in supermarket refrigeration system models can be found: SuperSlim and EnergyPlus [77], [78], [115], [117], [118], [120], [133], [134]. SuperSim is based in TRNSYS simulation environment, using a refrigeration system, whose sub-models were specifically developed for the effect, enabling the simulation of the performance of centralized vapor-compression refrigeration systems, along with their interaction with the building envelope and the HVAC [77]. EnergyPlus is an energy analysis and thermal load simulation software, allowing multizone building simulations, with integrated simultaneous solutions, sub-hourly, user-definable time-steps, and detailed data for HVAC, solar collectors and photovoltaic, *etc*. Along with TRNSYS, they are the most-used simulation programs in buildings optimization research [135], versatile and with wide-range applications [101]. Despite TRNSYS greatest mathematical modeling flexibility, as demonstrated by Liu *et al.* [136] and Polzot *et al.* [120] (among others), the EnergyPlus

software is freely available, and it can be used for the simulation of complex systems (although made of conventional components) [120]. It is also considered as one of the commonly used public domain whole building energy simulation software that can be used for refrigeration systems modeling (along with eQUEST) [129]. Supermarket refrigeration capabilities were first added to EnergyPlus in 2004, and new models have been continually added and upgraded, responding to the development of modern systems configurations [133], making it also capable of modelling industrial applications [129]. Therefore, it provides two different approaches to model the refrigeration systems [137]:

- Refrigeration compressor rack objects, for simple supermarket-type refrigeration systems, including compressor racks, refrigerated cases and walk-in coolers, secondary loop equipment, and optional air or water heat reclaim coils. Schematic and circuit examples are shown in Figure 4.1 and Figure 4.3, respectively;
- Detailed refrigeration systems, used to model more complex systems, enabling, among others, load transfer between different systems, with secondary loops, cascade condensers, or mechanical subcoolers. Schematic and circuit examples are depicted in Figure 4.2 and Figure 4.4 respectively.

According to the EnergyPlus Engineering Reference [137], the main differences between both models are related to the detailed data input requirements, flexibility in the system configuration, outputs and other features, inherent to the detailed system method, namely:

- Requirement for performance data for each compressor and air- and evaporative-cooled condensers;
- Explicit calculation of the amount of superheat available for reclaim (air or water heating optional coil);
- Realistic behavior of the suction temperature, according to the refrigeration loads, and affecting the compressor efficiency;
- Load transfer from other refrigeration systems (cascade condensers, secondary loops, mechanical subcoolers), or within the own refrigeration system (LSHX);
- Possibility for modelling constant, constant linear, two speed, and variable speed fan types in evaporative and air cooled condensers, as well as in air chillers;
- Refrigerant inventory available for output tracking;
- Realistic limitation on the compressor and condenser capacities, carrying the unmet load over to the next time step;
- Calculation of the suction piping heat gain (non-useful heat gain).

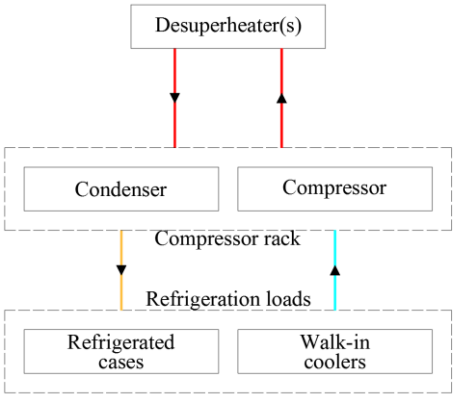

Figure 4.1: Typical compressor rack equipment schematic (source: adapted from [137])

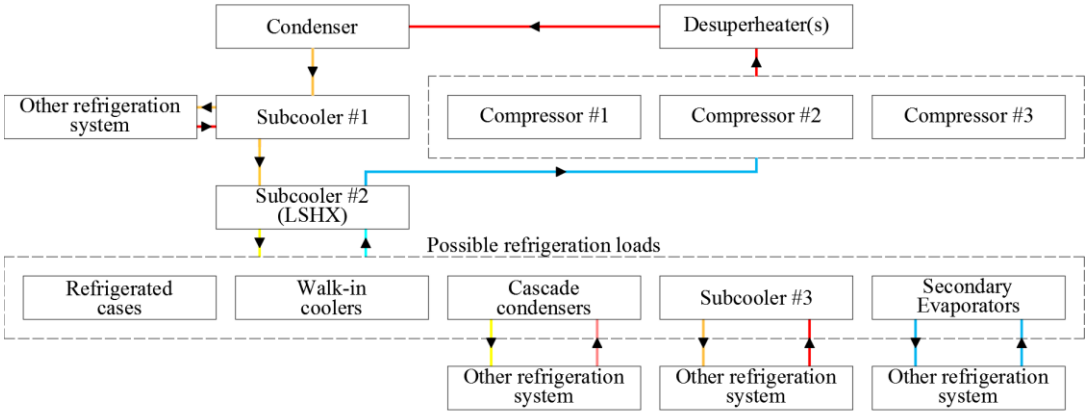

Figure 4.2: Typical detailed refrigeration system schematic (source: adapted from [137])

The most-recent versions of EnergyPlus include the following system types [129], [137]:

- Direct-expansion (DX) systems: including multiplex DX systems;
- Two-stage compression systems: including shell-and-coil or flash intercoolers;
- Cascade systems: exchanging heat from low- to high-temperature detailed systems;
- Secondary loop systems: using either single- or two phase heat transfer fluids;
- Transcritical CO_2 booster systems: standard configuration (see section 2.2.5.2);

and include the following refrigeration objects:

- Refrigerated cases: typical supermarket open refrigerated display cases;
- Walk-in coolers and freezers: small volume cold store, inside a space or a zone;
- Air Chillers: *i.e.* evaporators, when the operating fluid is a two-phase fluid (refrigerant) or air cooler, for single-phase fluids (glycol water or brine);
- Condensers: dry air-cooled, evaporative-cooled, water-cooled and cascade condensers (rejecting heat from a low- to a high-temperature refrigeration system);
- Compressors: for subcritical and transcritical operation, whose performance curves are defined in ANSI/AHRI Standard 540 [48] (section 2.2.2.2, Eq.(2.59));

- Compressor racks (compressor plus condenser unit): working in conjunction with refrigerated cases and walk-in coolers, typically for simple refrigeration systems;
- Subcoolers: suction line heat exchangers (LSHX) or mechanical heat exchangers (transferring a load from a lower- to a higher-temperature system);
- Air-cooled gas cooler: used for the transcritical CO_2.

EnergyPlus allows to model air mixing between two different zones (*e.g.* cold store and distribution corridor, allowing to choose between the absence of door protection, and the presence of air or strip curtains), according to density difference controlled air exchange model. Along with these objects (and besides the all non-mentioned others), EnergyPlus provides datasets for refrigerants' properties, namely for the R-11, R-12, R-22, R-123, R-134a, R-404A, R-407A, R-410A, R-507A, R-717 and R-744, and for glycol water (ethyleneglycol and propyleneglycol). Additional refrigerants or brines can be inserted. A set of examples files is provided, which can be adapted to define the simulation models. EnergyPlus offers a wide range of support documentation, including a valuable theoretical-based document: the Engineering Reference (reference [137]). Links to other software or internal programing is also possible to overcome eventual limitations.

Further, EnergyPlus has been used in the research unit to which the author belongs, it has been the subject of vocational training and a course (respectively, in ADAI, and at EfS MSc and PhD programmes, in the UC, with the author's contribution), and of some MSc theses, including a first iteration over EnergyPlus refrigeration systems modelling, applied to a conservation warehouse for frozen fish [138], also co-advised by the author. Following this lineage, EnergyPlus is the chosen software to perform energy simulations of refrigeration systems (and facilities) as those depicted in Figure 4.3 and in Figure 4.4.

Unitary direct-expansion system circuit, serving a walk-in freezer and a display case:

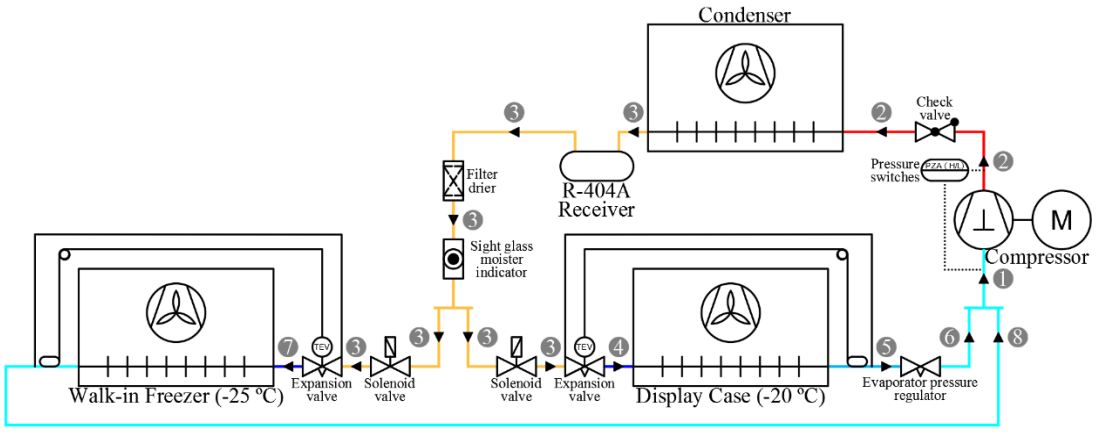

Figure 4.3: Unitary multiplex direct-expansion system: circuit (source: author)

Central system circuit (R-717), serving different freezing and cooling environments:

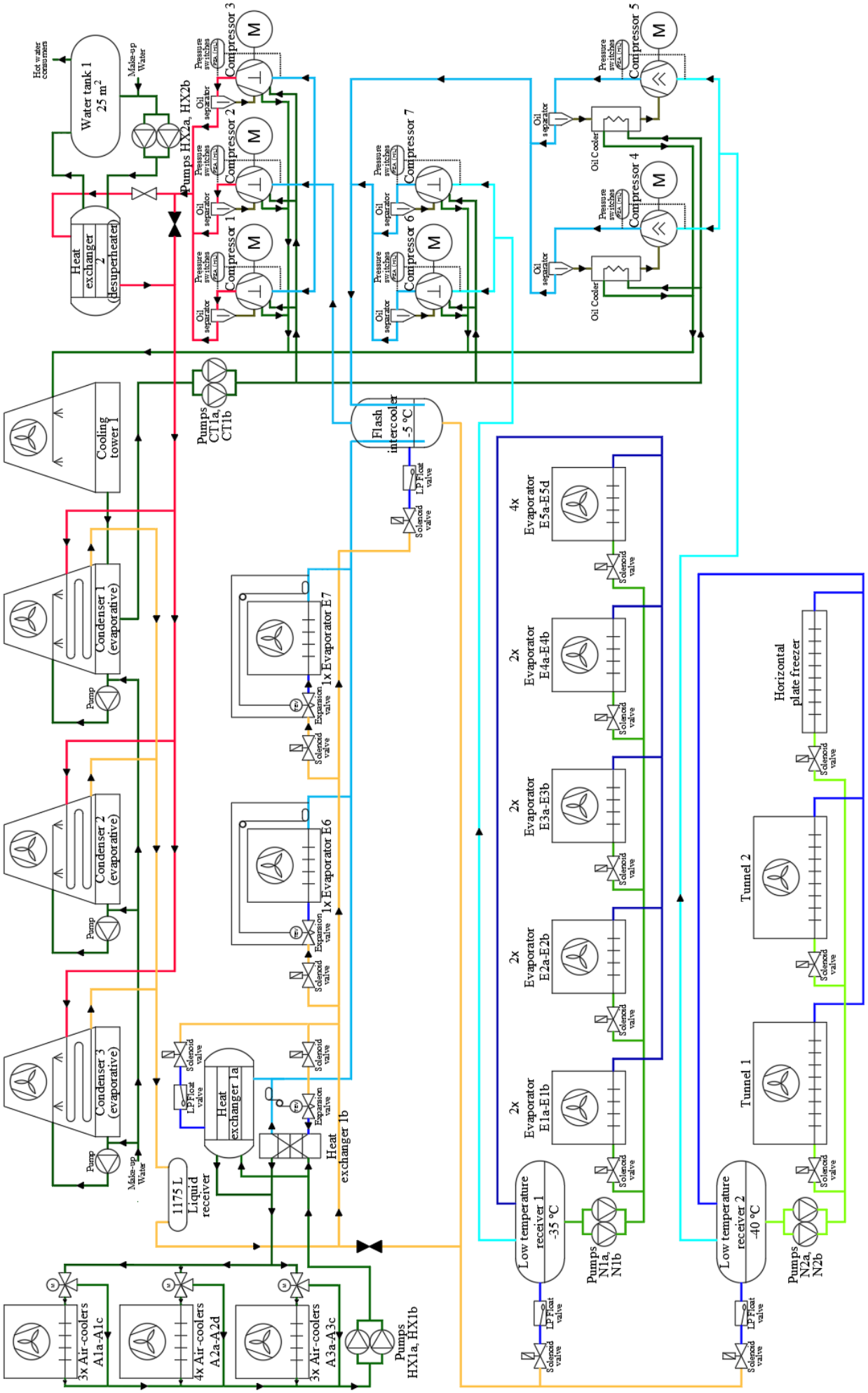

Figure 4.4: Ammonia-based refrigeration system - circuit (source: author)

5. CONCLUSIONS

5.1. RESEARCH SYNTHESIS

Energy efficiency is, undoubtedly, the main key to the reduction of GHG emissions worldwide. Particularly in the EU, it has become one of the most iconic issues/themes from energy and environmental policies, imposing targets for 2020 (20 % reduction on GHG emissions, 20 % increase the share of renewable-energy consumption, and 20 % reduction the energy consumption through energy-efficiency measures), recently redefined for 2030 (40 %, 27 % and 27 %, respectively). All the EU state members embraced these commitments, enforcing the legislation, albeit at different velocities and intensities, as it unfortunately happens in many other areas.

In Portugal, both current regulation on the implementation of energy-efficiency measures for the industry (SGCIE), and the energy programs aiming to mitigate the regulation gaps, have been proven to be ineffective, for the first case, and insufficient, for the latter, on transferring results and recommendations to the agro-food industry. The first main contribution to this failure is the SGCIE's application threshold, which is too high for the actuality of the national industry, dominated by non-intensive consuming companies. This reality is transversal to the agro-food sector, which, despite being the largest and the leading employer manufacturing sector, either in Portugal or in the EU, is highly fragmented, mostly constituted by SMEs, and out from the scope of SGCIE regulation. By the other hand, energy-efficiency measures resulting from by the energy programmes are presented at excessively large intervals. Such provides no reliable information nor conveys confidence to the decision-maker to take the risk on investing for retrofitting or acquiring a new equipment, or to change a manufacturing procedure. It is expected that energy simulation tools, applied to refrigeration systems and other energy systems, will be able to provide reliable and useful information, as long as the facilities, or building itself, and the most important, its systems are correctly defined and technically characterized, based in a deep knowledge on the existing technological solutions and its working parameters.

Starting with the storage temperature, which is highly dependent on the type of product and on the product intended shelf life, results in several categories for preservation of food quality in refrigerated storages: controlled atmosphere (for fruit and vegetables),

coolers, high-temperature freezers, and low-temperature storages and sub-freezers. The residence time in the cooling medium is a crucial design criterion to define cooling and pre-cooling methods: hydrocooling, forced-air and forced-air evaporative cooling, package icing, or vacuum and water spray vacuum cooling.

Regarding the components and their configurations: (1) the most-used refrigerant supply method for the evaporators is the direct-expansion. It is commonly used with halocarbon refrigerants, for small applications and moderate refrigerating temperatures. As disadvantages, it produces higher temperature differences between the cooling medium and the refrigerant, lowering the humidity (for air-coil evaporators). However, it is the least expensive, simpler and the most feasible refrigerant supplying method. The flooded feed method is appropriate for small temperature differences between the cooling medium and the refrigerant, and for low-temperature applications (particularly ammonia applications below -18 ºC). It is more efficient, has lower operating expenses and energy costs, fewer operating hours and lowers discharge temperature at the compressor outlet than the direct-expansion method, although it requires higher refrigerant charges. (2) Air-cooled is the costless, and the lowest acquisition and maintenance costs condenser type, although having higher noise levels and requiring higher condensation pressures than those from the evaporative type condensers. Cooling towers and evaporative condensers operate with a lower condensing temperature, resulting in lower condensation pressure, therefore, less consumption. Nevertheless, both are inevitably related with legionella. Cooling towers waste less water, while evaporative condensers are more compact and deliver lower condensing temperatures, reducing the energy consumption. (3) Reciprocating compressors are the most-common compressors up to 75 kW, having an applicability range from 0.25 kW to 1000 kW, and pressure ratios between 2.5 and 8 or 9. Screw compressors are the most used above 75 kW, in both single- and multistage systems, with applicability range up to 6000 kW, and providing pressure ratios up to 20. Machines with isentropic efficiencies above 70 % are reasonably efficient compressors. (4) Considering the expansion components, the thermostatic expansion valve is mainly used in direct-expansion circuits, while the high- and low-pressure float valves are used in flooded systems. The latter is much more common in industrial refrigeration.

With respect to the influence of the parameters over the system performance, as the pressure ratio decreases, both volumetric and isentropic efficiency increase, increasing the compressor's overall efficiency (it has more impact for reciprocating

compressors, while for twin-screw type, the isentropic efficiency might drop for low pressure ratios). A temperature variation (ΔT) in the evaporating temperature (T_{evap}) has a higher impact than the same variation (ΔT) in the condensation temperature (T_{cond}). (1) The reduction of the condensing temperature, or pressure, leads to an increase of the system's efficiency. Although, it should be adequately controlled, to ensure a lower-as-possible, yet functional condensing pressure level, particularly for the "winter operation", where further lowering of the condensing temperate or pressure might be less than the possible saves in pumps and fan motors of the condensers. (2) The increase of evaporating temperature, or pressure, results in an increased system efficiency, although limited by the conditions of the refrigerated medium and by operational parameters, such as the $DT1$. (3) An increase in the subcooling degree, always leads to an increase of the system efficiency, which is more important as the higher the subcooling degree is, and the lower the refrigeration effect is. (4) By opposition, superheating degree has not always an enhancing effect over the efficiency, depending on the refrigerant has it happens to NH_3. (5) The combined effect of subcooling and superheating degree depends on the strength of the variation of the specific volume *versus* the increment on the refrigeration effect. (6) The existence of pressure drops increases the pressure ratio, increasing the necessary specific compression work, decreasing the overall system's efficiency.

On the topic of the systems configurations and reduction of compression work, multistage arrangements are applied whenever the single-stage compression is not an economic and technically feasible process. Phenomena such as unacceptably high discharge temperatures, serious drops in the volumetric efficiency, excessive stress on the compressor moving parts, and especially the increase in the work input, are either harmful or excessively energy consuming for the reciprocating compressors. Therefore, for the pointed reasons, the multistage compression is used. The most effective and feasible procedure to minimize the compressor work is keeping the specific gas volume as small as possible, during the compression process, maintaining the gas temperature as low as possible during the process, *i.e.* cooling (desuperheating) the gas while it is compressed. (1) Liquid injection is the simplest, most compact and least-expensive desuperheating strategy, and it is used in low and medium-capacity systems. It is advantageous for cycles using ammonia, disadvantageous for R-502, and it has practically no benefits for R-22. (2) Liquid subcooling method reduces the irreversibilities from the isenthalpic expansion through a multistage expansion. The refrigeration effect increases, although the mass flow

decreases. It is advantageous for R-502, but should not be used with R-22 or ammonia. (3) Liquid injection with subcooling avoids the constrains imposed for R-22 or ammonia. (4) Intercooling is particularly efficient for high-capacity and low-temperatures applications using ammonia. Its efficiency can be improved incorporating a liquid subcooler, providing an interstage expansion (increasing the refrigeration effect). (5) Another multistage compression configuration is the indirect or cascade type, improving the COP, through the reduction of the compressor work and the increase in the refrigeration capacity. Owing the low quantity demand in the high-temperature cycle, there is a reduction the primary refrigerating charge. In industrial ammonia applications, it can be approximately 90 %, comparing to a conventional system of the same capacity.

Carbon dioxide has been recovering its place in vapor-compression system¸ used as a secondary refrigerant in the low-stage of cascade systems, or in secondary loop systems or as a primary refrigerant, in transcritical cycles. The transcritical CO_2 cycle has been commonly used in commercial refrigeration (in the US and Northern Europe), while in industry, it has been used as a secondary refrigerant in two-phase cascade systems. Regarding the other refrigerants, CFCs and HCFCs have been progressively phased out. The HCFs solved the chlorine containing problems of CFCs and HCFCs, although being thermodynamically less efficient than the HCFC R-22, and having high GWP values. The European "F-gas Regulation" has introduced restrictions for controlling the emissions from the fluorinated greenhouse gases, which triggered a quick response in the production of a new generation of refrigerants, wherein the synthetic fluids HFOs fit. Natural refrigerants, such as ammonia and carbon dioxide have been through a renewed interest.

Among the thermally driven technologies, such as adsorption and ejector refrigeration cycles, only vapor absorption technology might be a feasible alternative, as long as there is available waste heat. Other emerging technologies such as gas, Stirling, thermoelectric, magnetic or thermoacoustic refrigeration cycles are merely used in niche applications or specific HVAC equipment, and in some refrigeration systems, without a significant penetration in the agro-food refrigeration. Vapor compression technology provides the greatest energy performance coefficients, making it the leading refrigeration technology.

In the Portuguese agro-food industry, rather like it happens worldwide, refrigeration is dominated by the vapor-compression technology. Reciprocating compressors are the most-used compressor type, followed by screw compressors. The main refrigerant supply

method is the direct-expansion, although the liquid-overfeed method is used in ammonia-based flooded evaporators. The most-used refrigerants are the R-404A, ammonia (R-717 or NH_3) and R-22 among others, with a share lower than 10 %. Generally, the equipment has an advanced age, more than ten-year-old, being fragmented and diverse: unitary systems, condensing units, compressor racks (direct and secondary loop), compact units and air handling units (drying processes).

Regarding the energy simulation programs, there are several options. However, most of them without integration in a whole-building analysis (*e.g.* EES and MATLAB based computational models, CoolPack, Pack Calculation Pro), or oriented to the commercial refrigeration, *i.e.* supermarkets (*e.g.* IMST-ART, Econu Koeling , ORNL Supermarket Spreadsheets, CyberMart, SuperSlim). Among the conventional building-oriented energy simulation programs, only EnergyPlus offers refrigeration models, suitable either for commercial or industrial refrigeration. It includes the main existent configurations for the refrigeration systems, such as direct-expansion, multistage compression (two-stage), cascades, secondary loops and transcritical CO_2 booster systems. It includes diverse refrigeration equipment object models, such as refrigerated air chillers, walk-in coolers and freezers, air chillers (evaporators/air coolers), dry air-cooled, evaporative-cooled, water-cooled and cascade condensers, compressors for subcritical and transcritical operation, compressor racks, subcoolers and air-cooled gas coolers. EnergyPlus provides also datasets for several refrigerants' properties, and for glycol water, where additional information can be inserted. It has also an extensive support documentation, example files and datasets. Additionally, and besides all the energy models and other features, EnergyPlus allows internal programing and external connections to other software, overcoming its eventual limitations. For such reasons, EnergyPlus is adequate for the energy simulation of industrial refrigeration systems and for predicting the impact of energy-efficiency measures.

The calibration of an energy simulation model is not expected to be a trivial task, demanding for result comparisons with consumption breakdowns and energy analysis, obtained from detailed energy audits, previously conducted. Energy audits are essential to gather the information for the model inputs and its energy consumption's calibration.

5.2. FUTURE WORK AND RECOMMENDATIONS

EnergyPlus, an energy simulation software, will be then the engine to reproduce current operating conditions, and evaluate the impact on the energy consumption from the different measures. As previously indicated, it is mandatory to perform an exhaustive survey of the facilities and their operating conditions, through detailed energy audits. Energy audits should be carried out on several refrigeration plants and systems, and the corresponding dynamic simulation models should be developed, tested and calibrated. From the results, simplified and standardized models should be designed, to the different agro-food subsectors, where either geometrical characteristics, energy consumption or the impact of the energy-efficiency measures, should match to those from the detailed models. It is expected that these simplified models, when applied to other facilities, from the same agro-food subsectors and possessing equivalent refrigeration systems, allow to replicate the actual energy consumption, with a small amount of introduced information and without needing to perform the costly energy audits. In this way, it would be gathered the conditions for evaluating energy-efficiency measures, electing the most suitable and feasible options, providing reliable and useful information for this industrial sector. Among all the possible energy-efficiency measures, the following present a high potential for achieving these objectives:

- Passive solutions optimization (*e.g.* light, medium and heavyweight envelope, insulation level, orientation, thermal mass, phase change materials);
- System configurations (*e.g.* cascades, indirect *versus* direct systems, central *versus* unitary systems, different condensers types);
- Equipment and facilities (*e.g.* variable-frequency drives for compressors, fans and pumps, efficient lighting, evaporators defrost type, piping at outdoor conditions, PVC and air curtains);
- Control strategies *(e.g.* head pressure, evaporating pressure, air chiller scheduling, "peak shifting" or "peak shaving" loads);
- Heat recovery and combined heat and power (*e.g.* thermal driven chillers, solar, heat recover for HVAC systems), among others.

Further theoretical and experimental research should be conducted in the future for these fields, increasing the competitiveness of the SMEs, and contributing to the global effort regarding the energy independency and the reduction on GHG emissions.

REFERENCES

[1] European Commission, “Reference document on best available techniques for energy efficiency”, 2009.

[2] European Commission, “A policy framework for climate and energy in the period from 2020 to 2030”, 2014.

[3] European Commission, “Green paper: Towards a European strategy for the security of energy supply”, 2000.

[4] European Commission, “European energy security strategy”, 2014.

[5] European Commission, “Energy 2020. A strategy for competitive, sustainable and secure energy”, 2010.

[6] European Commission, “Energy roadmap 2050”, 2011.

[7] Eurostat - Statistical Office of the European Union, “Panorama of energy: Energy statistics to support EU policies and solutions”, 2009.

[8] J. Nunes, “Avaliação do desempenho dos sistemas de refrigeração nas indústrias agroalimentares da Beira Interior”, University of Beira Interior, Portugal, 2013.

[9] Exxon Mobil Corporation, “The outlook for energy: A view to 2040”, 2016.

[10] International Energy Agency, “World energy outlook 2015, Executive summary”, 2015.

[11] International Energy Agency, “Scenarios and projections”, *OECD/IEA*, 2016. [Online]. Available: http://www.iea.org/publications/scenariosandprojections/. [Accessed: 15-Feb-2016].

[12] International Energy Agency, “World energy outlook 2011, Executive summary”, 2011.

[13] International Energy Agency, “Energy and climate change. World energy outlook special report”, 2015.

[14] N. Jollands, P. Waide, M. Ellis, T. Onoda, J. Laustsen, K. Tanaka, P. de T’Serclaes, I. Barnsley, R. Bradley, and A. Meier, “The 25 IEA energy efficiency policy recommendations to the G8 Gleneagles Plan of Action”, *Energy Policy*, vol. 38, no. 11, pp. 6409–6418, 2010.

[15] N. Campbell and J. Park, “Work of the IEA’s energy efficiency unit”, in *IEA Headquarters*, 2012, pp. 1–31.

[16] Eurostat - Statistical Office of the European Union, “Final energy consumption by sector”, *Eurostat*, 2016. [Online]. Available: http://ec.europa.eu/eurostat/web/products-datasets/-/tsdpc320. [Accessed: 15-Feb-2016].

[17] European Commission - Directorate-General for Energy and Transport, “2020 Vision: Saving our energy”, Brussels, 2007.

[18] ICF Consulting Ltd under contract ENER/C3/2012-439/S12.666002 to the European Commission Directorate-General Energy, "Study on energy efficiency and energy saving potential in industry and on possible policy mechanisms", 2015.

[19] Resolução do Conselho de Ministros nº20/2013, *Plano Nacional de Ação para a Eficiência Energética (PNAEE 2016) e Plano Nacional de Ação para as Energias Renováveis (PNAER 2020)*. Portugal, 2013, pp. 2022–2091.

[20] E. A. Abdelaziz, R. Saidur, and S. Mekhilef, "A review on energy saving strategies in industrial sector", *Renew. Sustain. Energy Rev.*, vol. 15, no. 1, pp. 150–168, 2011.

[21] Grupo de Trabalho do PNAC 2020: Despacho nº.2441/2014, *Programa Nacional para as Alterações Climáticas 2020/2030 (PNAC2020)*. 2015, pp. 1–141.

[22] Decreto-Lei nº.71/2008 de 15 de abril, *Sistema de Gestão dos Consumos Intensivos de Energia (SGCIE)*. Portugal, 2008, pp. 2222–2226.

[23] Instituto Nacional de Estatística I.P., "Empresas em Portugal 2012", Instituto Nacional de Estatística I.P., Lisboa, 2014.

[24] Federação das Industrias Portuguesas Agro-Alimentares, "Federação das Industrias Portuguesas Agro-Alimentares web page", 2016. [Online]. Available: http://www.fipa.pt. [Accessed: 15-Feb-2016].

[25] Fooddrink Europe, "Data & trends. European food industry 2014-2015", Brussels, 2015.

[26] FoodDrink Europe, "FoodDrink Europe web page", 2016. [Online]. Available: http://www.fooddrinkeurope.eu. [Accessed: 15-Feb-2016].

[27] CITEVE – Centro Tecnológico das Indústrias Têxtil e do Vestuário de Portugal, "Plano setorial de melhoria da eficiência energética em PME - Setor agroalimentar", 2012.

[28] L. P. Andrade, J. Nunes, P. D. Silva, P. D. Gaspar, and C. Domingues, "Oportunidades de eficiência energética no setor agropecuário e agroindústrias." 2014.

[29] V. R. Ferreira, J. B. Ribeiro, A. R. Gaspar, J. J. Costa, and A. V. Oliveira, "InovEnergy – A project for energy efficiency in the agro-food industry sector", in *Energy efficiency for a more sustainable world*, 2012, pp. 1–8.

[30] L. P. Andrade, "Cooperação institucional na investigação aplicada : o caso do Project InovEnergy: eficiência energética no setor agroindustrial", *Rev. do Inst. Politécnico Castelo Branco*, vol. Ano 4º nº5, pp. 20–22, 2014.

[31] J. Nunes, D. Neves, P. D. Gaspar, P. D. Silva, and L. P. Andrade, "Predictive tool of energy performance of cold storage in agrifood industries: The Portuguese case study", *Energy Convers. Manag.*, vol. 88, pp. 758–767, 2014.

[32] L. P. de Andrade, J. Nunes, P. Dinho, P. Dinis, L. C. Domingues, T. Nobre, A. Gaspar, M. Feliciano, A. Araújo, P. Brito, and P. Félix, *Manual de boas práticas - InovEnergy*. 2014.

[33] InovEnergy – Eficiência energética no sector agroindustrial, “Divulgação”, 2014. [Online]. Available: http://inovenergy.inovcluster.pt/divulgacao.aspx. [Accessed: 15-Feb-2016].

[34] ASHRAE, *2010 ASHRAE Handbook - Refrigeration (SI Edition)*. Atlanta: American Society of Heating, Refrigerating and Air-Conditioning Engineers, Inc., 2010.

[35] W. F. Stoecker, *Industrial refrigeration handbook*. USA, 1998.

[36] S. Devotta, S. Sicars, R. Agarwal, J. Anderson, D. Bivens, D. Colbourne, G. Hundy, H. König, P. Lundqvist, E. McInerney, P. Nekså, and A. El-Talouny, “Refrigeration”, in *IPCC/TEAP Special report - Safeguarding the ozone layer and the global climate system: Issues related to hydrofluorocarbons and perfluorocarbons*, E. Calvo and I. Elgizouli, Eds. Geneva, Switzerland: Intergovernmental Panel on Climate Change, 2005, pp. 225–268.

[37] E. T. Alcaraz, *La produccíon de frío*. Valencia: Servicio de Publicaciones de la Universidad Politécnica de Valencia, 2000.

[38] G. H. Hundy, A. R. Trott, and T. C. Welch, *Refrigeration and air-conditioning*, 4th Ed. Elsevier Ltd, 2008.

[39] Y. A. Çengel and M. A. Boles, *Thermodynamics: An engineering approach*, 5th Ed., vol. 1. Boston: McGraw-Hill College, 2006.

[40] Á. L. M. Barreras and M. P. Rufes, *Ciclos de refrigeración*. Barcelona: Planeta DeAgostini Professional y Formación S.L., 2004.

[41] J. A. Creus, *Tratado prático de refrigeração automática*, VIII. Barcelona: Dinalivro, 1978.

[42] F. Cabeza, *Las bases del frío*, 5ª Edición. Madrid: Didafrio, 2014.

[43] N. Lior and N. Zhang, “Energy, exergy, and Second Law performance criteria”, *Energy*, vol. 32, no. 4, pp. 281–296, 2007.

[44] R. L. Akau and R. J. Schoenhals, “The second law efficiency of a heat pump system”, *Energy*, vol. 5, no. 8–9, pp. 853–863, 1980.

[45] A. L. Miranda, *Evaporadores*. Barcelona: Gráficas y Encuadernaciones Reunidas, S.A., 2000.

[46] P. R. Martínez, *Condensadores*. Barcelona: Gráficas y Encuadernaciones Reunidas, S.A., 2000.

[47] T. Q. Qureshi and S. A. Tassou, “Variable-speed capacity control in refrigeration systems”, *Appl. Therm. Eng.*, vol. 16, no. 2, pp. 103–113, 1996.

[48] ANSI/AHRI Standard 540-2015, *Standard for performance rating of positive displacement refrigerant compressors and compressor units*. Arlington, USA: Air-Conditioning, Heating, and Refrigeration Institute, 2015, pp. 1–19.

[49] N. Stošic, I. K. Smith, A. Kovacevic, and E. Mujic, “Three decades of modern practice in screw compressors”, in *International Compressor Engineering Conference*, 2010, pp. 1–8.

[50] S. K. Lohn and E. L. L. Pereira, “Numerical investigation of the gas leakage through the piston-cylinder clearance of reciprocating compressors”, in *International Compressor Engineering Conference*, 2014, pp. 1–9.

[51] N. Stošic, “Revew article: Screw compressors in refrigeration and air conditioning”, *HVAC&R Res.*, vol. 10, pp. 233–263, 2011.

[52] A. A. Kornhauser, “The use of an ejector in a geothermal flash system”, in *International Refrigeration and Air Conditioning Conference*, 1990, pp. 1–19.

[53] A. Subiantoro and K. T. Ooi, “Economic analysis of the application of expanders in medium scale air-conditioners with conventional refrigerants, R1234yf and CO2”, *Int. J. Refrig.*, vol. 36, no. 5, pp. 1472–1482, 2013.

[54] N. Lawrence and S. Elbel, “Experimental investigation of a two-phase ejector cycle suitable for use with low-pressure refrigerants R134a and R1234yf”, *Int. J. Refrig.*, vol. 38, no. 1, pp. 310–322, 2014.

[55] N. Lawrence and S. Elbel, “Analytical and experimental investigation of two-phase ejector cycles using low-pressure refrigerants”, in *International Refrigeration and Air Conditioning Conference*, 2012, pp. 1–11.

[56] A. Mota-Babiloni, J. Navarro-Esbrí, F. Molés, Á. B. Cervera, B. Peris, and G. Verdú, “A review of refrigerant R1234ze(E) recent investigations”, *Appl. Therm. Eng.*, vol. 95, pp. 211–222, 2016.

[57] C. C. Wang, “System performance of R-1234yf refrigerant in air-conditioning and heat pump system - An overview of current status”, *Appl. Therm. Eng.*, vol. 73, no. 2, pp. 1412–1420, 2014.

[58] Y. He, J. Deng, and Z. Zhang, “Thermodynamic study on a new transcritical CO2 ejector expansion refrigeration system with two-stage evaporation and vapor feedback”, *HVAC&R Res.*, vol. 20, no. 6, pp. 655–664, 2014.

[59] L. Zheng, J. Deng, Y. He, and P. Jiang, “Dynamic model of a transcritical CO2 ejector expansion refrigeration system”, *Int. J. Refrig.*, vol. 60, pp. 247–260, 2015.

[60] S. A. Klein, D. T. Reindl, and K. Brownell, “Refrigeration system performance using liquid-suction heat exchangers”, *Int. J. Refrig.*, vol. 23, no. 8, pp. 588–596, 2000.

[61] M. J. Skovrup, A. Jakobsen, and S. E. Andersen, “CoolPack.” IPU & Department of Mechanical Engineering - Technical University of Denmark, 2012.

[62] S. A. Tassou, J. S. Lewis, Y. T. Ge, A. Hadawey, and I. Chaer, “A review of emerging technologies for food refrigeration applications”, *Appl. Therm. Eng.*, vol. 30, no. 4, pp. 263–276, 2010.

[63] A. Pearson, “Refrigeration with ammonia”, *Int. J. Refrig.*, vol. 31, no. 4, pp. 545–551, 2008.

[64] A. Mota-Babiloni, J. Navarro-Esbrí, Á. Barragán-Cervera, F. Molés, B. Peris, and G. Verdú, “Commercial refrigeration – An overview of current status”, *Int. J. Refrig.*, vol. 57, pp. 186–196, 2015.

[65] W. Bingming, W. Huagen, L. Jianfeng, and X. Ziwen, “Experimental investigation on the performance of NH3/CO2 cascade refrigeration system with twin-screw compressor”, *Int. J. Refrig.*, vol. 32, no. 6, pp. 1358–1365, 2009.

[66] C. Sanz-Kock, R. Llopis, D. Sánchez, R. Cabello, and E. Torrella, “Experimental evaluation of a R134a/CO2 cascade refrigeration plant”, *Appl. Therm. Eng.*, vol. 73, no. 1, pp. 39–48, 2014.

[67] A. da Silva, E. P. Bandarra Filho, and A. H. P. Antunes, “Comparison of a R744 cascade refrigeration system with R404A and R22 conventional systems for supermarkets”, *Appl. Therm. Eng.*, vol. 41, pp. 30–35, 2012.

[68] V. Sharma, B. Fricke, and P. Bansal, “Comparative analysis of various CO2 configurations in supermarket refrigeration systems”, *Int. J. Refrig.*, vol. 46, pp. 86–99, 2014.

[69] J. M. Calm, “The next generation of refrigerants - Historical review, considerations, and outlook”, *Int. J. Refrig.*, vol. 31, no. 7, pp. 1123–1133, 2008.

[70] M. Chasserot, N. Masson, H. Jia, S. Burkel, A. Maratou, and K. Skačanová, “Guide 2014: Natural refrigerants - continued growth and innovation in Europe”, Brussels, 2014.

[71] J. Steven Brown and P. A. Domanski, “Review of alternative cooling technologies”, *Appl. Therm. Eng.*, vol. 64, no. 1–2, pp. 252–262, 2014.

[72] A. Pearson, “Carbon dioxide - New uses for an old refrigerant”, *Int. J. Refrig.*, vol. 28, no. 8, pp. 1140–1148, 2005.

[73] ASHRAE, *2008 ASHRAE Handbook - HVAC Systems and Equipment (SI Edition)*. Atlanta: American Society of Heating, Refrigerating and Air-Conditioning Engineers, Inc., 2008.

[74] K. Wang, M. Eisele, Y. Hwang, and R. Radermacher, “Review of secondary loop refrigeration systems”, *Int. J. Refrig.*, vol. 33, no. 2, pp. 212–234, 2010.

[75] L. Cecchinato, M. Corradi, and S. Minetto, “Energy performance of supermarket refrigeration and air conditioning integrated systems working with natural refrigerants”, *Appl. Therm. Eng.*, vol. 48, pp. 378–391, 2012.

[76] I. Sarbu, “A review on substitution strategy of non-ecological refrigerants from vapour compression-based refrigeration, air-conditioning and heat pump systems”, *Int. J. Refrig.*, vol. 46, pp. 123–141, 2014.

[77] Y. T. Ge and S. A. Tassou, “Performance evaluation and optimal design of supermarket refrigeration systems with supermarket model ‘superSim’, Part I: Model description and validation”, *Int. J. Refrig.*, vol. 34, no. 2, pp. 527–539, 2011.

[78] Y. T. Ge and S. A. Tassou, “Performance evaluation and optimal design of supermarket refrigeration systems with supermarket model ‘superSim’. Part II: Model applications”, *Int. J. Refrig.*, vol. 34, no. 2, pp. 540–549, 2011.

[79] New Buildings Institute, “Absorption chillers”, 1998.

[80] B. Le Lostec, N. Galanis, and J. Millette, “Simulation of an ammonia-water absorption chiller”, *Renew. Energy*, vol. 60, pp. 269–283, 2013.

[81] D. S. Kim and C. A. Infante Ferreira, “Solar refrigeration options - a state-of-the-art review”, *Int. J. Refrig.*, vol. 31, no. 1, pp. 3–15, 2008.

[82] R. Z. Wang and R. G. Oliveira, “Adsorption refrigeration-An efficient way to make good use of waste heat and solar energy”, *Prog. Energy Combust. Sci.*, vol. 32, no. 4, pp. 424–458, 2006.

[83] L. W. Wang, R. Z. Wang, and R. G. Oliveira, “A review on adsorption working pairs for refrigeration”, *Renew. Sustain. Energy Rev.*, vol. 13, pp. 518–534, 2009.

[84] M. Krause, R. Ghirlando, E. Podesser, M. Jaradat, R. Heinzen, L. Mesquita, P. Bourdoukan, E. Wurtz, K. Ellehauge, C. Bongs, C. Pollerberg, and P. Finocchiaro, “C1: State of the art – Survey on new solar cooling developments”, 2010.

[85] S. James, P. Nesvadba, M. Berry, J. Fletcher, P. McClure, J. Wilkinson, Q. T. Pham, A. Pearson, K. Fikiin, O. M. Magnussen, A. K. T. Hemmingsen, V. Hardarsson, T. S. Nordtvedt, T. M. Eikevik, C. L. M. Silva, E. M. Gonçalves, T. R. da S. Brandão, A. LeBail, H. D. Goff, R. Gormley, N. E. Zaritzky, A. G. F. Stapley, G. Panozzo, G. Cortella, and O. Laguerre, *Frozen food science and technology*. Blackwell Pubishing Ltd., 2008.

[86] ASHRAE, *2013 ASHRAE Handbook - Fundamentals (SI Edition)*. Atlanta: American Society of Heating, Refrigerating and Air-Conditioning Engineers, Inc., 2013.

[87] Regulation (EC) No 2037/2000, *Regulation (EC) No 2037/2000 of the European Parliament and the Council of 29 June 2000 on substances that deplete the ozone layer*. 2000, p. L244/1-24.

[88] Regulation (EC) No 842/2006, *Regulation (EC) No 842/2006 of the European Parliament and of the Council of 17 May 2006 on certain fluorinated greenhouse gases*. 2006, p. L161/1-11.

[89] Regulation (EU) No 517/2014, *Regulation (EU) No 517/2014 of the European Parliament and of the Council of 16 April 2014 on fluorinated greenhouse gases and repealing Regulation (EC) No 842/2006*. 2014, p. L150/195-230.

[90] CEN - European Committee for Standardization, *EN 378-1:2000 Refrigerating systems and heat pumps - Safety and environmental requirements - Part 1: Basic requirements, definitions, classification and selection criteria*. 2000, pp. 1–50.

[91] ANSI/ASHRAE Standard 34-2013, *Designation and safety classification of refrigerants*. USA, 2013, pp. 1–46.

[92] A. Mota-Babiloni, J. Navarro-Esbrí, Á. Barragán, F. Molés, and B. Peris, “Theoretical comparison of low GWP alternatives for different refrigeration configurations taking R404A as baseline”, *Int. J. Refrig.*, vol. 44, pp. 81–90, 2014.

[93] V. Ferreira, F. B. Lamas, A. Gaspar, J. Costa, and J. Baranda, “Caracterização dos sistemas de refrigeração da indústria agroindustrial”, in *“A indústria e a engenharia portuguesa - desafios e perspetivas” - 7º Encontro Nacional do Colégio de Engenharia Mecânica – Ordem dos Engenheiros*, 2014.

[94] Decreto-Lei nº.23/2010 de 25 de março, *Disciplina da actividade de cogeração*. Portugal, 2010, pp. 934–946.

[95] Decreto-Lei nº.68-A/2015 de 30 de abril, *Disposições em matéria de eficiência energética e cogeração*. Portugal, 2015, pp. 2–52.

[96] A. F. R. Couto, "Estudo de viabilidade de sistema de autoconsumo industrial com cogeração", University of Porto, Portugal, 2015.

[97] G. Ding, "Recent developments in simulation techniques for vapour-compression refrigeration systems", *Int. J. Refrig.*, vol. 30, no. 7, pp. 1119–1133, 2007.

[98] P. Brito, P. Lopes, P. Reis, and O. Alves, "Simulation and optimization of energy consumption in cold storage chambers from the horticultural industry", *Int. J. Energy Environ. Eng.*, vol. 5, no. 2–3, pp. 1–15, 2014.

[99] D. J. Cleland, "Modelling of refrigeration processes", in *IIR International Cold Chain Conference*, 2010.

[100] D. B. Crawley, L. K. Lawrie, F. C. Winkelmann, W. F. Buhl, Y. J. Huang, C. O. Pedersen, R. K. Strand, R. J. Liesen, D. E. Fisher, M. J. Witte, and J. Glazer, "EnergyPlus: Creating a new-generation building energy simulation program", *Energy Build.*, vol. 33, pp. 319–331, 2001.

[101] D. B. Crawley, J. W. Hand, M. Kummert, and B. T. Griffith, "Contrasting the capabilities of building energy performance simulation programs", *Build. Environ.*, vol. 43, no. 4, pp. 661–673, 2008.

[102] S. J. Lovatt, "A dynamic modelling methodology for the simulation of industrial refrigeration systems", Massey University, New Zealand, 1992.

[103] DOE, "EnergyPlus." U.S. Department of Energy - Energy Efficiency and Renewable Energy - Office of Building Technologies, Washington, D.C., USA, 2016.

[104] S. A. Klein et al, "TRNSYS 17: A transient system simulation program, Solar Energy Laboratory, University of Wisconsin, Madison, USA", 2010. [Online]. Available: http://sel.me.wisc.edu/trnsys. [Accessed: 19-Dec-2016].

[105] A. C. Cleland, "Simulation of industrial refrigeration plants under variable load conditions", *Int. J. Refrig.*, vol. 6, no. 1, pp. 11–19, 1983.

[106] A. C. Cleland, "Experimental verification of a mathematical model for simulation of industrial refrigeration plants", *Int. J. Refrig.*, vol. 8, no. 5, pp. 275–282, 1985.

[107] A. C. Cleland, "RADS - a computer package for refrigeration analysis, design and simulation", *Int. J. Refrig.*, vol. 8, pp. 372–373, 1985.

[108] S. J. Lovatt, M. P. F. Loeffen, and A. C. Cleland, "Improved dynamic simulation of multi-temperature industrial refrigeration systems for food chilling, freezing and cold storage", *Int. J. Refrig.*, vol. 21, no. 3, pp. 247–260, 1998.

[109] F-Chart Software, "Engineering Equation Solver." Madison, Wisconsin, USA, 2016.

[110] The Mathworks Inc., "MATLAB." Natick, Massachusetts, USA, 2016.

[111] K. A. Manske, "Performance optimization of industrial refrigeration systems", University of Wisconsin-Madison, USA, 2000.

[112] R. Stoeckle, “Refrigerated warehouse operation under real-time pricing”, University of Wisconsin-Madison, USA, 2000.

[113] P. Mumanachit, “Comparative analysis of low temperature industrial refrigeration systems”, University of Wisconsin-Madison, USA, 2009.

[114] P. Mumanachit, D. T. Reindl, and G. F. Nellis, “Comparative analysis of low temperature industrial refrigeration systems”, *Int. J. Refrig.*, vol. 35, no. 4, pp. 1208–1221, 2012.

[115] N. Fidorra, “Computational tools for supermarket planning”, 2016.

[116] H. Hasse and M. Becker, “Top-down model for dynamic simulation of cold-storage plants”, *Int. J. Refrig.*, vol. 19, no. 1, pp. 10–18, 1996.

[117] S. G. Gwanpua, P. Verboven, D. Leducq, T. Brown, B. E. Verlinden, E. Bekele, W. Aregawi, J. Evans, A. Foster, S. Duret, H. M. Hoang, S. Van Der Sluis, E. Wissink, L. J. A. M. Hendriksen, P. Taoukis, E. Gogou, V. Stahl, M. El Jabri, J. F. Le Page, I. Claussen, E. Indergård, B. M. Nicolai, G. Alvarez, and A. H. Geeraerd, “The FRISBEE tool, a software for optimising the trade-off between food quality, energy use, and global warming impact of cold chains”, *J. Food Eng.*, vol. 148, no. October 2007, pp. 2–12, 2015.

[118] A. M. Foster, L. O. Reinholdt, T. Brown, E. C. Hammond, and J. A. Evans, “Reducing energy consumption in cold stores using a freely available mathematical model”, *Sustain. Cities Soc.*, vol. 21, pp. 26–34, 2016.

[119] J. Khan and S. M. Zubair, “Design and performance evaluation of reciprocating refrigeration systems”, *Int. J. Refrig.*, vol. 22, pp. 235–243, 1999.

[120] A. Polzot, P. D’Agaro, P. Gullo, and G. Cortella, “Modelling commercial refrigeration systems coupled with water storage to improve energy efficiency and perform heat recovery”, *Int. J. Refrig.*, vol. 69, pp. 313–323, 2016.

[121] J. Arias, “Energy usage in supermarkets - modelling and field measurements”, KTH Royal Institute of Technology, Stockholm, Sweden, 2005.

[122] J. Arias, “CyberMart a whole-building simulation model for supermarkets.” pp. 1–37, 2006.

[123] Natural Resources Canada, “RETScreen - Clean Energy Project Analysis Software.” 2013.

[124] Modelica Association, “Modelica.” 2016.

[125] T. Pfafferott and G. Schmitz, “Modelling and transient simulation of CO2-refrigeration systems with Modelica”, *Int. J. Refrig.*, vol. 27, no. 1, pp. 42–52, 2004.

[126] R. Shi and J. Fan, “Dynamic Modeling of CO2 Supermarket Refrigeration System”, *Proc. Int. Refrig. Air Cond. Conf.*, pp. 12–15, 2010.

[127] S. Sawalha, “Theoretical evaluation of trans-critical CO2 systems in supermarket refrigeration. Part I: Modeling, simulation and optimization of two system solutions”, *Int. J. Refrig.*, vol. 31, no. 3, pp. 516–524, 2008.

[128] S. Sawalha, “Theoretical evaluation of trans-critical CO2 systems in supermarket refrigeration. Part II: System modifications and comparisons of different solutions”, *Int. J. Refrig.*, vol. 31, no. 3, pp. 525–534, 2008.

[129] M. Adams, J. Sanyal, B. Fricke, and K. Benne, “Refrigeration modeling components in OpenStudio”, in *International Refrigeration and Air Conditioning Conference*, 2014, pp. 1–10.

[130] S. M. van der Sluis, “Review of calculation programs for supermarket DX refrigerating systems year-round energy consumption”, *IIR/IIF D1-subcommission “Refrigerated Display Cabinets.”* Glasgow (UK) Meeting, pp. 1–13, 2004.

[131] H.-M. Getu and P. K. Bansal, “Simulation model of a low-temperature supermarket refrigeration system”, *HVAC&R Res.*, vol. 12, no. 4, pp. 1117–1139, 2006.

[132] Investigación y Modelado de Sistemas Térmicos - Universidad Politécnica de Valencia, “IMST-ART.” Valencia, Spain, 2016.

[133] T. K. Stovall and V. D. Baxter, “Modeling supermarket refrigeration with EnergyPlus ™”, *IEA Heat Pump Centre Newsletter*. pp. 1–5, 2010.

[134] H. Witt, S. Taylor, K. Lomas, and R. Liddiard, “Simulation of energy use in UK supermarkets using EnergyPlus”, in *Conference of International Building Performance Simulation Association*, 2015, pp. 1095–1102.

[135] A.-T. Nguyen, S. Reiter, and P. Rigo, “A review on simulation-based optimization methods applied to building performance analysis”, *Appl. Energy*, vol. 113, pp. 1043–1058, 2014.

[136] M. Liu, W. Saman, and F. Bruno, “Computer simulation with TRNSYS for a mobile refrigeration system incorporating a phase change thermal storage unit”, *Appl. Energy*, vol. 132, pp. 226–235, 2014.

[137] DOE, “EnergyPlus Engineering Reference.” U.S. Department of Energy - Energy Efficiency and Renewable Energy - Office of Building Technologies, Washington, D.C., USA, pp. 1–1723, 2016.

[138] J. A. B. M. da Silva, “Avaliação do desempenho energético de câmaras de refrigeração industrial”, University of Coimbra, Portugal, 2014.

[139] L. Theodore and F. Ricci, *Mass transfer operations for the practicing engineer*. New Jersey: John Wiley & Sons, Inc., 2010.

APPENDIX

Appendix A

Owing the lack of equipment information, it has been developed an Excel spreadsheet, using ASHRAE's methodology [34], in order to obtain the refrigeration capacity of the evaporators (for specific applications and products). All thermal properties of foods present in its database, such as freezing point, latent fusion and sensible heats, among others, have been calculated using thermal property models and tables from ASHRAE's Refrigeration Handbook [34]. It has been validated comparing results to the output of commercial equivalent tools.

Process Selection		
Choose refrigerated process type	Chilling	

External Design Conditions			
Elevation	elev	m	0,0
Atmosferic pressure	p_{atm}	Pa	101325,0
External air conditions			
Air temperature	t_{air}	°C	32,0
Relative humidity air	RH_r	%	30,0
Humidity ratio at saturation room air	Ws_r	$kg_W.kg_{da}^{-1}$	0,0306
Humidity ratio room air	W_r	$kg_W.kg_{da}^{-1}$	0,0089
Specific volume room air	ν_r	$m^3.kg^{-1}$	0,8768
Density room air	ρ_r	$kg.m^{-3}$	1,151
Enthalpy room air	h_r	$kJ.kg_{da}^{-1}$	54,9

Internal Design Conditions			
Geometry			
Area	A_r	m^2	400,0
Volume	V_r	m^3	1200,0
Room length (N, S)	L_r	m	20,0
Room width (E, W)	W_r	m	20,0
Room height	H_r	m	3,0
Air room conditions			
Room temperature	t_r	°C	0,0
Relative humidity room air	RH_r	%	90,0
Humidity ratio at saturation room air	Ws_r	$kg_W.kg_{da}^{-1}$	0,0038
Humidity ratio room air	W_r	$kg_W.kg_{da}^{-1}$	0,0034
Specific volume room air	ν_r	$m^3.kg^{-1}$	0,778
Density room air	ρ_r	$kg.m^{-3}$	1,290
Enthalpy room air	h_r	$kJ.kg_{da}^{-1}$	8,5

Miscellaneous			
Alloted time for the process (Cooldown/Freezing Time)	n	h	18
Safety factor (Transmision gains)	SF_{Tg}	%	10
Safety factor (Total loads)	SF_{Tl}	%	10
Compressor working time	$n_{compressor}$	h	18
Defrosting working time	$n_{defrosting}$	h	2
Fan motors working time	$n_{compressor}$	h	22

Envelope				
Overall heat transfer coefficient				
	Floor heat transfer coefficient	U_F	$W.m^{-2}.K^{-1}$	0,18
	Roof heat transfer coefficient	U_R	$W.m^{-2}.K^{-1}$	0,14
	Wall heat transfer coefficient (N)	U_N	$W.m^{-2}.K^{-1}$	0,18
	Wall heat transfer coefficient (E)	U_E	$W.m^{-2}.K^{-1}$	0,18
	Wall heat transfer coefficient (S)	U_S	$W.m^{-2}.K^{-1}$	0,18
	Wall heat transfer coefficient (W)	U_W	$W.m^{-2}.K^{-1}$	0,18
Adjacent temperatures				
	Floor adjacent temperature	t_{adjF}	°C	35,0
	Roof adjacent temperature (if not external)	t_{adjR}	°C	
	Wall adjacent temperature (N, if not external)	t_{adjN}	°C	
	Wall adjacent temperature (E, if not external)	t_{adjE}	°C	
	Wall adjacent temperature (S, if not external)	t_{adjS}	°C	
	Wall adjacent temperature (W, if not external)	t_{adjW}	°C	
	Roof boundary conditions	External (Light color)		
	Wall boundary conditions (N)	External (Light color)		
	Wall boundary conditions (E)	External (Light color)		
	Wall boundary conditions (S)	External (Light color)		
	Wall boundary conditions (W)	External (Light color)		

Infiltration and Ventilation				
Method		Infiltration by direct flow through doorways		
	Leakage area per door (0.03 - 0.1m²/door)	A	m²	0,03
	Average air velocity (0.3-1.5m.s⁻¹)	v	$m.s^{-1}$	0,3

Infiltration and Ventilation				
Infiltration by Air Exchange (Doors)				
	Doorway height	H	m	2,0
	Doorway width	W	m	1,0
	Number of doors	N_{doors}	-	1
	Doors Area	A	m^2	2,0
	Parent surface	S		
	Temperature incoming air	t_i	°C	32,0
	Relative humidity incoming air	RH_i	%	60,0
	Humidity ratio at saturation incoming air	Ws_i	$kg_W.kg_{da}^{-1}$	0,0306
	Humidity ratio incoming air	W_i	$kg_W.kg_{da}^{-1}$	0,0180
	Specific volume incoming air	ν_i	$m^3.kg^{-1}$	0,8895
	Density incoming air	ρ_i	$kg.m^{-3}$	1,144
	Enthalpy incoming air through doorway from adjacent area	h_i	$kJ.kg_{da}^{-1}$	78,3
	Door protection	No protection		
	Number of doorway passages	P	-	1
	Door open-close time per passage	θ_p	s	30
	Time door simply stands open	θ_o	min	2,0
	Daily (or other) time period, h	θ_d	h	1

Products				
Products		Vegetables	Vegetables (average)	
	Initial temperature of product above freezing	t_1	°C	10,0
	Lower temperature of product above freezing	t_2	°C	0,0
	Freezing temperature of product	t_f	°C	-0,9
	Specific heat of product above freezing	cp_1	$kJ.kg^{-1}.K^{-1}$	3,80
	Specific heat of product below freezing	cp_2	$kJ.kg^{-1}.K^{-1}$	1,89
	Latent heat of fusion of product	h_{if}	$kJ.kg^{-1}$	279
	Specific respiratory heat generation at t1 (10°C)	W_{t1}	$W.kg^{-1}$	0,1409
	Specific respiratory heat generation at t2 (0°C)	W_{t2}	$W.kg^{-1}$	0,1503
Storage density factor [$kg.m^{-3}$]		450	Daily rate [%]	10
	Total storage capacity	m_{total}	kg	540000
	Total mass of product	m	kg	54000
Product container (Material and utilization)		Cardboard	General (low)	
	Specific heat	$cp_{container}$	$kJ.kg^{-1}.K^{-1}$	1,3
	Relative mass	$\%m_{container}$	%	10%

Internal Gains				
People				
	Number of persons	n_{people}	persons	1
Lighting				
	Lighting level	q_{ligh}	$W.m^{-2}$	12,0
Trucks and Forklifts				
	Number of trucks	n_{truck}	truck	0
	Power per truck	P_{truck}	$kW.truck^{-1}$	0,00
Fan motors				
	Number of evaporators	$n_{evaporators}$	evap	10
	Number of fans per evaporator	$n_{fan/evap}$	fan/evap	4
	Heat gain per fan	q_{fan}	$kW.fan^{-1}$	0,07
Motors				
	Number of motors	n_{motor}	motor	0
	Heat gain per motor	q_{motor}	$kW.motor^{-1}$	0,00
Defrosting				
	Resistances	$q_{resistances}$	$kW.evap^{-1}$	3,00

Total load (+10%)	Q_{total}	kW	143,05
Safety factor	SF	%	10
Subtotal	ΣQ	kW	130,05
Load ratios	kW	%partial	%total
Envelope (+10%)	6,67	-	5,1%
Floor	2,77	41,6%	2,1%
Roof	2,28	34,2%	1,8%
Wall (N)	0,38	5,7%	0,3%
Wall (E)	0,42	6,2%	0,3%
Wall (S)	0,40	6,1%	0,3%
Wall (W)	0,42	6,2%	0,3%
Ventilation and Infiltration	1,94	-	1,5%
Products	113,44	-	87,2%
Sensible cooling above freezing	31,70	27,9%	24,4%
Latent cooling while freezing	0,00	0,0%	0,0%
Sensible cooling below freezing	0,00	0,0%	0,0%
Respiration	80,66	71,1%	62,0%
Containers	1,08	1,0%	0,8%
Internal gains	7,99	-	6,1%
People	0,27	3,4%	0,2%
Lighting	4,80	60,1%	3,7%
Trucks and Forklifts	0,00	0,0%	0,0%
Fan motors	2,92	36,5%	2,2%
Motors	0,00	0,0%	0,0%
Defrosting	Included in safety factor		

Transmission		$Q_{transmission}$	kW	6,67
Safety factor		SF	%	10
Subtotal		$\Sigma Q_{transmission}$	kW	6,06
Floor		$Q_{transmissionF}$	kW	2,52
	Area	A	m²	400,0
	Lenght	L	m	20,0
	Width	H	m	20,0
	Floor heat transfer coefficient	U_F	$W.m^{-2}.K^{-1}$	0,18
	Temperature difference	Δt	°C	35,0
	Adjacent temperature	t_{adjF}	°C	35,0
	Room temperature	t_r	°C	0,0
Roof		$Q_{transmissionR}$	kW	2,07
	Area	A	m²	400,0
	Lenght	L	m	20,0
	Width	H	m	20,0
	Roof heat transfer coefficient	U_R	$W.m^{-2}.K^{-1}$	0,14
	Temperature difference	Δt	°C	37,0
	Adjacent temperature	t_{adjR}	°C	32,0
	Room temperature	t_r	°C	0,0
	Sun effect, function of color and orientation (H)	Δt_{sunR}	K	5
Wall (N)		$Q_{transmissionN}$	kW	0,35
	Area	A	m²	60,0
	Lenght (L_r)	L	m	20,0
	Height	H	m	3,0
	Wall heat transfer coefficient	U_N	$W.m^{-2}.K^{-1}$	0,18
	Temperature difference	Δt	°C	32,0
	Adjacent Temperature	t_{adjN}	°C	32,0
	Room Temperature	t_r	°C	0,0
	Sun effect, function of color and orientation (N)	Δt_{sunN}	K	0
Wall (E)		$Q_{transmissionE}$	kW	0,38
	Area	A	m²	60,0
	Lenght (W_r)	L	m	20,0
	Height	H	m	3,0
	Wall heat transfer coefficient	U_E	$W.m^{-2}.K^{-1}$	0,18
	Temperature difference	Δt	°C	35,0
	Adjacent Temperature	t_{adjE}	°C	32,0
	Room Temperature	t_r	°C	0,0
	Sun effect, function of color and orientation (E)	Δt_{sunE}	K	3
Wall (S)		$Q_{transmissionS}$	kW	0,37
	Area	A	m²	60,0
	Lenght (L_r)	L	m	20,0
	Height	H	m	3,0
	Wall heat transfer coefficient	U_S	$W.m^{-2}.K^{-1}$	0,18
	Temperature difference	Δt	°C	34,0
	Adjacent Temperature	t_{adjS}	°C	32,0
	Room Temperature	t_r	°C	0,0
	Sun effect, function of color and orientation (S)	Δt_{sunS}	K	2
Wall (W)		$Q_{transmissionW}$	kW	0,38
	Area	A	m²	60,0
	Lenght (W_r)	L	m	20,0
	Height	H	m	3,0
	Wall heat transfer coefficient	U_W	$W.m^{-2}.K^{-1}$	0,1800
	Temperature difference	Δt	°C	35,0
	Adjacent Temperature	t_{adjW}	°C	32,0
	Room Temperature	t_r	°C	0,0
	Sun effect, function of color and orientation (W)	Δt_{sunW}	K	3

Infiltration by direct flow through doorways		$Q_{infiltration/ventilatio}$	kW	0,03
1	Leakage area per door (0.03 - 0.1m²/door)	A	m²	0,03
	Average air velocity (0.3-1.5m.s⁻¹)	v	m.s⁻¹	0,3
	Enthalpy incoming air through doorway from adjacent area	hi	kJ.kg⁻¹	78,3
	Enthalpy room air	h_r	kJ.kg⁻¹	8,5
	Density incoming air	ρi	kg.m⁻³	1,144
	Doorway open-time factor (decimal portion of time doorway is op	D_t	-	0,04167

Infiltration by Air Exchange (Doors)		$Q_{infiltration}$	kW	1,91
Doorway height		H	m	2,0
Doorway width		W	m	1,0
Doorway area		A	m²	2,0
Enthalpy incoming air through doorway from adjacent area		h_i	kJ.kg⁻¹	78,3
Enthalpy room air		h_r	kJ.kg⁻¹	8,5
Density incoming air		ρ_i	kg.m⁻³	1,144
Density room air		ρ_r	kg.m⁻³	1,290
Gravitational acceleration		g	m.s⁻²	9,81
Density factor		F_m	-	0,97
Doorway flow factor		D_f	-	0,8
Doorway open-time factor (decimal portion of time doorway is open)		D_t	-	0,04167
	Number of doorway passages	P	-	1
	Door open-close time per passage	θ_p	s	30
	Time door simply stands open	θ_o	min	2,0
	Daily (or other) time period, h	θ_d	h	1
Effectiveness factor for open-doorway protective device such as AC or		E_f	-	0,00

Products		$Q_{products}$	kW	113,44
Alloted time for the process		n	h	18
Heat removal from t_1 to t_2, above freezing (Chilling)		Q_1	kJ	2053855,65
1	Total mass of product	m	kg	54000
	Mass flow	ṁ	kg.h⁻¹	3000,00
	Initial temperature of product above freezing	t_1	°C	10,0
	Lower temperature of product above freezing	t_2	°C	0,0
	Specific heat of product above freezing	cp_1	kJ.kg⁻¹.K⁻¹	3,80
Heat removal from t_1 to t_f at freezing point (Freezing, sensible heat)		Q_2	kJ	0,00
0	Total mass of product	m	kg	0
	Mass flow	ṁ	kg.h⁻¹	0,00
	Initial temperature of product above freezing	t_1	°C	0,0
	Freezing temperature of product	t_f	°C	0,0
	Specific heat of product above freezing	cp_1	kJ.kg⁻¹.K⁻¹	0,00
Heat removal to freeze the product (Freezing, latent heat)		Q_3	kJ	0,00
0	Total mass of product	m	kg	0
	Mass flow	ṁ	kg.h⁻¹	0,00
	Latent heat of fusion of product	h_{if}	kJ.kg⁻¹	0,00
Heat removal from tf at freezing point to t3 (SubFreezing, sensible heat)		Q_4	kJ	0,00
0	Total mass of product	m	kg	0
	Mass flow	ṁ	kg.h⁻¹	0,0
	Freezing temperature of product	tf	°C	0,0
	Final temperature of product below freezing	t_3	°C	0,0
	Specific heat of product below freezing	cp_2	kJ.kg⁻¹.K⁻¹	0,00
Product container heat removal from t1 to final product temperature		$Q_{container}$	kJ	70200,00
1	Total mass of product	m	kg	54000
	Mass flow	ṁ	kg.h⁻¹	3000,0
	Relative mass of container regarding product	$\%m_{container}$	%	10%
	Initial temperature of container	$t_{containeri}$	°C	10,0
	Final temperature of container	$t_{containerf}$	°C	0,0
	Specific heat of product container	$cp_{container}$	kJ.kg⁻¹.K⁻¹	1,30
Heat of respiration (only for fresh fruits, vegetables and fresh cheese)		$Q_{respiration}$	kW	80,66
1	Specific respiratory heat generation at t1 (10°C)	W_{t1}	W.kg⁻¹	0,1409
	Specific respiratory heat generation at t2 (0°C)	W_{t2}	W.kg⁻¹	0,1503
	Mass of product at t1 (10°C)	m_{t1}	kg	54000
	Mass of product at t2 (0°C)	m_{t2}	kg	486000

People	Q_{people}	kW	0,27
Number of persons	n_{people}	persons	1
Room Temperature	t_r	°C	0,0

Lighting	Q_{lights}	kW	4,80
Lighting level	q_{ligh}	$W.m^{-2}$	12,0
Floor Area	A_r	m^2	400,0

Trucks and Forklifts	Q_{trucks}	kW	0,00
Number of trucks	n_{truck}	truck	0
Power per truck	P_{truck}	$kW.truck^{-1}$	0,00

Fan motors	Q_{fans}	kW	2,92
Number of fans	n_{fan}	fan	40
Heat gain per fan	q_{fan}	$kW.fan^{-1}$	0,07

Motors	Q_{motors}	kW	0,00
Number of motors	n_{motor}	motor	0
Heat gain per motor	q_{motor}	$kW.motor^{-1}$	0,00

Total Load	Q_{total}	kW	143,05
Safety factor	SF	%	10
Subtotal	ΣQ	kW	130,05